ENERGY AND VALUE ADDED PRODUCTS FROM MARINE BIOMASS AND WASTELAND DERIVED BIOMASS

A Thesis submitted to Gujarat Technological University

For the Award of

Doctor of Philosophy

In

Chemical Engineering

by

PRASANTA DAS

Enrolment No. 139997105007

Under Supervision of

Dr. Subarna Maiti

GUJARAT TECHNOLOGICAL UNIVERSITY

AHMEDABAD

July – 2018

ENERGY AND VALUE ADDED PRODUCTS FROM MARINE BIOMASS AND WASTELAND DERIVED BIOMASS

A Thesis submitted to Gujarat Technological University

For the Award of

Doctor of Philosophy

In

Chemical Engineering

by

PRASANTA DAS

Enrolment No. 139997105007

Under Supervision of

Dr. Subarna Maiti

GUJARAT TECHNOLOGICAL UNIVERSITY

AHMEDABAD

July – 2018

Annexure - II

Annexure – III

DECLARATION

I declare that the thesis entitled "**Energy and value added products from marine biomass and wasteland derived biomass**" submitted by me for the degree of Doctor of Philosophy is the record of research work carried out by me during the period from March, 2013 to July, 2018 under the supervision of **Dr. Subarna Maiti**, Sr. Scientist, CSIR-CSMCRI, and this has not formed the basis for the award of any degree, diploma, associateship, fellowship, titles in this or any other University or other institution of higher learning.

I further declare the material obtained from other sources has been duly acknowledged in this thesis. I shall be solely responsible for any plagiarism or other irregularities, if noticed in the thesis.

Signature of the Research Scholar: ……Date: 20th July, 2018.

Name of Research Scholar: **Prasanta Das.**

Place: CSIR-CSMCRI, Bhavnagar-364002, Gujarat, India.

Annexure – IV

CERTIFICATE

I certify that the work incorporated in the thesis "**Energy and value added products from marine biomass and wasteland derived biomass**" submitted by shri **Prasanta Das** was carried out by the candidate under my supervision/guide. To the best of my knowledge:

(i) the candidate has not submitted the same research work to any other institution for any degree/diploma, Associateship, Fellowship, or other similar titles

(ii) the thesis submitted is a record of original research work done by the Research Scholar during the period of study under my supervision, and

(iii) the thesis represents independent research work on the part of the Research Scholar.

Signature of Supervisor: ……Date: 20th, July, 2018.

Name of Supervisor: **Dr. Subarna Maiti.**

Place: CSIR-CSMCRI, Bhavnagar-364002, Gujarat, India.

Annexure – V

Originality Report Certificate

It is certified that PhD Thesis titled "**Energy and value added products from marine biomass and wasteland derived biomass**" by **Mr. Prasanta Das** has been examined by us. We undertake the following:

a. Thesis has significant new work / knowledge as compared already published or are under consideration to be published elsewhere. No sentence, equation, diagram, table, paragraph or section has been copied verbatim from previous work unless it is placed under quotation marks and duly referenced.

b. The work presented is original and own work of the author (i.e. there is no plagiarism). No ideas, processes, results or words of others have been presented as Author own work.

c. There is no fabrication of data or results which have been compiled / analysed.

d. There is no falsification by manipulating research materials, equipments, or processes, or changing or omitting data or results such that the research is not accurately represented in the research record.

e. The thesis has been checked using "Turnitin" software (copy of originality report attached) and found within limits as per GTU Plagiarism Policy and instructions issued from time to time (i.e. permitted similarity index 16% <=25%).

Signature of the Research Scholar: ……Date: 20th, July, 2018.

Name of Research Scholar: **Prasanta Das.**

Place: CSIR-CSMCRI, Bhavnagar-364002, Gujarat, India.

Signature of Supervisor: ……Date: 20th, July, 2018.

Name of Supervisor: **Dr. Subarna Maiti.**

Place: CSIR-CSMCRI, Bhavnagar-364002, Gujarat, India.

VNK

ORIGINALITY REPORT

16%	4%	15%	2%
SIMILARITY INDEX	INTERNET SOURCES	PUBLICATIONS	STUDENT PAPERS

PRIMARY SOURCES

1	Das, Prasanta, Milan Dinda, Nehal Gosai, and Subarna Maiti. "High Energy Density Bio-oil via Slow Pyrolysis of Jatropha curcas Shells", Energy & Fuels, 2015. Publication	8%
2	Submitted to Savitribai Phule Pune University Student Paper	2%
3	library.certh.gr Internet Source	1%
4	Prasanta Das, Samir Charola, Milan Dinda, Himanshu Patel, Subarna Maiti. "Hydrogen from empty cotton boll agro-waste via thermochemical route and feasibility study of operating an IC engine in continuous mode", International Journal of Hydrogen Energy, 2017 Publication	1%
5	Slopiecka, Katarzyna, Pietro Bartocci, and Francesco Fantozzi. "Thermogravimetric analysis and kinetic study of poplar wood pyrolysis", Applied Energy, 2012. Publication	1%
6	tel.archives-ouvertes.fr Internet Source	1%
7	Prabir Basu. "Biomass Characteristics", Biomass Gasification Design Handbook, 2010 Publication	1%
8	mospi.nic.in Internet Source	1%
9	www.environet.eu Internet Source	1%
10	Maiti, S.. "Thermal characterization of mustard straw and stalk in nitrogen at different heating rates", Fuel, 200707 Publication	1%

Exclude quotes	On	Exclude matches	< 1%
Exclude bibliography	On		

Draft Annexure – VI

PhD THESIS Non-Exclusive License to GUJARAT TECHNOLOGICAL UNIVERSITY

In consideration of being a PhD Research Scholar at GTU and in the interests of the facilitation of research at GTU and elsewhere, I, Prasanta Das having enrolment No. 139997105007 hereby grant a non-exclusive, royalty free and perpetual license to GTU on the following terms:

a) GTU is permitted to archive, reproduce and distribute my thesis, in whole or in part, and/or my abstract, in whole or in part (referred to collectively as the "Work") anywhere in the world, for non-commercial purposes, in all forms of media;

b) GTU is permitted to authorize, sub-lease, sub-contract or procure any of the acts mentioned in paragraph (a);

c) GTU is authorized to submit the Work at any National / International Library, under the authority of their "Thesis Non-Exclusive License";

d) The Universal Copyright Notice (©) shall appear on all copies made under the authority of this license;

e) I undertake to submit my thesis, through my University, to any Library and Archives. Any abstract submitted with the thesis will be considered to form part of the thesis.

f) I represent that my thesis is my original work, does not infringe any rights of others, including privacy rights, and that I have the right to make the grant conferred by this non-exclusive license.

g) If third party copyrighted material was included in my thesis for which, under the terms of the Copyright Act, written permission from the copyright owners is required, I have obtained such permission from the copyright owners to do the acts mentioned in paragraph (a) above for the full term of copyright protection.

h) I retain copyright ownership and moral rights in my thesis, and may deal with the copyright in my thesis, in any way consistent with rights granted by me to my University in this non-exclusive license.

i) I further promise to inform any person to whom I may hereafter assign or license my copyright in my thesis of the rights granted by me to my University in this non-exclusive license.

j) I am aware of and agree to accept the conditions and regulations of PhD including all policy matters related to authorship and plagiarism.

Signature of the Research Scholar: ……
Name of Research scholar: **Prasanta Das**.
Date: 20th, July, 2018. Place: CSIR-CSMCRI, Bhavnagar-364002, Gujarat, India.

Signature of Supervisor: ……
Name of Supervisor: **Dr. Subarna Maiti.**
Date: 20th, July, 2018. Place: CSIR-CSMCRI, Bhavnagar-364002, Gujarat, India.
Seal:

Draft Annexure - VII

Thesis Approval Form

The viva-voce of the PhD Thesis submitted by Shri ~~/ Smt. / Kum.~~ **Prasanta Das**…… (Enrolment No.139997105007) entitled "**Energy and Value added Products from Marine biomass and Wasteland derived biomass**"…… was conducted on 20th, July, 2018……. at Gujarat Technological University.

(Please tick any of the following option)

- ☐ The performance of the candidate was satisfactory. We recommend that he/she be awarded the PhD degree.
- ☐ Any further modifications in research work recommended by the panel after 3 months from the date of first viva-voce upon request of the Supervisor or request of Independent Research Scholar after which viva-voce can be re-conducted by the same panel again.

(Briefly specify the modifications suggested by the panel)

- ☐ The performance of the candidate was unsatisfactory. We recommend that he/she should not be awarded the PhD degree.

(The panel must give justifications for rejecting the research work)

Dr. Subarna Maiti **…….**

Name and Signature of Supervisor with Seal (1) (External Examiner 1) Name and Signature

…… …….

(2) (External Examiner 2) Name and Signature (3) (External Examiner 3) Name and Signature

Annexure – VIII

ABSTRACT

Biomass – either terrestrial or marine biomasses are essential source of renewable energy in terms of syn-gas production or extraction of valuable chemicals. Nowadays, energy crisis is a major problem not only in India, but all across the world due to shortage of conventional fuels. Researchers, today mostly focus on efficient way of utilization of bioenergy for thermochemical conversions such as pyrolysis, gasification, liquefaction, carbonization and combustion. These methods are promising technology in the recent times for its low carbon footprint and less carbon dioxide emission. While in case of conventional energy source caused several problems due to high emission of greenhouse gases. So the current trend is to find out alternate energy source and is simultaneously to investigate different pathways for reduction of pollution level in the atmosphere. For this to meet the energy consumption, although addressing the importance of energy security and environmental impact has grown interest in the alternate fuels instead of fossil fuels. Biomass is one of the solutions to meet the above challenges due to its carbon neutral energy sources and huge available around the world. So thermochemical conversions can be more fruitful to convert solid fuel to convenient gaseous form or liquid form in the downstream process. Direct combustion of biomass produces NOx, SOx from fuel-bound nitrogen and sulphur. Gasification provides the opportunity to control the level of gaseous and particulate emission, which is leading to lower down concentration particulate matters, soot particles, NOx, SOx, and the production of clean energy or valuable chemicals (e.g., CO, H_2, or CH_4). Much of the mass degraded during biomass decomposition at lower pyrolysis temperatures. Again, steam-gasification or gasification offers thermal treatment at elevated temperature under a reducing atmosphere that leads to fuel-bound nitrogen and sulphur formed into N_2 or H_2S or any other gases can be removed by absorption beds. By this way the fuel hydrogen rich syn-gas can be improved significantly in the downstream process.

The whole thesis is comprised of different thermochemical conversion routes such as gasification, pyrolysis, different kinetic models, steam gasification as well the physiochemical properties of the selected biomass. The selection of biomass is extremely important in this study as edible crops cannot be used in the thermochemical routes. For this some wasteland derived biomass, marine macroalgae, and some agricultural waste are selected in the present study. The wasteland derived biomasses are *Jatropha* curcas shells, *Cassia auriculata, Cassia tora, Jatropha gossypifolia, Dichanthium annulatum, Sphaeranthus indicus, Eclipta alba, Desmostachya bipinnata, Solanum xanthocarpum, Butea monosperm*a, *Prosopis* juliflora and the marine seaweed species are *Kappaphycus alvarezii* granules, *Ulva fasciata*, *Gracilaria corticata*, and *Sargassum tenerrimum*

and some agricultural residues are also characterized as a solid fuel. The present study is comprised of the physiochemical characterization of the selected biomass species as it is extremely important in thermochemical conversion processes. Some experimental case studies were validated on some selected biomass species. The gasification of a wasteland derived biomass and a seaweed species named *Jatropha carcass* shells and *Kappaphycus alvarezii* granules (KAG), respectively is investigated in a typical downdraft gasifier. The pyrolysis study is involving with the *Jatropha curcas* shells along with four seaweed species named *Kappaphycus alvarezii* granules, *Ulva fasciata*, *Gracilaria corticata*, and *Sargassum tenerrimum*. The pyrolysis mechanism was well described by the different kinetic models with TGA analysis for each kind of biomass that best elaborated by devolatilization process. And finally, steam gasification of *Jatropha curcas* shells char is also investigated as potential source of hydrogen rich clean energy. The outcome of each experimental case studies are briefly describing below. Three different distinguished case studies of *Jatropha curcas* shells were investigated in gasification, pyrolysis, and steam gasification.

(1) The gasification of jatropha shells was demonstrated in a typical downdraft gasifier having feed rate 15 kg h^{-1}. After the characterization of this feedstock it exhibited excellent calorific value 17.2 MJ kg^{-1} and the producer gas having calorific value 5.2 MJ Nm^{-3} obtained during gasification, with an efficiency of 64.8% over 8 h continuous operation. The temperature profile of the air gasifier measured as drying, pyrolysis, oxidation, and reduction are 130, 326, 752, 480°C, respectively. The gasifier was connected to a 100% producer gas engine and continuous power generation (ca. 10 kW) was showed off along with overall efficiency of 24.5%. Thus, captive power could be utilized for external sources of power for the operations of deshelling, screw pressing, oil refining, transesterification, glycerol purification, and soap making in the intermediate integrated biodiesel production process. CSIR-CSMCRI has built-up an integrated bio-diesel demonstration plant. In this process, the total electrical energy requirement of 500 kWh, and 50 kg furnace oil to obtain the following products starting from 6.06 t/day dry jatropha fruit can be worked out: 1 t jatropha biodiesel; 0.08 t neat glycerol; 2.54 t oil cake; 0.056 t soap cake; 0.022 t potassium sulphate; 2 t empty shells. The jatropha shells have good calorific value and the power and steam requirement can be met from the shells. The requirement of jatropha shells would be around 0.85 – 0.90 t based on the findings of the present study. So naturally the rest jatropha shells ca. 1.1 t could be utilized for the bio-oil production which can meet the requirement of furnace oil and the requirement of energy for the steam gasification. Thus the whole process would be sustainable.

(2) Again, jatropha shells were utilized for the bio-oil production in a fixed bed reactor at the temperatures of 300, 400, 500, and 600°C in order to obtain the optimum yield. The heating was

carried out using heater coil made of canthal-A1 and conduction, convection, and radiation were the modes of heat transfer. The heating rate could be controlled by PID controller and was optimized by experiments. The kinetic study was carried out by TGA method. For this kinetic study at the heating of 5°C min^{-1} was found suitable and the optimum result was obtained at 400°C, with yield of 31.14 wt.% and holding 4 h. The obtained bio-oil was containing ca. 40% carbonyl derivatives (>C=O) converted into corresponding methylene group (-CH_2-) derivative by the treatment of hydrazine hydrate and sodium hydroxide. The resulted oil was mostly containing with ethylbenzene, had a high calorific.

(3) The produced bio-chars at the temperatures of 300, 400, 500, and 600°C were obtained from the slow pyrolysis of jatropha shells in the above same fixed bed reactor and the bio-chars were characterized as solid fuel. The steam gasification was carried out at 700 and 800°C temperature and the bio-char produced from slow pyrolysis at 500°C has been selected for the steam gasification. The parametric studies were also investigated which included the effect of reactor temperature, the effect of steam flow rate. The detailed discussion was done how these two parameters influenced on hydrogen rich syn-gas yield.

(4) The macroalgae *Kappaphycus alvarezii* granules (KAG) were characterized as solid fuel for the thermochemical conversion processes, mainly in gasification and pyrolysis process. The granules obtained after recovery of sap (a liquid plant stimulant) is a promising biomass feedstock for energy application. The different kinetic models assist the devolatilization process through thermogravimetric analysis (TGA) in nitrogen atmosphere under different heating rates 5, 10, 15, and 20 K min^{-1}. Sawdust as lignocellulogic biomass was considered for comparative study. The selected kinetic models are (i) multilinear regression technique, (ii) Friedman method, (iii) Flynn-Wall-Ozawa (FWO) (iv) Kissinger-Akahira-Sunose (KAS) methods are used to evaluate the apparent activation energy (E_a), the pre-exponential factor (A_α) and overall reaction order (n). From the chemical constituents it was found that the seaweed species contained with around 50 % (wt.) κ-carrageenan composed of organic sulphur derivatives. So from TG-MS it is indicated that the SOx found maximum at 300°C and 950°C temperature which concluded the pyrolysis at 500°C, with a packed bed lime scrubber at the outlet during temperature rise is the best suitable thermochemical route for energy generation. For the gasification of KAG two case studies were investigated separately in the 10 kWe and 5 kWe downdraft gasifier. To avoid the problem existing in the 10 kW gasifier, an improved gasifier (5 kg h^{-1}) was designed. In this system a screw-driven conveyer with programmable timer was attached to remove ash in order to avoid agglomeration/slagging.

(5) The slow pyrolysis of three seaweed species named Red seaweed *Gracilaria corticata* (GC), brown seaweed *Sargassum tenirimum* (ST) and green seaweed *Ulva fasciata* (UF) were collected from Veraval (20.55°N and 70.20°E) west coast of India have been investigated for energy application. The sap (a potential liquid plant stimulant) has extracted from the seaweed species before pyrolysis which adds value addition. The devolatilization process well described by thermogravimetric analysis (TGA) with Arrhenius approach for evaluating the kinetic parameters and find out the best suitable pyrolysis temperature. It was found out that the best suitable pyrolysis temperature 500°C with the heating rate was 10°C min^{-1}. The obtained moisture free bio-oils were characterized and the reasonable calorific value in the range of 27 to 34 MJ kg^{-1} was obtained. The solid residue that is bio-chars left after the pyrolysis was also characterized. The bio-oils could be a suitable solution for the replacement of conventional diesel fuel. LCA (Life Cycle Assessment) has been selectively investigated for *Ulva fasciata* for the potential of industrial application.

Annexure - IX

Acknowledgement

I feel great pleasure in expressing my deepest respect and wish to thank Dr. Subarna Maiti, Senior Scientist in PDEC, CSIR-CSMCRI, Bhavnagar, Gujarat, India for her kind guidance and valuable suggestions and gracious initiation and inspiration without this I could not be completed this PhD thesis.

At the outset, there are many people who have been assisted during my PhD works I would like to thank them warmly and some of them are listed here. I would like to thank Mr. Pratyush Maiti, Principle Scientist in PDEC, CSIR-CSMCRI has provided project assistantship during my PhD work.

I also grateful to my DPCs (Doctoral Progress committee) members Dr. Parimal Paul, Chief Scientist, CSIR-CSMCRI, Bhavnagar, Dr. M. Shyam, a former director of SPRERI (Sardar Patel Renewable Energy Research Institute), Vallabh Vidhyanagar, Anand, Gujarat who have been given valuable suggestions in doctoral progress review committee meetings and provided continuous support in research. Dr. Piyush B. Vanzara is also acknowledged for attending open seminar in CSMCRI.

I would like to thank Hon. Vice Chancellor Prof. (Dr.) Navin Sheth and I/C Registrar Mr. Bipin J, Bhatt of Gujarat Technological University, in providing necessary support in PhD. I would also like to thank Director Dr. R. K. Gajjar of Gujarat Technological University and other supporting staff Mr. Dhaval, Ms. Radhika, Ms. Krutika, and Ms. Arpita at GTU office for facilitation of my PhD from administrative point of view.

I would like to thank former Director Dr. Pushpito K. Ghosh and the present director Dr. Amitava Das of CSIR-CSMCRI for giving me necessary approval to carry out the research in the institution. I am also grateful to Dr. C. R. K Reddy, Dr. Arup Ghosh, Dr. J. R. Chunawala, Dr. Subhadip Neogi, Dr. P.S. Bapat, Mr. Bhupendra K. Markam, Mr. Pankaj Patel and Mr. Vijayanand and Dr. Ravi Singh Bhagel. Other supporting staff Mr. Abhisek Joshi, Mr. Jaydip, Ms. Nehel Gosai, Mr. Jigar, Mr. Rathod, Mr. Pintu, Mr. Zala are acknowledged. I would like to thank Mr. Samir charola, a PhD colleague, Mr. S. Prajapati, Dr. Hiren D. Raval and Mr. Jatin Sir who have been given me moral support during my PhD work. And finally, all the supporting technical persons in CSIR-CSMCRI are also acknowledged.

Dedicated to,

Myself and Almighty God

(*Those who help me out from difficult situation in my life and thank them for their constant inspiration and motivation to complete my PhD thesis*)

Annexure - X

Table of content

turnitin

Digital Receipt

This receipt acknowledges that Turnitin received your paper. Below you will find the receipt information regarding your submission.

The first page of your submissions is displayed below.

Submission author:	Shantilal Shah Engineering College...
Assignment title:	Final Report_359
Submission title:	VNK
File name:	Final_full_PhD_thesis_12.pdf
File size:	6.05M
Page count:	185
Word count:	57,241
Character count:	289,563
Submission date:	06-Nov-2017 02:22PM (UTC+0530)
Submission ID:	875140330

CHAPTER – 1

General Introduction

1.1 Introduction

Today, energy crisis and environmental issues are two paramount problems confronting the world. Energy and environment are integral part of our daily life. The consequence of energy crisis triggers monumental problems in environment related areas especially from burning of conventional sources of energy. Nonetheless, the mankind is still substantially relying on the conventional sources of energy such as coal, oil and natural gas. The formation of conventional sources of energy such as fossil fuels in the earth entails thousands of years and their reserves are finite. In spite of these fossil fuel constraints, the rate of depletion of these fuels is extremely faster (about 100,000 times faster) than their formation [1]. The conventional energies are largely hinged on coal, oil and natural gas. The present civilization consumes the conventional energies rapidly and voraciously as compared to last few decades. So, naturally it can be predicted that the whole mankind in the universe might pass through relentlessly huge energy crisis in the ensuing future. A general outlook of energy distribution in India has been classified sector wise e.g., installed capacity of conventional fuel and overall installed capacity as shown in Fig. 1.1 (a, b, c). The scenario of energy distribution in India covered by state sector is 34%, central sector is 26% and private sector is 40%. As India is a diverse country, the private sector predominantly occupies energy sector percentagewise which is followed by state and central sector. Fig. 1.1 (b) shows the installed capacity of conventional fuel in India. The highest installed capacity is noticed for coal, followed by natural gas and oil. Most of the

Ph.D Thesis of Prasanta Das Page 1

Annexure – XI

List of Abbreviation

GDP: Gross Domestic Product

MW: Mega Watt

GWh: Gigawatt hours

CAGR: Compound Annual Growth Rate

MT: Metric Ton

EJ: Exajoules

NREL: National Renewable Energy Laboratory

HTL: Hydrothermal Liquefaction

py-GC/MS: pyrolysis-Gas-Chromatography/Mass-Spectroscopy

TGA: Thermogravimetric analysis

TG-MS: Thermogravimetric-Mass-Spectroscopy

HHV: Higher heating value

LHV: Lower heating value

NCV: Net Calorific Value

h_l: The latent heat of the steam

BTR_r: Base-to-acid ratio

BAI_r: Bed Agglomeration Index

GHG: Green House Gas

d.b.: Dry basis

FTIR: Fourier Transform Infrared

FID: Flame Ionization detector

t: Ton

NMR: Nuclear Magnetic Resonance

GCV: Gross Calorific Value

DEPT (-135): Distortionless Enhancement by Polarization Transfer

Annexure – XII

List of symbols

moc_o: Mass of carbon (decayed)

moc_i: Mass of carbon (initial)

n_i: Moles of carbon in components

V: Total volume of gas

η_{cge}: The cold gas efficiency

Q_s: Energy content of the syn-gas.

M_b: Moisture content of solid fuel or biomass

M_s: The product syn-gas

$(LHV)_b$: Lower heating value of the biomass

η_{hge}: The hot gas efficiency

T_f: Temperature of exist point at the gasifier

T_i: Temperature of entrance at the gasifier

M_d: The weight of dried biomass

M_w: The weight of wet biomass

ρ_b: Bulk density

k_1 to k_5: Reaction rate constant

1,4-DB eq : 1,4-Dichlorobenzene

U235 eq : Uranium equivalent (isotope 235)

P eq : Phosphorus equivalent.

N-Equiv: Nitrogen equivalent.

Fe eq: Iron equivalent.

CFC-11 eq: Chlorofluorocarbon equivalent.

PM10 eq: Particulate Matter 10 equivalent.

NMVOC: *Non-methane volatile organic compound*

SO_2 eq: Sulphur di-oxide equivalent.

Annexure – XIII

List of Figures

Annexure – XIV

List of Tables

Annexure – XV

List of Appendices

Appendix A: Pictures of ash fusion temperatures of ash cone for wasteland derived biomass and for three other seaweed species, *Ulva fasciata, Sargassum tenerrimum, Gracilaria corticata, and Kappaphycus alvarezii (washed granules).*

CHAPTER – 1

General Introduction

1.1 Introduction

Today, energy crisis and environmental issues are two paramount problems confronting the world. Energy and environment are integral part of our daily life. The consequence of energy crisis triggers monumental problems in environment related areas especially from burning of conventional sources of energy. Nonetheless, the mankind is still substantially relying on the conventional sources of energy such as coal, oil and natural gas. The formation of conventional sources of energy such as fossil fuels in the earth entails thousands of years and their reserves are finite. In spite of these fossil fuel constraints, the rate of depletion of these fuels is extremely faster (about 100,000 times faster) than their formation [1]. The conventional energies are largely hinged on coal, oil and natural gas. The present civilization consumes the conventional energies rapidly and voraciously as compared to last few decades. So, naturally it can be predicted that the whole mankind in the universe might pass through relentlessly huge energy crisis in the ensuing future. A general outlook of energy distribution in India has been classified sector wise e.g., installed capacity of conventional fuel and overall installed capacity as shown in Fig. 1.1 (a, b, c) [2]. The scenario of energy distribution in India covered by state sector is 34%, central sector is 26% and private sector is 40%. As India is a diverse country, the private sector predominantly occupies energy sector percentagewise which is followed by state and central sector. Fig. 1.1 (b) shows the installed capacity of conventional fuel in India. The highest installed capacity is noticed for coal, followed by natural gas and oil. Most of the

coal reserves in eastern part of India, especially Jharkhand, Odisha, Chhattisgarh, West Bengal, Madhya Pradesh, Andhra Pradesh and Maharashtra account for more than 99% of the total coal reserves in the country. But, India lacks the quality of coal and the majority of estimated coal is lignite with reserve amounting to around 43.24 billion tons at present [3]. India is not energy secure country, so mainly depends on the imports of oil and natural gas. Fig. 1.1 (c) shows the overall outlook of energy installed capacity including thermal, nuclear, hydro (renewable) and others renewable sources (excluding hydro). Apart from thermal energy, renewable energy has immense potential to sustain in near future. Hydro energy is generally assumed as renewable energy in India, but it is assumed as primary energy source in our country. Renewable energy includes mainly, solar energy, bioenergy, and wind energy available in India.

1.2 Energy Scenario in India

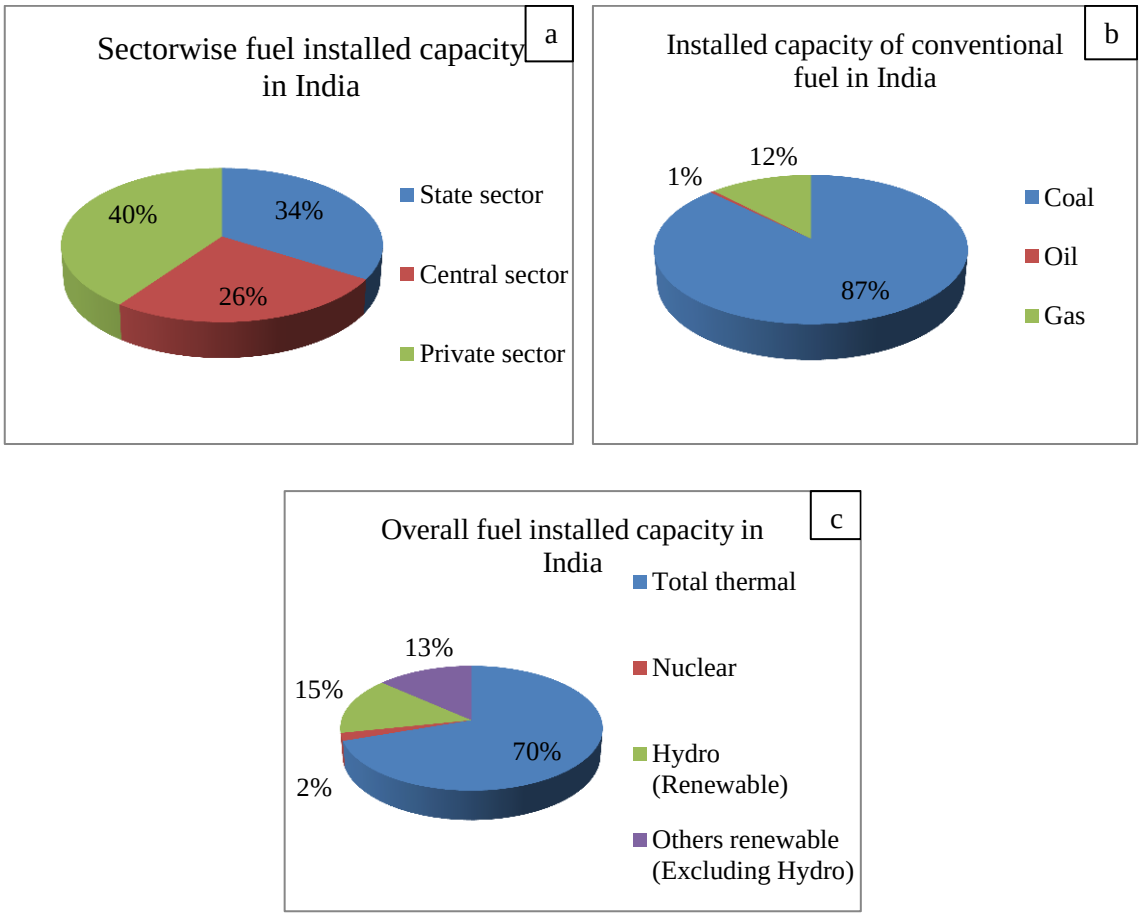

FIGURE 1.1: Sector wise conventional fuel installed capacity in India (a,b,c).

India is the world's second largest populous country after China in the world. The estimated reserves of fossil fuel in India are depicted in Table 1.1. India has the world's 4th largest coal reserves and this prime source of energy contributes hugely to India's economy i.e. GDP. India is the third top coal producer in 2013 with 7.6% production share of coal (including lignite) in the world. The present data describe the estimated reserve of coal is 301.05 billion tons, production is 565.77 million tons and the consumption is 571.89 million tons as illustrated in Tables 1.1, 1.2 and 1.3 [4]. So, now the equation is clear if the consumption rate is an indication, then it will last for around 526 years. But, till now 30% of rural area in India is not electrified, so in the near future consumption could be higher which is not accounted in this study.

TABLE 1.1: Estimated reserves of fossil fuel in India at present.

Resources	**Estimated quantity**	**Units**
Coal	301.05	billion tons
Oil	762.74	million tons
Natural gas	1427.15	billion cubic meters
Renewable sources	147615	MW

TABLE 1.2: Estimated production of fossil fuel in India at present.

Resources	**Estimated quantity**	**Units**
Coal	565.77	million tons
Oil	37.79	million tons
Natural gas	34.64	billion cubic meters
Total electricity generation	1,022,614	GWh

One of the major drawbacks of lignite coal is that the low calorific value due to the presence of large amount of ash. Generally, lignite coal with high ash content is washed by

water in order to remove ash content to make it an efficient fuel. There are certain alternative options to use this coal in thermal power plants. One such option is the gasification of coal or lignite producing syngas or coal gas or coke oven gas which is a fusion of hydrogen, carbon monoxide and carbon dioxide gases.

Coal gas can be converted into synthetic natural gas (SNG) by using Fischer–Tropsch process at low pressure and high temperature [5]. In oil sector, India imports nearly 74% of its 4.4 million barrels per day crude oil to meet its needs but exports refined petroleum products nearly 1.34 million barrels per day which is approximately 29% of its total production of refined oil products. India has now established enormous world class refining capacity using imported crude oil for exporting refined petroleum products. The net imports of crude oil is lesser by one fourth after accounting exports and imports of refined petroleum products. So, India lacks both in reserved and production of oil [6]. Tables 1.1, 1.2 and 1.3 show reserves, production and consumption of oil. Middle-east countries are main suppliers of crude oil to India.

TABLE 1.3: Estimated energy consumption in India at present.

Resources	**Estimated quantity**	**Units**
Coal	571.89	million tons
Oil	222.5	million metric tons
Natural gas	33.96	billion cubic meters
Total electricity consumption	8,82,592	GWh

In case of natural gas, the high production in the estimated reserves over the same period was 5.34%. The highest contribution to this enhancement has been from Eastern Offshore (12.26%), followed by Western Offshore (3.6%). It was found that CAGR (compound annual growth rate) for natural gas and electricity were 1.06% and 3.99% respectively and lignite coal showed the highest CAGR i.e. 4.33%. The reserved, production and consumption of natural gas are shown in Tables 1.1, 1.2 and 1.3.

Table 1.1 shows the total potential for renewable power generation in the country at present which is estimated as 147615 MW. This includes wind power potential of 102773

MW (69.7%), SHP (small-hydro power) potential of 19748 MW (13.37%), biomass power potential of 17,537 MW (11.87%) and 5000 MW (3.39%) from bagasse-based cogeneration in sugar mills. The total electricity production and consumption are shown in Tables1.2 and 1.3.

1.3 Global Energy Scenario

The World Energy Council (WEC) has developed two possible scenarios modelled by characteristics, which, from their own perspective, may completely envelope the large part of the world in 2050 - these are Jazz scenario and Symphony scenario. Although scenarios are imagined with music, they are completely different in nature. Jazz has a focus on energy equity with priority given to achieving individual access and affordability of energy through economic growth and Symphony has a focus on achieving environmental sustainability through internationally coordinated policies and practices [7]. The WEC primarily estimated the total primary energy supply (equivalent to consumption) which is bound to increase globally from 545 EJ in 2010 to 878 EJ in the Jazz scenario and 696 EJ in the Symphony scenario in 2050. From 1990 to 2010 - this is approximately half the time period covered in this scenario study – total global primary energy consumption rose by roughly 45%. Predictably, the global primary energy consumption will continue to phenomenally rise, but at much lower rate than in previous decades. Fig. 1.2 shows the production and consumption of coal, oil and natural gas from 2007 to 2014. The total production of coal has increased from 2007-08 to 2012-13 about 20.75% which happens to be quite high than from 2012-13 to 2013-14 (about 0.93%) (Fig. 1.2, a, b).

Similarly, the consumption of coal has increased from 2007-08 to 2012-13 about 14.49% and from 2012-2013 to 2013-14 to about 0.61% [7]. The total estimated production of crude oil in the world has increased from ~ 3950 MT in 2007-08 to about 4114.8 MT during 2012-13, and further increased to 4132.9 MT during 2013-14 (as shown in Fig. 1.2, c, d). During the same period, the production increased by 0.4% from 2012-13 to 2013-14. Distribution of total world production as per estimates showed that Saudi Arabia and Russian Federation were the first and second highest producers with 13.12% and 12.86% respectively. They were followed by USA (10.80%), China (5.04%), Canada (4.67%), Iran (4.02%), UAE (4.01), Kuwait (3.66), Mexico (3.43%) and Venezuela (3.27%). India accounted to only 1.02% of the world production. The total world production of natural gas increased from 2674.2 million tons oil equivalent (Mtoe) in 2007-08 to 3041.6 Mtoe in 2013-14. The production has increased by 0.8% from 2012-13 to 2013-14 (Fig. 1.2, e, f).

Distribution of production of natural gas over major regions showed that Europe & Eurasia (30.56%) and North America (26.88%) are the highest and the second highest producers, cumulatively accounting for 57.44% of the total world production [3].

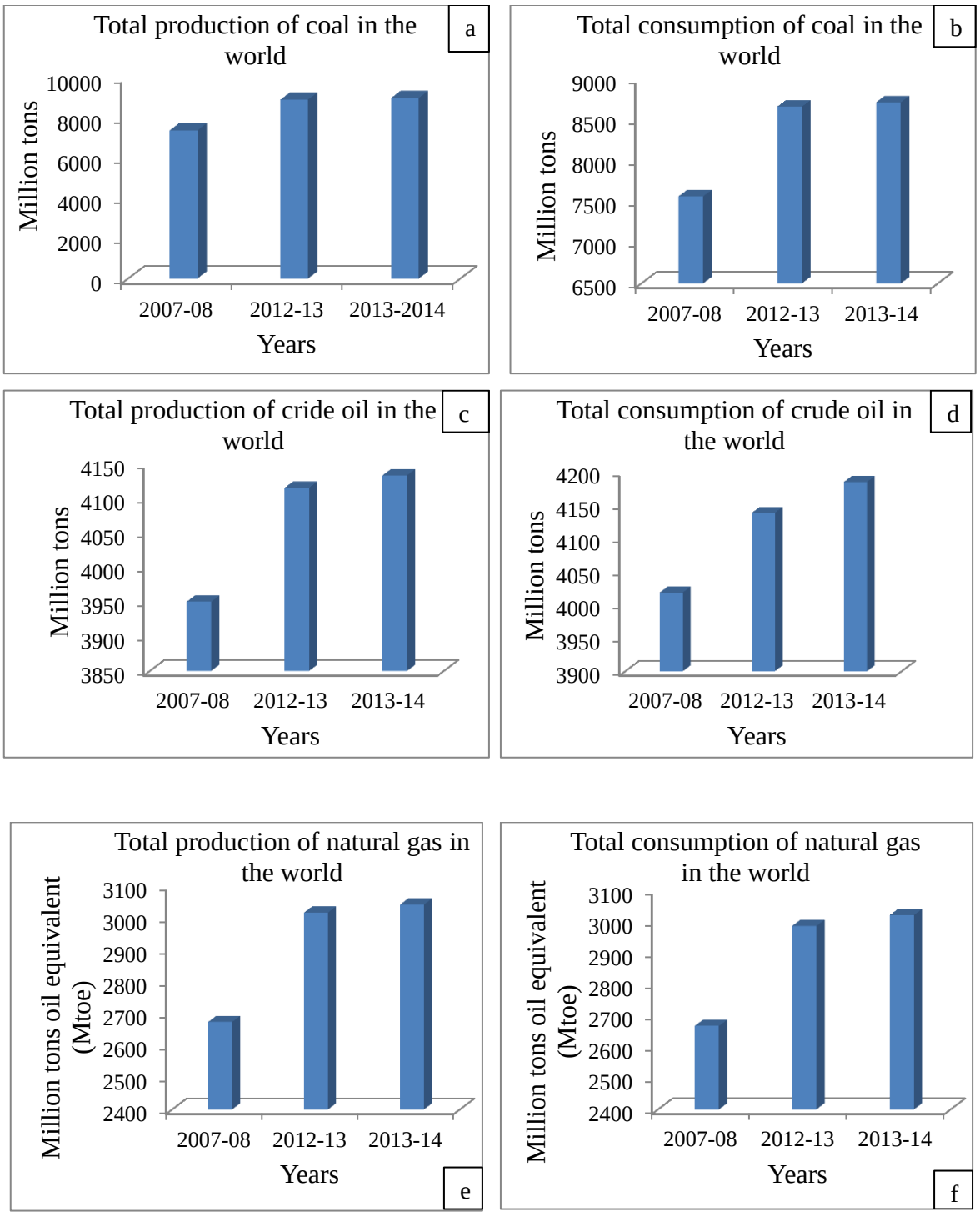

FIGURE 1.2: The production and consumption of coal, oil and natural gas in the world (a,b,c,d,e,f).

Apart from conventional sources of energy, biomass is the most bountifully available and is an advantageous renewable energy source over others energy sources. It can be used as a substitute for fossil fuels. The availability of biomass is that it is abundantly found in nature throughout the year anywhere in the world. Biomass consists of mostly organic matters with less inorganic matters. It is developed through photosynthesis process as indicated in the following reaction:

$$nCO_2 + nH_2O \xrightarrow{Sunlight+chlorophyll} (CH_2O)n + nO_2$$

There are different kinds of biomass available, especially classified from source of origin such as, aquatic biomass, marine biomass, agricultural residues, terrestrial biomass, and waste-land derived biomass. Some kinds of biomass are cultivated only for consumption purpose as animal or human feed. Hence, food vs. energy dilemma should not come into the picture and selection of proper biomass for energy application is a vital issue. The evaluation of particular type of biomass can be determined by physical and chemical properties of large molecules from which it is derived. However, since it takes millions of years to convert biomass into fossil fuels, these are not renewable within a time frame. Burning fossil fuels termed as ‘‘old’’ biomass and converts it into ‘‘new’’ CO_2 after burning of fossil fuel; which helps to produce the ‘‘greenhouse’’ effect and depletes a non-renewable resource.

1.4 Description of Thermochemical Process

Biomass is one of the most renewable sources of energy and it produces fewer amounts of greenhouse gases during thermochemical process. Conversion of biomass to energy can be considered generally through three pathways - thermochemical and biochemical or biological. Again, thermochemical process can be classified into three processes viz. combustion, gasification and pyrolysis, as shown in Fig. 1.3.

1.5 Combustion

Combustion is one of the most common phenomenon in thermochemical processes. Burning of biomass in the presence of air produces carbon dioxide, water and heat. The reaction is given below:

$$Biomass + O_2 = CO_2 + H_2O + heat$$

The heat produced during combustion of solid fuel is utilized for several purposes like mechanical power, or electricity, using various items of process equipment boilers, steam turbines, furnaces etc. Combustion characteristics are extremely important for the energy application and they depend on various other factors. Factors like moisture content, carbon content, hydrogen content, heating value, particle size, bulk density, extractive and ash fusion temperature are crucial factors for determining the combustion characteristics [8]. Generally, combustion of biomass or solid fuel generates hot gases temperatures around 700 - 1000°C. This temperature is quite enough to burn all kinds of biomass if the moisture content of biomass is less than 20% or if it is pre-dried. High moisture content biomass is more likely to be fruitful to use in biological conversion. The particle size of biomass should be around less than 0.6 cm in combustion.

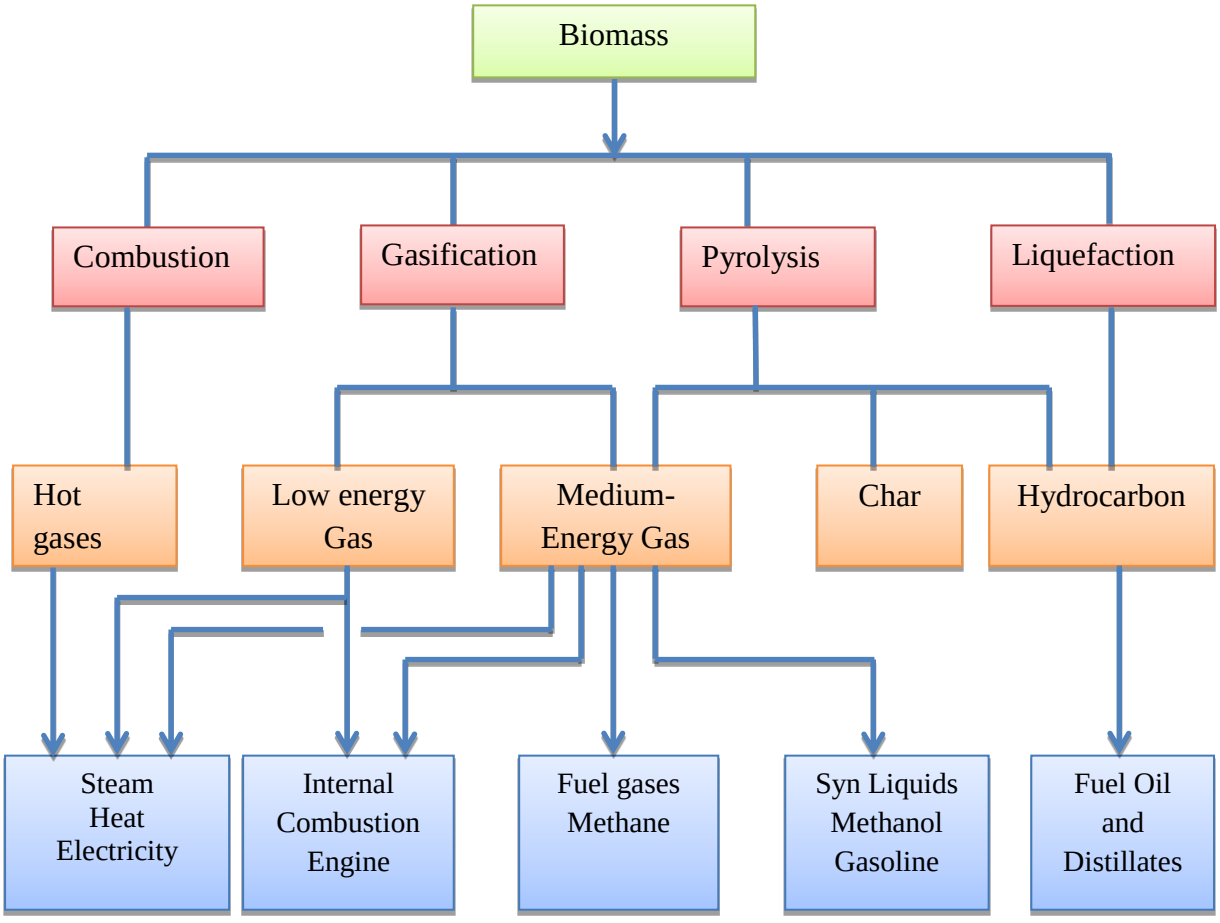

FIGURE 1.3: The thermochemical process, intermediate process and final energy output products from the conversion of biomass.

Ash content in biomass plays a significant role on heating value of biomass. Ash is generally contained with soluble and insoluble inorganic compounds. Soluble compounds assist to make catalytic effect on pyrolysis and combustion process, whereas insoluble compounds generally downgrade combustion efficiency like moisture does the same thing. High ash content in plant biomass makes it unfavourable as a solid fuel [9]. Ash content varies from biomass to biomass and generally terrestrial biomass contains less mineral matters (~ 1.5-20 wt. %) in comparison to marine biomass (~ 30 wt. %). Fuel analysis of biomass can be classified into two types, proximate and ultimate analysis. Fixed carbons in proximate analysis and carbon content in ultimate analysis are responsible for the heating value of biomass. In addition, biomass consists of biopolymers, namely hemicellulose, cellulose and lignin. The heating value of a biomass gradually increases with increasing lignin content [10]. The system efficiency could be improved by co-firing with coal; otherwise conversion of biomass combustion power plants lies between 25 – 45% [11].

1.6 Gasification

Gasification is very old technology and its use started in 1800 or more than 180 years. Initially, it was developed to produce town gas for cooking and lighting, later due to shortage of petroleum it was replaced by natural gas and electricity during World War II. During this period, wood gas generator was developed which was generally named as gasogene, was used to power motor vehicles in Europe. Trucks, buses and agricultural machineries were powered by gasification technology.

But now gasification technology stands much technologically upgraded and through designing and offers better efficiency and better sys-gas production. However, there are some technological issues related to maintenance, cleaning and associated heat loss.

Biomass gasification is defined as partial oxidation at elevated temperature, typically around 700 - 900°C in presence of air/steam/CO_2 or O_2. The process produces syn-gas i.e. carbon monoxide, hydrogen and methane – gases which are of low calorific value and used in boilers, dual-fuel engine etc. The gas is more versatile in relevance with solid biomass because it can be burnt to produce heat and steam or used in gas turbines to produce electricity. Due to shortage of fossil fuel across the world, renewable energy technologies like gasification technology came into market to meet the global energy demand. Based on feeding of biomass, gasifiers can be classified into counter-current (updraft) and co-counter

(downdraft) – both are fixed-bed type gasifier. Some other gasifier designs incorporating moving bed type such as circulating or bubbling or entrained fluidized bed are also available. One of the good techniques obtained is integrated gasification combined cycle (IGCC) useful for producing electricity from gas turbine and steam which contributes to higher conversion of efficiency.

The emission profile of syn-gas from biomass produces fewer pollutants and comparatively lower than that of emission from petrol or diesel or thermal power plants. So, syn-gas is much more environment-friendly than fossil fuel in terms of chemical compositions. The composition of syn-gas can be controlled by varying the process parameters and gasifying agents such as air-fuel ratio, temperature profile of the gasifier etc. as described below: carbon monoxide (15 – 30%), hydrogen (20 – 40%), methane (10 – 15%), carbon dioxide (15 – 20%), water vapour (7%) and nitrogen (1%) for oxygen blown gasifier [12]. But in case of air blown gasifier the composition of syn-gas is carbon monoxide (10 – 18%), hydrogen (15 – 25%), methane (4 – 10%), carbon dioxide (10 – 18%), water vapour (5 – 9%) and nitrogen (45 – 60%). For nitrogen blown gasifier, the higher heating value is around ~ 5 MJ/Nm^3 and for oxygen blown gasifier ~ 15 MJ/Nm^3.

1.7 Pyrolysis

Pyrolysis is a kind of thermochemical conversion process, similar to gasification, the difference being that pyrolysis occurs in absence of oxygen at temperatures of around 300 - 600°C depending on chemical composition of feedstock. The product yield is also different from gasification. The major components of gasification process is syn-gas, while in pyrolysis process three major products are generated viz. bio-char, bio-oil and syn-gas which are quantitatively less compared to the syn-gas produced in gasification. The products yield of pyrolysis process is dependent on some factors such as residence time, type of reactors used, particle size and process conditions. Accordingly, pyrolysis can be classified into slow, medium, fast and flash pyrolysis as shown in Table 1.4 and the products yield is also indicated. Depending upon the objective of usage, type of pyrolysis can be chosen in terms of getting the final products. Slow pyrolysis provides almost equal products of bio-oil, bio-char and gas. The gas is mainly consisting of hydrogen and carbon monoxide.

The chemistry behind the pyrolysis process is the thermal breakdown of cellulose and hemicellulose into smaller molecule like hydrogen, methane, carbon monoxide, etc. Lignin is not much degraded like cellulose and hemicellulose and is left over as char.

Apart from type of pyrolysis process, the physical and chemical properties do have effect on products yield. The calorific value of bio-oil lies in between 17 – 30 MJ/kg, while in case of bio-char, its value is around 18 – 26 MJ/kg.

TABLE 1.4: Different technologies in thermochemical process and estimated products yield and residence time.

Technology	Temperature (°C)	Residence time	Char (wt. %)	Liquid (wt. %)	Gas (wt. %)
Flash pyrolysis	~500	<1 sec	9	80	11
Fast pyrolysis	~500	~1 sec	12	75	13
Medium pyrolysis	~500	~10-20 sec	20	50	30
Slow pyrolysis	~500	~5-30 mints	35	30	35
Gasification	>750	~10-20 sec	10	5	85

1.8 Steam gasification

With increasing energy demand across the world, thermochemical conversion process has become very promising in terms of either gasification or pyrolysis or steam gasification. Thermochemical conversion process improves the energy quality of biomass or solid fuel and the versatility of fuel used as an end product. After pyrolysis of biomass, the left over is the char residue that can be used as solid fuel in gasification, combustion, fertilizer or activated carbon preparation. From the point of view of fuel quality, steam gasification provides better quality of fuel in terms of H_2/CO ratio as compared to other processes. The produced hydrogen can be used for different purposes. The steam gasification is a two

stepped process. The first step produces char, tar and volatile matters and the second step involves steam gasification of the char.

1.9 Conclusion

After studying the overview of energy scenario both in India and World, it was found that the most difficult situation will come in near future as an energy crisis all over the world. Renewable energy sources will become an important factor during this crisis time in near future. Nonetheless, researchers or scientists are vigorously working on renewable energy in order towards sustainability. Solar energy is now widely used renewable energy followed by bioenergy and wind energy around the globe. But, still the efficient way of utilization of energy from different technologies is an area of concern. In this background, thermochemical conversion processes of biomass e.g. gasification, pyrolysis and steam gasification plays a vital role regarding harnessing energy from biomass efficiently.

References:

1. Suman Dey's Ph.D Thesis. Some studies on the gasification of hydrocarbon based materials. School of Energy Studies, Jadavpur University, Kolkata - 70032.

2. http://powermin.nic.in/. Ministry of power, Government of India.

3. www.petroleum.nic.in. Shastri Bhavan, New Delhi - 110 001, India.

4. Central Statistics office, National Statistical Organization, Ministry of statistics and programme implementation, Government of India. www.mospi.gov.in.

5. Dieter Leckel, (2009), Diesel Production from Fischer-Tropsch: The Past, the Present, and New Concepts, Energy & Fuels, 23, 2342–2358.

6. https://www.cia.gov/library/publications/the-world-factbook.

7. www.worldenergy.org.World Energy Scenarios: Composing energy futures to 2050, World Energy Council, Copyright © 2013 World Energy Council.

8. Ayhan Demirbas, (2005), Potential applications of renewable energy sources, biomass combustion problems in boiler power systems and combustion related environmental issues, Progress in Energy and Combustion Science, 31, 171–192.

9. A. Demirbas¸ (2002), Relationships between heating value and lignin, moisture, ash and extractive contents of biomass fuels, Energy Exploration & Exploitation, 20, 105–11.

10. A. Demirbas, (2003), Relationships between lignin contents and fixed carbons of biomass samples, Energy Conversion Management, 44,1481–6.

11. Peter McKendry, (2002), Energy production from biomass (part 2): conversion technologies, Bioresource Technology, 83, 47–54.

12. A. Demirbas, (2004), The importance of biomass, Energy Sources, 26, 361–6.

CHAPTER – 2

Review of Earlier Research Works in the Relevant Field

2.1 Literature review – I; Biomass for thermochemical conversion process

2.1.1 Introduction

Lignocellulosic biomasses are organic material and have certain definite calorific value, and are considered renewable energy sources. These biomass can be utilised for both heat and electricity generation in the future. Apart from organic matter, inorganic matter is also found in plants in the form of ions, salts and inorganic species bound to organic species. Biomass can be classified as woody type, shrub type, grass type, herb type, and marine algae including both microalgae and macroalgae. The most important thing for biomass conversion into liquid or gaseous fuel is its bulk and inconvenient in nature. There is a significant difference of biomass handling as they cannot be stored or transported like gas or liquid fuel. So naturally biomass conversion into gas or liquid fuel is quintessential. The energy conversion processes involved in biomass are, (1) biochemical conversion, (2) thermochemical conversion. These conversions are further classified and particulars are shown in Fig. 2.1.1. Biochemical conversion is probably discovered in ancient times than thermochemical processes such as gasification or pyrolysis. Some countries like India and China generated methane gas for domestic purposes by anaerobic microbial digestion of animal wastes such as cow-dung, etc.

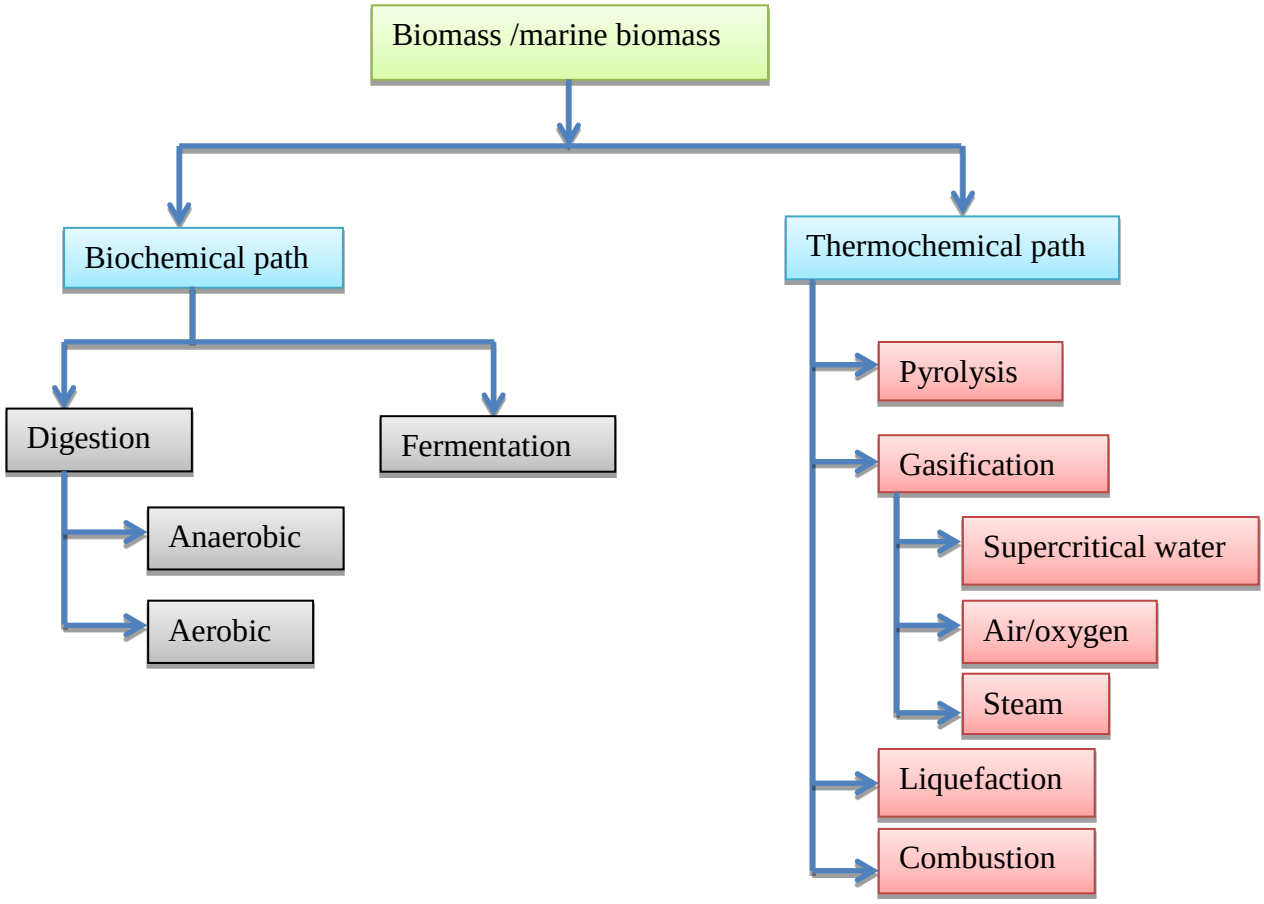

FIGURE 2.1.1: Different path ways for conversion of biomass/marine algae into fuel, gases or valuable chemicals.

In the recent times, fermentation technology has gained popularity for the production of bioethanol to be mostly used in automobile industry. While, for thermochemical conversion of biomass, syn-gas is produced this appeared later than earlier. Fig. 2.1.1 shows different forms of thermochemical routes such as pyrolysis, gasification, liquefaction, and combustion. The definition of pyrolysis, gasification, and steam gasification is briefly described in general introduction.

Fig. 2.1.2 shows the typical example of a biochemical process for the production of bioethanol from lignocellulosic biomass. The comparison between thermochemical and biochemical process shows biochemical process has gained more commercial acceptability than the previous one. According to the NREL reports, some analysts and process engineers made a huge contribution in 2009 – 2010 to update the 2002 design report of Aden et al. [1, 2] that described the biochemical conversion of lignocellulosic biomass such as corn stover to bioethanol production. According to J. R. Mielenz's reports all

automobile manufacturers produce vehicle that can readily consume 10% ethanol or 85% ethanol (E85) blends for fuel and ethanol can replace fossil fuel diesel in heavy vehicles as well [3]. Similar experiment was carried out by D.C. Rakopoulos and his co-workers at 5% and 10% (by vol.) ethanol blended with conventional diesel and its performance characteristics were evaluated [4].

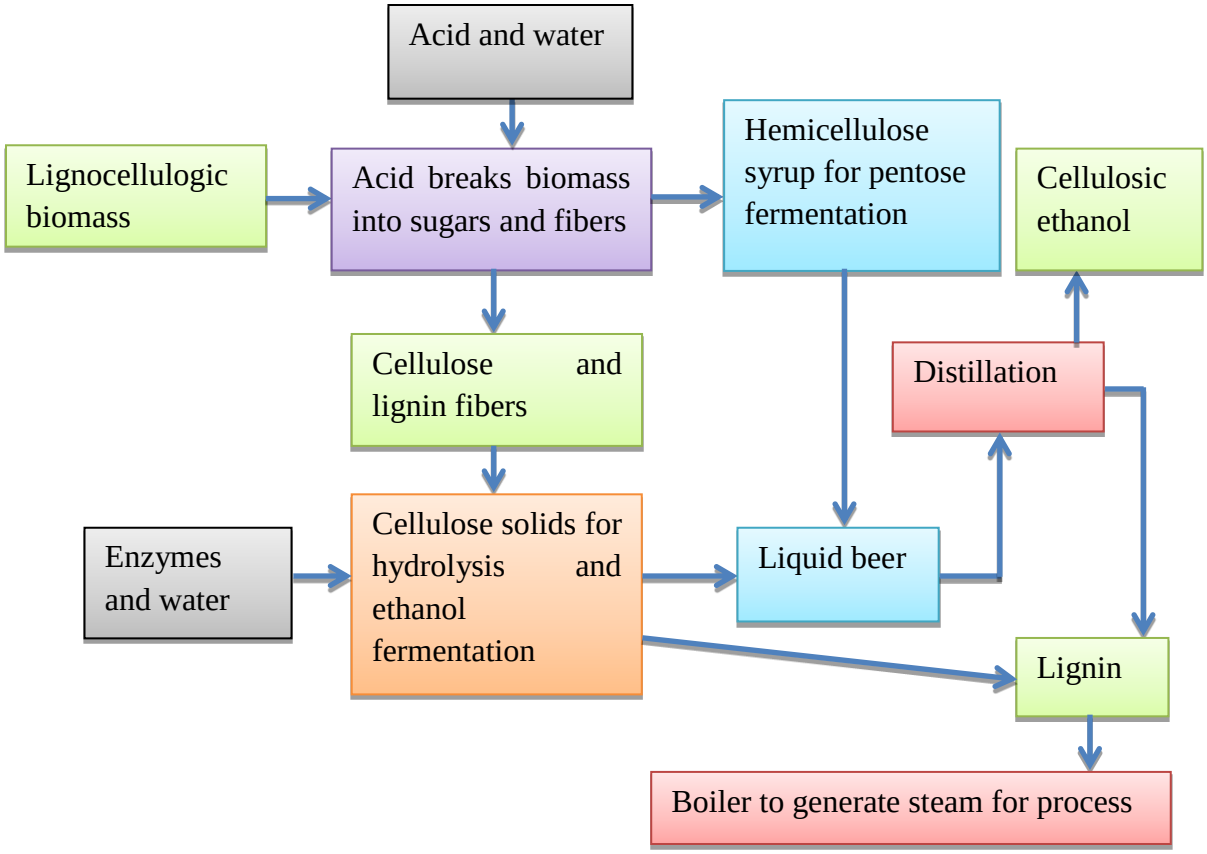

FIGURE 2.1.2: Typical example of biochemical conversion for the production of ethanol from biomass.

Other thermochemical conversion such as hydrothermal liquefaction (HTL) is a thermal depolymerisation process at certain temperature and pressure used to convert wet biomass into crude-like oil which is aptly referred as bio-oil. HTL method is mostly suitable with wet biomass such as marine algae as it is cultivated in seawater or other places. Some earlier research work about HTL is briefly described here, especially for marine algae. One such research work was investigated by F. Safari and his team [5] on the hydrothermal gasification of *Cladophora glomerata*, a macroalgae found in the southern coast of the Caspian Sea in a tubular batch reactor system. D. Zhou et al. investigated hydrothermal

liquefaction of macroalgae Enteromorpha prolifera to bio-oil at different temperatures in the presence of catalyst Na_2CO_3 [6].

M. J. Fernandez Llorente and his team [7] studied the concentration of elements in woody and herbaceous biomass as an ashing temperature depending function. Again, M. J. Fernandez Llorente et al. [8] investigated about the ash behaviour of lignocellulosic biomass such as woody type biomass poplar, and a herbaceous biomass, *Brassica carinata* in a bubbling fluidized bed combustion pilot plant (1 MWth) with silica as the bed material. M. J. Serapiglia et al. [9] investigated the variability in pyrolysis product yield from shrub willow genotypes by fast pyrolysis process and they established that the fast and flash pyrolysis is popular for its higher outputs. Fast pyrolysis is today more attractive thermochemical conversion route for the production of biofuels, as this biofuel is seamlessly compatible with the petroleum products. Some wasteland derived energy crops, like perennial grasses and short rotation woody crop, are the best feedstocks in fast pyrolysis. It was noticed that the shrub willow recently cultivated for high yield was evaluated for higher pyrolysis product yield using py-GC/MS. Jiele Xu et al. [10] did extensive research on Bermuda grass for the production of biofuel, especially bioethanol. Numerous experiments of chemical, physico-chemical, and biological pretreatment methods have been adopted to enhance the digestibility of Bermuda grass along with some other feedstocks such as Switchgrass, Corn stover, Wheat straw, Cotton stalk, and Rye straw and their compositions were listed in the literature (11 – 16).

B. Gabrielle et al. [17] pointed out that due to the paucity of conventional fossil fuel, renewable energy could meet the future policy targets for bioenergy improvement across the world facing major challenges for biomass supply chains in terms of competitiveness, reliability and sustainability. Evidently, the obtained bio-oil's physical and chemical characteristics are co-existing or compatible with the conventional fuels. The conversion of marine algae to biofuels by thermochemical routes pyrolysis, liquefaction, and gasification are excellent technology for this purpose [18].

Hernando Guerrero et al. had evinced their interest to produce more green chemicals from the renewable sources i.e. biomass rather than fossil sources [19]. Mariefel B. Valenzuela et al. had reported for the first time that the production of H_2 from actual biomass under aqueous-phase reforming by Pt/Al_2O_3 catalyst. The process was consisting of first acid

hydrolysis of biomass to pulverize into the smaller soluble molecules and these species are reformed by the above catalyst [20].

The thermochemical conversion is best explained by the kinetic study through thermogravimetric analysis (TGA). Numerous research activities were carried out for better justification of the thermochemical conversion process such as pyrolysis as well as gasification. One such experiment - pyrolysis of cellulose and global kinetics - was investigated at high heating rates (10^4 K/s) [21]. T. Sonobe et al. had reported the pyrolysis behaviour of several agricultural residues by TGA. The evolving rates of gaseous species such as CO_2, H_2, CH_4, CO, and H_2O were also measured by TG-MS. The most interesting aspect of this work is that without any assumption and mathematical fitting, they obtained the good kinetic parameters from the distributed activation energy model [22]. Haiping Yang et al. had studied in depth about the biomass pyrolysis based on three major components, hemicellulose, cellulose, and lignin [23].

2.2 Literature review – II; Review of earlier research work in gasification

2.2.1 Introduction

Gasification is a thermochemical conversion of biomass carried out at high temperature by partial oxidation process which produced syn-gas i.e. CO, H_2, and CH_4. [24].

In this chapter, review of earlier research work has been restricted to the area of gasification, pyrolysis and steam gasification. The following topics have been covered in gasification:

(a) Gasification technology and process

(b) Different kind of gasifiers

(c) Chemical reactions

(d) Gas cleaning and filtration systems

(e) Effect of mineral matters

2.2.2 An overview of gasification technology

Gasification technology is generally considered as ancient one. In 1846, Dr. Abraham Gesner, a native of Nova Scotia, Canada, discovered a methodology for extracting lighting

oil from solid fuels using pyrolysis technique. He named it as oil kerosene (it is a Greek word for wax and oil). In 1849, he developed a methodology for extracting kerosene from oil [25]. The last few decades have witnessed the successful emergence in gasification technology, especially in the area of conversion efficiency i.e. energy conversion efficiency, carbon conversion efficiency, cost effectiveness, high cold gas efficiencies, gas cleaning system and low harmful emissions. In a gasification system, the produced syn-gas can directly be used in duel-fuel engine for electric generation or for direct heating purpose.

Gasifier is a simple device constituting a set of gas filtration and cooling system attached with cylindrical reactor mainly made of either concrete or stainless steel or firebricks or any other material having resistance upto or more than 1000°C. The design of a gasifier depends on factors such as basic material and its fuel characteristics. Generally low calorific value and high ash content biomasses are more potent in fluidized bed or circulation bed gasifier than others.

2.2.3 Fundamentals of gasification technology

Gasification is primarily thermo-chemical conversion of organic materials at elevated temperature with partial oxidation process and is a complicated process due to the several reactions occurring concurrently. In a typical downdraft gasifier, the following physicochemical processes take place at temperatures indicated below (in Fig. 2.2.1):

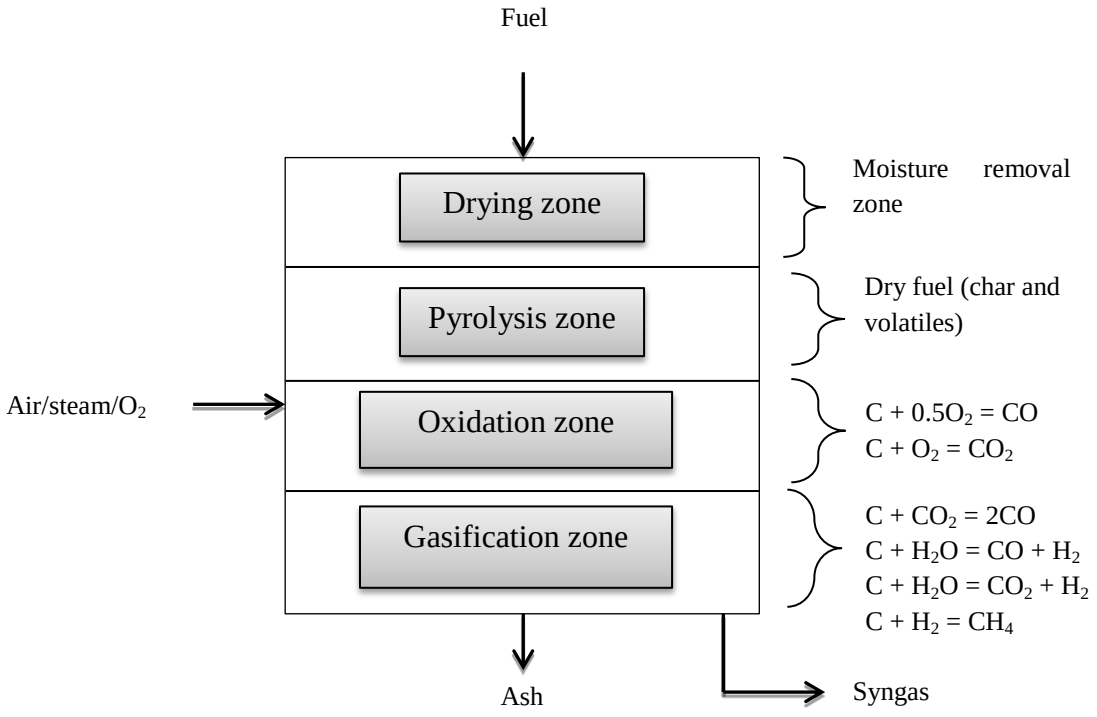

FIGURE 2.2.1: Different stages of gasification in a downdraft gasifier.

1. Drying (<150°C).

During initial phase of biomass drying at low temperature less than 150°C, unbound moisture and some amount of bound moisture are released. Bound moisture is directly attached with molecule which is very difficult to extract as it might form covalent bond with it.

2. Pyrolysis or devolatilization (150-600°C).

Pyrolysis or devolatilization is a thermochemical conversion of biomass converted into liquid, syn-gas and solid residue in absence of air at elevated temperature. Pyrolysis is influenced by temperature. The initial phase of exothermic dehydration of temperature is around 100 – 250°C which produces water vapour along with low molecular gases like CO and CO_2. Beyond this temperature around 250 - 550°C, pyrolysis of biomass produces vapour like liquid i.e. bio-oil. The breakdown of large molecule is mainly from cellulose and hemicellulose which is decomposed into condensable gases, non-condensable gases and bio-char. Lignin is not much degraded and sometimes it is the left over residue as bio-char. After temperature of around 300 - 850°C, the secondary reaction takes place by cracking of volatiles or tars into char and non-condensable gases. The chemistry of pyrolysis is a complex one as numerous reactions take place simultaneously. Generally, kinetics of pyrolysis is well described by overall reaction mechanism instead of first or second order reactions. If residence time is further increased, relatively large molecules break into char and gases at higher temperature. If condensable gases are removed quickly from the reactor, they quench quickly outside in the downstream process in a reactor and are converted to bio-oil or tar.

3. Oxidation (500-1500°C).

Fig. 2.2.1 describes vividly the gasification process and its different stages of a typical downdraft gasifier. In a typical downdraft gasifier air, oxygen or steam passed through the middle section of gasifier into the highly exothermic combustion zone in the presence of excess air/oxygen. The released energy heats the downward moving gas after passing through pyrolysis zone.

4. Reduction (800-1100°C).

The hot gas, a mixture of CO_2, CO and steam move after passing through pyrolysis zone towards reduction zone, where char from the upper bed is gasified. Initially, the concentration of carbon dioxide in combustion zone abruptly increase and then the

concentration of oxygen decrease letting the carbon dioxide enter the reduction zone where gasification reaction takes place with char, resulting as syn-gas. The design of a gasifier is highly influenced by the process parameters such as temperature, air-fuel ratio and fuel characteristic, etc.

2.2.4 Chemistry of gasification process

No chemical reaction occurs in the drying zone due to the moisture removed at low temperature. However, the higher temperature in the pyrolysis zone causes the biomass to degrade. The thermal conversion process for pyrolysis can be delineated as follows.

$$\text{Biomass} + \text{Heat} \rightarrow \text{Char (C)} + \text{Volatiles (CO, } CO_2\text{, } H_2\text{, } H_2O\text{, } CH_4\text{)} + \text{Tar vapour} \quad (2.2.1)$$

The main reaction to occur in the combustion zone is oxidation of char, in which oxygen reacts with char to produce carbon dioxide and water vapour. Other than this, the oxidation of volatiles also takes place. These reactions can be represented by,

$$C + O_2 \leftrightarrow CO_2 - 394 \text{ kJ/mol} \quad (2.2.2)$$

$$CO + 1/2O_2 \rightarrow CO_2 - 284 \text{ kJ/mol} \quad (2.2.3)$$

$$CH_4 + 2O_2 \leftrightarrow CO_2 + 2H_2O - 803 \text{ kJ/mol} \quad (2.2.4)$$

$$H_2 + 1/2O_2 \rightarrow H_2O - 242 \text{ kJ/mol} \quad (2.2.5)$$

Besides the main char-carbon dioxide and char-water vapour reactions, hydrogasification and water-gas shift reactions also occur in the gasification zone or reduction zone.
They can be written as follows.

$$C + CO_2 \leftrightarrow 2CO + 172 \text{ kJ/mol} \quad \text{(Bouduoard reaction)} \quad (2.2.6)$$

$$C + H_2O \leftrightarrow CO + H_2 + 131 \text{ kJ/mol} \quad \text{(Water-gas reaction)} \quad (2.2.7)$$

$$C + 2H_2 \leftrightarrow CH_4 - 74.8 \text{ kJ/mol} \quad \text{(Hydrogasification reaction)} \quad (2.2.8)$$

$$CO + H_2O \leftrightarrow CO_2 + H_2 - 41.1 \text{ kJ/mol} \quad \text{(Water-gas shift reaction)} \quad (2.2.9)$$

The typical product gas yield has been mentioned earlier in both air blown and oxygen blown gasifier in chapter 1. Investigations have been carried out during the last couple of

decades on catalytic gasification of biomass or coal. There are certain advantages of catalytic gasification over normal gasification:

(1) Tar cracking using catalyst is beneficial to improve the quality of gas, especially in downstream application. As tar is a sticky in nature, cleaning is a major problem after few experiments.

(2) The development of catalytic gasification is simply acting as a driven force for tar reforming by reducing methane content and is simultaneously increasing syn-gas i.e. CO and H_2.

The reaction mechanism of catalytic gasification based on heterogeneous reaction can be written as:

$$C_nH_m + nCO_2 \xrightarrow{Catalyst} 2nCO + (m/2)H_2 \quad (2.2.10)$$

$$C_nH_m + nH_2O \xrightarrow{Catalyst} (n + m/2)H_2 + nCO \quad (2.2.11)$$

Catalytic gasification increases the amount of gas by tar reforming as well as increases the calorific value of gas. Apart from this, there is an option for tar removal that is thermal cracking, but it requires very high temperature more than 1000°C which is not economical. Another important thing is that the catalytic gasification is generally carried out for removal of methane from product gas by catalytic steam reforming or catalytic carbon dioxide reforming. So, in the case of steam reforming, methane reacts with steam at 700°C to 1000°C in this temperature range [26]. The reaction can be written as:

$$CH_4 + H_2O \xrightarrow{Catalyst} CO + 3H_2 + 206\ kj/mol \quad (2.2.12)$$

This reaction is most common for the production of carbon monoxide and hydrogen, nickel-based catalysts and CaO are most suitable in this case.

The carbon dioxide reforming of methane is not that much cost effective or economical as steam reforming of methane. Despite this problem it has attractive advantageous over steam reforming of methane as the two greenhouse gas i.e. CO_2 and CH_4 mitigate environmental related problem and the reaction is highly endothermic as follows:

$$CH_4 + CO_2 \xrightarrow{Catalyst} 2CO + 2H_2 + 247\ kj/mol \quad (2.2.13)$$

Nickel-based reaction is also effective for above reaction like earlier reaction [27, 28].

2.2.5 Mass and Energy balance

Mass and energy balance is an important parameter for gasification process as thorough knowledge and fundamentals are required to make a scaled up gasifier. Fig. 2.2.2 shows typical diagram of material balance of a gasifier.

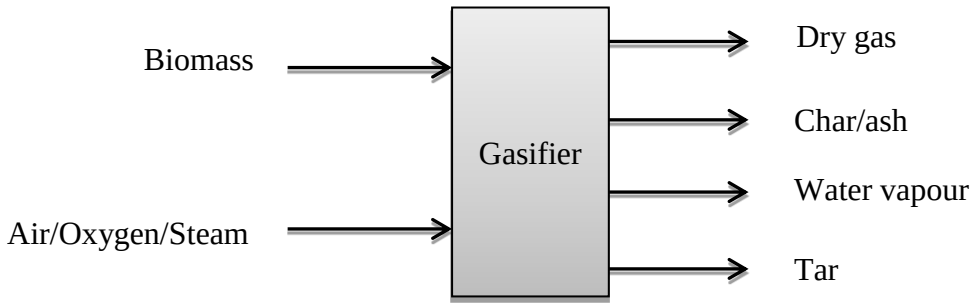

FIGURE 2.2.2: Typical diagram of material balance for gasifier.

As we know, one of the major drawbacks in any gasifier is it does not produce 100% conversion of biomass into ash. Some unburnt parts of biomass are still stuck with ash. So, it is a mixture of char and ash. Some earlier data from literature was listed in the article [29].

K. Patil et al. carried out mass and energy balance based on the input and output data in literature. They found mass balance varying between 82 – 91%, while in case of energy balance it varied between 71 – 81%. The most difficult problem is to obtain data of tar contents, outgoing moisture content and solid residue by practical ways [30].

2.2.6 Conversion efficiency

In thermochemical conversion process, conversion efficiency is bifurcated as the one carbon conversion or carbon conversion efficiency and the other efficiency of gasifier which implies the energy content in primary fuel to the energy content in secondary fuel that is syn-gas. Carbon conversion and carbon conversion efficiency are defined as follows: moles of carbon from parental biomass or bio-char and moles of carbon converted into syn-gas. They are calculated as [31]:

$$\textit{Carbon conversion (\%)} = [1 - \frac{moc_o}{moc_i}] \times 100 \qquad (2.2.14)$$

Carbon conversion efficiency (%) = $[(\sum n_i \,.V)/moc_i] \times 100$ (2.2.15)

The abbreviation of these equations represent as, moc = mass of carbon and subscripts 'o' and 'i' represents decayed molecules and initial molecules, respectively. n_i is the moles of carbon in component 'i' and *V* is the total volume of the gas. Overall efficiency of the gasifier is described as below:

Efficiency = $\frac{output\ energy}{input\ energy} \times 100$ (2.2.16)

The typical downdraft gasifier has efficiency around 60 – 70% excluding electrical efficiency. The average electrical efficiency via gasification process is around 15 – 30% as reported by earlier research work [32, 33]. The heat loss can be minimized by properly insulating associated parts of gasifier and cleaning the tar at regular intervals. By this way efficiency can also be improved.

2.2.7 Gasification efficiency

Gasifier efficiency is highly influenced by the quality and quantity of gas produced. Generally, conversion into gaseous product from solid fuel through gasification should be more efficient in order to get better efficiency. Gasification efficiency is classified into cold gas efficiency, hot gas efficiency and net gas efficiency as described below:

2.2.8 Cold-gas efficiency and hot-gas efficiency

Cold-gas efficiency defined as the energy input over the energy output. Suppose, M_b is the mass of solid fuel or biomass in kg gasified to produce M_s kg of product syngas with a LHV of Q_s, then efficiency is calculated as:

$$\eta_{cge} = \frac{Q_s M_s}{LHV_b M_b} \quad (2.2.17)$$

Where, η_{cge} is the cold-gas efficiency, LHV_b is the lower heating value of the solid fuel.

Hot-gas efficiency is almost similar to cold-gas efficiency in addition considering sensible heat. Some special cases like IGCC (integrated gasifier combined cycle), furnace or boiler gas is burnt as a continuous process for large scale. So, the hot-gas efficiency is computed as:

$$\eta_{hge} = \frac{Q_s M_s + M_s C_p (T_f - T_i)}{LHV_b M_b} \quad (2.2.18)$$

Where, η_{hge} is the hot-gas efficiency, T_f and T_i are the temperature of exit point of gasifier or burner and entrance temperature of gasifier of feed material, respectively.

2.2.9 Influence of fuel properties and type of material used on gasification

A wide range of biomass fuels such as wood, charcoal, wood wastes (branches, twigs, roots, bark, wood shavings and saw dust etc.) as well as multitude of agricultural residues (maize cobs, coconut shells, cereal straws, rice husks etc.) and peat and marine biomass both in macroalgae and microalgae (only selective marine biomass) and municipal solid waste (MSW) can also be used as fuel for biomass gasification. Each biomass has unique properties based on the source of origin as earlier mentioned and is dependent on physiochemical properties of biomass which is extremely important while choosing the type of gasifier. For ligno-cellulosic biomass more than 90% constitutes organic material that assists extremely well in gasifier for continuous operation and the moisture content of this kind of biomass is quite low around 5 – 20% on dry basis which is ideal for gasification. Marine biomass contains large fraction of ash or mineral contents difficult to operate in gasifier, however some special type of gasifier can help continuous operation.
Numerous research works investigated incineration of MSW and it is a proven technology. Industrialized nations have the basic problem with the waste management by MSW. Landfill is an option for waste disposal, but not so much popular over incineration as it creates some issues. Again, recycling or reuse of MSW is not much ideal over incineration [34]. Unlike fossil-fuel-fired power plant, incineration power plant exhibits extremely low energy efficiencies (12 – 25%) due to lower steam temperature. Also fouling or slagging problems cause an insulating effect for heat transfer. In addition higher emission of greenhouse gases per kWh converted energy is produced [35]. Pyrolysis and gasification are indeed promising technologies to tackle the above challenges in better way. These two technologies can avoid and reduce corrosion and emission by retaining alkali metals and heavy metals, sulphur, chlorine, etc. within the process residue, and other hazardous gases such as NO_x, metallic oxide vapour, etc. can be prevented [36]. Forest or agricultural residues are ligno--cellulosic biomass constituting more than 80% organic matters that are cellulose, hemicellulose and lignin and rest is moisture and ash content. Some forest or agricultural residues cause clinker or slag inside the reactor due to presence of mineral

contents such as K, Na, Si, S, Cl, P, Ca, Mg etc. [37]. So, selection of gasifier is a crucial factor depending on types of material being used. The most important factors playing on the optimum result encompasses the energy content, moisture content, volatile matter content, ash content and ash chemical composition, reactivity, size and size distribution, bulk density and charring properties of the starting biomass. Before choosing a gasifier for any individual fuel purpose, it is vital to ensure that the fuel meets the requirements of the gasifier or it can be treated to meet these requirements. Practical tests are needed if the fuel has not previously been successfully gasified.

In this section, the most important properties of fuel that influence the gasification are described elaborately.

2.2.9.1 Moisture content in biomass

Moisture content in biomass is an inherent characteristic. During the growth of biomass water is absorbed by different parts of plant by capillary mechanism through root. That is why the source of origin of each biomass is highly influenced by surrounding environment. Generally, moisture content in biomass is in two forms: (1) unbound or free moisture and, (2) bound moisture or inherent moisture. Free or unbound moisture resides on outer cell walls, whereas bound or inherent moisture is absorbed within the cell walls.

High moisture content in biomass is influenced on gasification or pyrolysis process especially on gasification efficiency. Generally, gasification efficiency is reduced as surplus moisture takes energy from the system. For example, M_w kg of wet biomass becomes M_d kg of dried biomass after drying and it is expressed as:

$$M_d = \frac{M_w - M_d}{M_d} \times 100 \tag{2.2.19}$$

Whereas, the moisture content on a wet basis is defined as:

$$M_w = \frac{M_w - M_d}{M_w} \times 100 \tag{2.2.20}$$

2.2.9.2 Energy content in biomass

The choice of a fuel for gasification will be partly decided by its heating value either lower (LHV) or higher heating value (HHV). Fuel with higher energy content is always better for gasification. Energy content of fuel is obtained in an adiabatic, constant volume bomb

calorimeter. The bomb calorimeter determines higher heating value of the fuel. It includes the heat of condensation from water formed in the combustion of fuel.

The amount of inert material that is ash content and moisture content in biomass is a crucial factor in determining the calorific value of fuel. The different test conditions of two wood species, known as Red Lauan (RL) and White Lauan (WL) were reported by His et al [38]. The most interesting observation was that the higher heating value decreases with increasing moisture content.

HHV defined as the amount of heat released when unit mass or volume (initially 25°C) is combusted in oxygen atmosphere and products returned at initial temperature i.e. 25°C. It includes the latent heat of vaporization of moisture and it is also called as GCV (gross calorific value). LHV is also defined as the amount of heat released by fully combusting a specified quantity devoid of the heat of vaporization of moisture in the combustion products and it is called as NCV (net calorific value).

The relationship among the HHV, LHV and moisture is as following:

$$LHV = HHV - h_l\left(\frac{9H}{100} - \frac{M}{100}\right) \quad (2.2.21)$$

Where h_l is the latent heat of steam in kCal/kg, H and M are the hydrogen content and moisture content, respectively.

2.2.9.3 Volatile matter in biomass

Volatile matter of a fuel has two parts, condensable and non-condensable vapour released when the fuel is heated. The amount of these two parts depends on the rate of heating and the temperature of heating. Volatile matter has several significant effects on physiochemical properties of biomass. If the biomass contains high volatile matter, oil yield during pyrolysis, might increase due to high condensable gases condensed as liquid oil. The ignition temperature is also lower for high volatile matter content biomass that might be helpful during combustion or pyrolysis or gasification. The yield of volatile matter is highly influenced by the rate of heating. If the rate of heating is increased, the products yield increased proportionately. Some data in this regard find mention in their literature [24, 39 – 42].

2.2.9.4 Ash content in biomass

Ash content in biomass is generally inorganic solid residue left after the biomass or solid fuel is burnt out completely. Its primary constituents are silica, sodium, potassium, aluminium, iron, calcium, magnesium sulphur and phosphorous oxides etc. In thermochemical processes these inorganic matters such as alkali metals (Na, K) or halides (Si, Cl, S) or alkaline earth metals (Ca, Mg) can create problems to the reacting vessels. These components can cause serious problems leading to form slagging or fouling or corrosion and agglomeration [43, 44]. So, naturally high ash content biomass is not the right choice for gasifiers.

2.2.9.5 Fixed carbon in biomass

Fixed carbon is the organic residue left after removal of moisture, volatile matter and ash content from biomass or solid residue. It is determined by the following equation as follows:

$$FC = (100 - M - VM - ASH) \quad (2.2.22)$$

The subscripts are *FC, M, VM,* and *ASH* stand for fixed-carbon, moisture, volatile matter and ash, respectively. In thermochemical conversion, fixed carbon is an important factor.

2.2.10 Ultimate analysis of biomass

Ultimate analysis is the individual chemical species present in biomass except for its moisture, *M*, and inorganic constituents. It is expressed as the following,

$$C + H + O + N + S + ASH + M = 100\% \quad (2.2.23)$$

In the above expression C stands for carbon, similarly H, hydrogen, O, oxygen, N, nitrogen, and S, sulphur in weight percentage in the fuel. It was found that not all the fuels contain all of above elements. For example, sulphur is hardly present in the biomass except some selected biomass. Again, the moisture content in biomass is expressed individually as *M*. Hence, hydrogen or oxygen in ultimate analysis does not hold any hydrogen and oxygen in the moisture, only the hydrogen and oxygen are present in the organic components of the biomass or fuel. The significance of atomic ratios of (H/C) and (O/C) determined from ultimate analysis help to understand the fuel value of a solid fuel. The van Krevelene diagram interprets it more promising way [45]. When the (O/C) ratio increases,

it means the effective heating value is reduced and vice-versa. Again, when the hydrogen-to-carbon ratio increases, the effective heating value of the fuel also decreases.

2.2.11 Reactivity of biomass or Bio-char

Reactivity of solid fuel is defined as the value of reaction rate under the following conditions, temperature, pressure and gasifying agent. The exact value of reactivity of solid fuel or bio-char is valuable to design a gasifier model. Keigo Matsumoto et al. studied gasification reaction kinetics on bio-char obtained as a by-product of gasification in an entrained-flow gasifier with steam and oxygen at 900 - 1000°C in four different bio-char, named Japanese cedar char, Japanese cedar bark char, a mixture of hardwood char, and Japanese lawn grass char. Final results showed that the random pore model was best in the bio-char gasification reaction due to constant particle size, surface porosity, specific surface area profile and gasification rate were obtained from Arrhenius expression. And the reaction order was found in the order of - a mixture of hardwood > cedar char > (cadar bark char, lawngrass char) [46]. F. Marquez-Montesinos et al. elaborated on CO_2 and steam gasification of grapefruit skin char and the specific reactivity of char evaluated from the weight loss curve by the following equation:

$$r = \frac{1}{w}\frac{dw}{dt} \tag{2.2.24}$$

Whereas, r is the specific reactivity (min^{-1}), w being remaining sample weight (dry basis) at each time obtained from thermogravimetric analysis (TGA). [47].

2.2.12 Particle size and size distribution

In thermochemical process particle size and its distribution is important especially in fluidized bed or circulating bed gasifier that influences the pressure drop and power. The characteristics of particle size were determined by some physical factors such as volume diameter, surface diameter, sieve size, surface-volume diameter, and sphericity. Geldart D. had vast experience in the field of fluidization, based on this knowledge solid particles were classified into four groups, A, B, C, D and their distinguished features are listed in the article [48, 49]. They described group C particles to be very fine, smaller than 20 μm if the bulk density is constant (2500 kg/m^3). Due to inter-particle forces, the particles are very difficult to fluidize. To avoid this problem channelling might be one of the best options or otherwise some special techniques are required in order to prevent the problem. Group A particle is little coarser than group C and has an excellent property to fluidize freely, but

expands a bit after exceeding minimum fluidization velocity. These particles are best suitable for circulating fluidized bed gasifier. Group B particles fluidize very well and start bubbling after crossing minimum fluidization. These categories can be used in almost every fluidized bed or boilers, etc. Finally, group D particles are coarser than other classified particle. To fluidize these particles require a much higher velocity is mostly suitable in spouted or some bubbling fluidized bed or boilers [49].

2.2.13 Bulk density of biomass

Bulk density is one of the important properties of biomass which can influence product yield of syn-gas, gasifier efficiency and carbon conversion efficiency. It is defined as the overall space occupied by biomass or solid particles and its governing equation as follows:

$$\rho_b = \frac{Total\ mass\ of\ biomass\ or\ solid\ particle}{Bulk\ volume\ occopied\ by\ biomass\ or\ solid\ particle} \quad (2.2.25)$$

2.2.14 Effect of mineral matter

The mineral matters in different biomass are present in various amounts. Mineral content is pre-eminently influenced by source of origin. Generally, terrestrial biomass contains Si, K, Na, Ca, Mg, Al, and Fe, with smaller amount Mn, S, P, and Ti. The mineral content in marine biomass is quite high including all above elements. These constituents are present as silicates, oxides, carbonates, sulphate, chlorides and phosphates. The influence of these compositions on ash deformation and fusion temperatures on various biomasses was studied extensively. G. Skodras et al. studied how the mineral matters affected lignite gasification in presence of H_2 and CO_2. It was found that the alkali index (AI) influenced gasification rate and the inorganic constituents in lignite coal played a controlling role in determining gasification reactivity. For both H_2 and CO_2, gasification rate increased with increasing concentration of Ca, but in case of K and Na, they did not have any effect on gasification rate due to the lower concentration of these two components. Mg had similar effect like Ca, but Fe did not have any effect on gasification rate [50]. The most problematic ash forming elements are alkali metals (Na, K), alkaline metal earth metals (Ca, Mg) and halides (S, Cl, and Si) [43, 44, 51]. Ash melting behaviour and deposition tendencies can be predicted through some empirical indices for biomass type ashes. These indices might be helpful at certain point in making large scale reactors or boilers before their final design. So, in this circumstance, the measurement of this mineral content needs to be highly accurate so that results can be predicted precisely. One such index is alkali

index, as a threshold indicator of slagging and fouling. The alkali index abbreviates the amount of alkali oxide in fuel per unit fuel energy:

$$AI = \frac{(K_2O + Na_2O)\ (in\ kg)}{GJ} \tag{2.2.26}$$

The limitation value for alkali index in the range of 0.17 – 0.34 kg/GJ indicates that slagging or fouling is possible, when this value crosses the limitation i.e. if the value is more than 0.34 fouling or slagging readily occurs [44, 51].

Another index such as base-to-acid ratio is given below [37, 52]:

$$BTA_r = \frac{(Fe_2O_3 + K_2O + Na_2O + CaO + MgO)\%}{(SiO_2 + TiO_2 + Al_2O_3)\%} \tag{2.2.27}$$

All the oxide of metals is in weight percentage of biomass ash.

And finally, bed agglomeration index has been developed for moving bed gasifier relating to ash agglomeration into the moving bed [53].

$$BAI_r = \frac{(Fe_2O_3)\%}{(K_2O + Na_2O)\%} \tag{2.2.28}$$

When this value lowers then 0.15 it is certain to cause bed agglomeration.

These empirical indices mainly predict the ash deposition and fouling tendencies. But, this problem can be overcome by some chemical treatment such as demineralization or deashing carried out by diluted hydrochloric acid (10% wt.) or hydrofluoric acid or simply distilled water to remove water soluble elements. The limitation comes when acid treatment to be carried out at large scale is not practically feasible, but water might be a good option. K. Raveendran et al. studied wood and twelve other types of biomass and the results showed that after deashing, the volatile yield, initial decomposition temperature and pyrolysis rate increased [54].

2.2.15 Types of gasifier

Gasifier designing is highly influenced on the final product yield. Tar generation, product gas yield and efficiency might be effected on types of gasifier. A brief description of updraft, downdraft, fluidized bed, circulating bed and entrained bed gasifier is elaborated below:

2.2.16 Updraft gasifier

The most common schematic diagram of updraft gasifier is shown in Fig. 2.2.3. The solid fuel or biomass is fed at the top of the gasifier and air or oxygen or steam is fed from the bottom as depicted in below figure. The product gas with tar escapes through the top and residue ash comes out at the bottom. The highest temperature is generated proximate to combustion zone, where carbon dioxide and heat are produced. After gasification reactions the hot gas passes through the pyrolysis zone at relatively lower temperature zone.

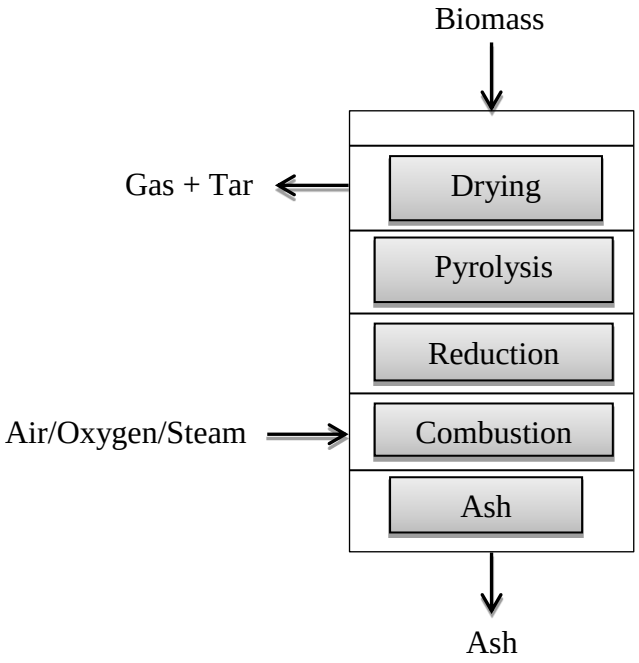

FIGURE 2.2.3: Typical diagram of an updraft gasifier.

During pyrolysis the tar which is produced at this zone is called as primary tar and it moves to cooler zone, as a result, there is no scope for conversion of tar into secondary tar and gases. Despite the above problem, some positive features of the construction of this gasifier are its easiness to make and its high thermal efficiency.

2.2.17 Downdraft gasifier

Fig. 2.2.1 shows the schematic diagram of a typical downdraft gasifier. The solid fuel or biomass is fed at the top of the gasifier similar to updraft gasifier. The highest temperature is in the combustion zone. The hot gases and primary tar produced in both the combustion

zone and pyrolysis zone passes through gasification zone towards upstream. So, the produced tar in pyrolysis moves towards hotter zone i.e. the combustion and gasification zone where mostly the primary tar is cracked into gaseous products. Due to this reason, the amount of tar produced in downdraft gasifier is less. A small scale application with internal combustion engine can be fruitful for the generation of electricity.

2.2.18 Fluidized bed gasifier

Fluidized bed gasifiers are a more recent development that offers advantage of excellent mixing characteristics and high reaction rates between gas-solid contacting. In early 1921 Fritz Winkler of Germany, who first invented the fluidized bed gasifier, especially an air-blown gasifier was used for running a gas engine. Now, fluidized bed is popular for energy conversion and is around 20% of gasifier market share in the world [49]. The basic phenomenon is the mixing of solid and air in hot bed of granules solid such as sand. Due to excellent mixing of gas – solid into all the zones – drying, pyrolysis, combustion and reduction, temperature is almost uniform throughout the bed. Fluidized bed reactors are the only gasifiers with isothermal bed operation. A typical operating temperature for biomass gasification is as low as 800 - 1000°C compared to fixed bed gasifiers. A schematic design of the fluidized bed gasifier is illustrated in Fig. 2.2.4. Air is blown through a bed of solid particles at a sufficient velocity to keep particles in a state of suspension. Actually, the bed is externally heated and the feedstock is introduced as soon as a sufficiently higher temperature is reached.

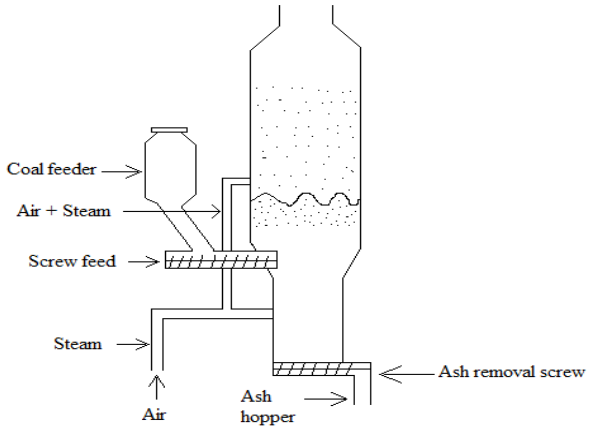

FIGURE 2.2.4: Schematic diagram of a typical fluidized bed gasifier.

The fuel particles are injected at the bottom of the reactor through screw feeder which is followed by quickly mixing with the bed material which instantaneously heats up to the bed temperature. As a result of this treatment the pyrolysis of the fuel is very fast – i.e secondary tar is cracked, resulting in a component mix with a relatively large amount of gaseous products. Further gasification and tar-conversion reactions occur in the gas phase. Most systems are equipped with an internal cyclone in order to minimize char blowout as much as possible. Ash particles are also carried through the bottom of the reactor which has to be removed from the gas stream if the gas is used in engine applications. There are certain advantages:

1. Higher yield of product gas

2. Better heat and mass transfer from fuel due to mixing intermolecular particles.

3. Higher heating value.

4. Reduced tar and char content.

5. No ash melt or slagging or fouling.

And finally, fluidized bed gasifier is developed to avoid the bed agglomeration problem that exists in fixed bed gasifier.

2.2.19 Circulating fluidized bed gasifier

A circulating fluidized bed gasifier is shown in Fig. 2.2.5. The fluidizing velocity in circulating bed gasifier is high enough to entrain large amount of solid product gas.

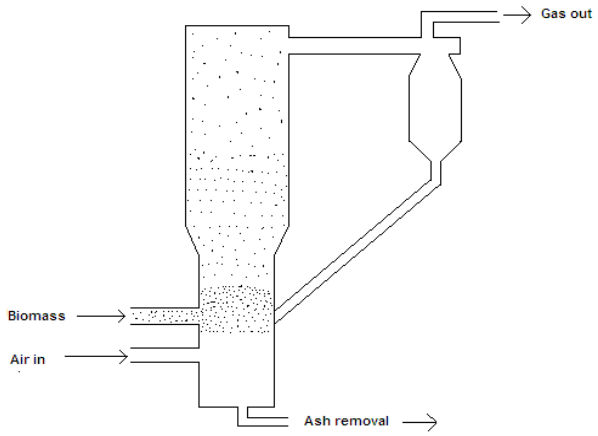

FIGURE 2.2.5: Schematic diagram of a circulating bed gasifier.

So, it exhibits excellent heat and mass transfer, longer residence time and better conversion. It is also capable of wider range of particles without the penalty of entrainment loss. In every recycle loop the bigger size particles are converted into smaller particles until they are converted into gases or entrained loss [55].

2.2.20 Bubbling fluidized bed gasifier

Bubbling fluidized bed (BFB) gasifier is another type of fluidized bed gasifier. It has several advantages such as the overall simplicity of the bubbling bed design and a number of other characteristics which makes its application more suitable for coal gasification than spouted or circulating fluidized beds. In biomass industries it finds the use in small to medium is less than 25 MW capacities.

2.2.21 Entrained bed gasifier

Entrained bed gasifier is one of the most promising technologies in modern thermochemical conversion process. Fig. 2.2.6 shows the schematic diagram of entrained bed gasifier. It has several advantages over other types of gasifiers. This system enacts to gasify pulverized fuel particles suspended in a downstream flow of air or oxygen or steam. As entrained bed gasifier operates at higher temperature, slag is removed from the bottom of reactor.

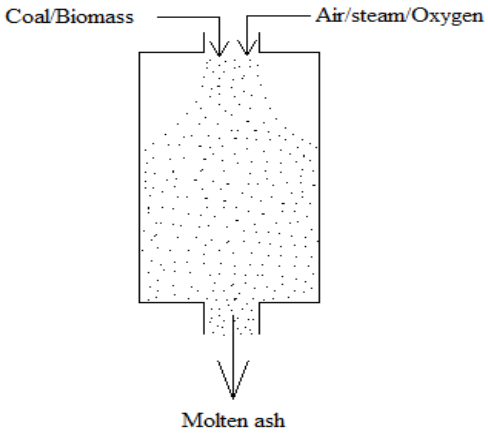

FIGURE 2.2.6: Schematic diagram of an entrained bed gasifier.

Entrained bed gasifier can be built in larger capacities (more than 100 MW) and it has wide versatility in application such as coal, refinery, wastes, etc. Despite this advantages, it has certain limitation in particle size distribution is most suitable around 70 – 100 µm.

2.2.22 Other types of gasifier

Notwithstanding, there are a wide variety of gasifiers, which do not fit into any of the categories described in the previous sections and are classified as other gas producing gasifiers. Some units are built to combine the advantages of cross draft with downdraft or updraft gas producers. A number of other biomass gasifier systems (double fired, molten bath etc.) are currently under development. In some cases these systems incorporate unnecessary refinements and complications, while others both the size and sophistication of the equipment make near term application in developing countries unlikely. For these reasons they are omitted from this account.

2.2.23 Gas filtration and cooling systems

Gases formed during gasification of biomass contaminated by tar and particulates. The levels of contamination vary depending on the gasification process and the nature of feedstock. Gas clean up and conditioning systems, including tar separation and hot gas particulate removal must be applied to prevent erosion, corrosion in downstream equipment and to minimize environmental hazards. Small carbon containing particles in the gas streams are difficult to remove by cyclone separator. Cyclone separator is partly helpful to remove hot soot particles and the rest is deposited in next to the filter or scrubber. However, they result in reduction in overall efficiency in the production of electricity or mechanical power using a gas engine. Furthermore, gas cleaning greatly adds to the capital investment of the plant. For this tar cracking with a suitable catalyst or using high temperature can be effective for running gas engine. The emission profile of electricity-generation from different sources is listed [45, 56]. The particulates are also truly responsible for polluting atmosphere irrespective chemical contamination [57]. They are basically;

(1) Particles formed due to incomplete combustion including soot, tar and char.

(2) Particles formed due to presence of inorganic material in fuel-ash.

In combustion process of wood pellets, wood logs and wood chips, mass concentration of particles in the flue gas have been reported earlier to be in the range of 35 – 1500 $mgNm^{-3}$ [58]. Particle size has showed a wide range of variation in between 50 to 200 nm. The concentration in particle numbers emitted from domestic combustion show large variation in the range of 10^7 – 10^{10} particles per Ncm^3 [59]. Municipal solid waste management system has been studied and several analyses were carried out by several researchers [60, 61, 62]. Globally, waste management systems are operating successfully in terms of thermochemical route or biochemical route. Both routes are efficient for utilization of energy. Certain problems existed in all types of gasifiers that constrain both from the technical point of view as well as socio-environment aspects. But, the major problem in gasifier is difficulty in cleaning up due to formation of tar and slag inside the reactor. Now, each gasifier has specific problem as elaborated and the performance of some kind of gasifier based on physiochemical characteristics listed in literature [63, 64].

2.3 Literature review – III; Slow pyrolysis for bio-oil production

2.3.1 Introduction

Pyrolysis is an old technology that came into being during ancient Egyptian times and was used for making caulking boats and certain embalming agents [65]. Extensive work has been done on the pyrolysis of wood or biomass to convert into liquid fuel and valuable chemicals since the oil crisis of mid-1970s. Pyrolysis is now so popular across the world that it is commercialized at the industry level.

More than 90% of all transportation energy in United States comes from non-renewable petroleum. Energy consumes more than 60% of oil in transportation sector in United States. Foreign oil accounts for more than half of all oil being used in United States. As United States is heavily reliant on foreign sources for non-renewable energy, there exists an excellent opportunity for developing renewable energy sources. The problem is not only associated with the United States, but sprawled to huge extent in Asia, especially India and China. These two countries lack inherent oil resources to meet all energy demands. So, huge opportunity exists for renewable energy sources in these two countries [66]. Another disadvantage of burning of non-renewable energy sources is that it produces carbon dioxide which pollute environment and increases greenhouse gas. In comparison with fossil fuel, the use of biomass for energy provides significant advantages over burning of

fossil fuel. Plant growth required to generate biomass feedstocks absorbs atmospheric carbon dioxide, which compensates the increase in atmospheric carbon dioxide that results from fuel combustion. There is currently no commercially accepted panacea to eliminate the carbon dioxide added to the atmosphere, as well as the resultant greenhouse gases from the combustion of fossil fuel. Climate change today is facing serious problems caused due to formation of carbon dioxide from fossil fuel combustion. Kyoto protocol established in 1992 and signed in 1997 by UNFCCC (United Nations Framework Convention on Climate Change) is the main tool focussed on greenhouse gas mitigation involving many countries. These countries have committed to reduce their emission level during this period by 18% compared to base year i.e. 1990 [67]. Carbon dioxide is mainly responsible for increasing the concentration of GHG. GHGs are generated due to the combustion of fossil fuel caused by anthropogenic CO_2 emissions. The global share of emission existed more or less in almost all the countries. Numerous papers are published on the thermochemical conversion of pyrolysis process. Most processes convert biomass into liquid fuel by slow, fast or flash pyrolysis process, and followed by catalytic upgrading of the resulting bio-oil obtained. Kinetics and thermal degradation mechanism for pyrolysis in case of biomass plant material and its chemical constituents were extensively studied [68 - 78]. Apart from this some studies focussed on the use of catalysts for biomass cracking (in situ upgrading) to improve either calorific value or produce valuable chemicals.

2.3.2 Pyrolysis process

Before one goes into elaborate details of pyrolysis process, it is important to understand the different thermochemical routes as shown in line diagram in Fig. 2.3.1. The conversion of biomass/marine algae into fuel, gases or valuable chemicals can be done by two major paths, one is biochemical path and other is thermochemical path, and it is further classified in details as shown in Fig. 2.1.1.

Pyrolysis is a thermochemical process unlike combustion which takes place in absence of oxygen, except in some cases where partial combustion is allowed in order to provide some external source of thermal energy as needed for the process. Fundamentally, slow pyrolysis is a thermal degradation of biomass in absence of oxygen and generates gas, liquid and solid products. In chapter 1 (general introduction) and table 1.4, which divide different technologies of pyrolysis with different time, names them accordingly such as torrefaction or mild pyrolysis, slow pyrolysis, fast pyrolysis and flash pyrolysis. In

pyrolysis the large molecules of biomass's chemical composition tend to degrade into smaller molecule mainly gases which are either condensable organic fragments or noncondensable gases. The distinguishing feature between slow pyrolysis and fast pyrolysis is the difference in yield of liquid or bio-oil and the yield of solid bio-char. The yield of products depends on process conditions such as residence time, quenching time, etc. It also greatly reduces its weight, thus enhancing the commercial value for transportation liquid fuel.

Fig. 2.3.1 depicts the products from pyrolysis process and their uses for different purposes. Today, pyrolysis has gained overwhelming popularity just because of versatility of the products. The physical changes that occur during pyrolysis are described below [79]:

(1) Heat transfer to material/fuel from heat source simply increases the temperature of the material/fuel.

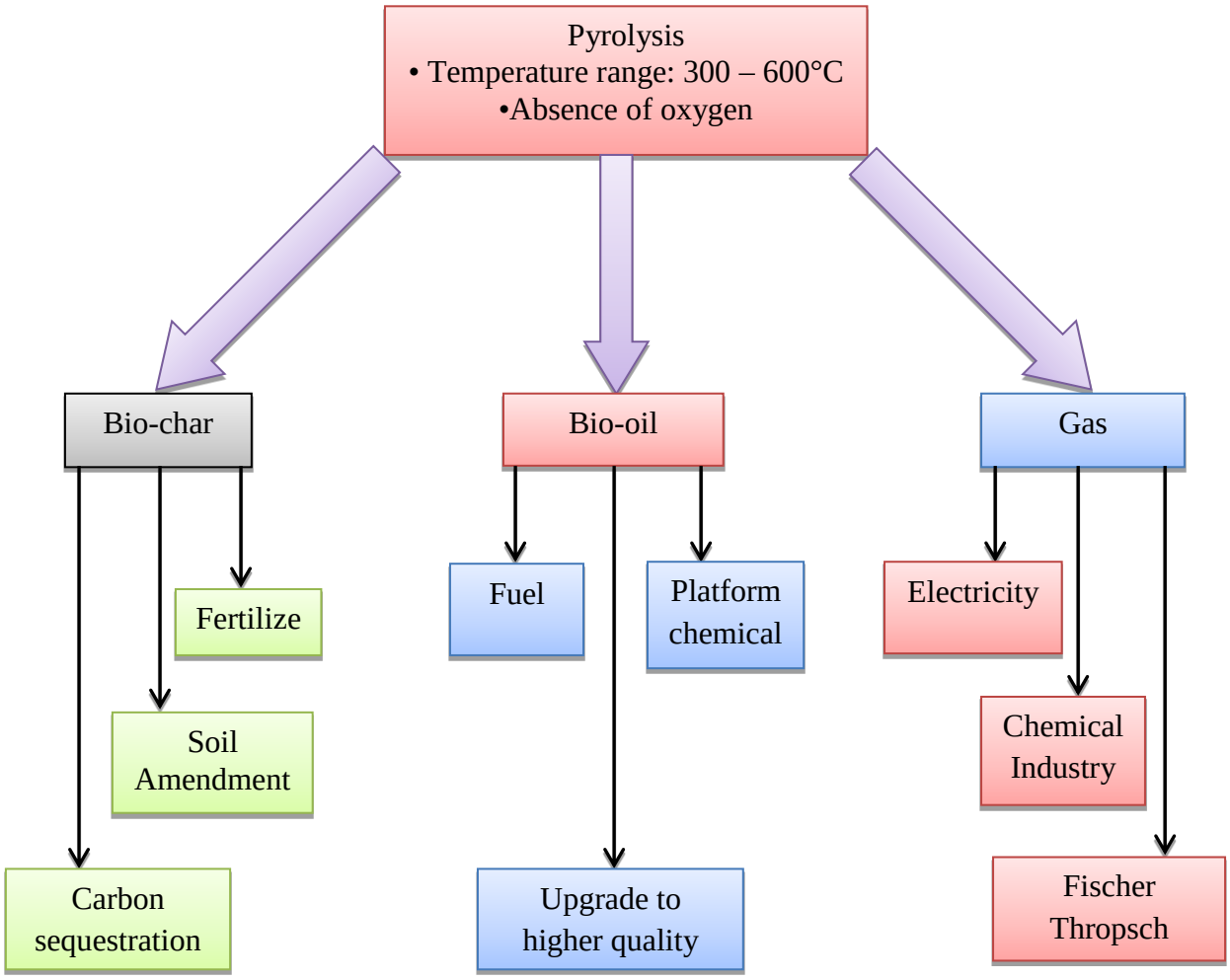

FIGURE 2.3.1: Schematic diagram of outlet products from pyrolysis process.

(2) The start-up of primary pyrolysis occurs when proposed temperature is reached to produce volatiles and char. The start-up pyrolysis temperature of every material is different due to variation of composition inside the material and the heat transfer limitation.

(3) The hot volatile gases flow towards cooler zone of solids resulting in heat transfer between hot volatiles gases and cooler side of the material/fuel.

(4) Some parts of volatile matter condense in the cooler parts of the material/fuel, followed by secondary reactions, to produce tar.

(5) Primary pyrolysis reactions proceed while secondary reactions occur simultaneously and continuously.

(6) Finally, thermal decomposition, water gas shift reactions, reforming, and dehydrations, etc. can also occur partially. But, whole process is largely affected by the process condition such as residence time/temperature/pressure profile.

Fast or flash pyrolysis is more beneficial in terms of oil yield from mild or slow pyrolysis. Over the last two decades, fast or flash pyrolysis has become the rib bone in research as it produces high yield of liquid or oil from which valuable chemicals, chemical intermediates, petrochemicals, and fuels can be obtained.

2.3.3 Physical and chemical properties of biomass

The physical properties of biomass was described well in the literature review of gasification technology which includes moisture content, energy content, volatile matter, ash content, fixed carbon, reactivity, particle size, bulk density, mineral matters in biomass. Apart from the physical properties, temperature plays a crucial role in both pyrolysis and gasification. In gasification the requirement of temperature is comparatively higher than pyrolysis. So, at higher temperature, the problems that crop up in gasification may not occur in pyrolysis. Mostly, mineral matters in gasification at higher temperature cause slagging or fouling on reactors.

Moisture content in biomass effect on the quality of bio-oil in terms of calorific value and some others properties such as carbon, hydrogen content etc. are also degrades the oil

quality. Proximate and ultimate analysis of biomass plays a significant role in pyrolysis or gasification process described in the literature review of gasification.

Thermodynamic properties of biomass influence on both gasification and pyrolysis. Biomass particles are subjected to heat conduction along and across the fibre, which in turn affects both pyrolysis and gasification. So, the thermal conductivity of biomass is an important subject in this context. The thermal conductivity can be calculated based on large samples developed by Maclean (1941) from the following correlations (from Kitani and Hall, 1989) [80].

$$K_{bio}\left(\frac{w}{m.K}\right) = sp.g\ (0.2 + 0.004m_d) + 0.0238 \qquad \text{for } m_d > 40\% \tag{2.3.1}$$

$$= sp.g\ (0.2 + 0.0055m_d) + 0.0238 \qquad \text{for } m_d < 40\% \tag{2.3.2}$$

Where, K_{bio} is the thermal conductivity of the biomass, $sp.g$ is the specific gravity of the fuel and m_d is the moisture content in biomass in percentage on dry basis.

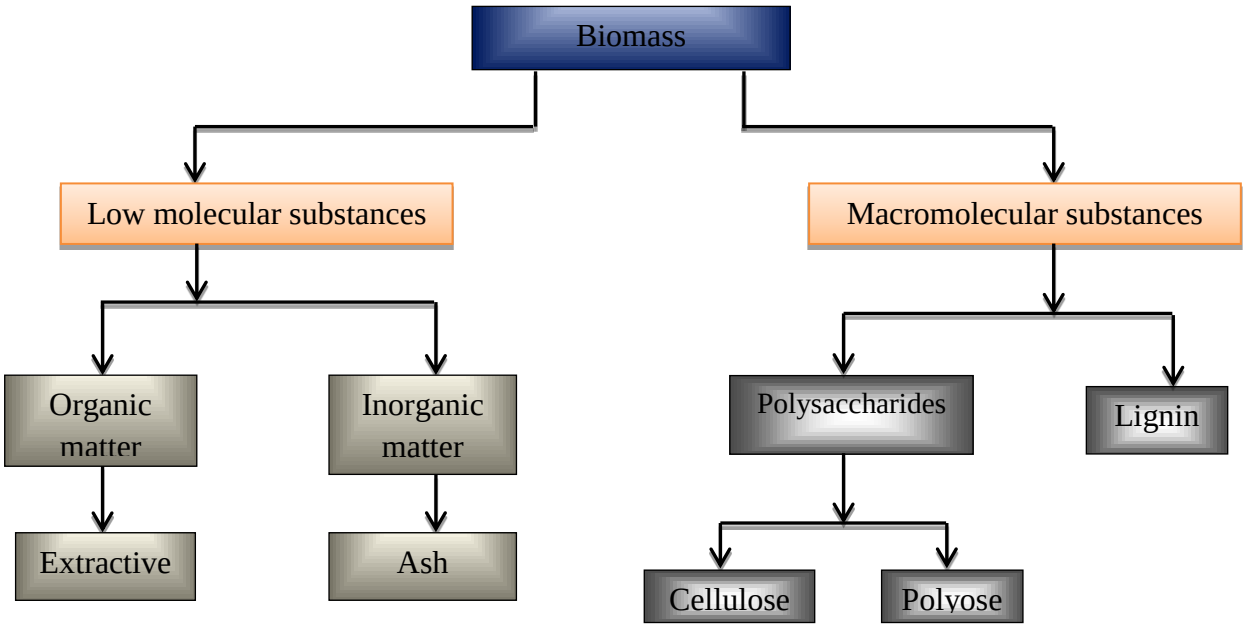

FIGURE 2.3.2: Typical components in biomass.

Unlike metal or any solid, biomass is highly anisotropic due to that reason its thermal conductivity is different across its fibre. Some factors such as moisture content, porosity, and temperature also affects the thermal conductivity and detailed study is not included here. Biomass generally consists of organic and inorganic material. Fig. 2.3.2 depicts typical components in biomass. The physical and chemical properties of biomass are

mainly dependent on the chemical constituents of biomass. Lignocellulosic biomass is a composite material in which its chemical constituents consisting of cellulose (40 – 50%, d.b.), hemicellulose (20 – 30%, d.b.), and lignin (15 – 25%, d.b.) are linked together in order to obtain structural strength in combination with flexibility. In addition, biomass also contains moisture and extractives and inorganic compound i.e. ash. The chemical constituents for marine algae are completely different from terrestrial biomass i.e. lignocellulosic biomass. In early research work, it was reported that the chemical composition of seaweeds is very versatile, depending on some external factors, such as harvesting season. In general, on dried weight basis, they contain proteins (5 to 30% wt.), carbohydrates (5 to 60% wt.), lipids (5 to 15% wt.), fibres (2-5% wt.) and ashes (10 to 50% wt.) [81, 82].

2.3.4 Physio-chemical properties of bio-oil

Pyrolysis is a thermochemical process that produces solid, gas and liquid or oil in absence of air/oxygen at a specified rate to a maximum temperature. Pyrolysis products depend on a specified rate of heating and temperature. The fundamental reaction mechanism of pyrolysis is as follows.

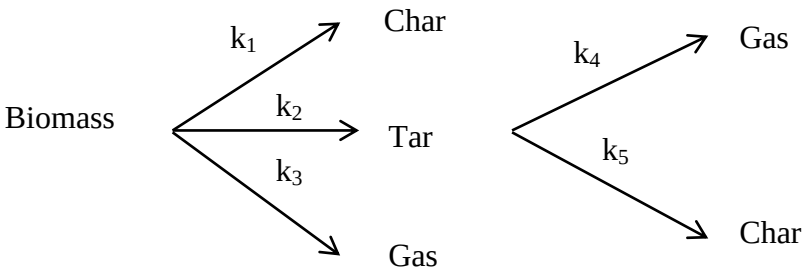

FIGURE 2.3.3: Pyrolysis reaction mechanisms including primary and secondary reaction.

The first stage of pyrolysis process produces solid and condensable gases. Condensable species are further broken down into noncondensable gases (CO, CO_2, CH_4, and H_2), liquid and char as shown in Fig. 2.3.3. The physical phenomenon of thermal decomposition is dependent on two different phases; one is partly involved with gas-phase homogeneous reactions and another is partly gas-solid-phase heterogeneous reactions. In gas-phase reactions, the condensable gases are further broken down into smaller molecules of noncondensable gases. The condensable gases condenses as bio-oil or pyrolytic oil and the

noncondensable gases leaves the reactor as product gas or syn-gas which is useful in a burner or boiler to provided heat or any supplementary application can be made. Solids left in the reactor are generally used as a commercial fuel or any other purposes.

Bio-oil is produced rapidly due to thermal split up of large molecules, simultaneously depolymerizing and fragmenting of hemicellulose, cellulose and lignin. During pyrolysis biomass undergoes a rapid increase in temperature followed by a quick quenching to freeze the intermediate products. The most important thing is that rapid quenching is necessary as it simply prevents further degradation of the intermediate products. The physical properties of bio-oils were well elaborated in earlier research work [83, 84]. The liquid looks like black-brown tarry fluid containing with 15 – 30% (wt.) moisture and having calorific value of around 15 – 32 MJ/kg [85]. It exhibits lower calorific value than hydrocarbon fuels as contains highly oxygenated compounds [86]. Bio-oil shows solubility in methanol and ethanol but is immiscible in hydrocarbon fuels. But, moisture free bio-oils have certain extent of miscibility in toluene, hexane, etc. Bio-oil can be easily stored, transported from one place to another in a similar fashion like petroleum-based products. Typical properties of bio-oil, light oil and heavy fuel oil are compared in the literature [87]. Some authors mooted NO_x emission can be reduced from bio-oil by the proper adjustment of injection timing and introducing exhaust gas recirculation (EGR) technique [88, 89, 90].

Table 2.3.1 shows probable composition of bio-oil and it was reported that more than hundreds of compounds are present, even though it depends on the chemical compositions of biomass. For detailed characterization of this oil mixture GC-MS, FT-IR and NMR spectra are helpful for identification of discrete compounds. Mainly, large and major peaks are isolated by GC-MS technique which primarily consists of fatty acids, alkanes, alkenes, amides, aldehydes, pyrrolizidines, terpenes, phytol and phenol its derivatives [91]. N_2 found in bio-oil was probably due to the presence of protein content and chlorophylls in algae or biomass or agricultural residues having high above two contents. Apart from this higher molecule or aromatic compounds such as benzene or toluene were also detected by GC-MS. Significant number of compounds booked in the $C_{16} - C_{20}$ bracket were also detected. [92].

TABLE 2.3.1: Thermal breakdown of the major constituents of biomass through thermochemical conversions and the respective probable components in bio-oil.

Components	Through	Probable major components

	thermochemical conversions	
Hemicellulose	thermal breakdown	acetic acid, furfural, furan, furanone, methanol, formaldehyde, hydroxyacetaldehyde, acetone, acetol, lactones
Cellulose		levoglucosan, hydroxyacetaldehyde, 1,6 anhydro-β-D glucofuranose, furfural, hydroxymethylfurfural, furan
Lignin		2-methoxyphenol, catechol, phenol, methanol, furfural, formaldehyde, formic acid, acetone, acetol, alkyl-phenol, lactones

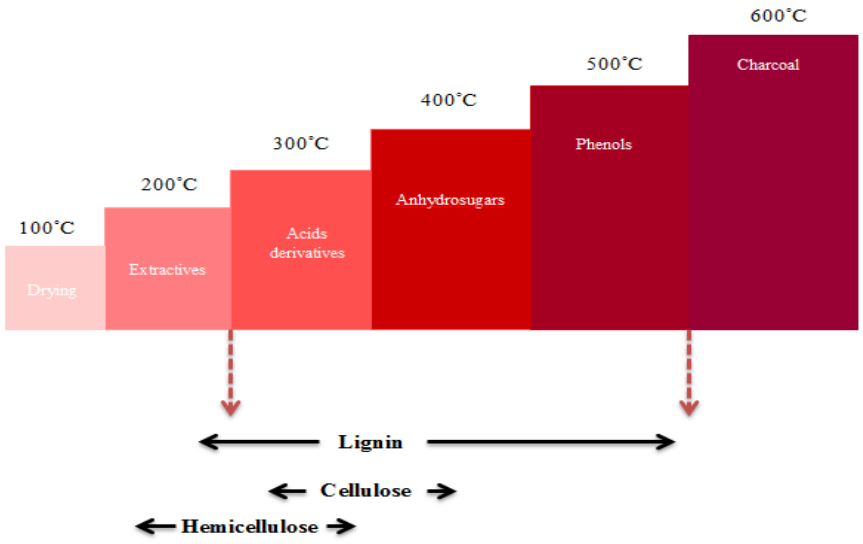

FIGURE 2.3.4: Different steps of thermal degradation along with foremost valuable products of biomass during pyrolysis process.

Paul de Wild described in details about the valuable chemicals and others products that were produced from pyrolysis process in his Ph.D thesis [93]. Fig. 2.3.4 shows thermal degradation temperature zone of three components, named hemicellulose, cellulose and lignin and their main products in all temperatures as shown in the above table 2.3.1. Hemicellulose breaks down in the temperature range of 200 – 300°C and the probable main products are acetic acids, furfural, furan, and some oxygenated compounds C_1 – C_4

such as formaldehyde, etc. Cellulose degrades in between 250 – 400°C temperature and the main products are levoglucosan, hydroxyacetaldehyde and some other products 1, 6 anhydro-β-D-glucofuranose, furfural, etc. used as glucose, polymers, and binders, etc. Lignin starts to degrade from 150 – 600°C and its degradation rate is comparatively slower than other two components due to giant and strong molecule. The phenolic compounds are present as monomeric units and oligomers are derived from the coniferyl and syringyl building blocks of lignin. Lignin consists of a large number of phenolic compounds which break down into smaller molecules such as 2-methoxyphenols or 2, 6-dimethoxyphenols, catecols etc. as listed in table 2.3.1. From earlier literature survey highest concentration of any single compound (except water) is hydroxyacetaldehyde (upto 10% wt.), followed by acetic acid and formic acid (at 5% wt., and 3% wt, respectively) [94, 95, 96]. This is why bio-oil exhibits acidic pH around 2 – 5.

2.3.5 Physical and chemical characterization methods of bio-oil

The physical properties of bio-oils are well established in literature [97 – 100]. Pyrolysis liquids contain many organic compounds which need to be characterized in detail. Oasmaaa and Peacocke worked on different bio-oils and discussed various physical and chemical properties along with their methods of estimation [101, 102, 103]. They studied in detail about the different types of pyrolysis liquid provided by different producers. The round-robin tests are recommended as following:

(1) The homogeneity of bio-oil should be verified by water distribution or microscopic determination.

(2) Karl – Fischer titration is recommended for analysing water content in bio-oil.

(3) pH determination is also recommended and the value should be reported in decimal place.

(4) The kinematic viscosity at 40°C is accurate in case of pyrolysis liquids. The Newtonian behaviour utilizing a closed-cup rota-viscometer should be checked for this liquid.

(5) The stability test of bio-oil should be performed in each pyrolysis liquid from different producers, in exactly the same way. The best comparisons among the pyrolysis liquid can be obtained when the differences in the water contents of the sample are least. The viscosity of pyrolysis liquid is measured at 40°C; at this temperature measuring error is smaller.

(6) Ethanol or methanol can be used for the solid content determination, but it is mostly depending on the types of feedstock being used, so the solubility of the liquid should be checked using solvents of different polarity.

(7) The sample size for elemental analysis should be as large as possible, and should be carried out at least thrice.

(8) It is necessary to calibrate gas and liquid chromatographic systems; using known amount of compounds with standard solution is being used during chemical characterization.

Some analytical methods such as GC are useful to measure the composition of bio-oil at certain level, but despite that it requires robust gas columns and the high temperature programs. Gas chromatography-mass spectroscopy (GC-MS) is most commonly used for characterization of bio-oil. In addition, bio-oil contains polar groups, non-volatile matters, and can be measured HPLC or GPC analysis. Overall the pyrolysis liquid can be measured by Nuclear magnetic resonance (NMR) (types of carbons, hydrogen in structural groups, bonds, etc.), GC-MS (condensed volatiles compounds), HPLC or HPLC/electrospray MS (non-volatile compounds), Fourier transform infrared (FT-IR) spectroscopy (functional groups), gel permeation spectroscopy (GPC) (molecular weight distributions).

2.3.6 Bio-oil production from various feedstocks

Due to wide variation of chemical composition in different feedstocks produced different bio-oil, sometimes it is very difficult to categorize as it is depending on species, age, portion of the plant selected, and many other parameters. Numerous research papers are published on pyrolysis and investigated based on different feedstocks available in nature. Here, some of them are listed so that reader may be able compare the difference in bio-oil properties obtained from different feedstocks. The most common feedstocks relevant to the present work are presented here as follows: wood, bark, agricultural wastes/residue, seeds, nuts, algae, aquatic biomass, grasses, forestry residue, cellulose, and lignin and others.

2.3.6.1 Bio-oil from Wood type biomass

Carmen Branca et al. [104] elaborated the conventional pyrolysis of beech wood carried out in the countercurrent fixed-bed gasification at the heating temperature in the range 327°C – 627°C. Again, the same author, Carmen Branca et al. [105] investigated the

combustion behaviour of bio-oils extracted from wood by means of fast pyrolysis techniques (i.e. BTG, Dynamotive, Ensyn, Pyrovac) which was studied by measuring weight loss curves in air under controlled thermal atmosphere. The physical and elemental analyses of bio-oil derived from different fast pyrolysis technologies were characterized.

Zhongyang Luo et al. [106] had devised a fluidized bed reactor with 3 kg h^{-1} throughput at atmospheric pressure and with varied temperature of 450 – 700°C. Nitrogen flow was introduced for fluidizing sand in the range of 3 – 6 Nm^3h^{-1} and four biomass were taken out of which three were wood type biomass, named, *Pterocarpus indicus, Cunninghamia lanceolata* and *Fraxinus mandshurica*, and the last one was rice straw. The most typical schematic diagram of pyrolytic oil set-up is shown in Fig. 2.3.6.

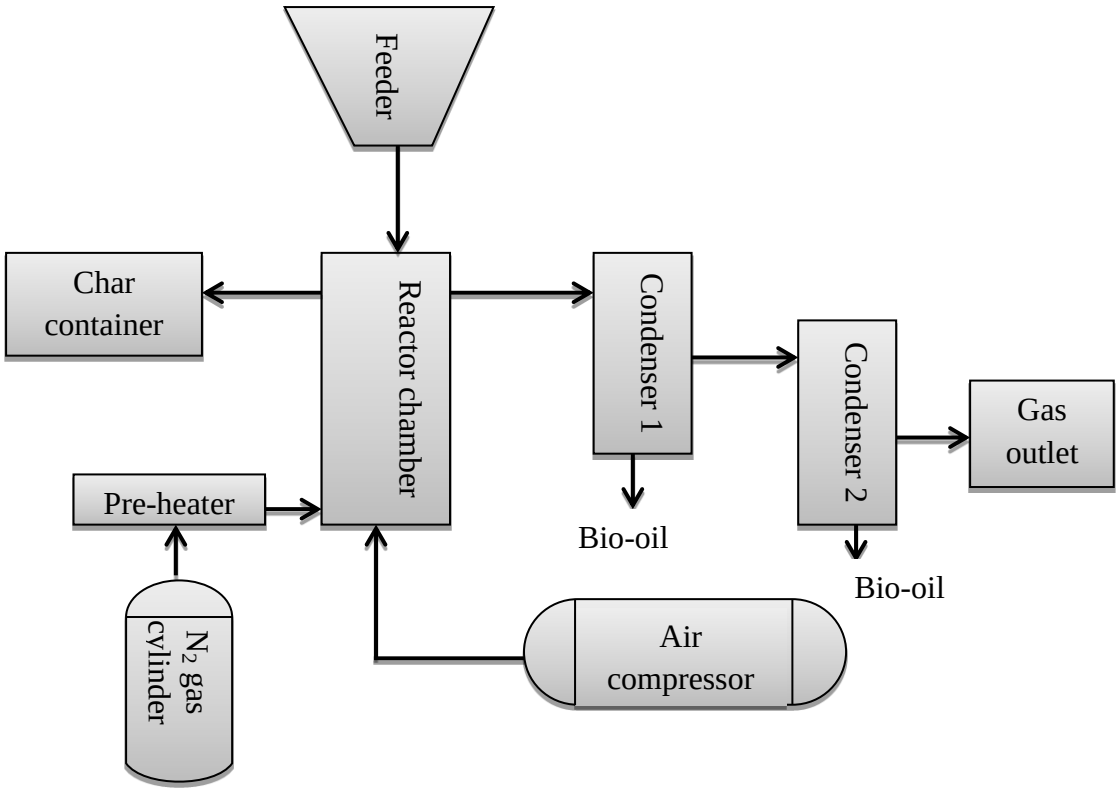

FIGURE 2.3.6: Typical schematic diagram of a pyrolytic oil set-up.

Oskar Paris et al. [107] investigated the pyrolysis of softwood (spruce and pine) in the temperature range of 25°C and 1400°C within the narrow intervals and the decomposition and carbonisation of this softwood was characterized by microstructural analysis by means of wide-angle X-ray scattering, small-angle X-ray scattering, and Raman spectroscopy. Bio-oil derived from slow pyrolysis of two Australian species, named red gum (*Eucalyptus*

camaldulensis) and blue gum (*Eucalyptus globulus*) was blended with ethanol and burnt in a circular jet spray at atmospheric pressure [108]. Again, pyrolysis behaviour of biomass could be modelled with different kinetic mechanism by thermogravimetric analysis as studied by Joaquin Reina et al. [109]. The experimental result showed a good agreement was established between the kinetic parameters obtained from either dynamic or isothermal techniques in three different waste woods, named forest wood, old furniture wood and used pellets. Maritha Nilsson et al. investigated small samples (wt. around 15 – 150 mg) from 8 different species of birch (Betula) which were pyrolyzed at 550°C [110]. The compounds produced from pyrolysis were analysed by GC methods: direct injection with GC/FTIR/FID and pre-connection with GC-MS. Maria Olsson et al. [111] studied the characterizations of smoke components produced from oxidative pyrolysis of softwood pellets carried out from compressed sawdust and wood shaving.

2.3.6.2 Bio-oil from algae

Marine algae either microalgae or macroalgae has potential to generate biofuels called third generation biofuel. Algae have several benefits over terrestrial biomass in terms of rapid growth rate, abundant availability in ocean or sea, no cultivation cost, no conflict over cultivation area, absorption of CO_2 via photosynthesis process, valuable minerals and chemicals could be extracted from different methods. The seaweeds are multicellar green, red, and brown algae which closely resemble with terrestrial biomass. T. Minowa and his co-workers performed experiment for producing bio-oil from algal cells of microalga, named *Dunaliella tertiolecta* having moisture content 78.4 wt. % by direct thermochemical liquefaction at around 300°C and 10 MPa [112]. The physicochemical properties of this microalga are important prior to liquefaction as listed in the article. The flowchart of liquefaction is shown in Fig. 2.3.7. The oil yield and its properties were found to be excellent; especially calorific value achieved 37.8 MJ kg^{-1}. Thomas A. Milne et al. investigated the catalytic conversion of microalgae and vegetable oils to premium gasoline by the shape-selective zeolite *HZSM-5*, a medium pore, shape selective, acid catalyst [113]. A. Bruhn and his co-workers studied the bioenergy potential of *Ulva lactuca*, which included yield, methane yield, and combustion characteristics prior to thermochemical process [114]. As it is well known that the mineral contents in marine algae are quite high as compared to terrestrial biomass. Some data accumulated by A. K. Siddhanta and his team who studied Indian seaweed species selectively listed in table 2.3.2 [115, 116]. The

sample preparation and chemical methods was tedious that involved cleaning of seaweed in sweet water to remove impurities, powdering in a rotating ball mill and storing in a plastic container.

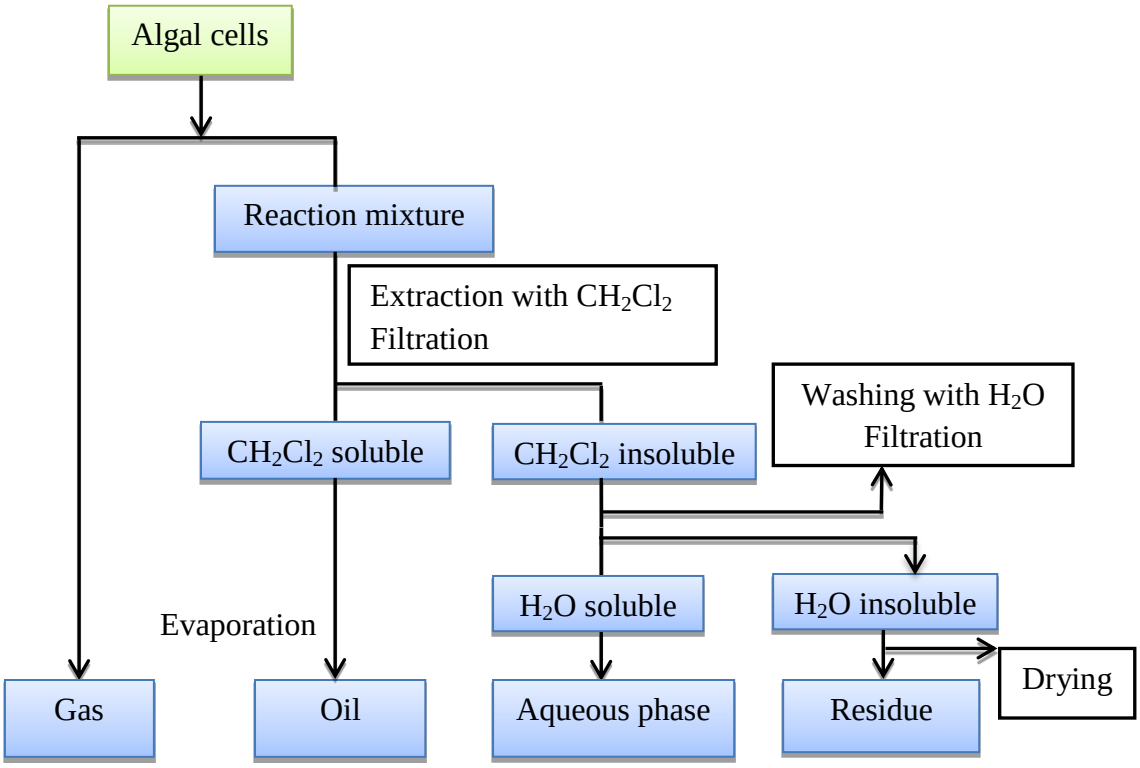

FIGURE 2.3.7: Procedure for separation of products yield.

TABLE 2.3.2: Yield of celluloses content in Indian seaweed species.

Seaweed (latitude and longitude)	**yield (%, ±SD)**			
	crude cellulose	α-cellulose	β-cellulose	ratio (α/β)
Ulva lactuca (09.28°N, 79.20° E)	5.6±0.4	1.12±0.2	2.86±0.1	0.39
Sargassum tenerrimum(20.54° N, 70.20°E)	10±0.5	8.5±0.3	1.03±0.2	8.25
Gracilaria edulis (09.9°N, 78.43°E)	5.3±0.2	3.38±0.08	0.70±0.04	4.83
Kappaphycus alvarezii (09.9°N, 78.43°E)	2.0±0.1	1.4±0.05	0.4±0.02	3.5

Shuang Wang et al. [117] analysed the composition of bio-oil derived from pyrolysis of seaweed, named *Enteromorpha clathrata* (EC) and *Sargassum natans* (SN) under three designated temperatures 400, 500 and 600°C along with nitrogen flow rate 150 L h^{-1}. Xiaoling Miao et al. and his co-workers [118] investigated the bio-oil production from fast pyrolysis by metabolic controlling of *Chlorella protothecoides*. Algae have huge potential to produce biofuels from either fermentation process or pyrolysis process that can replace fossil fuel in near future. Yasmin Khambhaty and his co-workers produced bioethanol from *Kappaphycus alvarezii* at laboratory and bench scales with 250 g and 16 kg, respectively [119]. Similar research was carried out by Seung-Soo Kim and his co-workers on pyrolysis characteristics and kinetics of alga *Saccharina japonica* [120]. The characteristics of *S. japonica* were investigated using a thermogravimetric analyser.

2.4 Literature review – IV; Kinetic study of thermochemical process

2.4.1 Introduction

Biomass from any source could produce renewable energy through thermochemical route by breaking its chemical structure consisting of some carbon-containing hydrocarbons. Biomass can be classified based on different sources as waste agricultural residue, wood softwood or hardwood, forestry residue, aquatic biomass, marine algae, etc. Pyrolysis converts biomass into high energy content biofuels required for the adequate temperature and heating rate to get proposed results and this may be used in internal combustion engines and gas turbines after an intermediate process that converts into liquid/gaseous fuels [121, 122]. Pyrolysis is the first step in all thermochemical conversion process after drying of feedstocks in inert atmosphere. Some of the factors such as heating rate, temperature, pressure, residence time, composition of biomass material, size of particles and moisture content are determinants of the thermal decomposition of biomass and it is a complicated series of chemical reactions. These chemical reactions are also highly influenced by the trace mineral matters present in biomass. So, interaction between constituents and the trace mineral matters in all the biomass that assists to catalyse numerous chemical reactions during pyrolysis caused the severity of reactions, making it more difficult to get an outlook of the lignocellulosic biomass [123, 124].

Numerous researchers intensively investigated the kinetic of biomass pyrolysis in detail [125 - 136]. Thermogravimetric analysis (TGA) is most general method used for kinetic analysis of devolatization. In literature many research works have been done on different

materials that described the pyrolysis behaviour by TGA methods. Such work was carried out by rubber-derivative [137], plastic [138], natural fibres [139], others types of biomass [140, 141] during thermal degradation. Usually, in case of lignocellulosic biomass with hemicellulose, cellulose and lignin, the pyrolysis behaviour was characterized by TGA method under nitrogen atmosphere and investigated by many researchers across the world. The pyrolysis behaviour of each material is unique and mainly dependent on its chemical compositions in the feedstocks. Gasparovic et al. [142] had studied the pyrolysis of wood and main wood compounds by thermogravimetry under nitrogen atmosphere and the results showed that the decomposition of wood occurred in three stages: water evaporation, active and passive pyrolysis zone. The decomposition of hemicellulose and cellulose occurred in active pyrolysis zone in the temperature range of 200°C to 380°C and 260°C to 380°C, respectively. Lignin decomposed in both active and passive pyrolysis zone in the temperature range of 180°C to 900°C. The thermal decomposition of corn stovers was carried out in both nitrogen and air atmospheres and it was observed that there were three distinct stages of weight loss in both the condition and kinetic parameters were also similar at lower rate of heating. With increasing heating rate, the second stage decomposition occurred rapidly and activation energy was higher than activation energy in nitrogen atmosphere. The activation energy during the main decomposition stage was in the range of 190 – 217 kJ/mol which was influenced by the conversion. But, at higher conversion, the activation energy started slowing down [143]. Similar effect was also noticed by S.Maiti et al. [144]. At lower rate of heating the curves are comparatively flatter than at higher heating rates. As it is well known that lower rate of heating meant more residence time. At lower rate of heating, the temperature profile along the cross-section of material can be assumed linear as both the outer surface and the inner core of biomass material achieved the same temperature at a particular time. For higher rate of heating, a major difference in temperature profile existed along the cross-section of biomass. The difference in the total degradation at a higher heating rate to the lower heating rate may also arise due to the kinetics of degradation that does not allow the completion of reaction at higher heating rate. Again, at lower rate of heating sufficient time is not provided to evolve the volatile matter. So, as a result with increasing temperature the degradation and rate of reaction had gone up. Song Hu et al. had studied the slow pyrolysis of six Chinese biomass by thermogravimetric experiment [145]. The selected biomass studied in this experiment were rice straw, camphor branch, rice husk, cherry bay branch, cotton straw, and maize straw. The result showed that the one-step model was not enough to elaborate the pyrolysis

of biomass. Thus, they examined on three-pseudocomponent models which were fruitful in simulating the biomass pyrolysis. It was found that the three-pseudocomponent model with *n*-order kinetics (model-II) was more prominent than that of first order kinetic (model-II). Activation energies were also higher in the case of model-II than model-I. V. Strezov et al. developed a suitable technique, named CATA (computer aided thermal analysis) which could measure the specific heat and heat of reactions during decomposition of biomass which were investigated to determine the heat requirement for maintaining the thermal conversion process of biomass to charcoal [146]. The experiments were carried out in four different species, named as sugar pine (*Pinus lambertiana*), radiate pine (*Pinus radiate*), meranti (*Shorea spp.*), tasmanian oak (*Eucalyptus obliqua*).

Chemical kinetic in thermochemical conversion is extremely helpful for predicting thermal and pyrolysis behaviour of a material. One such biomass sawdust along with hemicellulose, cellulose and lignin were investigated in detail about the thermochemical behaviour of pyrolysis in nitrogen atmosphere at the heating rate of 5, 10, 15 and 20°C min^{-1}. In this work, four synthesized samples were used for pyrolysis experiments.

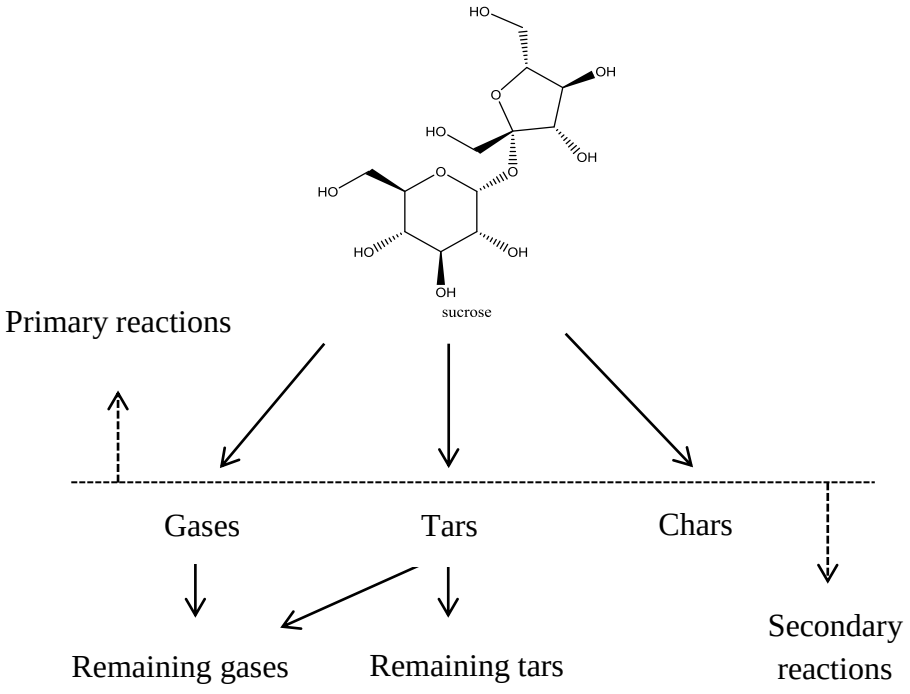

FIGURE 2.4.1: Different steps of pyrolysis of sucrose biomass.

They were CL (the weight ratio of cellulose to lignin = 1:1), CH (cellulose to hemicellulose = 1:1), LH (lignin to hemicellulose = 1:1) and CLH (cellulose : lignin : hemicellulose = 1:1:1). For kinetic study, the distributed activation energy model (DAEM) was used in this study as described in the literature [147, 148]. M. G. Gronli et al. [149] investigated the thermogravimetric analysis and devolatilization kinetics of different wood including softwood and hardwood Douglas fir, two pine species, redwood, spruce and beech, alder, birch, and oak, respectively at a heating rate of 5 K min^{-1}. The devolatalization mechanism was considered here as consisting of three parallel reactions and the same set of activation energies for hemicellulose, cellulose and lignin (100, 236 and 46 kJ/mol), that could describe the high temperature degradation behaviour of all of the woods with a perfect accuracy. M. Corbetta et al. examined the different pyrolysis models based on chemical reactions and transport of heat and species, implemented independently in two different software environments, namely (1) a particle-scale model implemented in the COMSOL environment and combining the pyrolysis kinetics with transport model, (2) the GASDS code, a multiphase and multiscale comprehensive mathematical model, coupling transport phenomena and kinetics schemes both at the particle and reactor scale [150]. Again, one such material sucrose biomass was investigated with a thermogravimetric analysis with gas chromatography (TGA-GC) system at different temperatures and various heating rates [151]. Fig. 2.4.1 shows the probable different steps of pyrolysis of sucrose biomass and the gaseous products consisted of a major amount of CO, CO_2, H_2 and CH_4.

2.4.2 Description of different kinetic models

There is several kinetics methods for analysing non-isothermal solid state kinetic data from thermogravimetric analyses and many literature were published based on this model. These methods were classified into two types: model-fitting and model-free (isoconversional) methods were presented in table 2.4.1 [152, 153].

Model-fitting methods are best described by the different fitting models to the data that assists the best statistical fit as the model from which the kinetic parameters are calculated. The isoconversional methods need numerous kinetics curves to elaborate the analysis. From this method the activation energy is calculated for a given value of conversion at different heating rates.

TABLE 2.4.1: Different methods for analysing solid-state kinetics.

Model-fitting		Model free	
Isothermal	Non-isothermal	Isothermal	Non-isothermal
conventional	Differential	Standard	Kissinger
	Freeman-Carroll	Friedman	Flynn-Wall and Ozawa
	Coats-Redfern	AIC	Vyazovkin and AIC
			Kissinger–Akahira–Sonuse

If we look back to the ancient times, model-fitting methods were most common which were used for solid state reaction because by a single TGA experiment evaluation of kinetic parameters was possible. There are certain problems regarding the inability to measure the kinetics model uniquely, especially for non-isothermal data [154]. Generally, model-fitting methods for non-isothermal data provided higher values for evaluating the kinetic parameters. So, these methods readily became defunct in favour of isoconversional methods. In order to avoid the problems in model-fitting methods, it was found advantageous to use model-free methods because of simplicity or ease of operation. These methods assist to determine estimated activation energy (E_a), for given value of conversion (α), for an independent model. It was possible to determine the estimated activation energy at each conversion [155]. Numerous literatures were published based on the thermal degradation of biomass at different heating rates. Their kinetic parameters were evaluated through TGA data and the degradation of biomass consisting of hemicellulose, cellulose and lignin were investigated by TGA data. Some of the numerical models were Arrhenius approach through multi-linear regression technique [143, 152, 156], model-free Friedman method isothermal [157], Model-free Flynn-Wall and Ozawa method (non-isothermal) [158, 159], and Model-free Kissinger–Akahira–Sonuse (non-isothermal) [160, 161].

2.5 Literature review – V; Steam gasification of bio-char/biomass

2.5.1 Introduction

Biomass gasification was very popular since ancient times for its power generation; gaseous product, and liquid fuel production, sometimes even valuable chemicals could also be recovered [162]. The most important thing is that the heterogeneous gasification reactions occurred during gasification process that includes solid carbon is: (1) the boudouard reaction, (2) water-gas reaction and (3) the heterogeneous methanation.

$$C + CO_2 \leftrightarrow 2CO \quad (2.5.1)$$

$$C + H_2O \leftrightarrow CO + H_2 \quad (2.5.2)$$

$$C + 2H_2 \leftrightarrow CH_4 \quad (2.5.3)$$

Bio-char steam gasification too was an interesting research topic, especially in the coal gasification research in 1980s. A lot of work has been done since on steam gasification of coal or bio-char with various mixed or impregnated alkali metals such as: K_2CO_3, KOH, KCl, $KHCO_3$, KNO_3, K_3PO_4, Na_2O_3, NaOH, NaCl [163 - 174]. Apart from this, calcium has also been investigated on char steam gasification as it is cheap substitute to alkali metals: CaO [165, 173] or iron in the form of Fe_2O_3 [166]. Some methods were adopted to deal with the steam gasification of demineralised coal char [175]. Hauserman [176, 177] showed that on mixing wood with wood ash (10 wt. %), the gasification rate (starting from wood) increased by a factor of 32 at 700°C. F. Yan and his co-workers [178] investigated the steam gasification of bio-char produced from the fast pyrolysis of liquefaction of pine sawdust in a fixed-bed, at final temperature of 500°C; particle size below 0.25 mm, with heating rate of 30°C/min. The main focus was to determine the effect of steam temperature and flow rate on syn-gas yield and its composition. After carrying out numerous experiments on varying temperature and steam flow rate, results showed that both high temperature and precise injection of steam lead to higher yield of dry gas and higher carbon conversion efficiency. The best result of dry gas yield was obtained at 850°C temperature and the steam flow rate of 0.165 g/min/g bio-char. M. Asadullah et al. [179] investigated the effect of bio-char structure on its gasification reactivity. To carry out this experiment, the bio-char was prepared from the fast pyrolysis of mallee wood in order to investigate the structural features and combustion reactivity by using Raman spectroscopy. The total Raman peak areas were obtained between 800 and 1800 cm^{-1} along with the combustion reactivity of chars and it evidently showed decrease with increasing the pyrolysis temperature due to the increasing aromatization of chars and loss of oxygen containing groups. H. Haykiri-Acma et al. [180] analyzed some agricultural residue and

waste biomass samples such as sunflower shell, pinecone, rapeseed, cotton refuse, and olive refuse were initially pyrolyzed in nitrogen atmosphere (40 cm^3 min^{-1}) at 20 K min^{-1} rate of heating from ambient to 1000°C. The obtained char was gasified in a mixture of steam and nitrogen exactly in the same condition as in thermogravimetric analyses. The final conclusion was made in which the gasification characteristics of bio-char were somehow found to be dependent on the biomass properties such as ash and fixed carbon and the constituents present in the ash. While, for the chars obtained from rapeseed and olive refuse were not satisfactorily gasified. F. Marquez-Montesinos et al. and his team [181] investigated the CO_2 and steam gasification of a grapefruit skin char along with a kinetic study. The chars obtained from this agricultural waste showed good reactivity due to the catalytic effect of inorganic matter. It was found that the ash content in the carbonised substrate had come down to 15% (dry basis) potassium being main alkali constituent. The result showed that for both CO_2 and steam gasification, the reactivity increased with increasing conversion along with increased reactivity per unit surface area due to catalytic effect as mentioned earlier. The increased reactivity was proven by after acid washing helped to reduce the reactivity, thus confirming the catalytic effect of inorganic matters present in ash. The apparent activation energy lied in the range 200 – 250 kJ mol^{-1} was obtained for CO_2 gasification, while for the steam gasification values had fallen down to between 130 and 170 kJ mol^{-1}. C. Franco et al. [182] investigated on the reactions influencing the biomass steam gasification process in an atmospheric fluidized bed. The variable parameters including temperature and steam to biomass ratio varied at 700 – 900°C and from 0.4 – 0.85 (w/w), respectively. So, to carry out this experiment, three types of forestry biomass were studied, namely *Pinus pinaster* (softwood), *Eucaluptus globulus* and holm oak (hardwood). The energy consumption, gas composition, higher heating value, and gas yields were also evaluated and correlated with temperature, steam/biomass ratio, and species of biomass used. After carrying out several experiments, the final results were optimised at 830°C temperature and a steam to biomass ratio 0.6 – 0.7 (w/w) found poorer in hydrocarbons and tars were produced with greater energy and carbon conversions were also found. The different class of biomass has versatility in the energy application as it offered numerous advantages in terms of transportation of fuel, conversion into different form of fuels such as liquid or gas, and the pollutants are much less compared to fossil fuel and it has wide applicability for small to medium scale at the industrial level. W. Close et al. [183] had studied the intrinsic reaction rate of biomass char gasification of beech wood char and oil palm shell char with carbon dioxide and steam. In

this experiment, special attention was paid in order to avoid heat and mass transport limitations during gasification, the particle size, amount of char, and flow rate were also varied in isothermal conditions. So, a rate expression Langmuir – Hinshelwood was also employed to match the experimental data at different partial pressures and reaction temperatures in the intrinsic regime. For evaluation of the experimental data, the reactive surface area of bio-chars was determined as a function of the degree of conversion by the temperature-programmed desorption technique. From this analysis it was concluded that the reaction rate was mostly influenced and dependent with the reactive surface area. As it was well known, the characteristics of biomass varied from place to place owing to the physical properties of soil across the world. K. Matsumoto et al. [184] investigated the gasification reaction kinetics on biomass char obtained as a by-product of gasification in an entrained-flow gasifier with steam and oxygen at 900 - 1000°C. The bio-chars were obtained from the wood portion of Japanese cedar char (JC), Japanese cedar bark char (JB), and a mixture of hardwood char (MH) and Japanese lawngrass char (JL). These chars were gasified in a drop tube furnace, where the parametric studies were also carried out as temperature (T_g), gasifying agent (CO_2 or H_2O) along with its partial pressure were varied in order to measure the gasification properties such as gasification reaction ratio, gasification reaction rate, change of particle size and change of surface area. The surface characteristics were analyzed by a scanning electric microscope (SEM). The final result showed that the random pore model was most convenient for the char gasification reaction due to the surface porosity, constant particle size, and specific surface area and gasification rate as experimentally obtained from Arrhenius equation along with the value was calculated by using random model. The reactivity order was found as MH > JC > (JB, JL) and was mostly influenced by the presence of the concentration of alkali metals in the feedstocks along with O/C ratio in biomass. C. Guizani and his co-workers [185] investigated the gasification reactivity of high-heating-rate chars in single and mixed atmospheres of H_2O and CO_2 in a new macro-TG experimental device. The most important thing in this study was to compare between the higher reactivity of the high-heating-rate chars vs.at a low heating rate chars. The reactivity of chars in a mixed atmosphere of steam and carbon dioxide was derived as the sum of the individual reactivity's achieved in single atmosphere gasification experiments. The final result showed the heating rate greatly affected the char reactivity to H_2O along with CO_2. It was found that high-heating-rate reactivity was 3.5 times higher in H_2O gasification and was found to be four times higher in CO_2 gasification in comparison with LHR-chars. S. Turn et al. [186] investigated on an

experimental basis hydrogen production from biomass performed in a fluidized bed gasifier. The parametric study was extremely important for the process optimization which included the effect of reactor temperature, equivalence ratio, and steam to biomass ratio as listed in the article. S. T. Chaudhari and his co-workers [187] carried out steam gasification of two biomass-derived chars obtained from (1) bagasse char-from Natural Resources Canada, and (2) commercial char-obtained from ENSYN Technologies Inc. were investigated at 700, 750 and 800°C in a fixed bed microreactor at different steam flow rates in the range of 1.25 to 10 g/h/g of char. It was found that the both chars were highly reactive at 800°C with steam flow rate of 5 and 10 g/h/g of char. The experimental result showed for baggase char was maximum conversion of 81% achieved at 800°C with a steam flow rate of 10 g/h/g of char, while for commercial baggase maximum conversion of 69% was achieved at 800°C with steam flow rates of 5 and 10 g/h/g of char. Y. Li and his team [188] demonstrated the hydrogen production from coal gasification in supercritical water with a continuous flowing system by which it can convert coal to hydrogen rich gaseous products efficiently. For this the experimental device was developed to sustain the temperature upto 800°C and the pressure upto 30 MPa. The gasification characteristics of coal were determined by a set of parameters such as temperatures range of 650 – 800°C, pressure of 23 – 27 Mpa, flow rate from 3 kg h^{-1} to 7 kg h^{-1}. Some other parameters such as Raney-Ni, K_2CO_3 were used as a catalyst along with H_2O_2 as an oxidant. The effects of these parameters were evaluated in order to optimize the process. The highest hydrogen yield was achieved (72.85%) in this experiment. A. Sattar et al. and his co-workers [189] investigated the steam gasification of rapeseed, wood, sewage sludge, and miscanthus bio-chars for the production of hydrogen-rich syngas. The parametric study included the effect of temperature, steam flow rate and particle size was evaluated for process optimization. The final result showed that the dry gas yield increased with increasing temperature and steam flow rate, but hydrogen fraction decreased with increasing temperatures, while particle size had little impact on gaseous composition. The highest hydrogen yield of 58.7 vol % at 750°C was obtained for rapeseed bio-char.

2.5.2 An overview of steam gasification process of bio-char

Bio-char is generally obtained from the slow pyrolysis of biomass at elevated temperature in nitrogen atmosphere or in vacuum condition in order to avoid ash formation. The characteristic of this bio-char is further improved in terms of as a fuel value against the raw

biomass. Owing to removal of oxygen content during pyrolysis of biomass, the carbon content is improved to a large extent which amends the calorific value of bio-char along with carbon content. The reactivity of bio-char is extremely good over biomass could be easily gasified with gasifying agents steam, CO_2, oxygen, and hydrogen to gaseous fuel. Apart from this, it can be used as a soil nutrient for enrichment of good fertility [190]. So, now-a-days steam gasification of bio-char is becoming vastly popular to convert solid fuel to gaseous fuel. Other option is that the syngas can also be converted into liquid fuels using Fischer – Tropsch technology. And also, the product gas could be directly used in the production of electrical power in fuel cells or combusted in gas turbines.

2.5.3 Reaction mechanism

In general, steam gasification reactions are complicated as main constituents are CO_2, CO, H_2, and CH_4. The steam gasification is a heterogeneous reaction mechanism as the steam reacts with the surface area of carbon. It was well known that the steam gasification reactions are some exothermic or endothermic as listed following [178, 191]:

$$C_pH_qO_r \rightarrow aCO_2 + bH_2O + cCH_4 + dCO + eH_2 + fC_2 \text{ (pyrolysis reaction)} \quad (2.5.4)$$

$$CO_2 + C \leftrightarrow 2CO \quad (+172 \text{ kJ/mol}) \quad (2.5.5)$$

$$C + H_2O \leftrightarrow CO + H_2 \quad (+131 \text{ kJ/mol}) \quad (2.5.6)$$

$$C + 1/2O_2 \rightarrow CO \quad (-111 \text{ kJ/mol}) \quad (2.5.7)$$

$$CH_4 + H_2O \leftrightarrow CO + 3H_2 \quad (+206 \text{ kJ/mol}) \quad (2.5.8)$$

$$CO + H_2O \leftrightarrow CO_2 + H_2 \quad (-41.2 \text{ kJ/mol}) \quad (2.5.9)$$

$$C + 2H_2 \leftrightarrow CH_4 \quad (-74.8 \text{ kJ/mol}) \quad (2.5.10)$$

So, naturally the reaction mechanism in the steam – carbon reaction, the chemisorption stage includes dissociation of water at the carbon surface into a hydroxyl radical and hydrogen atom, which adsorbs on next to carbon sites [178]. At high temperature it is supposed to assert the dissociation of water molecule forms hydroxyl groups which are highly oxidizing agents. This phenomenon exists in a similar fashion of water gas shift reaction. Carbon-oxide intermediate plays a crucial role in the reaction and hydrogen atoms freely diffuse across carbon at most likely higher temperature (> 600°C). The most

important thing is that the relative rates of these reactions are highly influenced by the reaction conditions. The product syn-gas in gasification reactions is interdependence of molecules, mostly varying with reactor design and operating conditions.

2.6 Research gap identification

The most challenging part of research gap identification is to bring out novelty or innovative feature that might be different from the conventional approach. Our research asserts that the thermochemical conversion of solid biomass to syn-gas or bio-oil or bio-char is important in the current literature. So, proper characterization of biomass is extremely important prior to choosing any thermochemical conversion process. Another objective of this study is the selection of biomass from waste-land derived sources that is from barren land, not from fertile land.

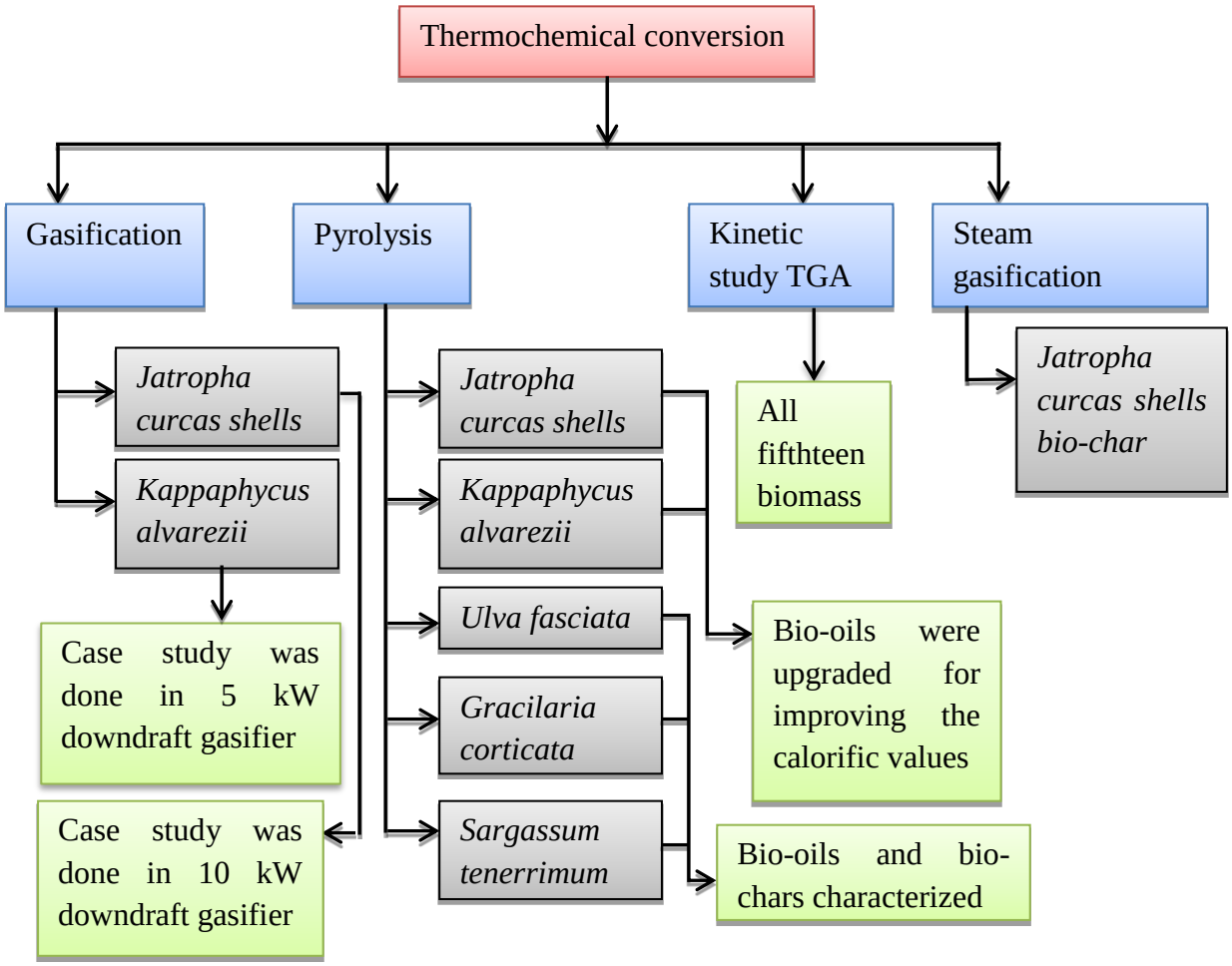

FIGURE 2.6.1: Schematic diagram of the experimental works carried out in the present study.

The speciality of this biomass is that it cannot be used as an animal fodder. Hence this biomass is suitable in thermochemical conversion process in order to produce clean energy. The present study mainly focuses on fifthteen different biomass from different category such as grass type biomass, herb type biomass, shrub type biomass, woody type biomass, and finally macroalgae. Previous literature is not available on these selected biomass and their thermochemical pathways. So, this problem is targeted in the present study. The thermochemical conversion processes are briefly outlined in Fig. 2.6.1 for some selected biomass. The kinetic study is a part of thermochemical process that's why it is included here and it is best described by the TGA (thermogravimetric analysis). Due to the limited scope of the research work time, it was yeoman task to carry out experiment for each biomass to get the valuable information. So, the full characterization of each biomass was investigated in details and conclusions were derived from the results obtained.

References:

1. Aden A, Ruth M, Ibsen K, Jechura J, Neeves K, Sheehan J, Wallace B Montague L, Slayton A, Lukas J, (2002), Lignocellulosic Biomass to Ethanol Process Design and Economics Utilizing Co-Current Dilute Acid Prehydrolysis and Enzymatic Hydrolysis for Corn Stover. Report No. NREL/TP-510-32438. Golden, CO: National Renewable Energy Laboratory, http://www.nrel.gov/docs/fy02osti/32438.pdf.

2. Humbird D, Davis R, Tao L, Kinchin C, Hsu D, and Aden A, (2011), Process Design and Economics for Biochemical Conversion of Lignocellulosic Biomass to Ethanol. Report No. NREL/TP-5100-47764, National Renewable Energy Laboratory, http://www.nrel.gov/docs/fy11osti/47764.pdf.

3. Jonathan R Mielenz (2001), Ethanol production from biomass: technology and commercialization status, Current Opinion in Microbiology 4, 324–329.

4. DC Rakopoulos, CD Rakopoulos, EC Kakaras, EG Giakoumis, (2008), Effects of ethanol–diesel fuel blends on the performance and exhaust emissions of heavy duty DI diesel engine, Energy Conversion and Management 49, 3155–3162.

5. Farid Safari, Omid Norouzi, Ahmad Tavasoli, (2016), Hydrothermal gasification of *Cladophora glomerata* macroalgae over its hydrochar as a catalyst for hydrogen-rich gas production, Bioresource Technology, 222, 232-241.

6. Dong Zhou, Liang Zhang, Shicheng Zhang, Hongbo Fu and Jianmin Chen, (2010), Hydrothermal Liquefaction of Macroalgae Enteromorpha prolifera to Bio-oil, *Energy Fuels*, 24, 4054–4061.

7. Jiele Xu, Ziyu Wang, Jay J. Cheng, (2011), Bermuda grass as feedstock for biofuel production: A review, Bioresource Technology, 102, 7613–7620.

8. JM Lee, J Shi, RA Venditti, H Jameel, (2009), Autohydrolysis pretreatment of coastal Bermuda grass for increased enzyme hydrolysis, Bioresource Technology, 100, 6434–6441.

9. Michelle J Serapiglia, Charles A Mullen, Lawrence B Smart, Akwasi A Boateng, (2015), Variability in pyrolysis product yield from novel shrub willow genotypes, Biomass and Bioenergy, 72, 74 – 84.

10. MJ Ferna´ndez Llorente, JE Carrasco Garcı´a, (2006) Concentration of elements in woody and herbaceous biomass as a function of the dry ashing temperature, Fuel 85, 1273–1279.

11. MJ Ferna´ndez Llorente, JM Murillo Laplaza, R Escalada Cuadrado, JE Carrasco Garcı´a (2006), Ash behaviour of lignocellulosic biomass in bubbling fluidised bed combustion, Fuel 85, 1157–1165.

12. J Xu, JJ Cheng, RR Sharma-Shivappa, JC Burns, (2010a), Sodium hydroxide pretreatment of switchgrass for ethanol production, Energy Fuels 24, 2113– 2119.

13. NREL, (2006), Biomass Feedstock Composition and Property Database, Available from: <http://www1.eere.energy.gov/biomass/feedstock_databases.html>.

14. J Shi, (2007), Microbial Pretreatment of Cotton Stalks by Phanerochaete chrysosporium for Bioethanol Production, Ph.D. dissertation, North Carolina State University, Raleigh.

15. Y Sun, JJ Cheng, (2005), Dilute acid pretreatment of rye straw and Bermuda grass for ethanol production, Bioresource Technology, 96, 1599–1606.

16. S Reshamwala, BT Shawky, BE Dale, (1995), Ethanol production from enzymatic hydrolysates of AFEX-treated coastal Bermuda grass and switchgrass, Applied Biochemistry and Biotechnology 51–52, 43–55.

17. B Gabrielle, L Bamière, N Caldes, S DeCara, G Decocq, F Ferchaud, C Loycef, E Pelzer, Y Perez, J Wohlfahrt, G Richard, (2014), Paving the way for sustainable bioenergy in Europe: Technological options and research avenues for large-scale biomass feedstock supply, Renewable and Sustainable Energy Reviews 33, 11–25.

18. MC Chow, WR Jackson, A L Chaffee, and M Marshall, (2013),Thermal Treatment of Algae for Production of Biofuel, Energy Fuels, 27, 1926−19.

19. Hernando Guerrero, Carlos Lafuente, Felix Royo, Laura Lomba, and Beatriz Giner , (2011), *PρT* Behavior of Several Chemicals from Biomass. Energy Fuels, 25, 3009–3013.

20. Mariefel B Valenzuela, Christopher W Jones, and Pradeep K Agrawal, (2006), Batch Aqueous-Phase Reforming of Woody Biomass, Energy & Fuels, 20, 1744-1752.

21. Alexander L Brown, David C Dayton, and John W Daily, (2001), A Study of Cellulose Pyrolysis Chemistry and Global Kinetics at High Heating Rates, Energy & Fuels, 15, 1286-1294.

22. Taro Sonobe, Nakorn Worasuwannarak, (2008), Kinetic analyses of biomass pyrolysis using the distributed activation energy model, Fuel, 87, 414–421.

23. Haiping Yang, Rong Yan, Hanping Chen, Chuguang Zheng, Dong Ho Lee, and David Tee Liang, (2006), In-Depth Investigation of Biomass Pyrolysis Based on Three Major Components: Hemicellulose, Cellulose and Lignin, Energy & Fuels, 20, 388-393.

24. Shayan Karimipour, Regan Gerspacher, Rajender Gupta, Raymond J. Spiteri, (2013), Study of factors affecting syngas quality and their interactions in fluidized bed gasification of lignite coal, Fuel, 103, 308–320.

25. AC Koufopanos, G Maschio, A Lucchesi, (1989), Kinetic modelling of the pyrolysis of biomass and biomass components, Canadian Journal of Chemical Engineering, 67, 75–84.

26. B Li, S Kado, Y Mukainakano, T Miyazawa, T Miyao, S Naito, K Okimura, K Kunimori, K Tomishige, (2007), Surface modification of Ni catalysts with trace Pt for oxidative steam reforming of methane, Journal of Catalysis, 245, 144–155.

27. S, Wang, GQ Lu, (1996), Carbon dioxide reforming of methane to produce synthesis gas over metal-supported catalysts: state of the art, Energy & Fuels, 10, 896–904.

28. H Liu, S Li, S Zhang, L Chen, G Zhou, J Wang, X Wang, (2008), Catalytic performance of monolithic foam Ni/SiC catalyst in carbon dioxide reforming of methane to synthesis gas, Catalysis Letters, 120, 111–115.

29. S.M. Char, Walter P. Walawender and L.T. Fan, Mass and energy balance analysis of a downdraft gasifier.

30. Krushna Patil, Prakash Bhoi, Raymond Huhnke, Danielle Bellmer, (2011), Biomass downdraft gasifier with internal cyclonic combustion chamber: Design, construction, and experimental results, Bioresource Technology, 102, 6286–6290.

31. Anwar Sattar, Gary A. Leeke, Andreas Hornung, Joseph Wood, (2014), Steam gasification of rapeseed, wood, sewage sludge and miscanthus biochars for the production of a hydrogen-rich syngas, Biomass and bioenergy 69, 276 -286.

32. Subarna Maiti, Pratap Bapat, Prasanta Das, Pushpito K. Ghosh, (2014), Feasibility study of jatropha shell gasification for captive power generation in biodiesel production process from whole dry fruits, Fuel, 121, 126–132.

33. AV Bridgwater, (2003), Renewable fuels and chemicals by thermal processing of biomass, Chemical Engineering Journal, 91, 87–102.

34. J Vehlow, (1996), Municipal solid waste management in Germany, Waste Management, 16, 367–374.

35. O Ayalon, Y Avnimelech, M Shechter, (2000), Alternative MSW treatment options to reduce global greenhouse gases emissions—the Isreali example, Waste Management Research, 18 , 538–544.

36. Thomas Malkow, (2004), Novel and innovative pyrolysis and gasification technologies for energy efficient and environmentally sound MSW disposal, Waste Management, 24, 53–79.

37. BM Jenkins, LL Baxter, TR Miles Jr., TR Miles, (1998), Combustion properties of biomass, Fuel Processing Technology, 54, 17–46.

38. Chih-Lun Hsi, Tzong-Yuan Wang, Chien-Hsiung Tsai, Ching-Yuan Chang, Chiu-Hao Liu, Yao-Chung Chang, and Jing-T. Kuo, (2008), Characteristics of an Air-Blown Fixed-Bed Downdraft Biomass Gasifier, Energy & Fuels, 22, 4196–4205.

39. Huanpeng Liu, Yujie Feng, Shaohua Wua, Dunyu Liu, (2009), The role of ash particles in the bed agglomeration during the fluidized bed combustion of rice straw, Bioresource Technology, 100, 6505–6513.

40. Samy S Sadaka, AE Ghaly, MA Sabbah, (2002), Two-phase biomass air-steam gasification model for fluidized bed reactors: Part III—model validation, Biomass and Bioenergy, 22, 479 – 487.

41. Bing Guo, Dingkai Li, Congming Cheng, Zi-an Lu, Youting Shen, (2001), Simulation of biomass gasification with a hybrid neural network Model, Bioresource Technology, 76, 77-83.

42. AB Ross, JM Jones, ML Kubacki, T Bridgeman, (2008), Classification of macroalgae as fuel and its thermochemical behaviour, Bioresource Technology, 99, 6494–6504.

43. D Vamvuka, D Zografos, (2004), Predicting the behaviour of ash from agricultural wastes during combustion, Fuel 83, 2051–2057.

44. TR Miles, TR Miles Jr., LL Baxter, RW Bryers, BM Jenkins, LL Oden, (1996), Biomass Bioenergy, 10(2–3), 125.

45. Prabir Basu, Biomass Gasification and Pyrolysis Practical Design and Theory.

46. Keigo Matsumoto, Keiji Takeno, Toshimitsu Ichinose, Tomoko Ogi, Masakazu Nakanishi, (2009), Gasification reaction kinetics on biomass char obtained as a by-product of gasification in an entrained-flow gasifier with steam and oxygen at 900 – 1000°C, Fuel, 88, 519–527.

47. F Marquez-Montesinos, T Cordero, J Rodriguez-Mirasol, JJ Rodriguez, (2002), CO_2 and steam gasification of a grapefruit skin char, Fuel, 81, 423 – 429.

48. D Geldart, (1972), The effect of particle size and size distribution on the behaviour of gas-fluidized beds, Powder Technology, 6, 201–215.

49. Prabir Basu. Combustion and Gasification in fluidized beds.

50. G Skodras, GP Sakellaropoulos, (2002), Mineral matter effects in lignite gasification, Fuel Processing Technology, 77–78, 151– 158.

51. DC Dayton, BM Jenkins, SQ Turn, RR Bakker, RB Williams, D Belle-Oudry, LM Hill, (1999), Energy Fuels, 13, 860.

52. LL Baxter, TR Miles, TR Miles Jr., BM Jenkins, T Milne, D Dayton, RW Bryers, LL Oden, (1998), Fuel Processing Technology, 54(1–3), 47.

53. DW Bapat, SV Kulkarni, VP Bhandarkar, (1997), Fluidized Bed Combustion, 1, 165.

54. K Raveendran, Anuradda Ganesh and Kartic C Khilar, (1996), Pyrolysis characteristics of biomass and biomass components, Fuel, 75, 987 – 998.

55. C Higman and M Burgt, Gasification, Elsevier, U.S.A., p. 105, 2003.

56. GJ Stiegel, (2005), Overview of Gasification Technologies, Global Energy and Energy Project (GCEP) Advanced Coal Workshop, Provo, UT.

57. LS Johansson, C Tullina, B Leckner, P Sj'ovall, (2003), Particle emissions from biomass combustion in small combustors, Biomass and Bioenergy, 25, 435 – 446.

58. J Dasch Muhlbaler, (1982), Particulate and gaseous emissions from wood-burning fireplaces, Environmental Science and Technology, 1982, 639–45.

59. C Hueglin, C Gaegauf, S K'unzel, H Burtscher, (1997), Characterization of wood combustion particles: morphology, mobility, and photoelectric activity, Environmental Science and Technology, 31, 3439–47.

60. A Porteous, (2005), Why energy from waste incineration is an essential component of environmentally responsible waste management, Waste Management, 25, 451–459.

61. CS Psomopoulos, A Bourka, NJ Themelis, (2009), Waste-to-energy: a review of the status and benefits in USA, Waste Management, 29, 1718–1724.

62. Umberto Arena, (2012), Process and technological aspects of municipal solid waste gasification. A review, Waste Management, 32, 625–639.

63. A V Bridgwater, (1994a), Catalysis in thermal biomass conversion, Applied Catalysis A: General, 116, 5–47.

64. V Belgiorno, G De Feo, C Della Rocca, RMA Napoli, (2003), Energy from gasification of solid wastes, Waste Management, 23, 1–15.

65. Dinesh Mohan, Charles U Pittman, Jr., and Philip H Steele, (2006), Pyrolysis of Wood/Biomass for Bio-oil: A Critical Review, Energy & Fuels, 20, 848-889.

66. SC Davis, (1998), Transportation Energy Data Book 18, Technical Report ORNL-6941, Oak Ridge National Laboratory, Oak Ridge, TN, (available via the Internet at http://cta.ornl.gov/data/Index.shtml).

67. Romain Morel and Igor Shishlov, (2015), Ex-post evaluation of the kyoto protocol: four key lessons for the Paris agreement.

68. AV Bridgwater, GVC Peacocke, (2000), Renewable and Sustainable Energy Reviews, 4 (1), 1-73.

69. AV Bridgwater, D Meier, D Radlein, (1999), Organic Geochemistry, 30, 1479-1493.

70. AV Bridgwater, (2003), Chemical Engineering Journal, 91 (2-3), 87-102.

71. AV Bridgwater, (1999), Journal of Analytical and Applied Pyrolysis, 51, 3-22.

72. D Meier, O Faix, (1999), Bioresource Technology, 68, 71-77.

73. SS Kelley, J Jellison, B Goodell, (2002), FEMS Microbiology Letters, 209, 107-111.

74. C Gerdes, CM Simon, T Ollesch, D Meier, W Kaminsky, (2002), Engineering Life Science, 2 (6), 167-174.

75. S Czernik, DK Johnson, S Black, (1994), Biomass Bioenergy, 7(1-6), 187-192.

76. A Oasmaa, DJ Meier, (2005), Journal of Analytical and Applied Pyrolysis, 73 (2), 323-334.

77. M E Boucher, A Chaala, C Roy, (2000), Biomass Bioenergy, 19, 337-350.

78. ME Boucher, A Chaala, H Pakdel, C Roy, (2000), Biomass Bioenergy, 19, 351-36.

79. S Sinha, A Jhalani, MR Ravi, AJ Ray, (2000), Solar Energy Society of India (SESI) 10 (1), 41-62.

80. Prabir Basu. Biomass Gasification and Pyrolysis, Practical Design and Theory

81. By Encarnacio´n Raymundo-Pin˜ero, Martin Cadek, and Franc¸ois Be´guin, (2009), Tuning Carbon Materials for Supercapacitors by Direct Pyrolysis of Seaweeds. Advanced Functioned Materials, 19, 1032–1039.

82. E Marinho-Soriano, P C Fonseca, M A A Carneiro, W S C Moreira, (2006), Bioresource Technology, 97, 2402.

83. S Czernik, AV Bridgwater, (2004), Energy Fuels, 18, 590-598.

84. ENSYN Group, Inc.: Greely, CA, (2001), The conversion of wood and other biomass to bio-oil.

85. Ayse Eren Putun, Eylem O¨nal, Basak Burcu Uzun, Nurgul O¨zbay, (2007), Comparison between the "slow" and "fast" pyrolysis of tobacco residue. Industrial Crops and Products, 26, 307–314.

86. A Oasmaa, S Czernik, (1999), Energy Fuels,13, 914-921.

87. http://dynamotive.com/biooil/whatisbiooil.html.

88. S Godiganur, CHS Murthy, RP Reddy, (2009), 6BTA 5.9 G2-1 Cummins engine performance and emission tests using methyl ester mahua (Madhuca indica) oil/diesel blends, Renewable Energy, 34, 2172–7.

89. B Baiju, MK Naik, LM Das, (2009), A comparative evaluation of compression ignition engine characteristics using methyl and ethyl esters of Karanja oil, Renewable Energy, 34, 1616–21.

90. MN Nabi, MM Rahman, MS Akhter, (2009), Biodiesel from cotton seed oil and its effect on engine performance and exhaust emissions, Applied Thermal Engineering 29, 2265–70.

91. Scott Grierson, Vladimir Strezov, Pushan Shah, (2011), Properties of oil and char derived from slow pyrolysis of Tetraselmis chui, Bioresource Technology, 102, 8232–8240.

92. X Miao, Q Wu, C Yang, (2004), Fast pyrolysis of microalgae to produce renewable fuels, Journal of Analytical and Applied Pyrolysis, 71 (2), 855–863.

93. Wild P de, (2011), Biomass pyrolysis for chemicals. ISBN: 978-90-367-4994-7.

94. Piskorz J, Scott D S, Radlien D, Composition of oils obtained by fast pyrolysis of different woods, In Pyrolysis Oils from Biomass:Producing Analyzing and Upgrading; American Chemical Society: Washington, DC, 1988; pp 167-178.

95. AA Boateng, CA Mullen, NM Goldberg, KB Hicks, CM McMahan, MC Whalen, K Cornish, (2009), Energy-dense liquid fuel intermediates by pyrolysis of guayule (*Parthenium argentatum*) shrub and bagasse, Fuel, 88, 2207–2215.

96. M Garcıa-Perez, A Chaala, C Roy, (2002), Vacuum pyrolysis of sugarcane bagasse, Journal of Analytical and Applied Pyrolysis, 65, 111–136.

97. GVC Peacocke, PA Russel, JD Jenkins, AV Bridgwater, (1994), Biomass Bioenergy 7, 169-178.

98. GVC Peacocke, ES Madrali, C Z Li, AJ Guell, R Kandiyoti, AV Bridgwater, (1994), Biomass Bioenergy, 7 (1-6), 155-167.

99. GVC Peacocke, PA Russel, AV Bridgwater, (1994), Biomass Bioenergy, 7, 147-154.

100. M Radovanovic, RH Venderbosch, W Prins, WPM van Swaaij, (2000), Biomass Bioenergy, 18, 209-222.

101. Oasmaa A, Peacock CA, (2001), Guide to Physical Property Characterization of Biomass DeriVed Fast Pyrolysis Liquids; Technical Research Centre of Finland, Espoo, Finland, VTT Publication No. 450.

102. A Oasmaa, D Meier, (2005), Journal of Analytical and Applied Pyrolysis, 73 (2), 323-334.

103. Oasmaa A, Meier D, (2005), Characterization, Analysis, Norms and Standards. In Fast Pyrolysis of Biomass, A Handbook, Volume 3; Bridgwater, A. V., Ed.; CPL Press: Newbury, U.K., pp 21-60.

104. Carmen Branca, Paola Giudicianni, and Colomba Di Blasi, (2003), GC/MS Characterization of Liquids Generated from Low-Temperature Pyrolysis of Wood, Industrial and Engineering Chemistry Research, 42, 3190-3202.

105. Carmen Branca, Colomba Di Blasi, and Rosario Elefante, (2005), Devolatilization and Heterogeneous Combustion of Wood Fast Pyrolysis Oils, Industrial and Engineering Chemistry Research, 44, 799-810.

106. Zhongyang Luo, Shurong Wang, Yanfen Liao, Jinsong Zhou, Yueling Gu, Kefa Cen, (2004), Research on biomass fast pyrolysis for liquid fuel, Biomass and Bioenergy, 26, 455 – 462.

107. Oskar Paris, Cordt Zollfrank, Gerald A Zickler, (2005), Decomposition and carbonisation of wood biopolymers—a microstructural study of softwood pyrolysis, Carbon, 43, 53–66.

108. V Stamatov, D Honnery, J Soria, (2006), Combustion properties of slow pyrolysis bio-oil produced from indigenous Australian species, Renewable Energy, 31, 2108–2121.

109. Joaquin Reina, Enrique Velo, Luis Puigjaner, (1998), Thermogravimetric study of the pyrolysis of waste wood, Thermochimica Acta, 320, 161-167.

110. Maritha Nilsson, Asa Ingemarsson, Jorgen R Pederson, and Jim O Olsson, (1999), Slow pyrolysis of birch (betula) studied with GC/MS and GC/FTIR/FID, Chemosphere, 38, 1469 – 1479.

111. Maria Olsson, Jennica Kjallstrand, Go¨ran Petersson, (2003), Oxidative pyrolysis of integral softwood pellets, Journal of Analytical and Applied Pyrolysis, 67, 135–141.

112. Tomoaki Minowa, Shin-ya Yokoyama, Michimasa Kishimoto and Toru Okakurat, (1995), Oil production from algal cells of *Dunaliella tertiolecta* by direct thermochemical liquefaction, Fuel, 74, 1735 -1738.

113. Thomas A Milne, Robert J Evans, and Nicholas Nagle, (1990), Catalytic conversion of Microalgae and Vegetable oils to premium gasoline, with shape-selective zeolite. Biomass, 21, 219 – 232.

114. Annette Bruhn, Jonas Dahl, Henrik Bangso Nielsen, Lars Nikolaisen, Michael Bo Rasmussen, Stiig Markager, Birgit Olesen, Carlos Arias, Peter Daugbjerg Jensen, (2011), Bioenergy potential of *Ulva lactuca*: Biomass yield, methane production and combustion, Bioresource Technology, 102, 2595–2604.

115. AK Siddhanta, Mahesh U Chhatbar, Gaurav K Mehta, Naresh D Sanandiya, Sanjay Kumar, Mihir D Oza, Kamalesh Prasad, Ramavatar Meena, (2011), The cellulose contents of Indian seaweeds, Journal of Applied Phycology, 23, 919-923.

116. AK Siddhanta, Kamalesh Prasad, Ramavatar Meena, Gayatri Prasad, Gaurav K Mehta, Mahesh U Chhatbar, Mihir D Oza, Sanjay Kumar, Naresh D Sanandiya, (2009), Profiling of cellulose content in Indian seaweed species, Bioresource Technology, 100, 6669–6673.

117. Shuang Wang, Qian Wang, Xiumin Jiang, Xiangxin Han, Hengsong Ji, (2013), Compositional analysis of bio-oil derived from pyrolysis of seaweed, (2013), Energy Conversion and Management, 68, 273–280.

118. Xiaoling Miao, Qingyu Wu, (2004), High yield bio-oil production from fast pyrolysis by metabolic controlling of *Chlorella protothecoides*, Journal of Biotechnology, 110, 85–93.

119. Yasmin Khambhaty, Kalpana Mody, Mahesh R, Sreekumaran Thampy, Pratyush Maiti, Harshad Brahmbhatt, Karuppanan Eswaran, Pushpito K Ghosh, (2012), *Kappaphycus alvarezii* as a source of bioethanol, Bioresource Technology, 103, 180–185.

120. Seung-Soo Kim, Hoang Vu Ly, Gyeong-Ho Choi, Jinsoo Kim, Hee Chul Woo, (2012), Pyrolysis characteristics and kinetics of the alga *Saccharina japonica*, Bioresource Technology, 123, 445–451.

121. H Goyal, D Seal, R Saxena, (2008), Bio-fuels from thermochemical conversion of renewable resources: a review, Renewable and Sustainable Energy Reviews, 12, 504–17.

122. F Fantozzi, B D'Alessandro, G Bidini, (2003), IPRP – Integrated pyrolysis regenerated plant – gas turbine and externally heated rotary-kiln pyrolysis as a biomass waste energy conversion system. Influence of thermodynamic parameters. Proceeding of the Institution of Mechanical Engineers part-A, Journal of Power and energy, 217, 519–27.

123. JF Gonzalez, A Ramiro, CM Gonzalez-Garcia, (2005), Pyrolysis of almond shells. Energy Applications of Fractions, Industrial and Engineering Chemistry Research, 44, 3003–12.

124. A Demirbas, (2000), Biomass resources for energy and chemical industry, Energy Education Science Technology Journal, 5, 21–45.

125. CJ Gomez, JJ Manya, JE Velo, L Puigjaner, (2004), Further applications of a revisited summative model for kinetics of biomass pyrolysis, Industrial and Engineering Chemical Research, 43, 901–6.

126. E Meszaros, G Varhegyi, E Jakab, (2004), Thermogravimetric and reaction kinetic analysis of biomass samples from an energy plantation, Energy Fuels, 18, 497–507.

127. MJ Antal, G Varhegyi, E Jakab, (1998), Cellulose pyrolysis kinetics: revisited, Industrial and Engineering Chemistry Research, 37, 1267–75.

128. MA Olivella, De las Heras, (2002), Kinetic analysis in the maximum temperature of oil generation by thermogravimetry in Spanish fossil fuels, Energy Fuels, 16, 1444–9.

129. G Varhegyi, P Szabo, MJ Antal, (2002), Kinetics of charcoal devolatilization. Energy Fuels, 16, 724–31.

130. VE Mangut, E Sabio, (2006), Thermogravimetric study of the pyrolysis of biomass residues from tomato processing industry, Fuel Processing Technology, 87, 109–15.

131. JJ Manya, E Velo, L Puigjaner, (2003), Kinetics of biomass pyrolysis: a reformulated Three-parallel-reactions model, Industrial and Engineering Chemistry Research, 42,434–41.

132. CJ Gomez, G Varhegyi, L Puigjaner, (2005), Slow pyrolysis of woody residues and an herbaceous biomass crop: a kinetic study, Industrial and Engineering Chemistry Research, 44, 6650–60.

133. M Grønli, MJ Antal, G Varhegyi, (1999), A round-robin study of cellulose pyrolysis kinetics by thermogravimetry, Industrial and Engineering Chemical Research, 38, 2238–44.

134. G Varhegyi, MJ Antal, E Jakab, P Szabo, (1997), Kinetic modeling of biomass pyrolysis, Journal of Analytical and Applied Pyrolysis, 42, 73–87.

135. JJM Orfao, FJA Antunes, JL Figueiredo, (1999), Pyrolysis kinetics of lignocellulosic materials-Three independent reactions model, Fuel, 78, 349–58.

136. H Teng, YC Wei, (1998), Thermogravimetric studies on the kinetics of rice husk pyrolysis and the influence of water treatment, Industrial and Engineering Chemical Research, 37, 3806–11.

137. O Senneca, R Chirone, S Masi, P Salatino, (2002), A thermogravimetric study of nonfossil solid fuels. 1. Inert pyrolysis, Energy Fuel, 16, 653–60.

138. Ja-Kong Koo and Seok-Wan Kim, (1993), Reaction kinetic model for optimal pyrolysis of plastic waste mixtures, Waste Management and Research, 11, 515-529.

139. F Yao, Q Wu, Y Lei, W Guo, Y Xu, (2008), Thermal decomposition kinetics of natural fibers: activation energy with dynamic thermogravimetric analysis. Polymer Degradation and Stability, 93, 90–8.

140. M Muller-Hagedorn, H Bockhorn, L Krebs, U Muller, (2003), A comparative kinetic study on the pyrolysis of three different wood species, Journal of Analytical and Applied Pyrolysis, 68-69, 231–49.

141. S Vecchio, G Luciano, E Franceschi, (2006), Explorative kinetic study on the thermal degradation of five wood species for applications in the archeological filed, Annali Di Chimica, 96,715–25.

142. L Gasparovic, Z Korenova, L Jelemensky, (2010), Kinetic study of wood chips decomposition by TGA, Chemical Papers, 64, 174–81.

143. A Kumar, L Wang, Y Dzenis, D Jones, M Hanna, (2008), Thermogravimetric characterization of corn stover as gasification and pyrolysis feedstock, Biomass Bioenergy, 32, 460–7.

144. S Maiti, S Purakayastha, B Ghosh, (2007), Thermal characterization of mustard straw and stalk in nitrogen at different heating rates, Fuel, 86, 1513–1518.

145. Song Hu, Andreas Jess, Minhou Xu, (2007), Kinetic study of Chinese biomass slow pyrolysis: Comparison of different kinetic models, Fuel, 86, 2778–2788.

146. Vladimir Strezov, Behdad Moghtaderib, John A Lucas, (2004), Computational calorimetric investigation of the reactions during thermal conversion of wood biomass, Biomass and Bioenergy, 27, 459–465.

147. K Miura, T Maki, (1998), Energy Fuel, 12, 864–9.

148. Gang Wang, Wen Li, Baoqing Li, Haokan Chen, (2008), TG study on pyrolysis of biomass and its three components under syngas, Fuel, 87, 552–558.

149. Morten Gunnar Grønli, Gabor Va rhegyi, and Colomba Di Blasi, (2002), Thermogravimetric Analysis and Devolatilization Kinetics of Wood, Industrial and Engineering Chemistry Research, 41, 4201-4208.

150. Michele Corbetta, Alessio Frassoldati, Hayat Bennadji, Krystle Smith, Michelle J Serapiglia, Guillaume Gauthier, Thierry Melkior, Eliseo Ranzi, and Elizabeth M Fisher, (2014), Pyrolysis of Centimeter-Scale Woody Biomass Particles: Kinetic Modeling and Experimental Validation, Energy Fuels, 28, 3884−3898.

151. Chao Wang, Binlin Dou, Yongchen Song, Haisheng Chen, Mingjun Yang, and Yujie Xu, (2014), Kinetic Study on Non-isothermal Pyrolysis of Sucrose Biomass, Energy Fuels, 28, 3793−3801.

152. P Simon, (2004), Isoconversional methods: fundamental, meaning and application. Journal of Thermal Analysis Calorimetry, 76, 123–32.

153. Katarzyna Slopiecka, Pietro Bartocci, Francesco Fantozzi, (2012), Thermogravimetric analysis and kinetic study of poplar wood pyrolysis, Applied Energy, 97, 491–497.

154. A Khawam, DR Flanagan, (2005), Complementary use of model-free and modelistic methods in the analysis of solid-state kinetics, Journal of Physical Chemistry B , 109, 10073–80.

155. D Zhou, E Schmitt, G Zhang, D Law, S Vyazovkin, C Wight, et al., (2003), Crystallization kinetics of amorphous nifedipine studied by model-fitting and model-free approaches, (2003), Journal of Pharmaceutical Sciences, 92, 1779–92.

156. Prasanta Das, Milan Dinda, Nehal Gosai, and Subarna Maiti, (2015), High Energy Density Bio-oil via Slow Pyrolysis of Jatropha curcas Shells, Energy Fuels, 29, 4311−4320.

157. HL Friedman, (1964), Journal of Polymer Science Part C: Polymer letters, 6, 183.

158. J Flynn, L Wall, (1966), A quick, direct method for the determination of activation energy from thermogravimetric data, Journal of Polymer Science Part C: Polymer letters, 4, 323–8.

159. T Ozawa, (1965), A new method of analyzing thermogravimetric data, Bulletin of the Chemical Society Japan, 38, 1881–6.

160. T Akahira, T Sunose, (1971), Joint convention of four electrical institutes, Sci TechnoL, 16, 22–31.

161. H Kissinger, (1956), Variation of peak temperature with heating rate in differential thermal analysis, Journal of Research of the National Bureau Standard, 57, 217–21.

162. AV Bridgwater, (2003), Renewable fuels and chemicals by thermal processing of biomass, Chemical Engineering Journal, 91, 87–102.

163. MJ Veraa, AT Bell, (1978), Effect of alkali metal catalysts on gasification of coal char, Fuel, 57, 194–200.

164. DW McKee, CL Spiro, PG Kosky, EJ Lamby, (1983), Catalysis of coal char gasification by alkali metal salts, Fuel, 62, 217–220.

165. Liu Z.-liang, Zhu H.-hui, (1986), Steam gasification of coal char using alkali and alkaline-earth metal catalysts, Fuel, 65, 1334–1338.

166. N Kayembe, AH Pulsifer, (1976), Kinetics and catalysis of the reaction of coal char and steam, Fuel, 55, 211–216.

167. DW McKee, D Chatterji, (1978), The catalyzed reaction of graphite with water vapor, Carbon, 16, 53–57.

168. R Köpsel, H Zabawski, (1990), Catalytic effects of ash components in low rank coal gasification with steam, Fuel, 69, 282–288.

169. RJ Lang, RC Neavel, (1982), Behaviour of calcium as a steam gasification catalyst, Fuel, 61, 620–626.

170. RJ Lang, (1986), Anion effects in alkali-catalysed steam gasification, Fuel, 65, 1324–1329.

171. D McKee, (1982), Gasification of graphite in carbon dioxide and water vapor – the catalytic effects of alkali metal salts, Carbon, 20, 59–66.

172. DW McKee, CL Spiro, PG Kosky, (1985), Eutectic salt catalysts for graphite and coal char gasification, Fuel, 64, 805–809.

173. Guo C.-tao, Zhang L.-ming, (1986), Kinetics of coal char gasification at elevated pressures, Fuel, 65, 1364–1367.

174. SJ Yuh, EE Wolf, (1983), FTIR studies of potassium catalyst-treated gasified coal chars and carbons, Fuel, 62, 252–255.

175. PL Walker Jr., S Matsumoto, T Hanzawa, T Muira, IMK Ismail, (1983), Catalysis of gasification of coal-derived cokes and chars, Fuel, 62, 140–149.

176. WB Hauserman, (1994), High-yield hydrogen production by catalytic gasification of coal or biomass, International Journal of Hydrogen Energy, 19, 413–419.

177. Pavlina Nanou, Héctor E Gutiérrez Murillo, Wim PM van Swaaij, Guus van Rossum , Sascha RA Kersten, (2013), Intrinsic reactivity of biomass-derived char under steam gasification conditions-potential of wood ash as catalyst. Chemical Engineering Journal, 217, 289–299.

178. Feng Yan, Si-yi Luo, Zhi-quan Hu, Bo Xiao, Gong Cheng, (2010), Hydrogen-rich gas production by steam gasification of char from biomass fast pyrolysis in a fixed-bed reactor: Influence of temperature and steam on hydrogen yield and syngas composition, Bioresource Technology, 101, 5633–5637.

179. Mohammad Asadullah, Shu Zhang, Zhenhua Min, Piyachat Yimsiri, Chun-Zhu Li, (2010), Effects of biomass char structure on its gasification reactivity, Bioresource Technology, 101, 7935–7943.

180. H Haykiri-Acma, S Yaman, S Kucukbayrak, (2006), Gasification of biomass chars in steam–nitrogen mixture, Energy Conversion and Management, 47, 1004–1013.

181. F Marquez-Montesinos, T Cordero, J Rodriguez-Mirasol, JJ Rodriguez, (2002), CO_2 and steam gasification of grapefruit skin char, Fuel, 81, 423 – 429.

182. C Franco, F Pinto, I Gulyurtlu, I Cabrita, (2003), The study of reactions influencing the biomass steam gasification process, Fuel, 82, 835–842.

183. Wolfgang Klose, Michael Wolki, (2005), On the intrinsic reaction rate of biomass char gasification with carbon dioxide and steam, Fuel, 84, 885–892.

184. Keigo Matsumoto, Keiji Takeno, Toshimitsu Ichinose, Tomoko Ogi, Masakazu Nakanishi, (2009), Gasification reaction kinetics on biomass char obtained as a by-product of gasification in an entrained-flow gasifier with steam and oxygen at 900–1000°C, Fuel 88, 519–527.

185. C Guizani , FJ Escudero Sanz, S Salvador, (2013), The gasification reactivity of high-heating-rate chars in single and mixed atmospheres of H_2O and CO_2, Fuel, 108, 812–823.

186. S Turn, C Kinoshita, Z Zhangt, D Ishimura and J Zhou, (1998), An experimental investigation of hydrogen production from biomass gasification, International Journal of Hydrogen Energy, 23, 64-648.

187. S T Chaudhari, A K Dalai, and N N Bakhshi, (2003), Production of Hydrogen and/or Syngas (H_2 + CO) via Steam Gasification of Biomass-Derived Chars, Energy & Fuels 17, 1062-1067.

188. Yongliang Li, Liejin Guo, Ximin Zhang, Hui Jin, Youjun Lu, (2010), Hydrogen production from coal gasification in supercritical water with a continuous flowing system, International Journal of Hydrogen Energy, 35, 3036 – 3045.

189. Anwar Sattar, Gary A Leeke, Andreas Hornung, Joseph Wood, (2014), Steam gasification of rapeseed, wood, sewage sludge and miscanthus biochars for the production of a hydrogen-rich syngas, Biomass and Bioenergy, 69, 276 – 286.

190. M Kumar, RC Gupta, (1998), Energy Sources, 20 (7), 575.

191. Basu P. Chapter 7-gasification theory. In: Basu P, editor. Biomass gasification, pyrolysis and torrefaction, (2013), 2nd edition Boston: Academic Press, 199-248.

CHAPTER – 3

Aim and Scope of the Work

3.1 Introduction

3.1.1 An overview of renewable technologies

It is well established that the renewable energy is one of the cleanest energy sources among all available energy sources in the nature. The impact of this energy source has explicitly or implicitly influenced humanity and society. Since the industrial revolution, energy has been an intrinsic force for developing civilization in the universe. Due to phenomenal increase in the demand for energy consumption, the conventional energy sources are now on the periphery of difficult situation and tend to exhaust in the near future. So, renewable energy sources provide promising feedstocks for converting into clean energy. Biomass is one of the renewable energy sources and it is the oldest source of renewable energy known to humans, since ancient times. The formation of this biomass is the presence of sun via photosynthesis process with chlorophyll converting carbon dioxide from the air and water from the ground into carbohydrates, complex compounds composed of carbon, hydrogen, and oxygen. When these carbohydrates are burnt, it produces carbon dioxide and water and release the energy as comes from the sun. So naturally, it can be said that biomass is just like a natural battery for storing solar energy. As long as biomass is produced sustainably, the natural battery will last indefinitely.

3.2 Objectives of the present work

India is basically an agriculture-driven country and biomass could be utilized as an energy carrier for different purposes and it has very good potential in India. It was found that more than 320 million tons of agricultural residues are produced every year of which a major chunk of this residue is burnt in an open atmosphere in situ farming land [1]. Now, with the present crisis of conventional energy sources shortage, the rural civilization is depending more and more to the burning of these agricultural residues for domestic cooking and other purposes [2]. In practice, it is highly inefficient and polluting the atmosphere causing health hazards. So naturally to avoid these adverse effects, these crop residues should be upgraded into convenient and less polluting forms. There are several established methods, one such method is the utilization and conversion of locally available residue by controlled burning or pyrolysis or carbonization. The resultant product solid fuel or bio-char has a higher heating value than original biomass, low ash content, and produces no smoke during burning. Again, high efficient small scale burner stove could be used for this purpose instead of the open challahs which produce more smoke and is also low energy efficiency. Also slow pyrolysis is one of options to produce syn-gas or bio-oil. This process is widely applicable for the production of useful energy or valuable chemicals.

Kinetic study of biomass is really helpful to describe the thermal degradation of any biomass. So there are several kinetic models that are used to ascertain process parameters of pyrolysis pathway.

Another thermochemical process i.e. the gasification technology generally produces syn-gas used for different purposes such as for running gas turbines, electricity generation, burning for domestic uses, etc. and this process is much more convenient and efficient than direct burning of biomass. Steam gasification is also another option for producing hydrogen rich syn-gas with the higher heating and less polluting combustible gases. Solid fuel to hydrogen rich syn-gas has several advantages. Hydrogen is a clean source of energy. But storage of this gas is really serious problem for commercial application. Magdalena Momirlan et al. [3] investigated on physical properties of hydrogen as a fuel substitute for future. One of the challenges faced is hydrogen storage.

The present research work comprises of thermochemical conversion of different kinds of biomass as basic feedstocks like wasteland derived biomass and marine macroalgae. So, the characterization of these biomasses as a potential for solid fuel is important prior to the selection of any thermochemical processes. Because each biomass is unique in terms of

chemical constituents, so naturally process parameters needs to be developed based on physical and chemical properties of biomass. In case of macroalgae, the chemical constitution is completely different from terrestrial biomass. For this suitable thermochemical conversions should be chosen for macroalgae. Generally, hydrothermal liquefaction, pyrolysis, and gasification are most common techniques adopted. The present work focuses on the pyrolysis and gasification of selected seaweed species.

The main objective of this work is the characterization of the selected biomass which includes some common wasteland derived biomass and marine macroalgae. Based on the characterization, some case studies are selected for harnessing energy from them via gasification, pyrolysis, or steam gasification.

To be more specific, the important objectives of this work are:

(1) Characterization of selected biomass species as solid fuel for thermochemical processes.

(2) Syn-gas production through downdraft gasifier for selected feedstocks for running an engine to produce electricity.

(3) Production of bio-oil via slow pyrolysis process of selected biomass and upgradation of this oil.

(4) Production of hydrogen rich syn-gas via steam gasification from obtained bio-char through slow pyrolysis.

The success of the present work will contribute to achieve the following objectives:

(a) The availability of data for the selected feedstocks as solid fuel would be more open for the researchers.

(b) Increase the competiveness of oil and gas industry in the world market with renewable energy sources, not only for developed nations, but also for developing countries like India having huge potential market.

(c) Development of indigenous sources and improve gross domestic product (GDP) for better economy.

(d) Accelerate the employment rate by creating new activities based on small, medium, even higher scale gasification units, especially for syn-gas production for domestic purpose or generating electricity for households.

(e) Biomass is a renewable energy source which could contribute to decrease in the greenhouse gas in place of fossil fuel with a sustainable way.

(f) Improve fuel security throughout the year.

(g) Valuable chemicals from renewable sources (i.e. value added products).

The contents of this thesis are disseminated and discussed in six chapters. All the chapters are correlated with each other in order to develop connectivity and sequence. The overall thesis contains general introduction, literature review, and aim and scope of the work and the experimental work is presented in chapter 4, chapter 5. The last chapter, chapter 6 includes the conclusion and future remarks. Chapter 4 contains characterization of selected wasteland biomass species and possible route to harness energy from each kind of biomass. The chapter 4 includes introduction, different instrument used for fuel characterization of the wasteland derived biomass and results Chapter 5 consists of all the case studies including utilization of *jatropha curcas* shells for energy application, thermochemical conversion of macroalgal biomass, *Kappaphycus alvarezii* granules seaweed for energy application, and lastly, harnessing energy from three selected seaweed species, named *Ulva fasciata*, *Gracilaria corticata*, and *Sargassum tenerrimum*. The case studies are briefly described in this chapter, and the chapter also includes detailed characterisation of macroalgal biomass used for the study. And finally LCA (Life Cycle Assessment) of three macroalgae have been investigated for the potential of industrial application.

The final conclusions obtained will help in charting out the future course of the work.

References:

1. PhD thesis of Subarna Maiti, Studies and investigation of value added products from agricultural waste, May, 2007, School of Energy Studies, Jadavpur University, Kolkata 70032, India.

2. Reddy A.K.N. (1981), An Indian village agricultural ecosystem-case study of Ungra village Part II. Biomass 1: 77 – 88.

3. M Momirlan, TN Veziroglu, (2005), The properties of hydrogen as fuel tomorrow in sustainable energy system for a cleaner planet, International Journal of Hydrogen Energy, 30, 795 – 802.

CHAPTER – 4

Wasteland Biomass as Feedstock for Thermochemical Conversion Processes

4.1 Introduction

The main objective of this chapter is to characterize the fuel properties of selected biomass in the present study. For this selection, the first priority is that food crops should not come in the energy application. Hence the biomass chosen from wasteland derived or agricultural wastes or macroalgae are all non-fodder and non-edible [1]. In India, there are some areas which are barren in nature and can be fully leveraged for the production of energy crop. More specifically, barren land can be aptly described as wastelands which are degraded lands and they have various inherent or imposed lacunae and hence there are restrictions with respect to growing of arable crops.

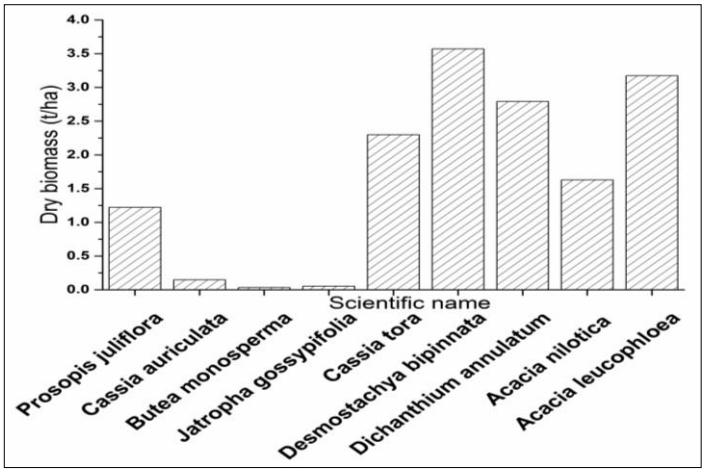

FIGURE 4.1: Production of different species of wasteland derived biomass per hectare.

However, there are many plant species including weeds which can grow luxuriantly on such types of land by virtue of their tolerance to extreme physico-chemical and environmental conditions. Such non-food crops offer profound scope to harness biomass and energy while reclaiming these degraded lands by proper agronomic management. According to NRSA, 2003 data based on satellite imagery, western state of Gujarat has ca. 2 million hectares of land under different categories of wasteland, majority of which fall under the category of land with shrub vegetation where plant species like *Prosopis juliflora*, *Cassia auriculata*, *Butea monosperma*, *Jatropha gossypifolia*, *Acacia nilotica*, *Acacia leucophloea* are abundantly found [2]. Many grasses and tussocks such as *Desmostachya bipinnata* and *Dicanthium annulatum* can thrive on waterlogged soils. In one such study carried out at Gujarat, abundant quantities of biomass were recorded from these types of wastelands (Figure 4.1). The biomass abundantly found in such types of wastelands may be gainfully used to derive energy through thermo-chemical conversion processes such as biomass gasification or pyrolysis process. Utilizing of such biomass from wastelands would also avert the food-vs-fuel dilemma as no arable crop production is anyway possible in these tracks. With a view to address the above problem, the present work was carried out to characterize biomass obtained from different plant species growing on wastelands. Ten plant species including trees, shrubs, herbs and grasses were collected from wasteland located in Panchmahal district of Gujarat, India (Altitude- 296 ft N 22° 41’ 376’’ E 073° 29’ 649’’). If we look at the India map, the wastelands are distributed accordingly state-wise and categorised based on the types barren lands projected by NRSA, 2003. They projected that such lands are estimated to be around 552692.26 square km in both cases excluding Jammu & Kashmir [2].

4.2 Fuel characterization of solid wasteland derived biomass

The basic and fundamental of biomass characterization consisting several analyses are listed here, as hot oven for drying biomass, mixer for crushing the biomass into powder form at different particle size depending on the requirement, the proximate analysis, ultimate analysis, calorific value, ash fusion test, fibre analyzer, TG analysis for kinetic study etc.

4.2.1 Proximate analysis

Figure 4.2 (a) shows the hot oven for drying the biomass as per the experimental requirement. The hot air oven has a measurement of temperature range of room temperature to 250°C, having precision of ± 2°C. The standard method according to ASTM method for determining the moisture content is 110°C temperature and 1 h. Similarly, for figure 4.2 (b), the automatic proximate analyzer (model no. APA-2, Advanced Research Instruments Company, New Delhi) were used for measuring the moisture content, volatile matter, fixed carbon and ash content. The method was adopted according to ASTM method as moisture: ASTM D3173; ash: ASTM D3174; volatile matter: ASTM D3175; and fixed carbon: by difference ASTM E1131-08. The operating principle of this instrument is here briefly elaborated.

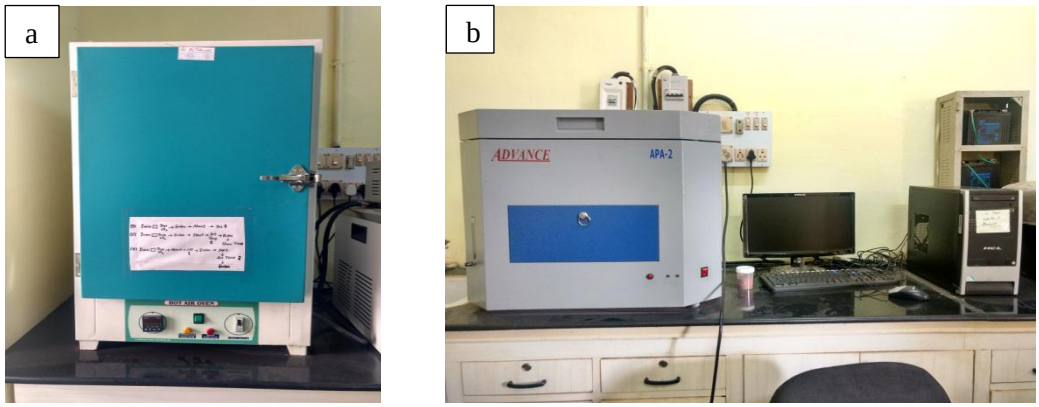

FIGURE 4.2: (a, b) Depict of the hot air oven and the proximate analyzer.

The automatic Proximate Analyzer is programmed to perform complete and automatic analysis of Air Dry Basis Moisture, Ash & Volatile Constituent in the biomass samples. Each measurement allows up to 19 samples in every batch. In the analyser, both oxidizing and inert atmospheres can be maintained as per ASTM guidelines. Provision is made to introduce a sweep gas or a reactant gas, and to remove product of drying, de-volatilization or combustion. The sample balance pedestal, crucible and the crucible covers are made of ceramic material as per ASTM guidelines. The crucible and the turn table are capable of withstanding high-temperatures and different furnace atmospheres and are not susceptible to wrapping at high temperature. The furnace is programmed to have maximum temperature control up to 1000°C and the furnace cover of the analyser is supported by two shafts for better stability and support. The instrument has two thermocouples which

include one thermocouple for over-temperature protection for safety and the other one to measure and record temperature near the test crucible. The instrument is configured with a built-in high precision electronic scale to ensure precise and accurate weighing of the samples. The electronic balance in this instrument has a measurement range of 110 g with an accuracy of 0.1 mg. The controlling precision of the instrument is ± 5°C. The total analysis time required 240 min along with analysis range 0.2 – 100%.

4.2.2 Ultimate analysis

Ultimate analysis is also another important fuel characteristic which determines the C, H, N, S of a solid fuel and O is determined by difference. It was found that mainly, carbon, hydrogen, nitrogen, sulphur and oxygen are the major constituents in biomass. In order to measure these constituents in biomass, the sample preparation is required. The sample should be in powder form and evenly distributed. So the ultimate analysis was performed in a CHNS analyzer (vario MICRO cube) where the combustion and reduction columns have the temperatures of 1150°C and 850°C, respectively. For this analysis, the standard was sulphanilamide and the sample requirement was 1 to 10 mg. The oxidizing agent was O_2 and the carrier gas was He.

4.2.3 Calorific value analysis

Calorific value is generally determines how much energy is stored in the biomass. This characterisation is extremely important prior to thermochemical process, especially in gasification and pyrolysis.

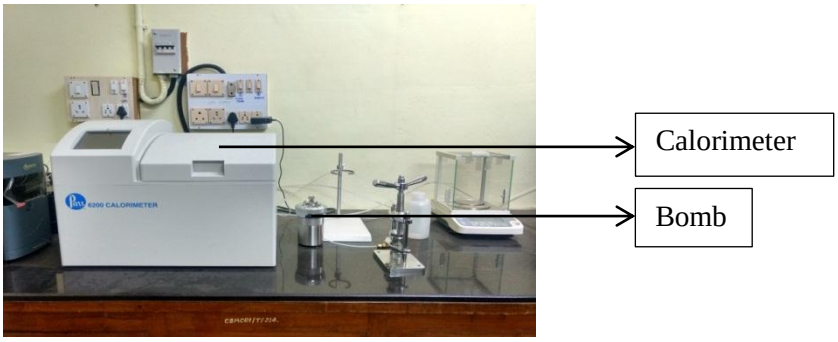

FIGURE 4.3: The picture of the automatic bomb calorimeter.

Figure 4.3 shows the picture of a typical automatic bomb calorimeter, supplied by Parr Instrument Company. 6200 is a microprocessor controlled isoperibol oxygen bomb calorimeter which is widely used for both routine and occasional calorific tests. It uses the time-tested Parr 1108 style oxygen bomb and oval bucket in a compact calorimeter, producing reliable results with good repeatability. All sensors, controls and jacketing in the 6200 Calorimeter are built into a single, compact cabinet to provide a self-contained operating unit consisting of a temperature-controlled water jacket with a built-in circulating system and an electric heater, an 1108P oxygen bomb with an oval bucket which fits into the insulating water jacket, a built-in automatic system for charging the bomb with oxygen, a high precision electronic thermometer. The operating principle of this instrument is very simple as it takes only 10 to 15 min per sample. The requirement of sample is around 0.1 to 1 g, depending the state of sample. Only oxygen filling system is automatic and the rest bucket fill and bomb wash operations are manually carried out. The temperature precision is extremely good at 0.0001°C and the instrument precision is 0.05 to 0.1%.

4.2.4 Ash fusion test analysis

This instrument is used for measuring the ash fusion temperature of ash produced from biomass or any organic matter. The ash fusion temperature has immense importance in thermochemical conversion process, especially in gasification process as it is essential to know the decomposition temperature of each biomass as gasifiers usually operates at high temperature of more than 700°C. Ash melting causes fouling or slagging inside the reactor which prevents the downstream process and it is not fruitful in a continuous process. The design of most gasifiers takes in to account the characteristics of the ash generated and whether it will remain in solid form or be fluid to some degree. The ash fusion analysis was performed in an ash fusion analyzer AFT of Advance Research Instrument company, New Delhi, India. This test performs the actual melting / fusion of the ash cone under controlled conditions and checks the corresponding deformation temperature of the sample biomass ash. The instrument complies with the ASTM standard to check the temperatures of four separate transitional states of the ash cone between dry and fluid conditions that will occur because of the heating. The auto image recognition feature in the higher versions enables auto detection of the various deformation temperatures. The instrument features an automatic temperature recording along with images of the ash cone using a high resolution CCD camera. The camera collects and records the images of the ash cone

as it deforms with increase in furnace temperature. A rugged high temperature heater used with high grade thermal insulating blocks ensure a long life of the heater element even after continuous and repeated use at temperatures up-to 1520/1620 °C.

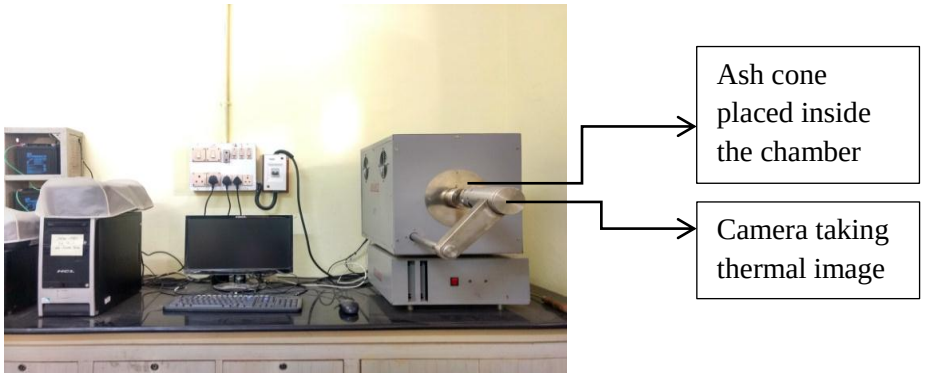

FIGURE 4.4: The picture of the ash fusion tester.

The operating principle of this ash fusion tester is briefly described and is shown in figure 4.4. The furnace temperature range was 0-1520^{o}C with temperature accuracy of < 5^{o}C and resolution of 1^{o}C. The ash fusion testing was carried out in weak reduction atmosphere by means of graphite. The temperature ramp was set as 20^{o}C min^{-1} from 30^{o}C to 900^{o}C; 4^{o}C min^{-1} for 900-1300^{o}C; 1^{o}C min^{-1} for 1300-1520^{o}C. The ash cone was prepared by a matrix provided by the same company.

4.2.5 Fibre analysis

Hemicellulose, cellulose and lignin are the major three constituents in biomass. Ligno-cellulosic biomass is a woody type plant material. This woody type plants include trees, shrubs, cactus, and perennial vines. Thus, the above biomass can be categorized as: (1) herbaceous and (2) non-herbaceous.

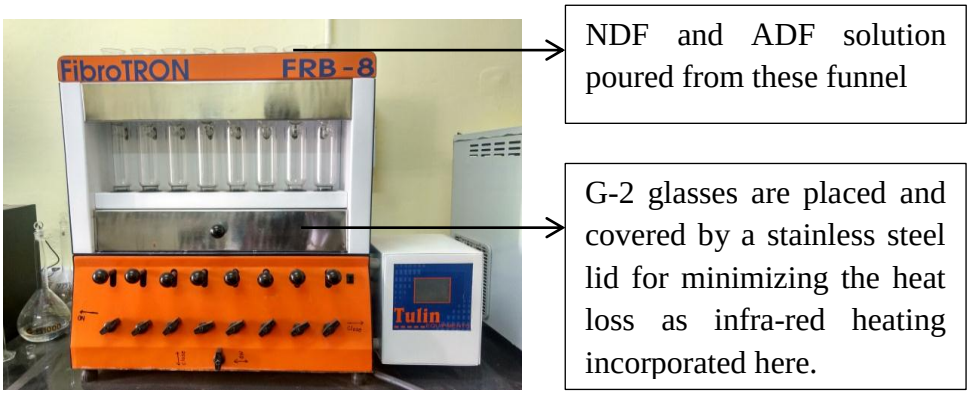

FIGURE 4.5: The schematic picture of the fibre analyzer.

An herbaceous biomass is a plant with leaves and stems that die annually at the end of the growing season such as wheat and rice, etc. Whereas, non-herbaceous plants are not seasonal, generally large trees fall in this category. The operating principle of fibre analyzer (FibroTRON, model no. FRB-8, supplied by Tulin equipments, India as shown in figure 4.5) is simple as the prepared solutions (NDF, ADF, etc.) are poured from the top where eight conical flasks are placed which are directly connected to the sintered glass (G-2), along with an infra-red heating system and refluxing system. The estimation of hemicellulose, cellulose and lignin is briefly described here.

4.2.5.1 Determination of hemicellulose

For the determination of hemicellulose, the neutral detergent solution (NDF) has to be prepared with the following quantity. Firstly, di-sodium ethylene-di-amine-tetra-acetate and sodium borate decahydrate is dissolved in about water by slow heating. Then, solution containing sodium lauryl sulphate in 2-ethoxy ethanol is added. Along with it is added a solution of di-sodium hydrogen phosphate. Finally pH is adjusted at 7 and the solution is made up to 1 litre NDS (neutral detergent solution). The biomass sample is refluxed with NDS and water soluble and materials other than the fibrous component are removed. The solid material is weighed after filtration and expressed as neutral detergent fibre (NDF). The hemicellulose content can be calculated as follows:

Hemicellulose = Neutral detergent fibre (NDF) – Acid detergent fibre (ADF)

4.2.5.2 Determination cellulose and lignin

Now, for the determination of acid detergent fibre, the acid detergent solution (ADS) has to be prepared. Firstly, cetyl trimethyl ammonium bromide dissolved in 1 (N) sulphuric acid. The sample along with ADS was boiled for 30 min at 250°C with the refluxing system. Then, washed, dried weights are taken and, ADF content is calculated as (W/S); where ‘W’ is the weight of the fibre and ‘S’ is the weight of the sample.

For determination of acid detergent lignin, the acid detergent fibre was transferred to G-2 crucible with 72 %w/w sulphuric acid and kept for 3 to 4 h. The residue was washed, dried and weighed. The residue was then ashed at 550°C for 4 h.

Cellulose = ADF – Residue after extraction with 72% H_2SO_4

Lignin = Residue after extraction with 72% H_2SO_4 – ash.

4.2.6 Complete ash analysis

Figure 4.6 shows the picture of the muffle furnace used in this study. The maximum heating capacity of the furnace was 1150°C, rate of heating 15°C min^{-1}.

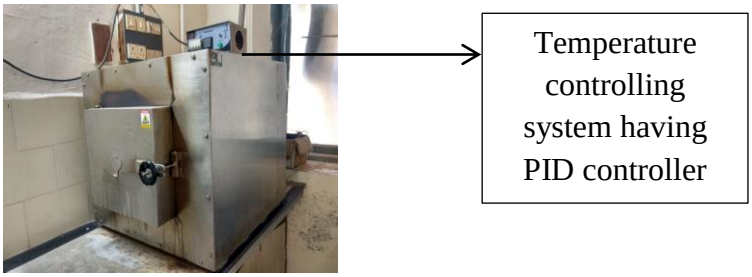

FIGURE 4.6: The picture of the muffle furnace.

The temperature controlling system was guided by the PID controller and the precision of the temperature is ±1°C. The complete ash component analysis was done in ICP Perkin Elmer Optical Emission Spectrometer (Model No. Optima 2000 DV). The ash was prepared at 550°C for 4 hr in muffle furnace and 1 g ash was digested in 10 to 15 ml aqua regia solution (HNO_3 + HCl: 1:3). The solution was evaporated slowly in order to obtain ash paste. This same procedure was repeated 3 to 4 times. This paste was mixed with 1(N) HCl in order to make homogeneous solution using magnetic stirrer and filtered. The residue was placed in muffle furnace at 900°C for 2 hrs in order to obtain SiO_2 (probable). The filtrate that contained compounds (mainly oxides) of Al, Fe, Ca, Mg, Na and K were made up to 500 ml with distilled water. 5 ml of 100 ml of this solution was mixed with 2% (wt. %) conc. HNO_3, made up to 500 ml using distilled water and filtered. The solution was now finally prepared for ICP. The other part, i.e. 400 ml solution was mixed with NH_4Cl in order to obtain the neutral pH and kept in heating for 15 to 20 min. This solution was filtered and the residue consisted of oxides of Al & Fe. The filtrate contained Ca, Mg, Na, K, SO_4--. The collected residue was dissolved in 2 (N) NaOH in which alumina was completely dissolved to form aluminium hydroxide. The solid residue, was probably $Fe(OH)_3$. It was washed till neutral. This was kept in oven for 110°C for 1 hr and was then transferred to a muffle furnace, kept for 900°C for 2 hrs in order to obtain Fe_2O_3. The other part i.e. liquor containing $Al(OH)_3$ was mixed with HCl (1:1) and heated for 15 to 20 min. 2 to 3 g ammonium chloride was added and after drying at 110°C for 1 hr, the residue was

placed in a muffle furnace at 900°C, for 2 h to obtain Al_2O_3. The other part of 400 ml solution was further treated by and Ca and Mg were determined by volumetric method. The nebulizer flow rate in the ICP was 0.80 lpm and the standard sample concentration limit was 10 ppm for ICP analysis. The element in the ash was selected based on those are important in thermochemical process.

4.2.7 Thermo-gravimetric analysis

The thermogravimetric (TG) analysis was carried out for determining the kinetic values obtained from different kinetic models and at different heating rates. The instrument used was Netzsch, TG209 F1, Libra and the studies were carried out in nitrogen atmosphere with N_2 flow rate of 50 ml min^{-1} .The heating rates chosen were 5 K/min, 20 K/min and 50 K/min for kinetic analyses.

4.3 The biomass selected in this study

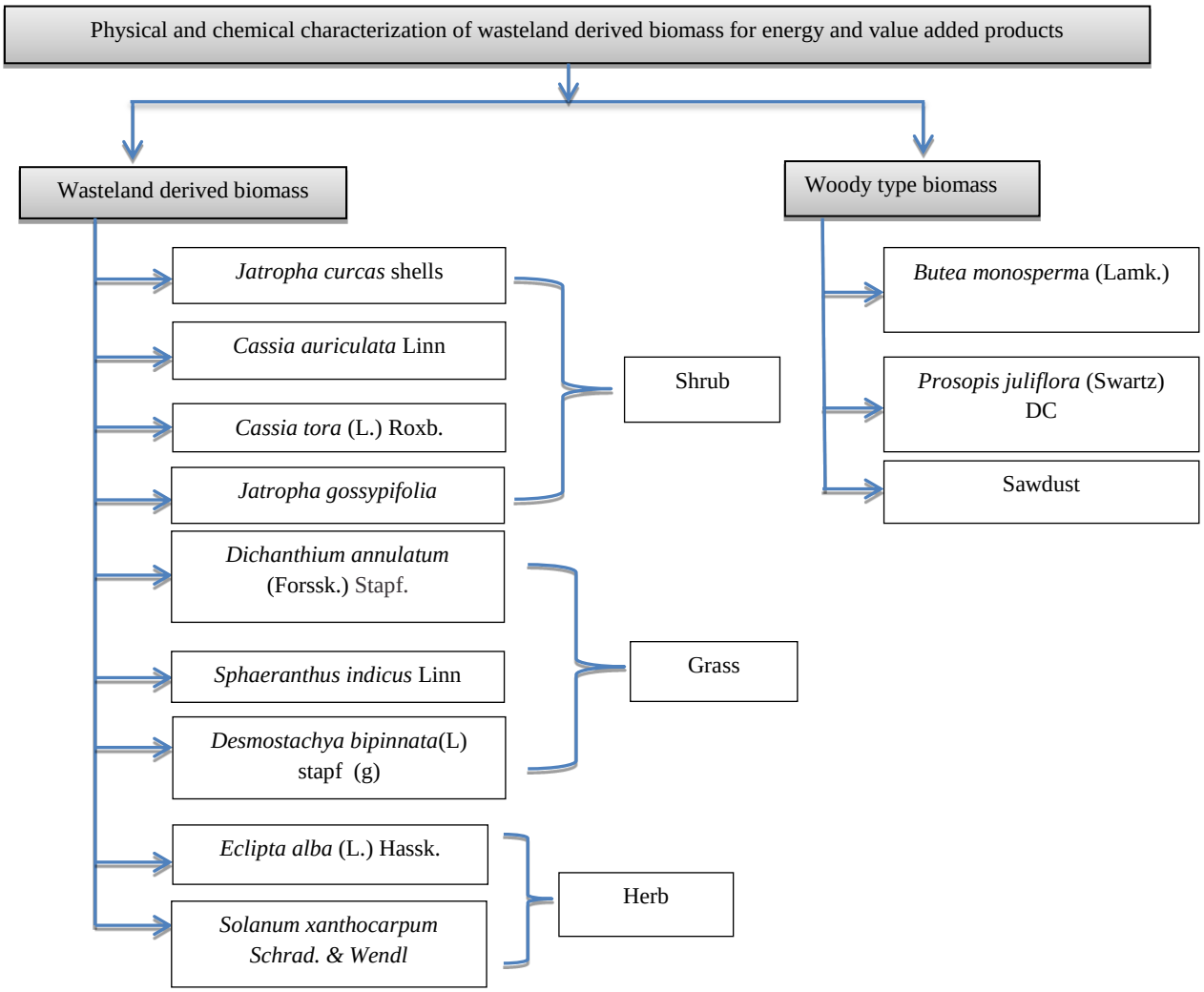

FIGURE 4.7: All the selected biomass classified as shrub, grass, herb, woody type wasteland biomass.

The wasteland derived feedstocks were characterized. The selected biomasses are abbreviated for shrub type as *Jatropha curcas* shells (JC), *Cassia auriculata* Linn (CA), *Cassia tora* (L.) Roxb. (CT), *Jatropha gossypifolia* (JG); for grass type biomass as *Dichanthium annulatum* (Forssk.) (DA), *Sphaeranthus indicus* Linn (SI), *Desmostachya bipinnata* (L) (DB); for herb type biomass as *Eclipta alba* (L.) Hassk. (EA), *Solanum xanthocarpum* (SX); for woody type biomass *Butea monosperm*a (Lamk.) (BM), *Prosopis juliflora* (Swartz) DC (PJ).

4.3.1 Moisture analysis of selected biomass

The most important parameter for characterization of biomass is the moisture content. The fundamental of a plant is to absorb moisture from the ground and the potential difference of the moisture pressure pushes upwards. Then, moisture passes to leaves through the capillary passages. The moisture assists in photosynthesis process and the rest is evaporated through leaves.

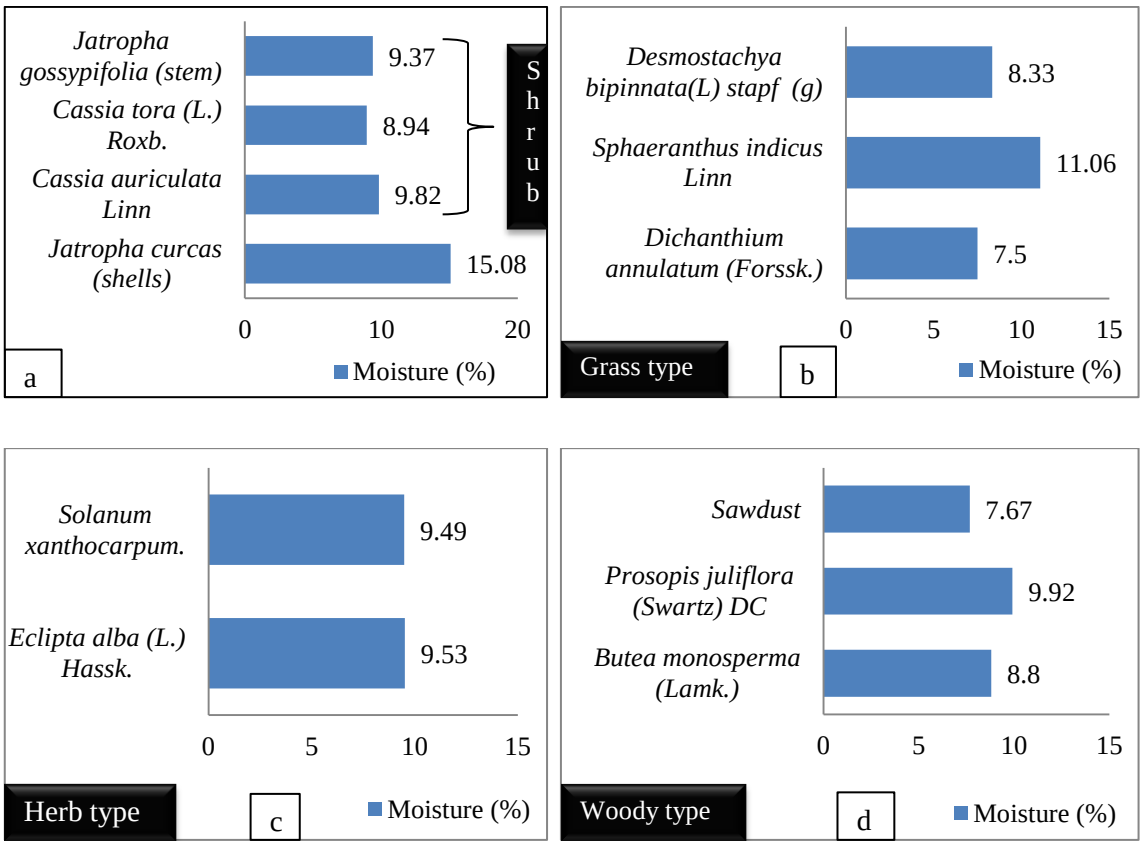

FIGURE 4.8: The moisture content in the selected biomass in this study (wt. %).

A fully grown biomass contains the moisture in two forms, (1) free or external, and (2) inherent or equilibrium. Free moisture called as unbound moisture generally remains on the outer surface of biomass. The inherent or equilibrium moisture is called bound moisture and is present in the plants internal structure. It is very intricate to remove bound moisture. As shown in figure 4.8, the shrub type biomass *Jatropha gossypifolia (stem)*, *Cassia tora (L.) Roxb*, *Cassia auriculata Linn*, and *Jatropha curcas* shells show reasonable moisture content except *Jatropha* curcas shells which exhibits quite high moisture content among the biomass and the values are 9.37, 8.94, 9.82 and 15.08%, respectively. The moisture content of each biomass is presented as, "as received basis" of biomass. The grass type biomass *Desmostachya bipinnata*, *Sphaeranthus indicus* and *Dichanthium annulatum* have moisture contents as 8.33, 11.06 and 7.5% respectively. The variation of moisture content among the herb, and woody biomass are found to be less as shown in figure 4.8 (c,d).

4.3.2 Fixed carbon and Volatile matter

Fixed carbon is the residual mass obtained after determining moisture content (*M*), volatile matter (*VM*), and ash content (*A*) as depicted in the following way, eqn. (4.1).

$$FC = 100 - M - VM - A \quad (4.1)$$

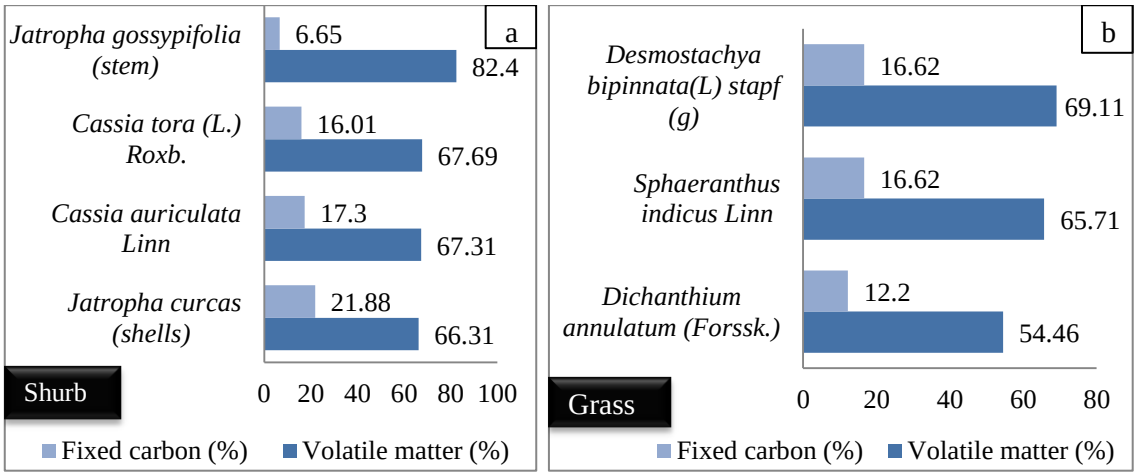

This fixed carbon (FC) is the solid residue left in the biomass mostly as bio-char in the pyrolysis process after devolatalization, i.e. after the volatile matter (VM) is liberated off.

The source of carbon in biomass comes from the photosynthesis fixation of CO_2 and thus it is organic matter.

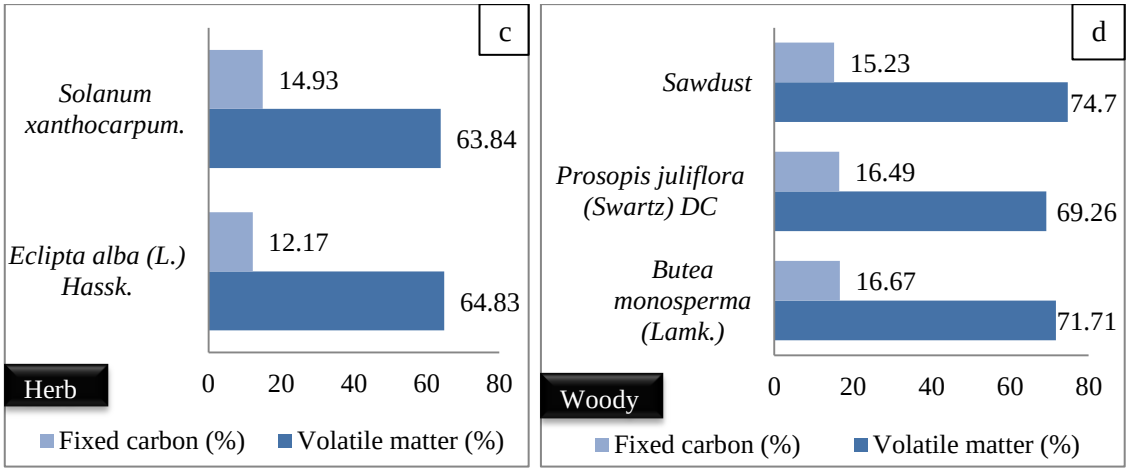

FIGURE 4.9: The fixed carbon and volatile matter in the selected biomass (wt. %).

Since *FC* depends on the amount of *VM*, it cannot be evaluated directly. *VM* in biomass varies with the rate of heating, and also the fixed carbon is not a fixed quantity but its value, under standard condition, provides a valuable fuel parameter. Figure 4.9 (a,b,c,d) shows the fixed carbon and volatile matter of the selected biomass. Apparently, all the biomass has good fixed carbon and volatile matter and these parameters have positive impact on thermochemical conversion.

4.3.3 Ash content

The ash content is the inorganic solid residue left after the fuel is completely burnt under the standard condition. The major constituents in ash are oxides of silicon, aluminium, iron, calcium, sodium, and potassium; some small amount of magnesium, titanium may also be present. Figure 4.10 shows the ash content of selected biomass in this study. Figure 4.10 (a) shows the ash content of shrub type biomass and that *Jatropha curcas* shells had the highest ash content. Many researchers have reported that *Jatropha* curcas shells are difficult to run in gasifier due to high ash content. In the grass type biomass, the reasonable ash contents (within 10 %) were found except *Dichanthium annulatum* which has 25.84% ash. This biomass might be difficult to apply in thermochemical process. The herb type biomass had within 15% ash content.

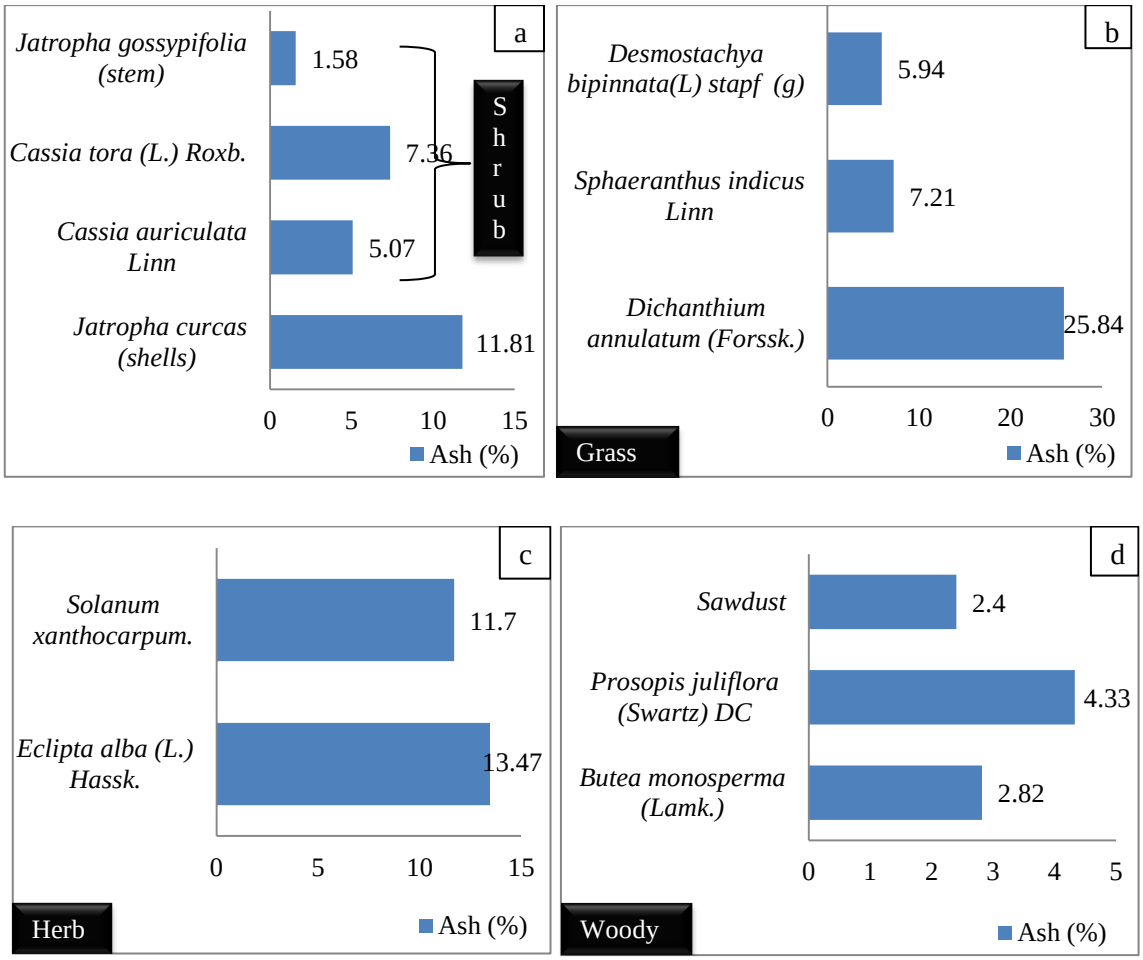

FIGURE 4.10: The ash content of the selected biomass (wt. %).

The woody biomass has very less ash content and may be the best feedstock in the thermochemical conversions. The ash content plays a significant role in biomass utilization especially if it contains alkali metals such as potassium or halides such as chlorine. Mostly, straw and grasses are particularly susceptible to this problem. These components in ash can lead to serious agglomeration, fouling and corrosion problem in gasifiers or reactors.

4.3.4 Calorific value analysis

Figure 4.11 (a,b,c,d) shows the calorific value (CV) of the selected biomass. The CV of the shrub type biomass figure 4.11 (a) is not much divergent within its group except CT as it has high ash content, low carbon content and high oxygen content. But in case of grass type biomass only *Dichanthium annulatum* exhibits somewhat low CV than others due to the presence of the high ash. Generally, high ash in fuel reduces the calorific value. The same reason could be applied for the herb type biomass as *Eclipta alba* has the low CV.

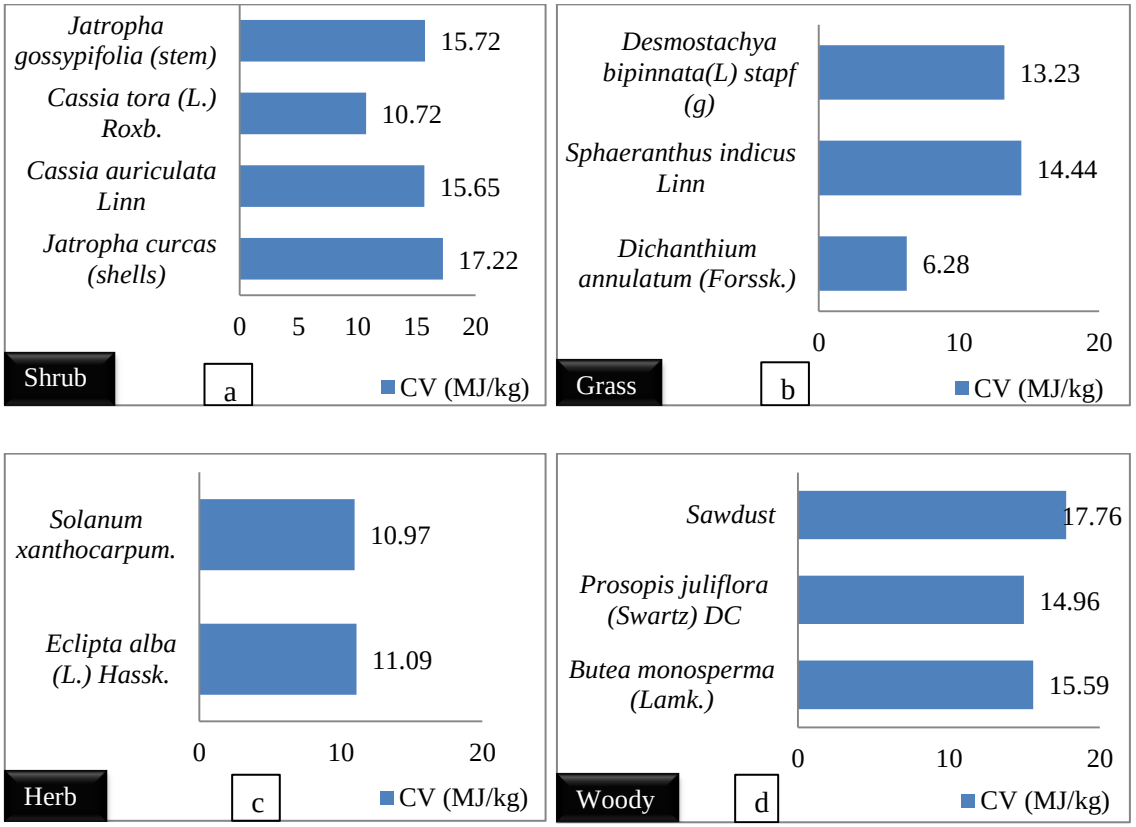

FIGURE 4.11: The calorific value of the selected biomass.

The CV does not depend only on ash content, but it also depends on carbon content, hydrogen content, moisture content, and oxygen content. The high moisture, oxygen and ash content are primarily responsible for reducing the calorific value of the fuel. The woody type biomass has excellent CV than other type of biomass.

4.3.5 CHNS analysis

Figure 4.12 (a,b,c,d) shows the ultimate analysis of the selected biomass was investigated in the present study. The composition of the fuel is expressed in terms of its fundamental elements which exclude moisture *M*, and ash content. The biomass common ultimate analysis can be expressed as

$$C + H + O + N + S + ASH + M = 100 \quad (4.2)$$

where, C stands for carbon, similarly H for hydrogen, N for nitrogen, and S for sulphur. The main objective of ultimate analysis is to find out the atomic ratios of (H/C) and (O/C)

which determines the fuel characteristics. Also the air-fuel ratio in gasifier is obtained from the ultimate analysis. Figure 4.12 (a) shows the shrub type biomass have almost nil sulphur content. The sulphur when combusted produces sulphur oxides which are hazardous to the environment.

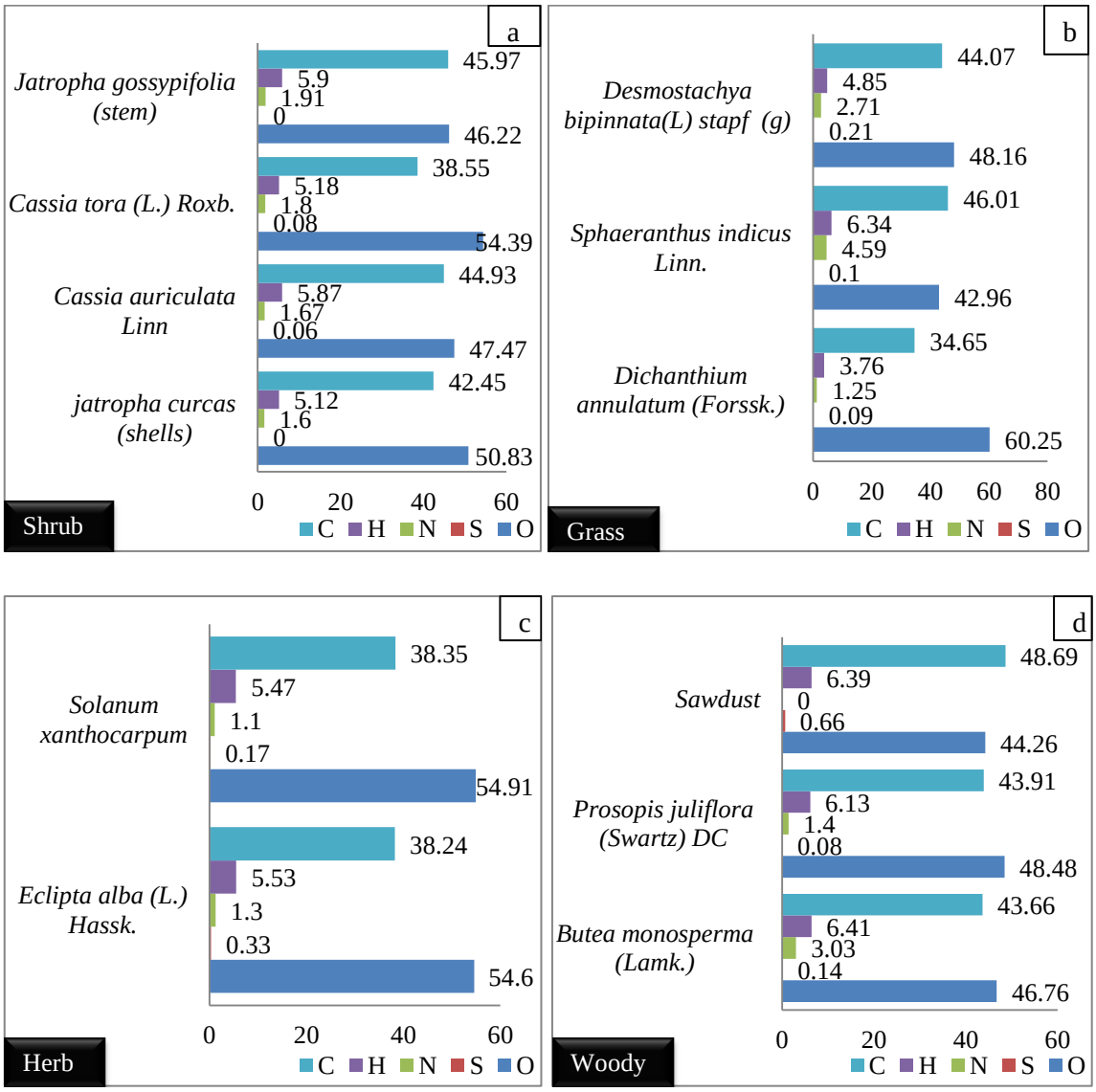

FIGURE 4.12: The CHNS of the selected biomass (in wt. %).

All biomass including shrub, grass, herb, woody have reasonable carbon, hydrogen and oxygen contents. To analyse in detail, the atomic ratios of (O/C) and (H/C) of the selected biomass were evaluated for each biomass, first for herb type biomass the values are (1.50, 1.54), (2.11, 1.61), (1.58, 1.56), (1.79, 1.44) for respective biomass in figure 4.12 (a). Similarly, for grass type biomass its values are (1.63, 1.32), (1.40, 1.65), (2.60, 1.29), for

herb type (2.14, 1.71), (2.14, 1.73), for wood type (1.36, 1.57), (1.65, 1.67), (1.60, 1.76 respectively.

4.3.6 Ash fusion test

The ash fusion tests were performed in the ash fusion tester as described earlier. Figure 4.13 (a,b,c,d) shows the ash fusion temperatures of the respective biomass.

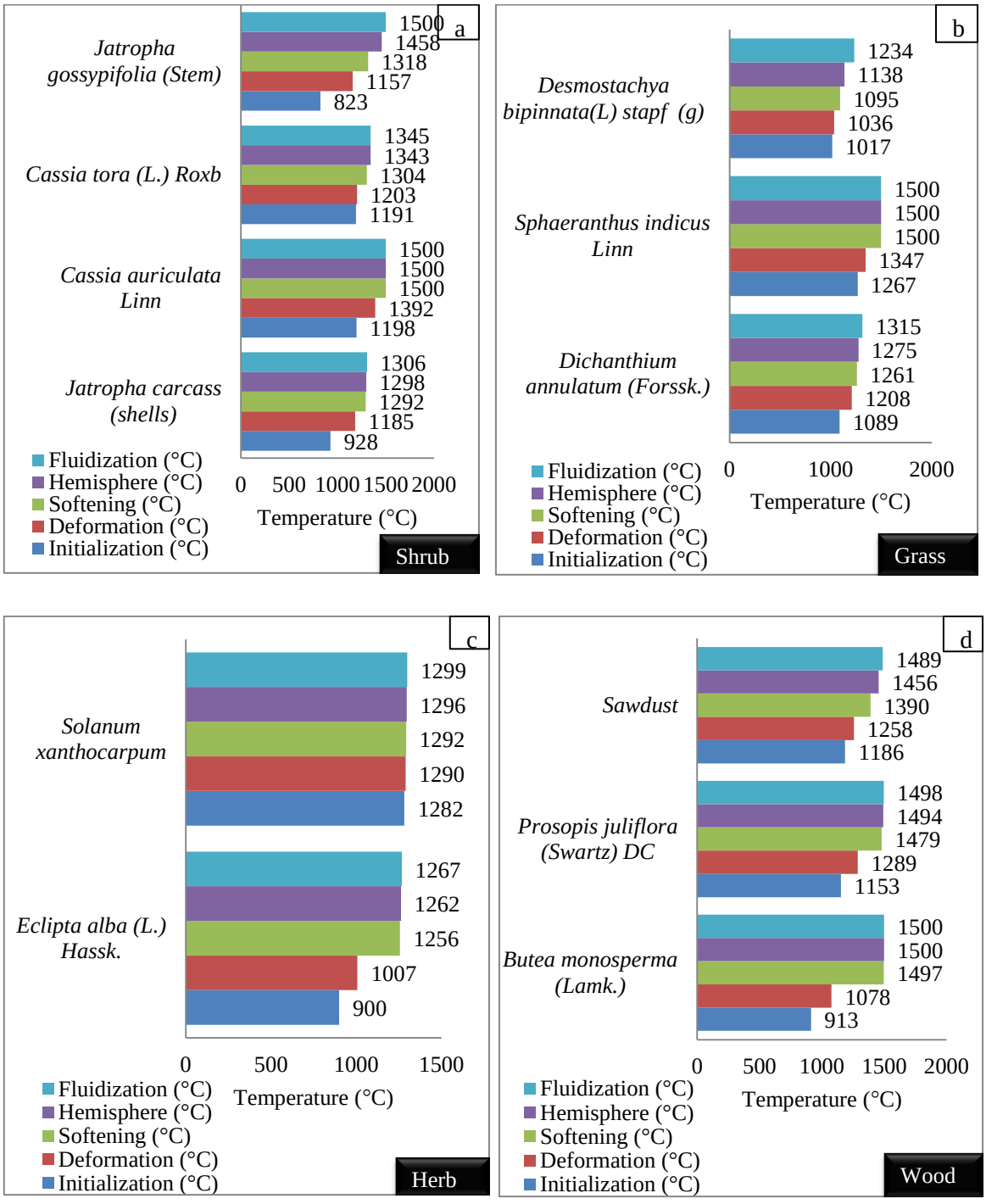

FIGURE 4.13: The ash fusion temperatures of the selected biomass.

In ash fusion test, the most important parameter is the fluidization temperature among as this represents the temperature at which the ash totally melts down. These ash fusion temperatures are extremely important prior to the design of any reactor in thermochemical conversion process. Another important parameter that must be taken into consideration is the material of construction, in order to resist high temperatures. It is well established that the thermochemical conversions such as gasification, pyrolysis are mainly operated at high temperature and this may lead to form fouling or slagging inside the reactor. The, shrub type biomass exhibited good initialization, deformation, softening, hemisphere and fluidization temperature characteristics. These biomasses can be used in gasifier without any trouble. For the grass type biomass and herb type, special attention is required in palletisation for improving the energy density of the biomass. All pictures of ash cones are provided in appendix – I.

4.3.7 Fibre analysis of all selected biomass

Selected biomasses were considered for fibre analysis - *Jatropha gossypifolia* (stem), *Cassia tora (L.) Roxb., Cassia auriculata Linn, Jatropha curcas* (shells), *Desmostachya bipinnata, Sphaeranthus indicus Linn, Dichanthium annulatum (Forssk.), Solanum xanthocarpum, Eclipta alba, Sawdust, Prosopis juliflora, Butea monosperm,* in this study.

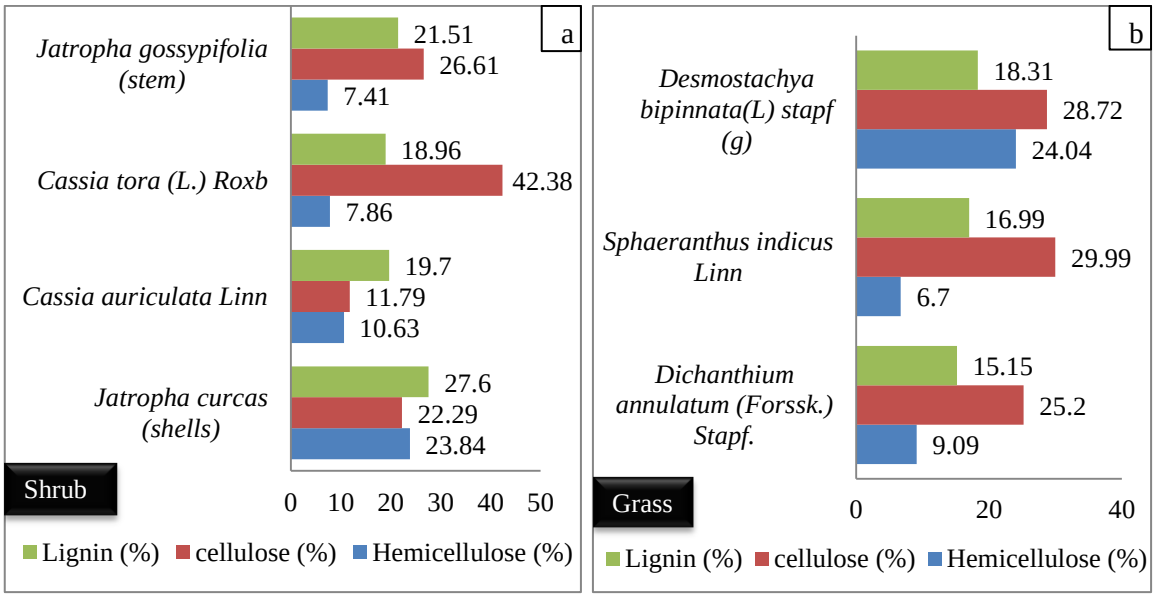

Figure 4.14 shows the typical values of the cellulose, hemicellulose and lignin content of the selected biomass.

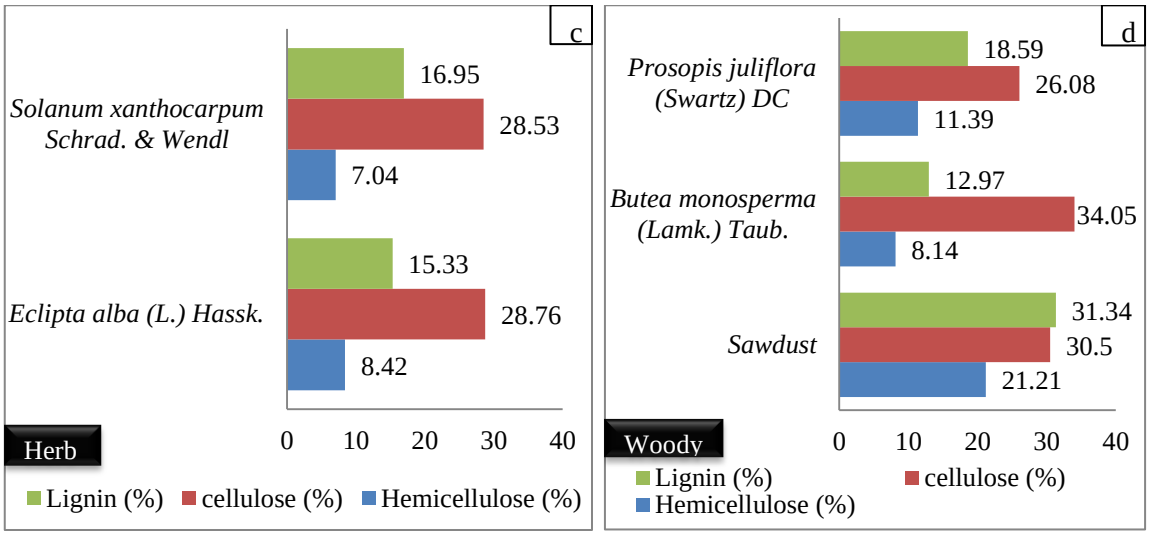

FIGURE 4.14: Fibre analysis of the selected biomass in the present study (dry wt. %).

Firstly, the shrub type biomass exhibited reasonable fibre content, while the grass type biomass has less lignin content compared to others as it contained high ash content as shown in figure 4.14 (a, b). The shrub type and wood type biomass contain a good amount of fibre content due to the low ash content as shown in figure 4.14 (c, d).

4.3.8 Mineral content analysis

The effect of mineral matter in biomass is important to explain the thermochemical behaviour. The presence of alkali metals (K, Na), alkaline earth metals (Ca, Mg), silicon, phosphorous, and iron in the ash makes the biomass prone to create slagging and fouling. The behaviour of the ash including melting and deposition tendencies towards reactor or any surfaces can be predicted or interpreted through some empirical indices. First, alkali index interprets the amount of alkali oxide present in the fuel per unit of fuel energy (kg alkali Oxide GJ^{-1}).

$$AI = \frac{A \times (K_2O + Na_2O)}{Q(GJ)} \quad (4.3)$$

Where, Q is the heating value of fuel in GJ kg^{-1} and K_2O and Na_2O are in mass fraction present in the ash. A is the mass fraction of ash content. If the value of AI belongs to the

range of 0.17 to 0.34 kg/GJ, then slagging or fouling might have occurred and above this value the slagging or fouling will be occur [3–5].

Secondly, base-to-acid ratio is given below.

$$P_{b/c} = \frac{\%(Fe_2O_3 + CaO + MgO + K_2O + Na_2O)}{\%(SiO_2 + TiO_2 + Al_2O_3)} \quad (4.4)$$

The compounds are present in ash on dry and in weight percentage basis. The base-to-acid ratio has primarily measured the tendency of fouling in fuel ash. When $P_{b/c}$ ratio increases, then fouling tendency of fuel increases [5, 6].

And finally, bed agglomeration has been brought out in order to interpret fouling tendency in fluidized bed reactors.

$$BAI = \frac{\%(Fe_2O_3)}{\%(Na_2O + K_2O)} \quad (4.5)$$

The compounds are in weight percentage and the bed agglomeration occurs when the values become lower than 0.15 [5, 7]. Figure 4.15 shows the acid (a, c, e, g) and basic (b, d, f, h) mineral content of the selected biomass. It is necessary to categorise the mineral compounds as an acidic components, Al_2O_3, P_2O_5, TiO_2, SiO_2 and basic mineral content, NaO_2, K_2O, MgO, CaO, Fe_2O_3.

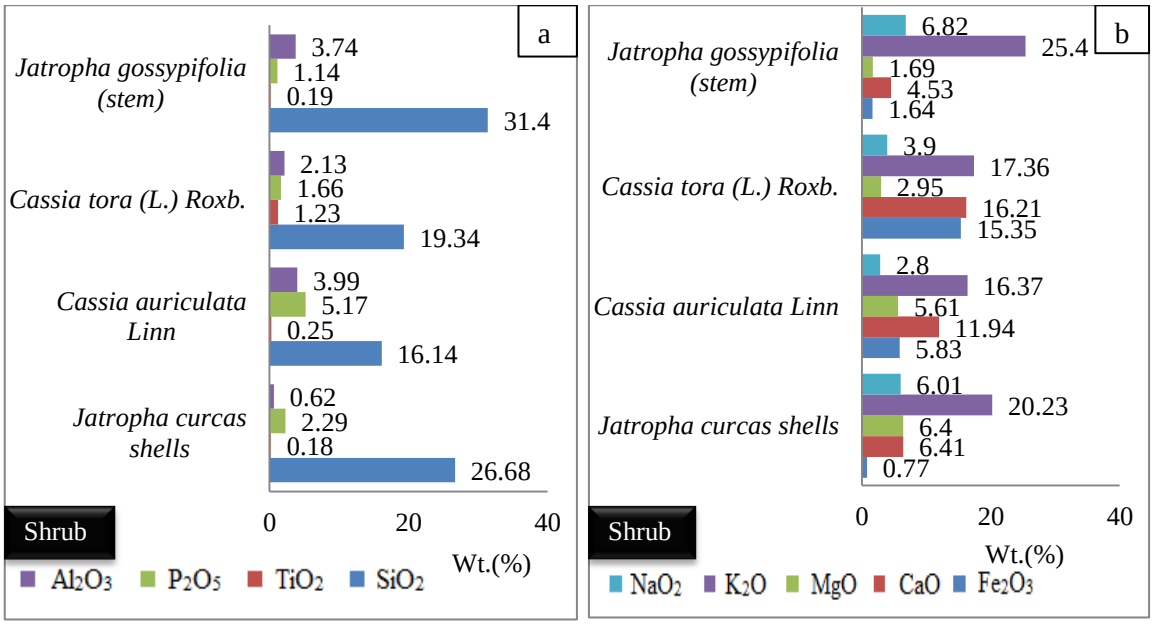

Now, for shrub type biomass such as *Jatropha gossypifolia* (JG), *Cassia tora* (CT), *Cassia auriculata* (CA), and *Jatropha curcas* (JC) shells are shown in figure 4.15 (a). JG (stem) has maximum SiO_2 and K_2O contents. The alkali index (AI), base-to-acid ratio ($P_{b/a}$), and bed agglomeration index (BAI) were found out as 0.031, 1.41 and 0.05, respectively. So it can suppose that there is minimum chance to form clinkers inside the reactors or gasifiers. Only BAI was found lower than standard value. But this would not create any major problem in case of a continuous process.

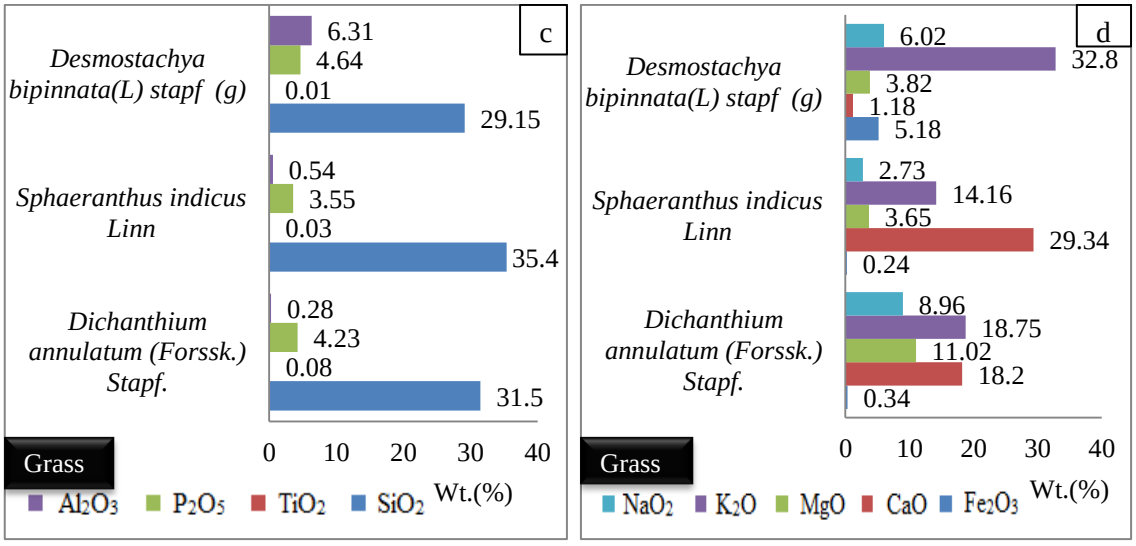

The three indices AI, $P_{b/a}$, and BAI were calculated for *Jatropha curcas* shells as 0.035, 1.73, and 0.029. These are quite similar with *JG* biomass indices. For CA and CT, the values are slightly higher than JG and JC shells as shown in table 4.1. In figure 4.15 (c) and 4.15(d) the acid and basic mineral compounds found in grass type biomass ash - *Desmostachya bipinnata* (DB), *Sphaeranthus indicus* (SI), *Dichanthium annulatum* (DA) are shown. The silica content in grass type biomass was high as expected, while for *DB* K_2O was found to be 32.8% and for SI it was 14.16 %, 18.75% was for DA. The calcium oxide content was found to be maximum in SI as 29.34%, followed by DA by 18.2%. Sodium contents among the biomass were found to be of reasonable amount. So based on this data the AI, $P_{b/a}$, and BAI are also tabulated for DA as 0.45, 1.80, 0.012, for SI as 0.062, 1.38, 0.014, for DB as 0.13, 1.38, 0.13. The alkali index was poor for DA followed by DB and SI. The base-to-acid ratios are also found to be high which is not good in gasification process due to the possibility of formation of clinkers or slagging inside the reactors. Similarly, BAIs were poor for all grass type biomass. So based on these indices it

can be concluded that the grass type biomasses are hardly suitable in thermochemical conversion processes.

For the herb type biomass, the acid and basic mineral contents are shown in figures 4.15 (e) and 4.15 (f). *Solanum xanthocarpum* (SX) and *Eclipta alba* (EA) are in the category of herb type biomass. In acid mineral contents, silica content is found maximum for EA followed by SX and the values are 20.58% and 9.36%, respectively.

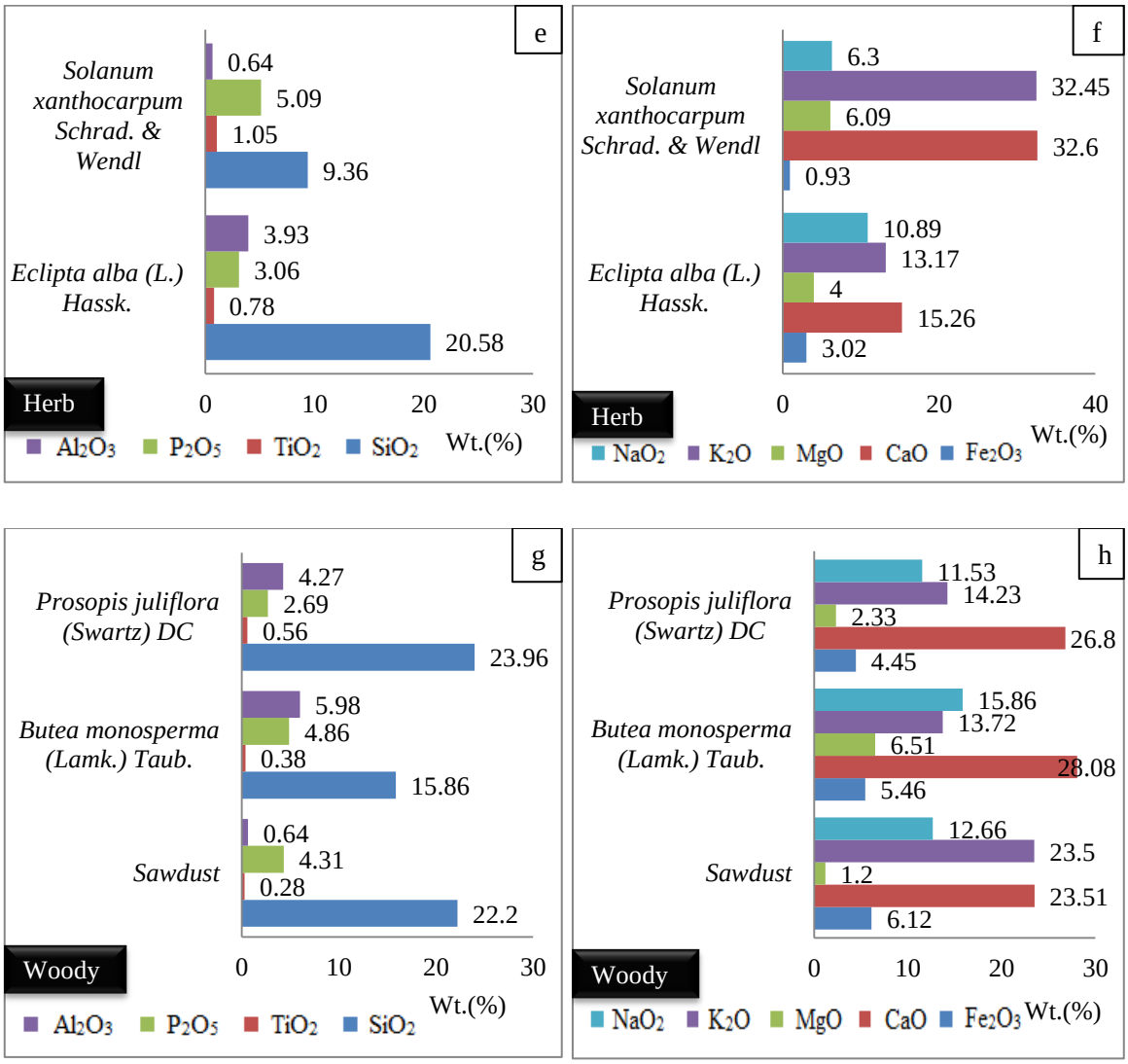

FIGURE 4.15: The acid (a, c, e, g, i) and basic (b, d, f, h, j) mineral contents in the selected biomass ash.

The AI, $P_{b/a}$, BAI were determined as 0.25, 7.83, 0.024 for *SX* and 0.21, 1.89, 0.12 for *EA* as shown in table 4.1. The indices are not so good for the above two herb type biomass in view of the presence of high silica, calcium, potassium, and sodium content in ash. Hence,

these biomass might find difficulty in utilization in the gasifier .The woody type biomass - *Prosopis juliflora*, *Betea monosperma*, and sawdust are shown in figures 4.15 (g) for acid and 4.15 (h) for basic mineral contents. The sawdust is considered as standard biomass for comparing these two biomasses. In acid content, the high silica was found for all woody type biomass, however, for basic contents it was found that the calcium, potassium, and sodium contents were high followed by iron and magnesium. The alkali index found was excellent for all woody type biomass, and the base-to-acid ratios were on the higher side due to the existence of more alkali metals which increased basicity. BAIs were also good, i.e just beyond the range of the standard value as shown in table 4.1. So it can be concluded that all woody type biomass have almost same characteristics. The presence of phosphorus and calcium in woody biomass ash improved the degradation temperature [8]. So biomass having less ash content, high calorific value, high volatile matter, and low moisture content are best suited in the thermochemical conversion process. Based on detailed fuel characterization of biomass, the reactor size and type are determined.

TABLE 4.1: Determination of alkali index (AI), base-to-acid ratio ($P_{b/a}$), bed agglomeration index (BAI) for the selected samples.

Family	**Samples**	**AI**	**$P_{b/a}$ (base-to-acid ratio)**	**BAI**	**Suitability in thermochemical conversions based on three indices**	
					Gasification	**Pyrolysis**
Grass	*Dichanthium annulatum (Forssk.) Stapf.*	0.45	1.80	0.012	Not suitable	Not suitable
	Sphaeranthus indicus Linn	0.062	1.38	0.014	Not suitable	Not suitable
	Desmostachya bipinnata(L) stapf (g)	0.13	1.38	0.13	Not suitable	Not suitable
Wood	*Butea monosperma (Lamk.) Taub.*	0.04	2.89	0.18	Suitable	Suitable
	Prosopis juliflora (Swartz) DC	0.05	1.99	0.17	Suitable	Suitable

	Sawdust	0.04	2.63	0.16	Suitable	Suitable
Shrub	*Cassia auriculata Linn*	0.05	2.08	0.63	Suitable	Suitable
	Cassia tora (L.) Roxb.	0.08	2.45	1.85	Suitable	Suitable
	Jatropha gossypifolia	0.031	1.41	0.05	Suitable	Suitable
	Jatropha curcas shells	0.035	1.73	0.029	Suitable	Suitable
Herb	*Eclipta alba (L.) Hassk.*	0.21	1.89	0.12	Not suitable	Suitable
	Solanum xanthocarpum Schrad. &Wendl	0.25	7.83	0.024	Not suitable	Suitable

References:

1. C Di Blasi, (2009), Combustion and gasification rates of lignocellulosic chars, Progress in Energy and Combustion Science, 35, 121–40.

2. Wastelands atlas of India, Government of India, Ministry of rural development, Dept. of land resources, New Delhi. National Remote Sensing Agency (NRSA), Hyderabad, 2005.

3. TR Miles, TR Miles Jr, LL Baxter, RW Bryers, BM Jenkins, LL Oden, (1996), Biomass Bioenergy, 10(2–3), 125.

4. DC Dayton, BM Jenkins, SQ Turn, RR Bakker, RB Williams, D Belle-Oudry, LM Hill, (1999), Energy Fuels, 13, 860.

5. D Vamvuka, D Zografos, (2004), Predicting the behaviour of ash from agricultural wastes during combustion, Fuel, 83, 2051–2057.

6. BM Jenkins, LL Baxter, TR Miles Jr, TR Miles, (1998), Fuel Process Technology, 54(1–3), 17.

7. DW Bapat, SV Kulkarni, VP Bhandarkar, (1997), Fluidized Bed Combustion, SciTech Connect, 1, 165.

8. E Kakaras, L Fryda, K Panopoulos, P Vourliotis, E Pavlidou, (2006), Experimental investigation of fluidized bed co-combustion of meat and bone meal with coals and olive bagasse, Fuel, 85, 1685–1699.

CHAPTER – 5

Utilization of Wasteland Biomass & Marine Macroalgae for Energy: Case Studies

5.1 Wasteland biomass *Jatropha curcas* shells for energy

5.1.1 A study of *Jatropha curcas* shells gasification for captive power generation

5.1.1.1 Introduction

Jatropha curcas (abbreviated as jatropha) is a hardy plant material easy to cultivate on barren land and is a wasteland derived biomass. The plant has earned acclaim in terms of high quality of bio-diesel obtained from its seeds. The mass of the whole fruit comprises of 60 – 65% of seed weight, remaining 40 – 35% comprising the weight of the empty shell. Most of the attention is paid to the seed as it contains an outer coating husk and a kernel within which the oil exists [1]. It was found that the weight ratio of husk to kernel is approximately 1:2. There have been several research work reported on different aspects of biodiesel production from jatropha oil, either alone or combination of other nonedible oils [2 – 16]. The integrated process developed at the Institute consists of the following steps: removing of raw oil from the whole seed, with oil cake as by product; removal of free fatty acid (FFA) and other impurities from the raw oil in addition to the calculated amount of caustic soda solution in order to avoid the saponification; single step KOH-catalyzed trasesterification with methanol; refinement of methyl ester through non-aqueous washing

followed by water wash; and use of dry hot air to remove the moisture from fuel. Potash fertilizer and pure glycerol are recovered from the glycerol layer while other residues are utilized in soap preparation [2]. The crude glycerol can be used as a substitute source for microbial synthesis of PHA (polyhydroxyalkanoate) [3]. The jatropha shell is also a potential source of energy for generating renewable energy to run any process. It has been evaluated by Waver et al. for its constituents [17]. The lignin content was reported to be 47.6%, the remaining comprising of mainly α-cellulose (22.29%) and hemicellulose (23.84%). It was earlier reported that the presence of high amount of ash content of the shell, and the presence of high amount of alkali metal contents were found to be very problematic in gasification process [17, 18]. Nonetheless, a large amount of shell generated during processing of oil production can be used in conducting trials on jatropha shells gasification. The main objective of this work is to develop a sustainable process to meet the energy consumption for any process. For this purpose, a calculation was done for a biodiesel production unit, in order to obtain the following products starting from 6.06 t/day dry jatropha fruit: 1 t jatropha biodiesel; 0.08 t neat glycerol; 2.54 t oil cake; 0.056 t soap cake; 0.022 t potassium sulphate; 2 t empty shells. If the power and steam consumptions are met from jatropha shells, its requirement would be between 0.85 – 0.90 t based on the findings of the present study. So, this would imply a surplus of ca. 1.1 t of shells, which can be used as a second fuel. Again, for the pyrolysis oil set-up, the requirement of energy is presently supplied from fossil fuel which could be replaced by the energy generation from a 10 kW gasifier in the present study. Thus the process will be sustainable.

5.1.1.2 Material and methods

The full characterization of jatropha shells was done and presented in chapter 4 which includes proximate, ultimate analysis, CV, ash fusion test, and the ash compositions. The most important parameters of jatropha shells were the calorific value and it was found to be 17.22 MJ kg^{-1} and detailed fuel characterization of this feedstock is described in chapter 4. So, naturally, it is an ideal solid fuel for gasification. The ultimate analysis showed a good understanding of the constituents (carbon, hydrogen, nitrogen, and oxygen) which are required for computation of the amount of air for efficient gasification, and the estimation of the volume and composition of the combustion gases. Proximate analysis of a fuel provides information about the moisture content, volatile matter, fixed carbon, and ash. It

was well established that the fuel moisture content has adverse effect on energy efficiency and the recommended moisture level is less than 20% for downdraft gasification.

The moisture content of jatropha shells estimated in this study was around 15.08% under this limit. The high volatile matter (66.31%) was also considered advantageous, as higher values assisted good ignition and result in an enhancement of flame length during burning of gas [19]. The fixed carbon was estimated to be 21.88% in present study. Ash, non-combustible component of the shells, was found to be 11.81% against the reported value of 14.88% [1]. The compositions of alkali and alkaline earth metals ions in the ash were also determined.

The most noticeable constituent K content (16.79%) was comparatively lower than the literature value (24.04%) [1]. Generally, high ash content has adverse effects on the heat transfer at the surface of a solid fuel as well as the diffusion of oxygen during char combustion [20]. Formation of clinkers, which prevent air distribution and also entraps the combustible matter across the reactor zone, depends on the temperature of operation and melting characteristics of ash. Thus ash melting behaviour is an important characteristic in thermochemical process. If the melting temperature is low i.e. less than 800°C, formation of clinkers inside, the reactor can be prevented through special design approach. For this the ash fusion characteristics of the jatropha shells ash was determined and it was found to be good.

It was found that the deformation temperature was 1185°C and the shells were therefore suitable for downdraft gasifier or any thermochemical process.

5.1.1.3 Description and operation of the 10 kW downdraft gasifier

Fig. 5.1.1.1 (a,b) shows typical diagram of the downdraft gasifier used in this study along with the downstream system and the picture of the installed unit. For removal of ash, perforations were made on the base plate in the reduction zone to improve the passage of ash particles. Before start-up, charcoal was charged below the hearth zone and the jatropha shells were manually loaded from the feed hopper having a capacity of 100 kg. Initial ignition was carried out through the firing ports at the air inlets, and a sustained flame was noticed within 5 minutes inside the reactor. The flame could be viewed through a glass mirror positioned at the air inlets. An air suction device was established by circulation of water through a venture scrubber connected to the gas outlet. The air velocity was

determined using a thermo anemometer (CET-6T8B) at the air inlets. About 30 minutes was required to attain the full gas production capacity. Pressure drops were measured across each part by U-tube manometer. Water was used as the manometric fluid. K-type thermocouples were used to measure temperature at different positions of the reactor. After drying and pyrolysis at the upper part of the reactor, the shells went in the combustion zone where air was sucked in. The gaseous combustion products reached the reduction zone having charcoal bed and the gases underwent further reaction to produce combustible producer gas mixture. The produced hot gas coming out at the reactor bottom passed through the scrubber through which water was circulated at room temperature. The cool gas – water mixture was then allowed into cyclone separator to remove the char and tar particulates along with water. The gas was further cleaned by a series of filters consisting of sawdust and two cotton bag filters. At the outlet the gas could be either let into the engine or to a burner.

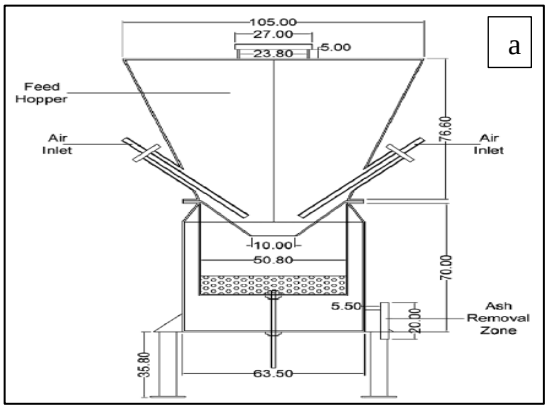

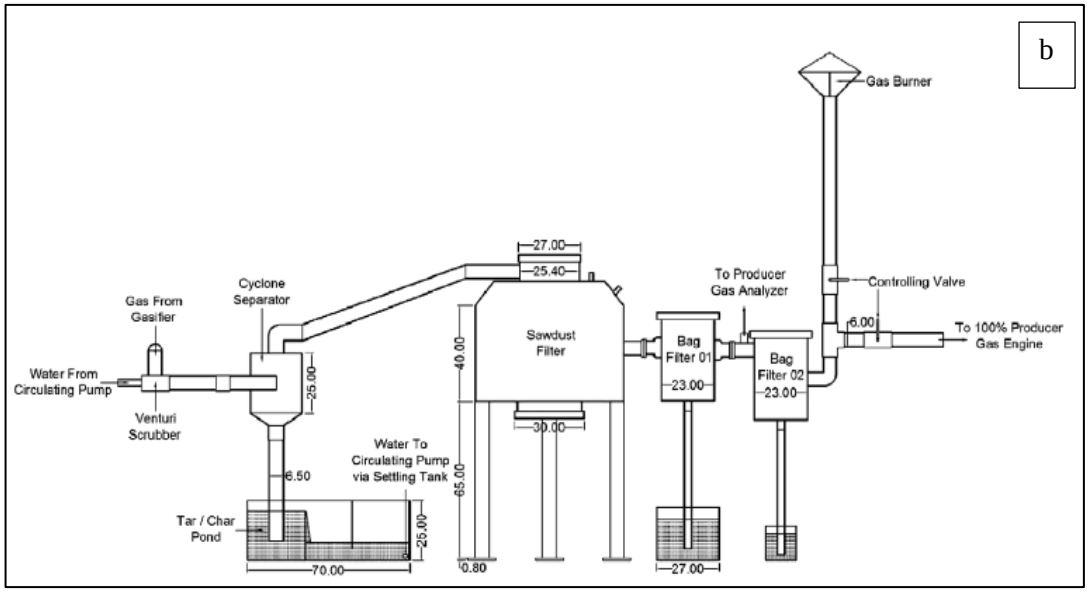

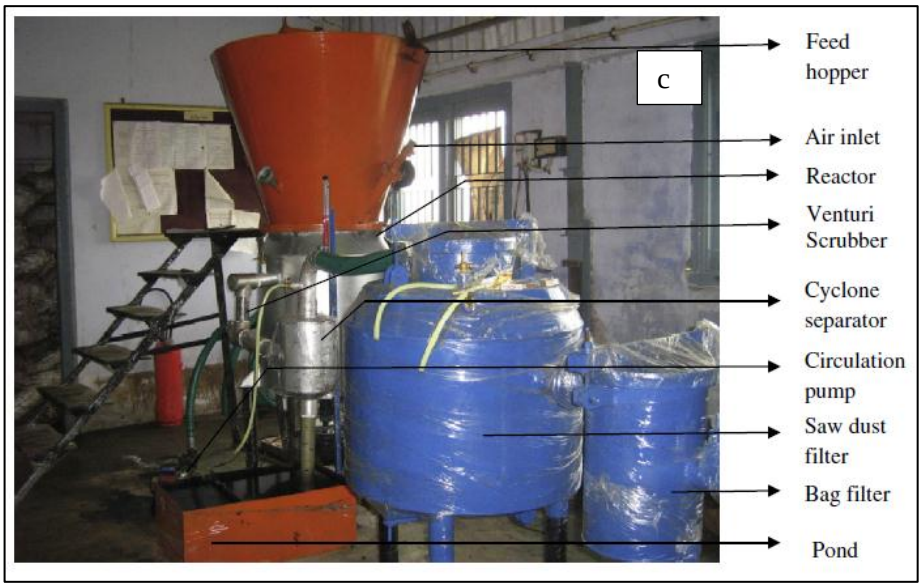

FIGURE 5.1.1.1: First, drawings of the downdraft gasifier (in cm) (a), second, gasifier in downstream system (b), and the picture of the installed unit gas cooling and cleaning systems (c).

Next step was the determination of gas composition by online producer gas analyzer (ESTECH) for volumetric proportions of CH_4, CO and H_2 prior to engine entry. Analytical data assisted to decide the timing of fresh charge of solid fuel. The gasifier has a rotating (2 rpm) grate, which simply allowed mechanical discharge from the base of the reactor. A vibrator assisted the process of ash removal and finally the ash was collected with the help of shovel through a gas-tight service opening after allowing the system cool as shown in Fig. 5.1.1.1 (c).

5.1.1.4 Description of the 100% producer gas engine

The specification of the 100% gas engine i.e. generator was important for optimum utilization of the producer gas for power generation. For this the model was chosen Prakash PNG – 15 BM with rated power of 12 kW. It has a water cooled, 4-stroke, spark ignition type, rpm-1500, continuous rating engine. The engine has a specially designed automatic air and fuel controller and mixing device for smooth and efficient working from nil to full load. It has a one/three-phase (230/414 V; 50 Hz) class F insulation alternator, conforming to IS: 4722/IS: 13364/BS: 5000 standard. The engine exhaust heat was used to dry the feed biomass in a tray type drier. Initially, the shells were placed in drier prior to

charging the gasifier. Start-up of the engine was carried out with battery (12 V, 100 Ah). Once the air – fuel was reached, the engine operation was self-sustained.

5.1.1.5 Operating of the gasifier

The gasifier was initially designed for wood species having moisture (10 – 15% moisture content) at full load (9 – 10 kWe) for period of 5 h on a continuous basis. For the experimental run, jatropha shells and the wood species were charged to the downdraft gasifier in the weight ratio of 1:2. In the present study, suitable modifications were made to improve the passage of ash particles. Electricity was generated on a continuous basis for a period of 6 h. Finally, at the end of experiment, it was observed that other than formation of small amounts of clinkers, no adverse effect was observed. The gasifier was adequately run entirely with jatropha shells and the performance evaluated under load-free conditions. Important parameters for gasification such as equivalence ratio, heating value of the producer gas and gasification efficiency were estimated based on the experimental results from the below equations (5.1) – (5.16) [21].

5.1.1.6 Operating parameters for downdraft gasification

5.1.1.6.1 Specific gas production – producer gas to biomass ratio

The best way to find out producer gas to fuel ratio is by carbon balancing of fuel as follows.

$$C_{biomass} = C_{gas} + C_{char\text{-}ash} + C_{tar} \quad (5.1)$$

$C_{biomass}$ = Rate of carbon input in the gasifier with biomass.

C_{gas} = Rate of carbon leaving the gasifier with producer gas.

$C_{char\text{-}ash}$ = Rate of carbon leaving the gasifier with char-ash.

C_{tar} = Rate of carbon leaving the gasifier with tar.

Assuming carbon in char-ash and tar is negligible compared to the carbon in the producer gas;

$$C_{biomass} = C_{gas} \quad (5.2)$$

From the proximate analysis the mass percentage of jatropha shell is taken as 42.45%.

$C_{biomass} = 0.4245 \times B$ (5.3)

B = Fuel consumption rate (kg/h).

C_{gas} is substituted with $C_{biomass}$.

$C_{gas} = 0.4245 \times B$ (5.4)

Volumetric fraction of carbon in the producer gas is computed as follows:

$$C_{vfg}=\sum \frac{Volume\ fractions\ of\ C\ containing\ components \times Density \times C\ wt.per\ mole}{Molecular\ Wt.\ of\ components} \quad (5.5)$$

$C_{gas} = C_{vfg} \times D$ (5.6)

Where D is the flow rate of the producer gas (m^3/h).

Now, C_{gas} is substituted in equation (5.6).

$0.4245 \times B = C_{vfg} \times D$

$$\frac{D}{B} = \frac{0.4245}{C_{vfg}} \quad (5.7)$$

5.1.1.6.2 Specific air consumption (or air to producer gas ratio)

Nitrogen balance is required in order to find out air to producer gas ratio.

Now, using the nitrogen balance:

$N_{biomass} + N_{air} = N_{gas}$ (5.8)

$N_{biomass}$ = Rate nitrogen input to the gasifier with fuel.

N_{air} = Rate nitrogen input to the gasifier with air.

N_{gas} = Rate of nitrogen leaving the gasifier with gas.

Assuming nitrogen in the fuel is very small compared to the nitrogen in the air.

$N_{air} = N_{gas}$ (5.9)

The volumetric fraction of nitrogen in air is 0.79.

$N_{air} = 0.79 \times E$ (5.10)

Where E is the air flow rate (m^3/h).

Now, N_{air} is substituted in equation (5.9)

$$N_{gas} = 0.79 \times E \tag{5.11}$$

$$N_{gas} = N_{vfg} \times D \tag{5.12}$$

Where, N_{vfg} volumetric fraction of nitrogen.

The value of N_{gas} is substituted in equation (5.12);

$0.79 \times E = N_{vfg} \times D$

$$\frac{E}{D} = \frac{N_{gv}}{0.79} \tag{5.13}$$

5.1.1.6.3 Operating air – fuel ratio and equivalence ratio

The air flow rate and the fuel flow rate largely depend on equivalence ratio. The ratio is defined as the ratio of actual or operating air –fuel ratio to stoicheometric air-fuel ratio.

$$ER = \frac{Operating\ or\ actual\ (\frac{A}{F})_o}{Stoicheometric(\frac{A}{F})_s} \tag{5.14}$$

$$(\frac{A}{F})_o = \frac{Mass\ flow\ rate\ of\ air}{Fuel\ jatropha\ shells\ consumption\ rate} = \left(\frac{D}{B}\right)(\frac{E}{D}) \times \text{Density of air} \tag{5.15}$$

Stoicheometric air-fuel ratio i.e. $(\frac{A}{F})_s$ is considered as 5.4 kg of air per kg of jatropha shells.

5.1.1.6.4 Heating value of the producer gas

The lower heating value of the producer gas reckoned from the chemical composition of the different gases.

$(LHV)_g = \sum Volumetric\ (\%)\ of\ the\ componenets\ \times LHV\ of\ the\ componenets.$

5.1.1.6.5 Gasification efficiency

$$\eta_g = \frac{Heating\ value\ of\ the\ gas\ (HV)_g \times Gas\ flow\ rate\ (D)}{Heating\ value\ of\ the\ fuel\ jatropha\ shells\ (HV)_b \times Fuel\ consumption\ rate\ (B)} \times 100\% \tag{5.16}$$

In this study, the downdraft gasifier was first operated without load for 8 h at a one hour interval and the producer gas burnt with a yellowish-blue flame as shown in Fig. 5.1.1.2.

FIGURE 5.1.1.2: Burning flame of producer gas in gasifier.

TABLE 5.1.1.1: The variation of gasifier performance factors during 8 h continuous operation of the gasifier without load.

Time	***D/B***	***E/D***	$(A/F)_0$	***ER***	$(HV)_g$ **(kJ m^{-3})**	η_g
12:00	2.39	0.67	2.01	0.37	3985.74	55.16
13:00	2.22	0.59	1.65	0.30	5140.64	66.18
14:00	2.04	0.54	1.37	0.25	5639.04	66.81
15:00	2.04	0.50	1.29	0.24	5840.76	69.25
16:00	2.18	0.58	1.60	0.29	5048.19	63.94
17:00	2.18	0.62	1.70	0.31	4576.70	57.94
18:00	2.04	0.54	1.38	0.25	5472.13	64.85
19:00	2.11	0.53	1.40	0.26	5725.65	70.13

Table 5.1.1.1 shows the values of D/B, E/D, $(A/F)_0$, ER, $(HV)_g$ and η_g for each hour starting from 12:00 to 19:00. It was found that the fresh charge of jatropha shells was required when the combustible gas composition showed declining proportions. All average data were tabulated in this study and found that the average gasification efficiency was 64.81% in 8 h operation and the average calorific value of the producer gas 5.2 MJ m^{-3}. The average fuel feed rate at no load condition was 13 kg h^{-1} and producer gas yield was 27.65

m^3 h at room temperature. The space velocity [22] was calculated using the following equation (5.17),

$$space\ velocity = \frac{volumetric\ gas\ production\ rate\ in\ Nm^3s^{-1}}{throat\ cross\ sectional\ area\ in\ m^2} \quad (5.17)$$

The space velocity was calculated and found to be 0.88 m s^{-1}. The value of gasification efficiency and the calorific value of the producer gas are comparable to results from other combustible biomass [23]. Fig. 5.1.1.3 shows combustible gas composition over the entire period. For experiment, a charge of 80 kg was provided at the beginning.

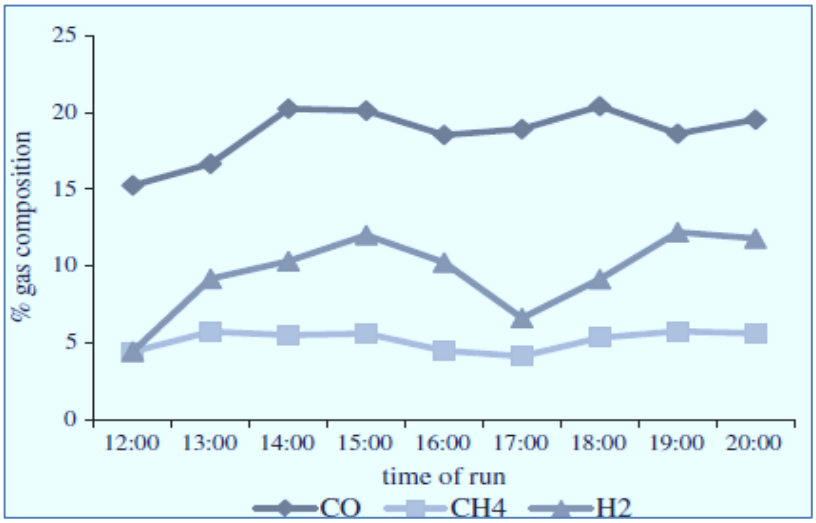

FIGURE 5.1.1.3: The variation of gas composition with time.

The curve shows that, as the biomass was consumed, combustible components in the producer gas increased and the efficiency of gasification also increased as shown in table 5.1.1.1. From 15:00 h, there was a sharp drop in combustible components which was more pronounced for H_2, and at around, 16:30 h, a fresh charge of the jatropha shells were required. Then again, it was found that the combustible gas composition rose and lasted till 20:00 h. After about 2 h of the start of experiment run, the temperatures were measured as 130°C, 326°C, 752°C, and 480°C at four different zones, drying, pyrolysis, combustion, and reduction zones, respectively. Control of the *ER* value was crucial during gasification since high *ER* decreases the heating value by lowering the concentration of combustible components such as CO, and H_2 and simultaneously, enhanced the CO_2 content in the product gas [23]. *ER* was varied in this experiment from 0.25 to 0.37 which has considerable range for gasification of biomass [24]. The regression was also performed to

correlate the $(A/F)_0$ combustible gases, equation (5.18) was derived from the experimental data having R^2 value 0.9976. The above equation interpreted that the higher air-fuel ratio leads to lower combustible components in the producer gas.

$$(A/F)_0 = 3.78 - 0.08CO - 0.10CH_4 - 0.03\,H_2 \quad (5.18)$$

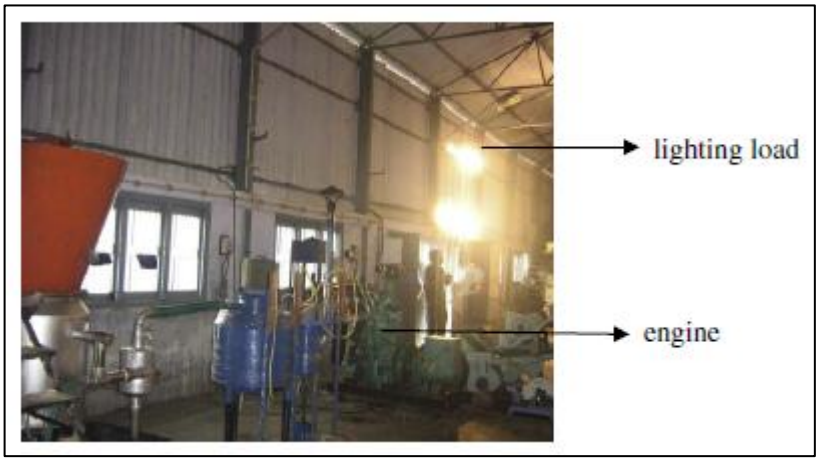

FIGURE 5.1.1.4: Gasifier being operated with 10 kWe lighting load.

TABLE 5.1.1.2: Performance of the 100% producer gas engine.

Time		Voltage (v)	Current (A)	Power factor	Frequencey	Power (kW)
12:00	R	232	13.5	1	47.1	3.2
	Y	231.1	13.6	1	47	3.27
	B	234.8	13.7	1	47.6	3.21
13:00	R	239	11.7	1	49	2.78
	Y	241	11.8	1	49	2.81
	B	240	11	1	48	2.72
14:00	R	222	13.3	1	45	3.07
	Y	229	13.4	1	46	3
	B	229	13.1	1	47	2.9
15:00	R	229	13	1	46	3.1

	Y	233.3	13.5	1	47.7	3.09
	B	220	12.6	1	35	2.9
16:00	R	237.6	13.5	1	48.9	3.2
	Y	238.6	13.5	1	48	3.3
	B	243	13.7	1	48.8	3.28
17:00	R	243.2	13.2	1	48.7	3.35
	Y	244.7	13.1	1	49.9	3.3
	B	247.4	13.8	1	50	3.44
18:00	R	232.5	13.5	1	48.5	2.88
	Y	228.8	13.2	1	47.2	2.95
	B	229.3	13.4	1	46.6	3.17
19:00	R	220.6	13.1	1	46.5	2.88
	Y	222.7	13.2	1	46.3	2.95
	B	233.7	13.3	1	46.9	3.17
20:00	R	195	12.4	1	42	2.35
	Y	208.6	12.7	1	43.7	2.63
	B	193.9	12.1	1	43	2.26

The downdraft gasifier was connected to the 100% producer gas engine directly in this study along with alternator in the following run. Three phase power was generated when nine 1 kW flood lights and three 0.5 kW flood lights (Fig. 5.1.1.4) were connected as load. The load was gradually increased at the start and the generator was then made to run at full load from 12:00 h to 20:00 h continuously in order to maintain load adding with biomass time to time. It measured the negative pressure in line was 470 mm of water column. The gas temperature of outlet was at room temperature. Table 5.1.1.2 shows the power generation data for 8 h continuous operation. R, Y, and B indicate the three phase system. The engine exhaust temperature was found to be 250 – 300°C, which assisted in drying the feedstock biomass. The arrangement for such system was a wire rack (0.4m × 0.4m ×

0.24m; standard mesh 4) containing the shells was placed over engine exhaust pipe and pre-dried in batch mode prior to charging in the gasifier. To carry out the experiment, 15 kg of the biomass was introduced at hourly basis. The overall efficiency of the gasifier including electrical energy was 24.46%. After cooling down the gasifier, the next day ash was collected and it was found that the some clinkers were formed having dimension 2.5 – 3.0 cm diameter in the gasifier grate. The reason may be due to the long residence time of 20 – 25 min of the ash on the grate and drop in temperature in the combustion zone. Meanwhile, the clinkers did not create any problem to flow the producer gas and power production during operation, some modification might be needed to reduce the formation of clinkers.

5.1.2 A study on pyrolysis of *Jatropha curcas* shells

5.1.2.1 Description of the pyrolytic oil set-up

This pyrolysis experiment was carried out in a fixed bed horizontal reactor made of 316 grade stainless steel having dimension of 105 cm length and 5 cm diameter with one end was fully shielded to prevent entry of air/oxygen and other end was adjoined with silicon tube which was connected to the condenser. The heating system is consisted of a heating element wire wound up directly round the outer surface of the reactor. The heater coil was insulated from the outside in order to minimize the heat loss. A K-type thermocouple was used to measure the temperature of the bulk sample bed and was placed in the middle of the reactor. To control the temperature of the bed, a PID controller was used to control the final temperature and heating rate along the axis of the reactor. The temperature distribution, especially in a tubular reactor was in the axial direction of the reactor, and it was found that the extreme ends displayed about 5% less temperature than the middle.

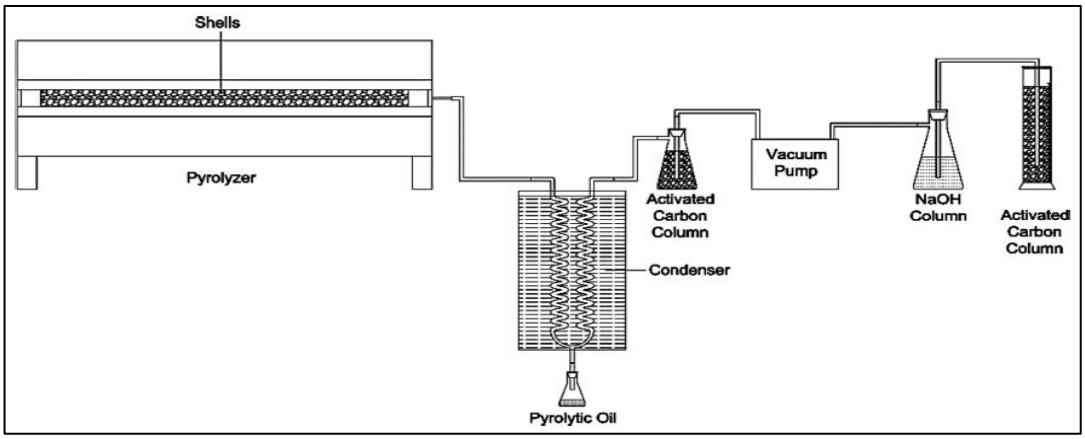

FIGURE 5.1.2.1: Schematic diagram of experimental set-up for the fixed-bed reactor.

The shells were fully packed in the reactor as shown in Fig. 5.1.2.1. The condenser was designed in this experiment in such way that maximum oil yield could be obtained for each experiment, and there were no carry-over of oil with the gas. The condenser was placed in an ice bath for efficient condensation. The non-condensable gas from the condenser was allowed to pass through two beds of activated carbon with a vacuum pump in between, and through a dilute solution sodium hydroxide to free it completely from the non-condensed tarry matter. The non-condessable gas was quantified through an ESTECH producer gas analyzer, and the following gases were quantified as CO, H_2 and CH_4. For experimental study, 100 g of jatropha shells was uniformly placed inside the reactor, and the experiments were carried out at the heating rate of 5°C min^{-1} upto final temperatures of 300, 400, 500 and 600°C with a holding time of 4 h until the oil yield became maximum and the non-condensable gas yield became close to zero. The yields were tabulated as the average of at least three with an experimental measurement error < ±1%.

5.1.2.2 Effects of kinetics parameters on pyrolysis

The rate of decomposition of a solid-state substance is a function of temperature, and the conversion is best described by the following equation [5.19 – 5.28] [25 – 31]:

$$\frac{d\alpha}{dt} = \text{k}\,(T) f(\alpha) \tag{5.19}$$

Conversion, α, is defined by the weight loss from a decomposed sample with increasing temperature.

$$\alpha = \frac{m_{pm} - m_{am}}{m_{pm} - m_{fm}} \tag{5.20}$$

m_{pm} is the initial mass, m_{am} is the mass at time t and m_{fm} is the final mass of the sample.

The temperature-dependent function or rate constant, i.e. *k (T)*, is best described by the Arrhenius equation as follows:

$$\text{k (T)} = A.\, e^{\frac{-E_a}{RT}} \tag{5.21}$$

where E_a is the apparent activation energy (kJ mol^{-1}), T is the absolute temperature (K), R is the gas constant (8.314 J mol^{-1} K^{-1}) and A is the pre-exponential factor (min^{-1}). Inserting eqs. (5.20) and (5.21) into (5.19) gives the eq. (5.22), which represents the equation for calculating the reaction kinetic parameters from the TGA results.

$$\frac{d\alpha}{dt} = A.f(\alpha).e^{\frac{-E_a}{RT}} \quad (5.22)$$

The function $f(\alpha)$ can be expressed as,

$$f(\alpha) = (1-\alpha)^n \quad (5.23)$$

Here, n is the reaction order, and substituting the value of $f(\alpha)$ in eq. (5.22) gives the expression of the reaction rate as follows:

$$\frac{d\alpha}{dt} = A.(1-\alpha)^n.f.e^{\frac{-E_a}{RT}} \quad (5.24)$$

For a non-isothermal case, the linear heating rate is $\beta = \frac{dT}{dt}$ and the following equation can be applied:

$$\frac{d\alpha}{dT} = \frac{A}{\beta}.(1-\alpha)^n.f.e^{\frac{-E_a}{RT}} \quad (5.25)$$

$$\ln(\frac{d\alpha}{dT}) = \ln(\frac{A}{\beta}) - \frac{E}{RT} + n.ln(1-\alpha) \quad (5.26)$$

The above equation can be written in the following simplified form;

$$y = P + Q.x + R.z \quad (5.27)$$

where $y = \ln(\frac{d\alpha}{dT})$, $P = \ln(\frac{A}{\beta})$, $x = \frac{1}{RT}$, $z = ln(1-\alpha)$, $Q = -E$ and $R = n$

$$\frac{d\alpha}{dT} = -\frac{1}{m_{im}-m_{fm}}\frac{dw}{dT} = -\frac{1}{[\beta(m_{im}-m_{fm})]}\frac{dw}{dt} \quad (5.28)$$

P, Q and R can now be calculated from multilinear regression from the data obtained from the TGA and DTG curves. The derivative mass loss (DTG) and TGA of thermal decomposition of shells pyrolysis is shown in Fig. 5.1.2.2.

It is well known that the jatropha shell is lignocellulogic biomass and, like any other biomass, were presumed to devolatilize through the degradation of three major constituents: hemicellulose, cellulose and lignin. From TGA and DTG curves it was

revealed that both heating rates, the first peak from 45 to 150°C showed the removal of moisture from the biomass.

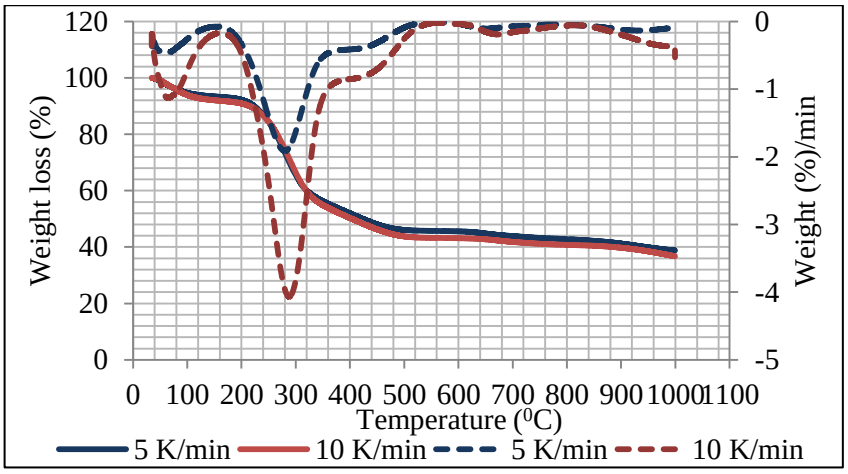

FIGURE 5.1.2.2: Weight loss and rate of weight loss with temperature from TGA.

The drying temperature zone sharpened or increased with an increasing heating rate due to reduction in the residence time in any given temperature range. The actual pyrolysis started at 200°C and continued to 600°C. It was observed that during entire pyrolysis process, weight loss occurred continuously until the weight became close to constant. Owing to the rate of heating it was increased from 5 K min^{-1} to 10 K min^{-1} the reaction time decreased and the curves for 10 K min^{-1} became sharper and shifted toward higher temperatures. Haiping Yang et al. [32] elaborated in detail about the thermal degradation of pure cellulose, hemicellulose and lignin at 10°C min^{-1}. They reported that the pyrolysis of hemicellulose started at 220°C and mass-loss increased with increasing temperature and the maximum mass-loss obtained at 260°C. Similarly, the pyrolysis of cellulose occurred in the range of temperature of 315°C to 390°C, maximum mass-loss obtained at 355°C and after that mass-loss reduced largely. In case of lignin from room temperature to 900°C, the DTG curve was almost flat and the solid residue left from the lignin devolatilization was about 45% of the original weight. It could be assumed that the slow carbonization of lignin occurred in wide range of temperature zone. In this present study jatropha shells promoted for thermal degradation, a 53.56% and 51.83% weight loss occurred at 5 and 10 K min^{-1}, respectively, from the active pyrolysis zone of 200−500 °C. Table 5.1.2.1 shows the thermal degradation of the biomass at the two heating rates is selectively chosen to correlate with the pyrolysis temperature. The active pyrolysis zone of 200−500°C was further divided into three specific zones: 200−260, 260−300, and 300−450°C based on the

degradation hemicellulose, cellulose and lignin. The thermal degradation for each zone is shown in table 5.1.2.1. The weight loss pattern for 450−750°C is also shown in table 5.1.2.1. Initially, the thermal degradation rates were slow. The thermal degradation of hemicellulose started at about 200°C and continued to about 260 °C, the degradation being 11.78% and 9.95% at 5 and 10 K min-1, respectively. However, at temperatures above 260°C, a rapid degradation was observed: 19.46% and 18.78% mass loss occurred within the temperature range of 260−300°C, marking the degradation of a large amount of cellulose in the biomass. The decomposition of the jatropha shells was found to be at a maximum in the third zone; 26.66% and 30.40% mass loss occurred within the zone of 300−450°C, which might have been presumably due to both cellulose and lignin. However, the rate of degradation was slow. At temperatures above 450°C, an insignificant rate of the degradation of the shells was observed. Lignin decomposed throughout a wide range of temperature, the start being even lower than that of cellulose and the end being about 750°C. The DTG curve was found to be relatively flatter at 5 K min^{-1}. This might have been due to the existence of a temperature gradient throughout the cross-section of the shells during its thermal degradation [33]. At a lower heating rate, sufficient time was provided for heating, and the temperature pattern along the cross-section could be presumed to be linear, and as a result the outer surface and the inner core of a single biomass particle attained an equivalent temperature at a particular time. On the other hand, a sufficient residence time was not provided for the required evolving of the volatile matter for a higher heating rate, and therefore, pyrolysis with optimum gas, oil, and char residues was achievable at a lower heating rate. The thermal decomposition of cellulose, hemicellulose, and lignin could be correlated with their chemical nature of the structure. Hemicellulose is easily pyrolyzed because of its amorphous characteristic and the randomly distributed molecular chain length. Cellulose is a long polymer of glucose units without any branches. It is crystalline in nature and it resists degradation.

TABLE 5.1.2.1: Thermal degradation and the rate of degradation of jatropha shells at 5 K min^{-1} and 10 K min^{-1}.

	Temperature zone (°C)			
	200-260	260-300	300-450	450-750
	Heating at 5 K min-1			
Total weight loss (%)	11.78	19.46	26.66	10.02
average degradation rate (% min^{-1})	0.98	2.43	0.88	0.16

		Heating at 10 K min^{-}1		
Total weight loss (%)	9.95	18.78	30.40	11.02
average degradation rate (% min^{-1})	1.65	4.69	1.57	0.36

TABLE 5.1.2.2: Kinetics parameters for jatropha shells.

Kinetics parameters	**Temperature Zone ($^{\circ}$C)**		
	200-260	260-300	300-450
	Heating at 5 K min^{-}1		
R^2	0.99	0.83	0.99
A (min^{-1})	7.57×10^{5}	1.15×10^{2}	1.74
E (kJ/mol)	67.26	30.65	13.21
n	0.0665	0.171	2.20
	Heating at 10 K min^{-}1		
R^2	0.99	0.89	0.94
A (min^{-1})	2.67×10^{6}	4.09×10^{2}	6.03×10^{3}
E (kJ/mol)	69.67	33.68	49.06
n	0.0672	0.0836	2.32

Lignin is composed of polysaccharides and is a cross-linked polymer consisting of three kinds of benzene−propane. The thermal stability of lignin is extremely good, and it is extremely hard to decompose [32].

The kinetic parameters for the shells were calculated using eqs (5.26) and (5.28) using a multilinear regression technique and the values are summarized in table 5.1.2.2. For all the temperature zones and at both heating rates, the reaction order was fractional, indicating chain reactions or complex reaction mechanisms as pyrolysis is a complex reaction mechanism. The results from the activation energy at the two heating rates revealed that the values at all the selected temperature zones were less at a heating rate of 5 K min^{-1}. So, naturally, increasing the heating rate did not increase the activation energy, and therefore, the heating rate of 5 K min^{-1} was chosen as the experimental heating rate for the pyrolysis intended for the production of bio-oil. A fall in activation energy was noted as the pyrolysis proceeded at 5 K min^{-1}. This might have been due to the genesis of lower molecular at higher temperatures due to slow heating. Notwithstanding, the activation energy increased for the third temperature zone at 10 K min^{-1}, which might have been because of the incompletion of the cellulose and lignin decomposition at the higher heating rate. The value of A increased with an increasing heating rate, as earlier found by Bilbao et al. [34]. The investigation of DSC of jatropha shells was carried out at 5 and 10 K min^{-1}

from ambient temperature to 600°C. The purge gas flow rate was 50 mL/min or 70 mL/min in the protective mode. The plot is shown in Fig. 5.1.2.3(a). The sharp endothermic peak at about 85 °C was owing to the removal of moisture from the biomass on heating. The curves have an exothermal pattern from 200 to 260 °C, which could be attributed to the pyrolysis of the hemicellulose. The prominent exothermic peak at about 285 °C was probably due to the degradation of the lignin in the biomass. The endothermic peak at about 300, 400, and 500°C was on account of the pyrolysis of the cellulose. The DSC curves were well explained by Ball et al. [35]. The researchers reported that the formation of solid char from a biomass during pyrolysis was highly exothermic in nature, whereas the evolution of the volatiles was endothermic. The rate of heating also affects the reaction pathway, and therefore the final products. The kinetic study and TGA plot in Fig. 5.1.2.2 show that the weight loss from ambient to 300, 400, 500, and 600°C at a heating rate of 5 K min^{-1} was 34.44, 48.11, 57.18, and 66.8%, respectively. During pyrolysis, the biomass was continuously heated to 1000°C, and presumably the weight loss was pre-eminently due to the loss of condensable and non-condensable matter, and that the residue was bio-char.

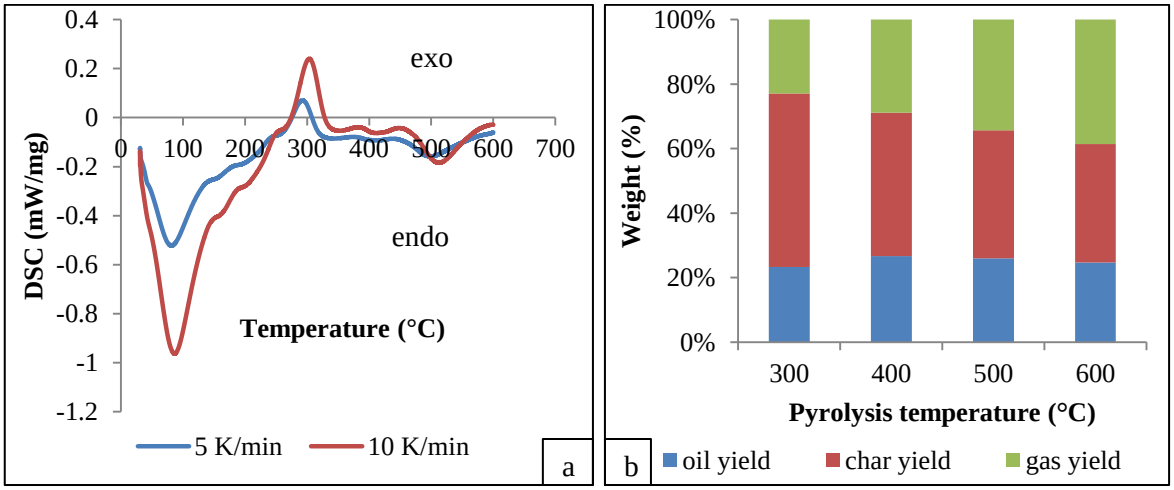

FIGURE 5.1.2.3: DSC curves (a) and effect of temperature on products (b) yield for jatropha shells.

Prior to start of the experimental pyrolysis in the fixed-bed horizontal reactor, a preset holding time of 4 h was considered to be enough for the complete removal of the gas and pyrolytic bio-oil. Moreover, bio-char was a valuable product for this study. Looking at the weight loss pattern from the kinetic study, temperatures of 400 and 500°C were found to

be most suitable as both produced 40−50% bio-char. Since, for the sake of optimization, pyrolysis was investigated at the four temperatures of 300, 400, 500, and 600°C at a heating rate of 5°C min^{-1}.

5.1.2.3 Effect of reactor temperature on product yield during pyrolysis

The percent product yields of oil, gases, and solid chars at varied temperatures are shown in Fig. 5.1.2.3(b). The maximum char yield of 53.71% was obtained at 300°C, after which it gradually decreased, the lowest being 36.74% at 600°C. On increasing the temperature, the reactions involving devolatilazation were successful, and as a result the gas production increased. The gas production increased from 20.36 to 37.30% when the pyrolysis temperature was raised from 300 to 600°C. Hence, the gas yield increased with temperature, but the solid char yield decreased. The liquid oil yield increased with temperature and was at a maximum at 400°C, its value being 31.14%; it then decreased at higher temperatures of 500 and 600°C. A similar trend has been observed by earlier reported work on other kind of biomass [36 – 38]. At 300°C, the oil yield was at a minimum due to lack of temperature for the thermal degradation of the solid biomass. At 600°C, the oil yield again reduced; the possible reason could be the evaporation of oil fragments, especially lower molecule, at higher temperatures. Nonetheless, in addition to the characteristic of the biomass, the type of pyrolytic reactor and the heating rate pre-eminently affect the product yield distribution. Pyrolysis at 400°C resulted in a combined oil and gas yield of 55.6%. The discrepancy of 7.5% was evaluated from the kinetic study and assumed that because of the holding time of 4 h at that temperature, it ensured the complete removal of the volatiles and condensates from the biomass structure.

5.1.2.4 Bio-oil characterization

The bio-oils obtained from jatropha shells were characterized by physical and chemical properties such as density, viscosity, and pH which were determined according to ASTM methods. The moisture content was determined by Karl-Fisher titration. The CHNS, GCV (gross calorific value), TGA were earlier described. The refractive index of the bio-oils was measured with refractometer model no. RE40D, Metler Toledo. The moisture free bio-oil was characterized by Shimadzu GC-MS-QP2010 gas chromatograph/mass spectrometer. The column over temperature was 400°C, and injection temperature was 250°C, the heating rate being 15°C min^{-1}. The holding times were 3 min and 10 min at

40°C and 240°C. The total pressure, total flow, column flow, linear velocity, purge flow, and split ratio were kept at 49.7 kPa, 34.1 mL min^{-1}, 1.0 mL min^{-1}, 36.1 cm s^{-1}, 3.0 ml min^{-1} and 30.0 respectively. Helium was used as a carrier gas, and the MS was operated in scan mode with a scan time of 0.5 s. The scan speed was 1250 scan s^{-1}, and the mass range was 30 – 600 m/z. The NMR spectrum analysis was carried out by Fourier transform (FT) nuclear magnetic resonance (NMR) spectroscopy at 500 MHz using Bruker Advance II 500 instrument, and $CDCl_3$ was used a solvent. The FT-IR analysis was carried out in a Perkin Elmer Spectrum GX FT-IR analyzer.

Bio-oil from jatropha shells has been characterized as a fuel and reported previously by several authors [33, 39, 40]. The cellulose, hemicellulose, and lignin components of the shells were experimentally [41 – 43] found to be 24.66, 21.45, and 39.01%, respectively. The bio-oil obtained by the pyrolysis of the shells at varied temperatures of 300, 400, 500, and 600°C were affirmed for physical properties such as viscosity, density, refractive index, and pH. The GCV of the extracted pyrolytic bio-oil was found to be almost identical at all the working temperatures. An elemental analysis was determined. Table 5.1.2.3 tabulated the physical properties of the crude bio-oil at varied carbonization temperatures. The bio-oils obtained at varied temperatures were characterized by GC-MS, FT-IR, and NMR spectra (^{1}H and ^{13}C) to recognize the different organic fractions present. Bio-oil is basically a mixture of different organic fragments which generally accrue from the thermal decomposition of cellulose, hemicellulose, and lignin within the temperature range. It is well known that acids, aldehydes, alcohols, and ketones are the key products of cellulose and hemicelluloses pyrolysis, and that phenolics and cyclic oxygenates are the key products of lignin [44]. Table 5.1.2.4 explains the matter comprehensively derived from the GC-MS data, and it shows the different type of fragments present in the oils and the % area occupied by each. It can be seen from table 5.1.2.4 that ketone and its derivatives are at a high at around 37.69−42.49%. Other functional groups such as phenols, carboxylic acid, and alcohols were also high (9.34−14.32%, 4.55−23.61%, and 20.45−29.23%, respectively). The oxygenated compounds containing the functional group O−H, C=O, C−O, and aromatic compounds made the bio-oil slightly acidic and reduced its calorific value [45]. A ^{1}H NMR analysis was investigated, and the results are shown in table 5.1.2.5. The types of hydrogen in ^{1}H NMR are classified into four groups as aromatic and olefinic, ether and ester, aliphatic hydrogen adjacent to aromatic/olefin/ketone, and other aliphatic groups. The aromatic and olefinic group was found to be the lowest at 600°C. ^{13}C DEPT-

135 NMR was also carried out to identify the position of the odd numbers of hydrogen containing carbon (−CH, $-CH_3$) and the even numbers of hydrogen containing carbon ($-CH_2$). The δ value of the odd number of hydrogenic carbon which comes on the positive signal whereas, the even number of hydrogenic carbon comes on the negative signal. The results are displayed in table 5.1.2.6. FT-IR was used to identify the chemical bonds and functional groups present in a bio-oil sample through an infrared absorption spectrum, which gave an assessment of the chemical properties of the bio-oil. The functional groups of the bio-oils were identified through the FT-IR analysis as shown in table 5.1.2.7. A simple organic reduction reaction was carried out with the oil obtained at a 400°C pyrolytic temperature. The oil yield was around 60% after the reduction. The calorific value of the upgraded bio-oil was enormously higher at 50 MJ kg^{-1}. GC-MS and FT-IR were performed for the upgraded bio-oil, and the results were compared with the compositional analysis of the crude. Fig. 5.1.2.4 and tables 5.1.2.8 and 5.1.2.9 clearly show the difference in the composition of the two oils. The aldehyde and ketones in the crude bio-oil were converted to alkanes, as can be seen from the absence of the 1714 cm^{-1} C=O stretching vibrations in the upgraded oil (Fig. 5.1.2.4). Table 5.1.2.8 shows the compositional analysis of the bio-oil obtained at a pyrolytic temperature of 400°C before the reduction, and table 5.1.2.9 shows the compositional analysis after the reduction. Table 5.1.9 shows the conversion of the aldehyde/ keto compounds in the unprocessed bio-oil to ethylbenzene (48.55%) and other benzene derivatives, thus making the calorific value of the upgraded oil 66% more than the unprocessed bio-oil from J. curcas shells. The density of the upgraded oil was measured to be 978.65 kg m−3. A GC-MS chromatogram of the crude bio-oil obtained at 400 °C and that of the upgraded bio-oil which are shown in Fig. 5.1.2.5 (Top).

TABLE 5.1.2.3: Physical properties of the *Jatropha* shells bio-oil at different pyrolytic temperatures.

Properties	**Temperatures (°C)**			
	300	400	500	600
GCV (MJ/kg)	29.9	29.13	31.0	29.94
viscosity (cP)[a]	0.96	1.11	1.15	1.77
density (Kg m^{-3})[b]	1026.3	1021.0	1010.0	1023.7
pH	6.5	6.5	6.5	6.5
refractive index	1.464	1.488	1.493	1.469
elemental analysis (wt. %)				

C	54.21	57.20	58.55	53.82
H	6.957	7.038	7.423	7.308
C/H	7.792	8.127	7.887	7.364
N	1.81	2.55	3.38	1.82
O	37.02	33.21	30.64	37.05
H/C molar ratio	1.54	1.47	1.52	1.62
O/C molar ratio	0.512	0.435	0.389	0.516
a @ 50^0C b @ 30^0C				

TABLE 5.1.2.4: Distribution of organic compounds (% area) at different temperatures by GC-MS.

Type of organic compounds	Temperatures (°C)			
	300	400	500	600
aromatic hydrocarbons	1.95	2.8	1.51	0.31
hydrocarbons	0.52	-	2.40	0.27
Total	2.47	2.80	3.91	0.58
nitrogen-containing organic compounds	-	0.17	1.23	5.4
total	-	0.17	1.23	5.4
other organic compounds				
alcohols	27.75	28.85	29.23	20.45
phenols	14.32	17.54	15.0	9.34
ethers	-	-	0.97	0.8
aldehydes	0.28	0.50	1.26	0.93
ketones	41.79	37.69	42.49	38.91
carboxylic acids and derivatives, etc.	13.39	12.43	4.55	23.61

TABLE 5.1.2.5: ^{1}H NMR results for the obtained bio-oil.

Type of hydrogen		Temperature (°C)			
	Chemical shift (ppm)	300	400	500	600
Aromatic and olefinic group	8.5 – 6.5	4.10 (20.79)[a]	3.00 (21.05)	4.00 (26.52)	1.5 (17.64)
Ether, ester related group	5 - 3	3.00 (15.21)	2.10 (14.73)	2.19 (14.52)	1.3 (15.29)
Aliphatic hydrogen adjacent to aromatic/olefin/ketone	3 - 2	9.24 (46.85)	6.57 (46.10)	6.09 (40.38)	4.0 (47.05)
Other aliphatic	2 - 1	3.38 (17.13)	2.58 (18.10)	2.80 (18.56)	1.7 (20.0)

[a]values are presented as the mol% and, in parenthesis, the % of total hydrogen at each

temperature.

TABLE 5.1.2.6: ^{13}C NMR result for the obtained bio-oil.

Type of carbon	Chemical shift (ppm)
Ketones, aldehydes	220 - 200
Esters, carboxylic	200 - 180
Amides, esters, carboxylic acid and aromatics	180 - 160
Aromatics, alkenes and heteroaromatics	160 - 140
Aromatics, heteroaromatics and alkenes	140 - 120
Nitriles, alkenes	120 - 100
Alkyne, phenols, and alcohols	100 - 80
Phenols, alcohols and nitro	80 - 60
Phenols, alcohols	60 - 40
Alkanes	40 - 20
Alkanes	20 - 10
Alkanes	10 -0

TABLE 5.1.2.7: FT-IR analysis of obtained bio-oil.

Frequency range (cm^{-1})	Groups	Class of compounds
900-690	O-H (bending)	Aromatic compounds
1300-1000	C-O (stretching)	Alcohols, ethers, esters, carboxylic acids, phenol.
1450-1375	C-H (bending)	Alkanes
1550-1350	-NO_2 (Stretching)	Nitrogenous compounds
1680-1600	C = C (Stretching)	Alkenes
1740-1700	C = O (Stretching)	Ketones, aldehyde, carboxylic acid
3000-2850	C-H (Stretching)	Alkanes
3150-3050	C-H (Stretching)	Aromatic ring
3650-3200	O-H (Stretching)	H-bonded, water impurities

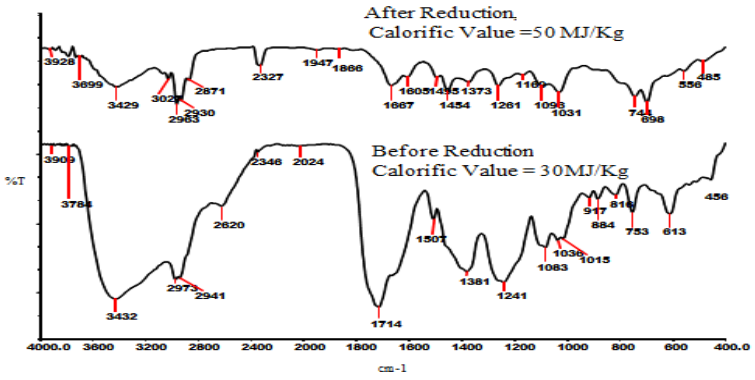

FIGURE 5.1.2.4: FT-IR analysis of obtained bio-oils before and after reduction.

TABLE 5.1.2.8: GC-MS data of the bio-oil obtained at 400°C.

Retention Time	Compound Name	Area (%)
3.186	2-butanone, 3-hydroxy- (CAS); Acetoin	0.89
4.243	1-hydroxy-2-butanone	3.17
4.500	cyclopentanone	0.44
4.760	3-hydroxy-2-pentanone	0.71
4.912	2-hydroxy-propionic acid isobutyl ester	0.76
5.341	2-cyclopenten-1-one (CAS); cyclopentenone	2.95
5.735	methyl butyric acid	0.51
5.950	2-furanmethanol (CAS); furfuryl alcohol	16.35
6.326	4-hydroxy-3-hexanone	0.96
6.478	2-cyclopenten-1-one, 2-methyl-	1.72
6.571	ethanone, 1-(2-furanyl)- (CAS); 2-acetylfuran	1.26
6.855	butyrolactone	5.15
7.293	2(3H)-furanone, dihydro-5-methyl-	0.43
7.405	2-cyclopenten-1-one, 3-methyl- (CAS); 3-methyl-2-cyclopentenone	2.37
7.661	2 methyl-2-Pentenal	0.41
7.735	3,4-dimethyl-cyclopent-2-enone	1.21
7.864	furan carbon saeure chlorid, tetrahydro-	7.02
8.152	4-cyclopentene-1,3-dione, 4-propyl-	0.76
8.318	2-cyclopenten-1-one, 2,3-dimethyl-	3.35
8.463	2-cyclopenten-1-one, 2-hydroxy-3-methyl-	6.79
8.567	2-cyclopenten-1-one, 2,3,4-trimethyl- (CAS); 2,3,4-trimethylcyclopent-2-ene-1-one	0.32
8.703	3,5-dimethyl cyclopentenolone	4.36
8.898	3,4-dimethyl cyclopentenolone	0.43
8.963	phenol, 2-methoxy-	5.40
9.176	2-amino-5,6-dihydro-4,4,6-trimethyl-4h-1,3-oxazine	0.35
9.416	3-ethyl-2-hydroxy-2-cyclopenten-1-one	4.95
9.601	4-isopropylcyclohexanone	1.12
9.663	2-hydroxy-3-propyl-2-cyclopenten-1-one	1.65
10.093	2-methoxy-4-methylpheno	0.51
10.297	2-hydroxy-3-propyl-2-cyclopenten-1-one	0.88
10.507	cyclohexanecarboxaldehyde, 3,3-dimethyl-5-oxo-	0.95
10.630	bicyclo[2.2.1]heptane-1,2-dicarboxylic acid	0.69
10.942	phenol, 4-ethyl-2-methoxy-	0.48
11.057	tricyclo[5.2.1.0(2,6)]deca-4,8-dien-3,10-dione	0.41
11.169	pentanoic acid, 4-methyl-, 1-buten-1-yl ester	0.39
11.535	tricyclo[5.2.1.0(2,6)]decan, 4-methyl-	0.63
11.714	phenol, 2,6-dimethoxy- (CAS); 2,6-dimethoxyphenol	9.60
12.038	2-buten-1-ol, propanoate (CAS); 2-Buten-1-ol, propionate	0.42

	(CAS); 1-propionyloxy-2-butene	
12.532	4-methoxy-3-(methoxymethyl)phenol	1.15
13.194	benzene, 1,2,3-trimethoxy-5-methyl-	0.92
13.337	2-propanone, 1-(4-hydroxy-3-methoxyphenyl)-	1.51
14.399	benzeneacetic acid, 4-hydroxy-3-methoxy- (CAS); homovanillic acid	0.71
15.213	3,5-dimethoxy-4-hydroxyphenylacetic acid	0.98

TABLE 5.1.2.9: GC-MS data of the reduced bio-oil from table 5.1.2.8.

Retention Time	Compound Name	Area (%)
5.672	ethylbenzene	36.79
5.965	ethylbenzene	11.76
6.277	benzene, 1,3-dimethyl-	25.70
6.698	benzene, (1-methylethyl)-	12.44
7.088	benzene, propyl-	6.20
7.192	benzene, 1-ethyl-3-methyl-	2.77
7.978	benzene, 1-methyl-2-(1-methylethhyl)-	1.76
8.638	benzenemethanol, .alpha. –methyl-	0.98
8.971	benzene, 1-ethyl-4-(1-methylethyl)-	0.49
11.316	benzene, cyclohexyl-	0.22
11.486	benzene, (2,4-dimethylcyclopentyl	0.31
11.816	benzene, (2,4-dimethylcyclopentyl)-	0.59

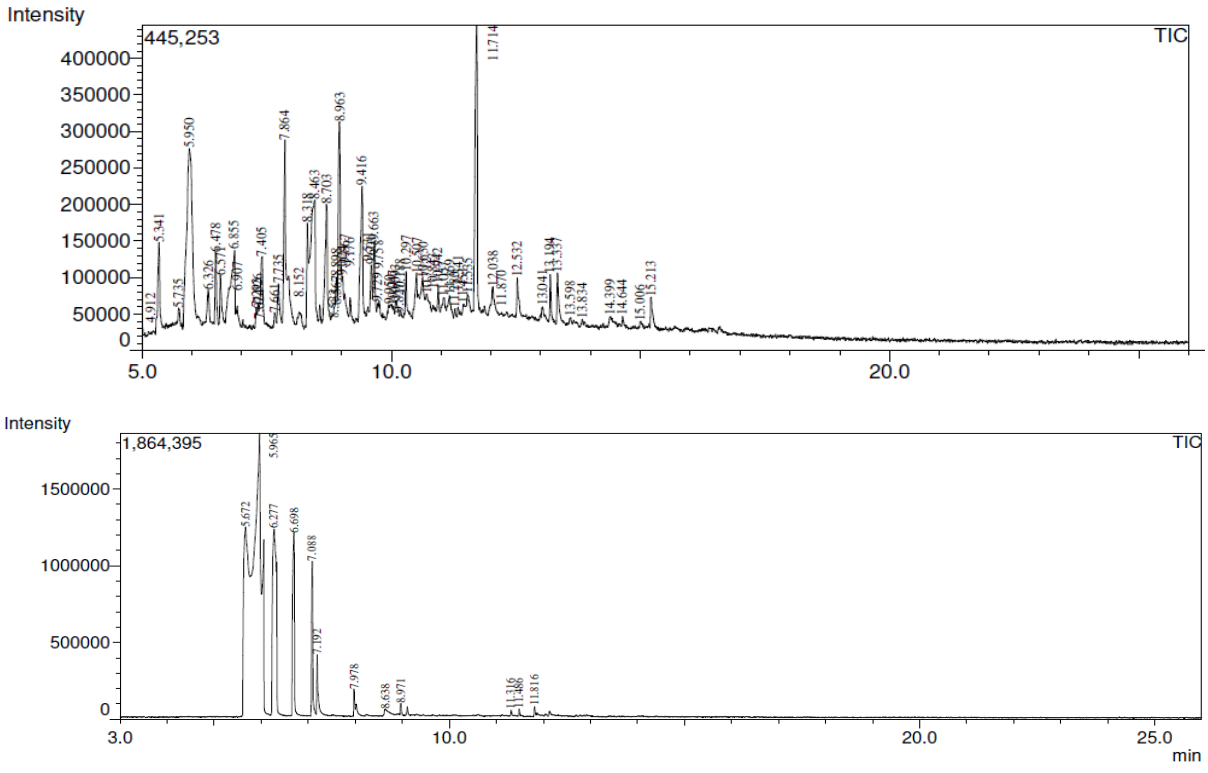

FIGURE 5.1.2.5: (Top) GC-MS chromatogram of the crude bio-oil obtained at 400°C. (Bottom) GC-MS chromatogram of the upgraded bio-oil.

5.1.3 A study of steam gasification of *Jatropha curcas* shells for hydrogen rich syn-gas

5.1.3.1 Description of the steam gasification set-up

The same above fixed bed reactor was utilized for the steam gasification of bio-char obtained from the slow pyrolysis of *Jatropha curcas* shells at temperatures of 300, 400, 500, and 600°C as shown in Fig. 5.1.3.1. The obtained bio-char at 500°C temperature proved to be the best in terms of balanced volatile matter and fixed carbon among the others was chosen for the steam gasification. At one end, a peristalitic pump (Maker: Cole Parmer, Masterflex L/S, and model no. 77800 – 60) was connected to the fixed-bed horizontal reactor for providing water at constant flow rate which can vary from wide range of flow rates including fraction also. The other end of the reactor affixed to a condenser (i.e. ice bath) was assisting to cool the hot gases that were coming out from the reactor. Two silica gel columns, one cloth filter, one activated carbon column and one calcium chloride column assisted to make the gases completely clean in order to avoid the damage of sensor in the online producer gas analyser. A one stage vacuum pump was attached in order to purge out the air constantly to keep the reactor in air-free condition, so that no oxidation occurred. The online producer gas analyser showed the compositions of the gas in terms of (v %) and is capable to measure the following compositions such as carbon monoxide, carbon dioxide, methane, hydrogen and acetylene and CV (MJ/m^3).

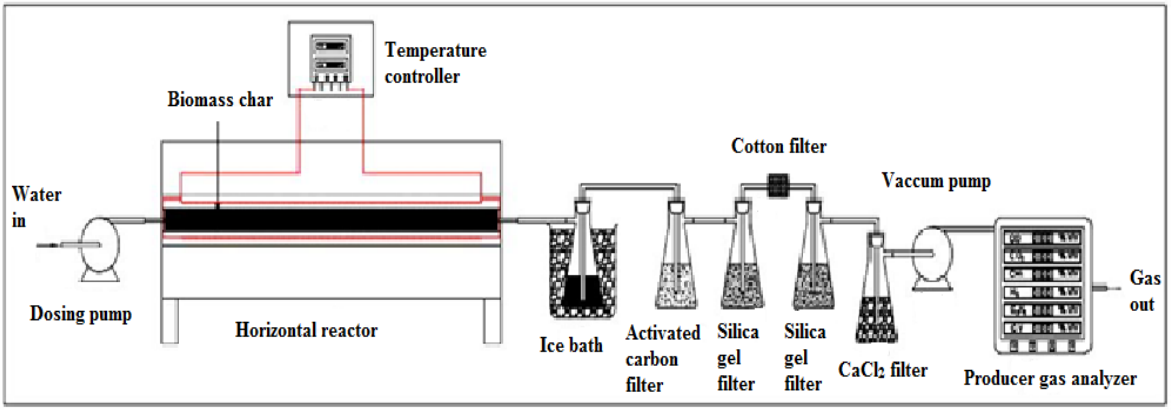

FIGURE 5.1.3.1: Schematic diagram of the steam gasification of *Jatropha* curcas shells bio-char.

In this study, 10.0 g of bio-char was placed in a trough made of stainless steel. As mentioned the two-stage vacuum pump was adjoined after the activated carbon column for keeping constant vacuum into the reactor during the experiment. Once the proposed temperature was reached then immediately removed the two-stage pump and is then connected to the online producer gas analyser for recording the data and the cold (room temperature) water was fed into the reactor by peristalitic pump. Three sets of experiments were carried out for optimization of the results at 700°C and 800°C for 1 ml/min. It was found that promising result was obtained at 700°C temperature and for optimization of flowrates, the experiments were carried out from 1, 2, 3, 4, and 5 ml/min. The optimum result was found at 700°C with 1 ml/min. The products consisting of little tar, different gases and steam were passed through a series of filtration system. This clean gas is fed into the producer gas analyser to detect the compositions of the gas. The pressure of the gas was measured by U-tube manometer and the pressure was found positive and it was 784 Pa. Each experiment was carried out for 30 min or more until it became almost zero and after that the SS trough was taken out to get the residue and weighed to measure the unconverted char.

5.1.3.2 Steam gasification mechanism of bio-char

The steam to biomass ratio was stoichiometrically calculated to be 0.98 and the stoichiometric yield of H_2 from bio-char was 239.60 mol H_2/kg bio-char. *Y* in Eq. (5.29) is the dry gas yield in Nm^3kg^{-1}.

$$\eta_c = \frac{(CO_2\%+CO\%+CH_4\%)\times Y\times 12}{22.4\times C\%}\times 100\% \quad (5.29)$$

$$CH_{0.577}O_{0.695} + 0.305H_2O \rightarrow 0.59\ H_2 + CO \quad (5.30)$$

$$C+H_2O \rightarrow CO+H_2 \text{ (Water gas reaction)} \quad (5.31)$$

$$C+2H_2O \leftrightarrow CO_2+2H_2 \text{ (Water gas reaction)} \quad (5.32)$$

$$CO+H_2O \leftrightarrow CO_2+H_2 \text{ (Shift reaction)} \quad (5.33)$$

$$C + CO_2 \rightarrow 2CO \quad \text{(Boudouard reaction)} \quad (5.34)$$

$$C + 2H_2 \rightarrow CH_4 \quad \text{(Methanation)} \quad (5.35)$$

$CH_4+H_2O \leftrightarrow CO+ 3H_2$ (Steam methane-reforming reaction) (5.36)

$CH_4+2H_2O \leftrightarrow CO_2+4H_2$ (Steam methane reforming reaction) (5.37)

$C_nH_m + {}_nH_2O \rightarrow nCO+ (n + 0.5m) H_2 >0$ (Tar cracking reaction) (5.38)

All the probable reactions occurring are listed from eqs. (5.29) to (5.38). The thermochemical conversion of steam gasification involved two steps. First step i.e., primary pyrolysis which involves the generation of char, tar, and volatiles, followed by tar cracking and reforming of the volatiles. The second step involved reactions of CO, H_2, CH_4, CO_2, hydrocarbon gases and carbon in the biomass char with steam producing gaseous products. Pyrolysis or gasification or steam gasification process is indeed complicated as it involves a lot of complex reactions.

Since temperature was a vital factor in the steam gasification process, total gas production, gas composition and heating value were checked at temperatures of 700 and 800^oC and the water flow rate through the pump was set at 1 ml min $^{-1}$. Overall, the hydrogen yield improved significantly at 700^oC, and dropped off at 800^oC. The maximum hydrogen yield (63.66 %) and CV (22.41 MJm^{-3}) was recorded at 700^oC. Higher H_2 might have been due to tar cracking and endothermic reforming reactions at 700^oC. Boudouard reaction and carbon gasification reaction at that temperature might have also been responsible. At 800^oC, reactions eqs. (5.33) and (5.34) were dominating as most of the reduction reactions occurred at this higher temperature resulting in higher CO_2 as compared to 700°C and the ratio of CO/CO_2 is determined as 0.39 and 0.11 at 700 and 800°C, respectively. From Fig. 5.1.3.2, it is clear that hydrogen yield lasted for only few minutes at 800°C.

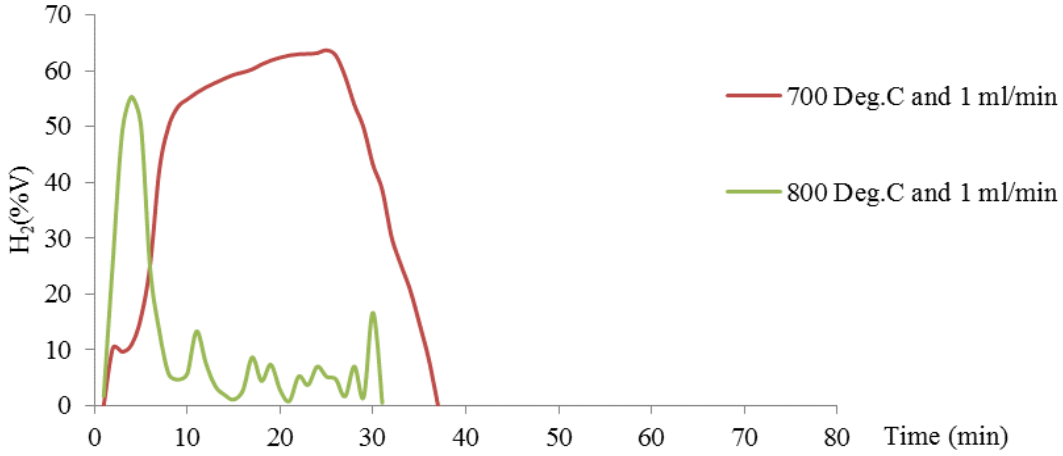

FIGURE 5.1.3.2: Hydrogen yield at 700°C and 800°C and water flow rate of 1ml min^{-1}.

The effect of water flow rates had significant changes on bio-char conversion, total amount of gas produced and its composition at different flow rates of 1, 2, 3, 4 and 5 ml min $^{-1}$ and temperature of 700°C as in Fig. 5.1.3.3.

As observed from Fig. 5.1.3.3, H_2 yield decreased with increasing water flow rates. It is possible that at high flow rate, the temperature inside the reactor dropped, and also the high rate might have caused improper reaction with the char and residence time might be playing a crucial factor.

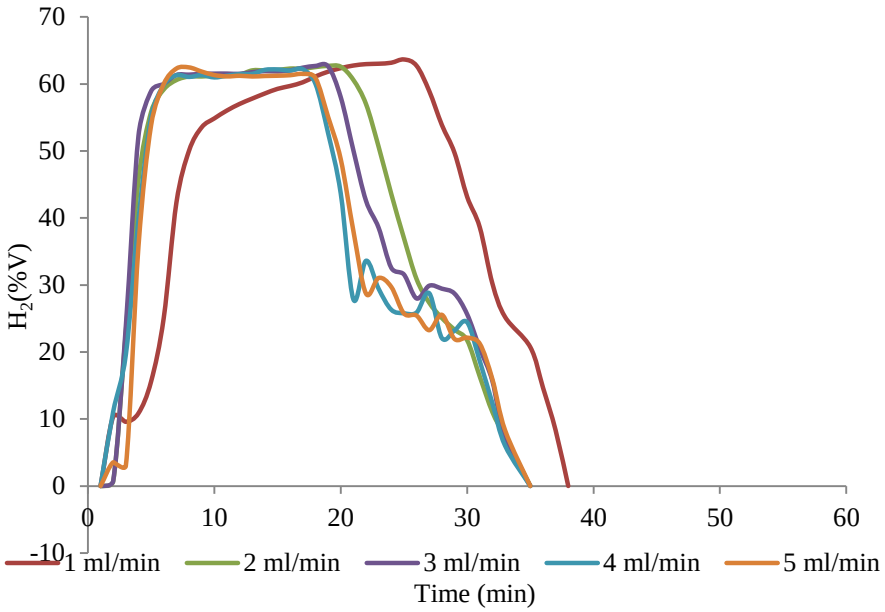

FIGURE 5.1.3.3: Hydrogen yield at 700°C and water flow rates of 1, 2, 3, 4 and 5 ml min^{-1}.

5.1.4 *Jatropha curcas* shells bio-char

The residue left as a bio-char after the pyrolysis in the reactor is a potential solid fuel and can be gasified to obtain producer gas for either thermal or electrical applications or preparation of activated carbon. The complete fuel characterization was done on the chars obtained at 300, 400, 500, and 600°C pyrolysis temperatures. Fig. 5.1.4.1 and table 5.1.4.1 show the proximate analysis (air-dried basis) and ultimate analysis (as received basis) results, respectively. From Fig. 5.1.4.1, it can be seen that there was a phenomenal reduction of volatile matter with an increase in the pyrolysis temperature. The reason could

be gasification reactions occurring at higher temperatures. So, at higher temperature the gas generation became more by reducing the mass of the remaining char and also reduced the volatile matter of the biomass. The fixed carbon is the combustible matter in the biomass that rests after the volatile matter has been driven off. It simply surges with increasing carbonization temperature. The higher ash content was obtained because of the lessening in the contents of the other elements like nitrogen, carbon, and hydrogen. Hence, with an increase in pyrolysis temperature, the ash content increased. A higher heating value points out the bio-char's potential to be used as a solid fuel. The optimum temperature for carbonization to obtain a char with a moderately high heating value was 400°C. However, the calorific values of the bio-char are reasonably good at all temperatures, and hence these also have the potential to serve as a solid fuel in the gasifier. The decomposition behaviour of the char produced at the different carbonization temperatures are shown in Fig. 5.1.4.2. In the ash fusion tester, the dark semicircle is the thermal image of the tube in which the char cone (triangular object made from chars) was placed on a board-shaped platform, and the white circle is the image of the thermocouple tip inside the tube. The ash forming steps could be divided into five different stages of physical changes; namely, initiation, deformation, softening, hemisphere formation, and total ash formation. The decomposition started at 571−584°C, and the char deformed within the range of 634− 708°C. Softening occurred within a temperature range of 756−749°C; for hemisphere formation, the temperature range was 772−844°C. The total ashing occurred between temperatures of 787−862°C. The determination of other physical properties of the chars such as bulk density, thermal conductivity, and specific heat capacity was also considered in this study. The bulk density value of the chars prepared at 300, 400, 500, and 600°C, determined according to ASTM E-873-06, were 409.92, 395.64, 470.83, and 476.59 kg m^{-3}, respectively. As shown, the general trend was a decrease in bulk density with an increase in temperature within a temperature range of 300−400°C, after which the bulk density improved because of the formation of high ash. The density of the carbonized products is hinged on the density of the original biomass. The bulk density and the heating value of the char influenced the size of the reactor if it is to be used as a solid fuel. The calculated thermal conductivities [45] were found to be 0.103, 0.105, 0.118, and 0.119 W m^{-1} K^{-1}, respectively. The thermal conductivity of char is a key parameter as the biomass is allowed to heat conduction along and across its structure during its application as solid fuel in any thermochemical process.

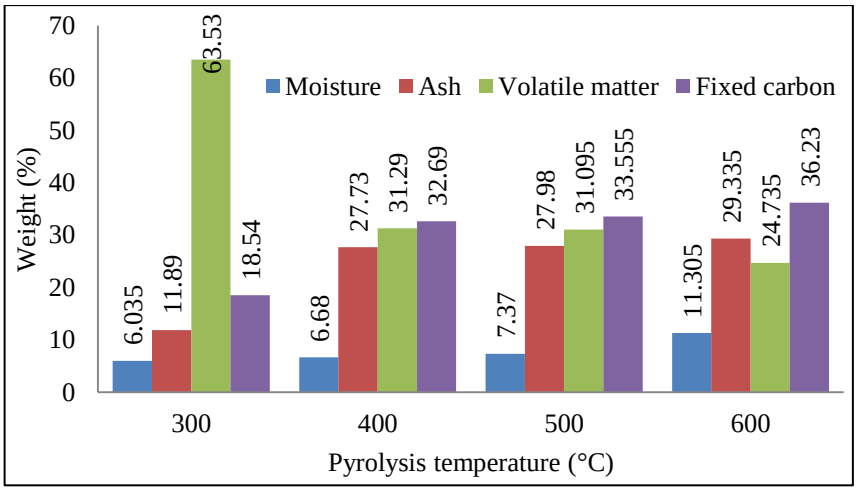

FIGURE 5.1.4.1: Proximate analysis of the bio-chars at respective pyrolytic temperatures.

TABLE 5.1.4.1: Ultimate analysis of bio-chars at respective pyrolytic temperatures.

	Temperatures (°C)			
	300	400	500	600
C	54.70	51.71	50.31	50.30
H	4.62	2.83	2.42	2.04
N	1.11	0.90	0.61	0.34
S	0.0	0.0	0.0	0.0
O	42.57	44.56	46.66	47.32
HHV (MJ kg^{-1})	18.84	20.79	20.62	18.59

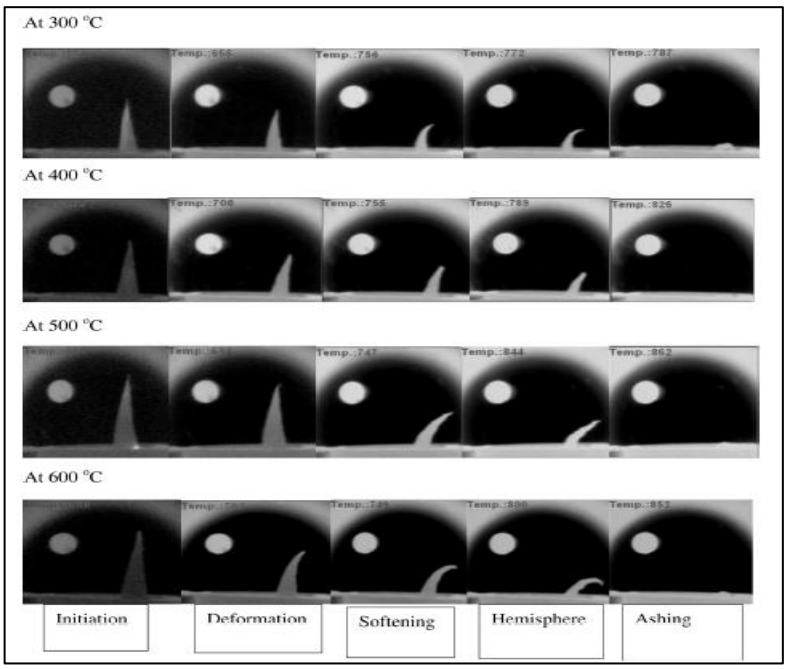

FIGURE 5.1.4.2: Deformation of bio-chars produced at different pyrolysis temperature until complete ashing.

The specific heat [45] is also another important thermodynamic property which deals with the heat capacity of the bio-chars formed at the different pyrolysis temperatures. They were calculated to be 0.836, 0.845, 0.862, and 0.976 kJ $kg^{-}1$ K^{-1}, respectively for the chars formed at 300, 400, 500, and 600°C carbonization temperatures. So, it can be predicted that the specific heat of each temperature is more or less same.

5.1.5 Conclusion

Jatropha shells can be a potential source of thermal and electrical energy generation through gasification in a downdraft gasifier which is elaborated in the present study belying the views expressed in the literature that such gasification may be difficult. The thermal and electrical efficiencies were calculated to be 64.8% and 24.5%, respectively, with respect to the calorific value of the shells. It was found that the continuous 8 h of operation could be sustained with intermittent charging of biomass. However, clinker formation was observed after the experiment, and it is expected that suitable modification in the design and programming of the residence time might help to reduce the clinker formation.

For the production of bio-oil , a fixed-bed pyrolytic reactor and allowed to be slow pyrolysed up to temperatures of 300, 400, 500, and 600°C, with the aim of producing bio-oil and solid fuel. Kinetics studied through TGA and DTG analyses showed the favourable heating rate to be 5°C min^{-1}. The most favourable temperature for the highest bio-oil yield (31.14%) was found to be 400°C. The crude bio-oil, having 23.5−24% moisture, was extracted with ethyl acetate and characterized in turn by GC-MS, FT-IR, and NMR spectral analyses. Along with the other oxygenated compounds, the bio-oil was found to contain about 40% carbonyl (>C=O) derivatives and has an energy density of 30.67 MJ L^{-1}. The obtained oil was then subjected to reduction by hydrazine hydrate/sodium hydroxide along with 130°C temperature and 7 h, which converted the carbonyl groups to corresponding methylene (−CH2−) derivatives to produce high energy density oil (48.92 MJ L^{-1}) with a yield of 60%. The bio-chars obtained during each experiment were characterized for their fuel properties. The results show that the bio-char obtained at 400

and 500°C has calorific values of 20.76 and 20.62 MJ kg−1, respectively, which asserted their potential as a solid fuel in thermochemical processes.

Considering the integrated biodiesel process, it was found that more than 45% of the shell amount would require meeting the captive energy requirement to obtain oil cake, soap cake, refined glycerol, and potash fertilizer along with jatropha biodiesel conforming to the international specifications and residual briquetted shells as a secondary fuel.

5.2 *Kappaphycus alvarezii* seaweed granules (KAG) for energy

5.2.1 Thermochemical conversion of *Kappaphycus alvarezii* seaweed granules (KAG)

5.2.1.1 Introduction

Augmenting the use of bio-energy requires a robust emphasis on marine biomass. There has been enough awareness about producing biofuel from algae, a supposed third-generation biofuel, in recent times. Seaweeds or macroalgae have huge potential to be used as biofuels for their rapid growth rate, high photosynthetic efficiency; no requirement of a cultivable land area and no competition with food crops [46]. Also, terrestrial biomass resources are tricky to use with varied applications because of their scattered nature, their availability being influenced by the seasons and the 'food-fuel' conflict. This is not the case with seaweed. Marine macroalgae grow mostly in intertidal coastal waters; they can capture a large amount of CO_2 and nutrients from the seawater and convert them into biomass through photosynthesis process. They can be converted into suitable biofuels through biological and thermochemical routes [47, 48]. Thermochemical conversion may be an option considered as a good method to overcome the existing problems associated with biochemical conversion due to long reaction time, meagre conversion efficiency by microbes and enzymes, and large production costs [49, 50]. Among the thermochemical conversion processes, hydrothermal liquefaction (HTL) is a very promising thermochemical technology to use the whole algae. HTL is most suitable for conversion of fresh water containing algae, since the feed to the conversion unit is water based slurry. Therefore no energy is required for evaporative algae drying. There are a number of HTL

experimental studies in the previous literature [51 - 63]. Numerous researchers have investigated the kinetic behaviour of a terrestrial biomass consisting mainly cellulose, hemicellulose and lignin [64 - 66] and have noticed that for the lignocellulosic biomass, the calculated activation energy of cellulose is ~ 238 kJ mol $^{-1}$, hemicellulose is 103.7-110.3 kJ mol $^{-1}$ and lignin is ~53 kJ mol $^{-1}$. Some other algal species like *Sagarssum sp*., *Saccharina japonica*, were also studied for the pyrolysis mechanism at different heating rates in order to calculate the apparent activation energy. The product yield of bio-oil, evolving gas and bio-char were also measured at different temperatures for these species [67, 68].

There are, in common, multitudes of methods for determining the kinetic model of any biomass from TGA data. In the case of model-fitting method, models are fit to the experimental data and the one providing the best fit is selected and apparent activation energy calculated. However, best selection of the suitable reaction model is one of the major snags of this method. Isoconversional (model-free) methods can predict the apparent activation energy without considering the reaction model and have the benefit of simplicity and ignorance of errors connected to choosing particular reaction models. Activation energy can be calculated on the same value of conversion at different heating rates. The drawbacks are related to reproducibility of same samples mass and the same volume flow rate of inert gas. Their fluctuation can cause errors when investigating a series of experimental runs for isoconversional (model-free) methods at different heating rates. Therefore, in order to get perfect results with high resolution curves, low ranges of heating rates should be accounted for experiments to accept the model-free methods [69]. The present study envisages model-free methods such as Friedman, Flynn-Wall-Ozawa (FWO) and Kissinger-Akahira-Sunose (KAS). The kinetic mechanism of marine macroalga – *Kappaphycus alvarezii* granules (KAG) – has been compared to terrestrial lignocellulosic biomass sawdust here. *Kappaphycus alvarezii* is typically a red alga, which is commercially produced for the linear sulfated polysaccharide, κ-carrageenan. A process was developed by the Institute (CSIR-CSMCRI) to get two products in an integrated form from seaweed [70, 71]. The fresh algae are harvested and first crushed and squeeze to expel sap. The whole mass of seaweed lump is thereafter centrifuged to split up “sap” and solid mass call seaweed granule. The complete constituents of the fresh seaweed sap and granules were already reported earlier [70]. Field trial of “sap” as a foliar spray in a variety of crops has shown significant growth and enhanced yields in diverse geographical locations across India. Taking into account, advantage of the India’s coastline, large

magnitudes of this seaweed species is thus needed to be generated through farming in the sea to fulfil the "sap" production requirement. To make the sap production process standalone and energy efficient, a suitable thermochemical conversion ought to be acquired by converting the large volume residual granules to gaseous/liquid form of energy. With this current objective, the present kinetic study was initiated. Some selected models were chosen to analyse the solid-state kinetic data obtained from TGA, and the findings from the kinetics of the thermal decomposition further assisted to describe the devolatization process.

5.2.1.2 Materials

The marine macroalga – *Kappaphycus alvarezii* – was collected from CSIR-CSMCRI field station located on the coast at Mandapam in Tamilnadu in southern India. After the 'sap' was extracted, the granules were washed to remove the surface salts and then kept open in direct sunlight for two days. Granules as received from the field station contained moisture ~15 % , soluble salt ~ 22% , fibre ~ 13 % , organic sulfate ~ 12 %, κ-carrageenan ~50 %, acid insolubles and other impurities ~ 12 % by weight % (checked in triplet over two batches). Raft cultivation of this alga in the sea is the usual practice. Over 6 harvesting cycles per annum on 3 m × 3 m raft, the fresh alga yield was ~ 1550 kg [72]. The biomass chosen for comparison was sawdust, collected from the Institute's carpentry department. This standard terrestrial biomass mainly comprises cellulose (40-55 %), hemicellulose (24-40 %) and lignin (18-25 %) [73]. All characterization including physical and chemical properties is listed below section.

5.2.1.3 Kinetic analysis

5.2.1.3.1 The Arrhenius approach and solving through multilinear regression

In section 5.1.2.2 the Arrhenius approach was considered for kinetic study analysis and was solved through multilinear regression technique.

5.2.1.3.2 The model-free isothermal Friedman method

This method [74], as in eq. (5.2), allows the apparent activation energy (E_a) to be obtained from the slope of the plot of ln ($\beta d\alpha/dT$) against 1/T at different heating rates for a given value of conversion (α).

$$\ln(\frac{\beta d\alpha}{dT}) = \ln[A_{\alpha} f(\alpha)] - \frac{E_a}{RT} \quad (5.2)$$

5.2.1.3.3 The model-free non-isothermal Flynn-Wall-Ozawa method

The FWO method, [75, 76], as in eq. (5.3), allows the calculation of apparent activation energy ($E_{a\alpha}$) from a plot of the natural logarithm of the heating rates, ln (β_j), against $1000/T_{\alpha j}$ for a given value of conversion at different heating rates.

$$\ln(\beta_j) = \ln(\frac{A_\alpha E_{a\alpha}}{Rf(\alpha)}) - 5.331 - 1.052\frac{E_\alpha}{RT_{\alpha j}} \quad (5.3)$$

where $f(\alpha)$ is the value of conversion, and subscripts j and α indicate the values of the heating rate and conversion, respectively.

5.2.1.3.4 The Kissinger-Akahira-Sunose method

The KAS method [77, 78] gives the following expression (5.4):

$$\ln(\frac{\beta_j}{T_{\alpha j}^2}) = \ln(\frac{A_\alpha R}{E_\alpha f(\alpha)}) - \frac{E_\alpha}{RT_{\alpha j}} \quad (5.4)$$

From the above explanation the apparent activation energy can be calculated from a plot of ln ($\beta_j / T_{\alpha j}^2$) against $1000 / T_{\alpha j}$ for a given value of conversion, α, and the activation energy can be obtained from the slope $-E_\alpha / R$.

By using model-free methods (isothermal and non-isothermal) and a multilinear regression technique were studied for the kinetics parameters from TGA analysis. The main objectives of choosing these four different methods were to elaborate the kinetics at different heating rates and to compare models each other. The apparent activation energy (E_α) and pre-exponential factor (A_α) were calculated using the FWO, KAS (non-isothermal) and Friedman methods (isothermal). Except from these methods, the activation energy (E_α), pre-exponential factor (A_α) and overall reaction order (n) were also obtained using a multilinear regression technique. In the first two methods the kinetics parameters were calculated by eqs (5.3) and (5.4), respectively, for a given value of conversion. For the KAG, the plots of ln (β) against $1000/T\ K^{-1}$ ln (β/T^2) against $1000/T\ K^{-1}$, and ln ($\beta\ d\alpha/dT$) against $1000/T\ K^{-1}$ for a given value of conversion are shown in Fig. 5.2.1.1(top). Similarly, for the sawdust the results are shown in Fig. 5.2.1.1 (bottom).

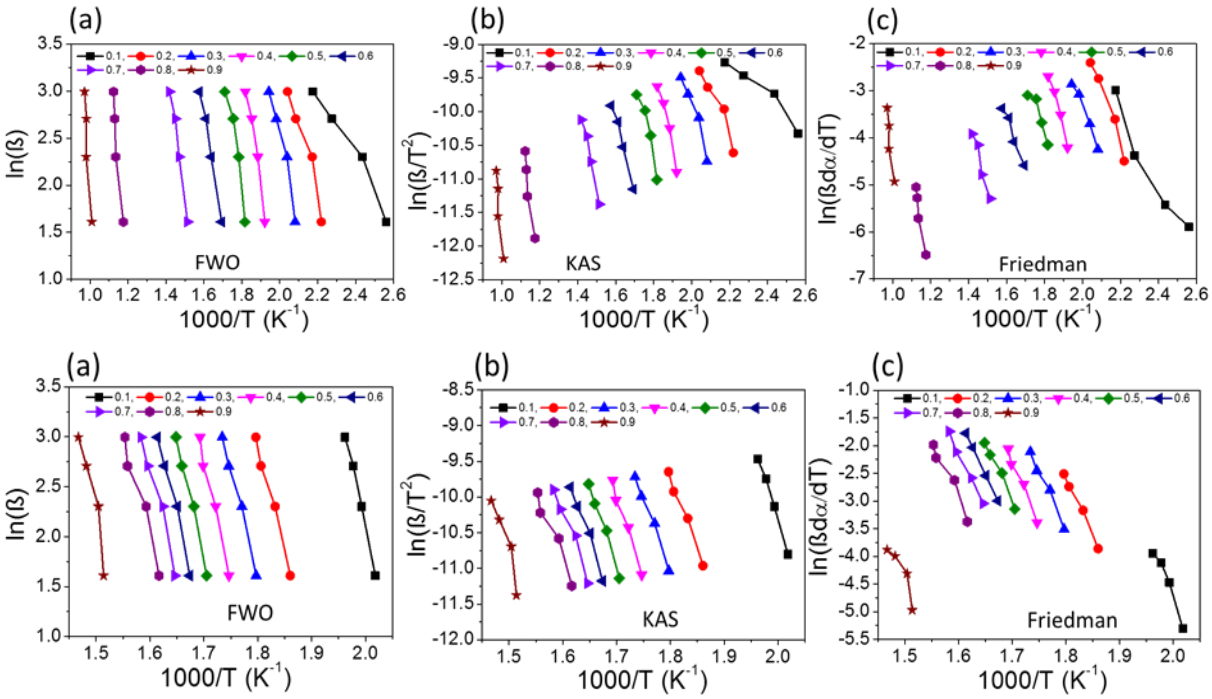

FIGURE 5.2.1.1: Flynn-Wall-Ozawa (FWO), Kissinger-Akahira-Sunose (KAS) and Friedman plots of KAG (top) and sawdust (bottom) at different values of conversion.

The apparent activation energies and the pre-exponential factors were obtained from the curves, and the corresponding values are provided in table 5.2.1.1 for the two biomass samples. The obtained regression coefficient (table 5.2.1.1) showed harmony with the models used. From Fig. 5.2.1.1 and 5.2.1.2 and table 5.2.1.1, it was noticed that for KAG, during stage-I of degradation, at α = 0.3 and 0.4, average values of E_a were 103.91, 91.13, 87.29 kJ mol^{-1} for Friedman, FWO, and KAS models respectively, while for sawdust , during same stage, the values were 179.21, 179.41, 179.19 kJ mol^{-1} respectively. Sawdust shown almost similar average E_a values in the second degradation zone as well. However for KAG, during stage-II the values of average E_a were decreased for the three kinetic models chosen. During stage-III, the average values of E_a were found to be on the much higher side at 172.27, 156.29, 151.53 kJ mol^{-1} respectively. Finally, at α =0.9, E_a values were 312.09, 267.67, 264.83 kJ mol^{-1} for corresponding methods.

The reason for this variation can be perceived to the variation in composition of KAG and breakdown of the intricate structures at each stage. Therefore, lower apparent energy was needed in the stages-I & II with more degradation as compared to the other two remaining zones. The high E_a values in the latter stages might be due to the volatilization of proteins

and complex carbohydrates and thermal breakdown of intricate inorganic salt present in the KAG structure at temperatures > 700^{o}C. Since sawdust is lignocellulosic in nature, stage-I indicated degradation of hemicellulose and cellulose and lignin mostly degraded in stage-II. For both the cases, the reaction mechanism was not uniform in every step of pyrolysis, and the activation energy was obviously dependent on the conversion. In the Friedman method, the apparent activation energy of the sawdust varied from 165.07 to 205.58 kJ mol $^{-1}$, and for KAG it varied from 60.68 to 312.09 kJ mol^{-1}. For the FWO and KAS methods, the variation in the apparent energy for the terrestrial lignocellulosic biomass sawdust was much less conspicuous than that of the KAG.

TABLE 5.2.1.1: Kinetic data of KAG and sawdust at different values of conversion.

Friedman Method						
	KAG			**Sawdust**		
α	**E_a [kJ/mol]**	**A_α [min^{-1}]**	**R^2**	**E_a [kJ/mol]**	**A_α [min^{-1}]**	**R^2**
0.1	60.68	2.86×10^{6}	0.93	205.58	2.56×10^{20}	0.95
0.2	95.04	6.79×10^{9}	0.97	170.99	4.52×10^{15}	0.99
0.3	84.25	7.32×10^{7}	0.98	177.37	4.65×10^{15}	0.98
0.4	123.57	1.01×10^{11}	0.97	193.23	3.72×10^{16}	0.97
0.5	84.11	3.40×10^{6}	0.87	171.37	1.66×10^{14}	0.98
0.6	89.36	1.36×10^{6}	0.95	170.48	6.66×10^{13}	0.99
0.7	126.69	7.37×10^{7}	0.94	165.47	1.15×10^{13}	0.99
0.8	217.86	4.30×10^{10}	0.93	165.07	4.13×10^{12}	0.95
0.9	312.09	2.19×10^{14}	0.86	174.02	5.54×10^{11}	0.82
Avg.	132.62	2.43×10^{13}		177.06	2.84×10^{19}	
FWO Method						
α	**KAG**			**Sawdust**		
	E_a [kJ/mol]	**A_α [min^{-1}]**	**R^2**	**E_a [kJ/mol]**	**A_α [min^{-1}]**	**R^2**
0.1	27.28	2.41×10^{2}	0.96	198.05	4.12×10^{19}	0.99
0.2	56.94	3.06×10^{5}	0.94	164.31	6.79×10^{14}	0.98
0.3	75.79	1.78×10^{7}	0.95	169.82	9.30×10^{14}	0.99
0.4	106.48	6.19×10^{9}	0.96	192.24	5.20×10^{16}	0.98
0.5	100.85	5.80×10^{8}	0.92	188.28	1.04×10^{16}	0.99
0.6	94.81	3.71×10^{7}	0.98	177.89	7.11×10^{14}	0.98
0.7	118.12	3.53×10^{8}	0.98	165.34	3.59×10^{13}	0.97
0.8	194.47	1.23×10^{11}	0.91	155.15	2.92×10^{12}	0.97
0.9	267.67	1.98×10^{13}	0.89	212.57	2.15×10^{16}	0.90
Avg.	115.82	2.21×10^{12}		180.47	4.58×10^{18}	
KAS Method						
	KAG			**Sawdust**		

α	E_a [kJ/mol]	A_α [min^{-1}]	R^2	E_a [kJ/mol]	A_α [min^{-1}]	R^2
0.1	21.66	7.52	0.93	200	6.14×10^{19}	0.99
0.2	52.09	3.90×10^{4}	0.92	163.76	5.80×10^{14}	0.98
0.3	71.47	3.70×10^{6}	0.94	169.23	7.9×10^{14}	0.98
0.4	103.12	2.25×10^{9}	0.96	192.57	5.39×10^{16}	0.98
0.5	96.66	1.66×10^{8}	0.90	188.15	9.83×10^{15}	0.98
0.6	89.90	8.60×10^{6}	0.97	177.03	5.73×10^{14}	0.98
0.7	112.93	9.61×10^{7}	0.97	163.64	2.39×10^{13}	0.96
0.8	190.14	5.71×10^{10}	0.90	152.71	1.64×10^{12}	0.94
0.9	264.83	1.31×10^{13}	0.88	212.47	2.04×10^{16}	0.89
Avg.	111.42	1.46×10^{12}		179.95	6.83×10^{18}	

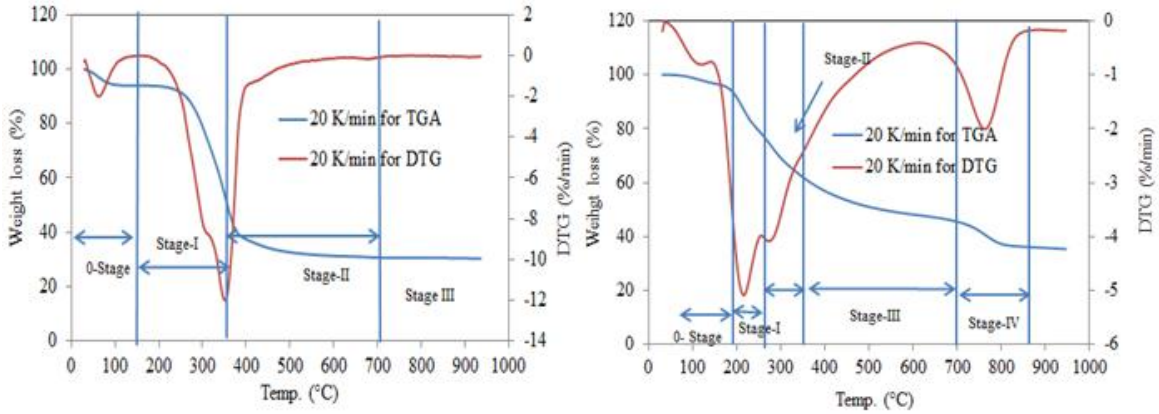

FIGURE 5.2.1.2: TGA (Thermogravimetric analysis) and DTG (Differential thermogravimetry) curves of sawdust and KAG at 20 K min^{-1} showing different stages of degradation corresponding to the temperature ranges selected.

Also, at the lower conversions levels (< 0.8) much less apparent activation energy was needed for the pyrolysis in the case of KAG than sawdust. However, at higher conversion levels a similar activation energy trend was noticed. A similar pattern was observed for the woody biomass, oak [79].

Fuel properties affect the thermogravimetric analysis of a biomass. Table 5.2.1.2 indicates the proximate and ultimate analysis of both the biomass samples. The ramification of the VM and FC content is that they give an extent of ease with which the biomass can be caused to catch fire and eventually used as an energy source. The lignocellulosic biomass, sawdust, has approximately 33% more VM and FC than KAG, therefore making it a better fuel. It can be seen in table 5.2.1.2 that KAG has a HHV of 9.19 MJ kg^{-1} compared to sawdust at 17.76 MJ kg^{-1}. The low value may be ascribed to less C and H content than the

lignocellulosic biomass. The high S and O content is the result of sulphated compounds found in its structure. This is interesting because the seaweed is commercially cultivated for linear sulfated polysaccharide, κ-carrageenan. Depending on the quantity of ash content, the net energy of the solid fuel reduces proportionately. Proximate analysis of two batches of granules with 9 times sampling was investigated to make sure of the dependency of moisture, ash and VM on the HHV. It was calculated that HHV=3.65-0.08 moisture-0.12ash+0.17VM, indicating that the moisture and ash contents influence the energy content of the biomass inversely, in case of the opposite is for the case with VM.

TABLE 5.2.1.2: Fuel characterization of Sawdust and KAG.

Proximate analysis	**Moisture (air dried, ad), %**	**Ash (ad), %**	**Fixed carbon (ad), %**	**Volatile matter (ad), %**	**HHV (MJ/kg)**
Sawdust	7.67	2.40	15.23	74.7	17.76
KAG	14.98	17.46	14.97	52.59	9.19
Ultimate analysis (% by wt)	C	H	N	S	O
Sawdust	48.69	6.39	0.0	0.66	44.26
KAG	31.36	5.66	0.6	4.41	57.97

In thermo-chemical conversion mechanism, the chemical composition of the ash is vital and the constituents can cause noteworthy operational obstacles. The ash can react to form 'slag' during the energy conversion, a liquid phase formed at elevated temperatures which can hinder the production throughput and result in increased operating costs. Table 5.2.1.3 gives data on the ash composition of the sawdust and KAG. It gives data on the average ash composition of the granules and statistical data for five sets of data points. Acidic content such as Si, Al and Ti are generally accepted to produce high melting ash, whereas basic contents such as Na, K, Ca, Mg and Fe have the converse effect. The basic constituents were substantially higher in the KAG ash. The presence of large amounts of K^+ is the reason why ash fusion temperature of KAG is somehow less than others (see Appendix-I). As would be obvious from the structure of κ-carrageenan, the seaweed builds up potassium selectively from seawater, and a fraction of this potassium is present as counter-ions in the sulfated polysaccharide. Since different methods were employed to determine the elemental composition in the ash, the sum total is not 100.

TABLE 5.2.1.3: Ash composition (wt. %).

Samples	Si	Al	Ca	K	Mg	Na	Fe	Ti	S
Sawdust	10.52	0.33	2.49	9.71	0.70	1.98	0.12	0.17	1.38
KAG	9.94	1.56	2.29	24.16	1.57	6.09	1.49	0.05	11.87

5.2.1.4 Thermogravimetric (TGA) analysis

In the present study, the thermal decomposition of sawdust and KAG were analysed at different heating rates i.e. 5, 10, 15 and 20 K min^{-1} in a nitrogen atmosphere. The derivative mass loss (DTG) and TGA are shown in Fig. 5.2.1.3. From the DTG curves, for sawdust, it can be observed that there are three peaks corresponding to moisture evaporation, active pyrolysis and passive pyrolysis in similar with the earlier reported work [80].

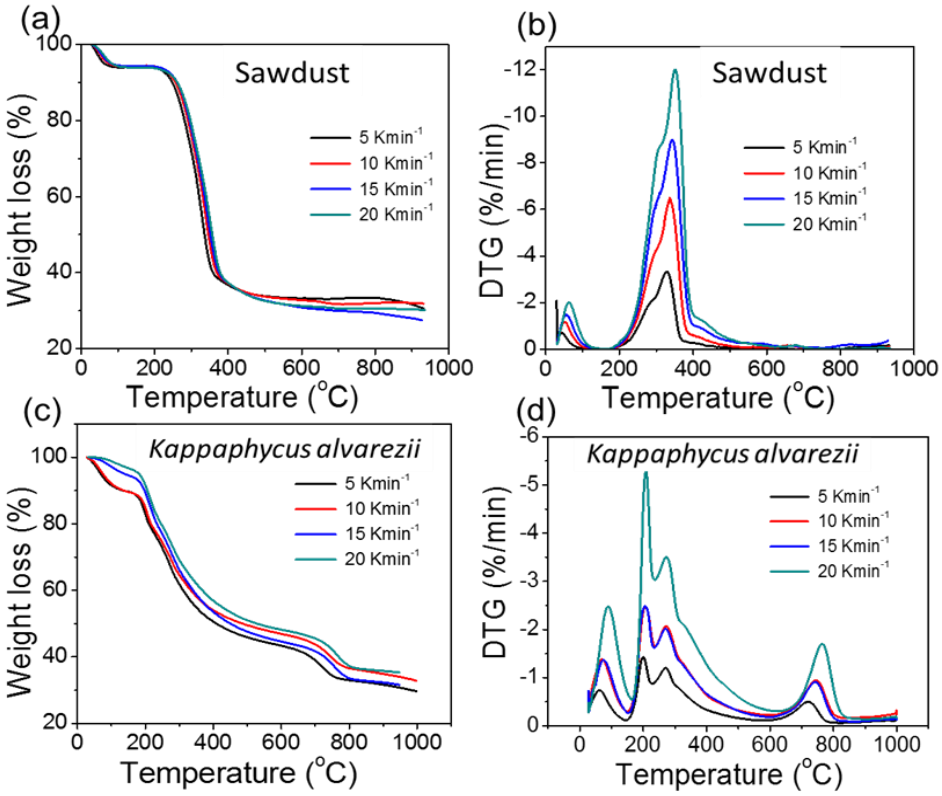

FIGURE 5.2.1.3: TGA (Thermogravimetric analysis) and DTG (Diffential thermogravimetry) plots of sawdust, and KAG at 5, 10, 15, and 20 K min^{-1} heating rates in N_2 atmosphere.

The effect of the heating rate impacts on the TGA curve, maximum temperature, maximum decomposition rate and maximum decomposition, as indicated in Fig. 5.2.1.3. As the heating rates increased in the present cases, the initial and final temperatures of the active pyrolysis and passive devolatilization zones shifted towards higher temperatures. At lower heating rates, in unit time, less thermal energy was provided to the system, so more time was needed for purging the gas to allow equilibrium with the temperature of the furnace. The converse effect occurred for higher heating rates, as reported by earlier researchers [27, 33]. Table 5.2.1.4 shows the rate of degradation, ROD (% min $^{-1}$) and weight loss (%). From this table, it can be noticed that the rate of degradation increased with increasing heating rate in both the samples. To investigate the TGA and DTG plots for kinetic analysis, varied temperature zones were chosen. Fig. 5.2.1.2 shows the different stages of decomposition for both biomasses. Only 20 K min $^{-1}$ was considered as representative figure for both cases. For the sawdust, the first peak from 45°C to 150°C revealed gradual moisture removal and the peaks became sharper on increasing the heating rate due to decreasing the residence time. The pyrolysis in case of sawdust started at 200°C and was completed under 400°C. This zone can be provided to as an active pyrolysis zone due to the thermal degradation of hemicellulose and cellulose content.

The lignin content in the biomass degraded throughout the entire temperature zone. In contrast, the pyrolysis of the KAG started at ~ 150° C and was finished at about 800°C. The second peak in the temperature zone of around 170-320°C for KAG could be attributed to the degradation of the 4-sulphate-β-D-galactose or the carbohydrate and protein.

TABLE 5.2.1.4: Weight loss (%) at different temperature zones of Kappaphycus alvarezii granules and sawdust.

Samples	**Heating rate (°K min^{-1})**	**Weight loss (%) in different temperature zones**							
		Stage-I (150-225°C)		Stage-II (225-325°C)		Stage-III (325-650°C)		Stage-IV (650-800°C)	
		Wt. loss (%)	ROD (%/min)	Wt. loss (%)	ROD (%/ min)	Wt. loss (%)	ROD (%/ min)	Wt. loss (%)	ROD (%/ min)
KAG	5	12.87	0.80	19.24	0.96	15.57	0.24	9.11	0.28
	10	11.61	1.45	17.22	1.72	15.02	0.46	9.33	0.58

	15	18.0	2.62	14.6	2.84	18.55	0.81	9.84	0.95
	20	17.65	3.51	13.92	3.72	18.75	1.04	9.18	1.42
Sawdust	5	6.83	0.54	15.48	1.87	35.93	1.43	Negligible	
	10	5.04	0.81	13.56	3.29	40.5	2.78		
	15	4.1	1.0	12.67	4.65	42.66	4.40		
	20	3.59	1.18	11.57	5.75	43.88	6.10		

The third peak noticed for KAG was because of the degradation of the insoluble polysaccharide and cellulose. The last peak was due to the thermal degradation of the Aphthitalite [$K_3Na(SO_4)_2$], as its melting point is around 750°C to 850°C. The weight loss behaviour and pattern of each biomass categorised in different temperature zones are shown in table 5.2.1.4. To perceive the kinetics of the thermal breakdown of KAG, 150-225°C, 225-325°C, 325-650°C and 650-800°C temperature zones were chosen. The weight loss and rate of decomposition were investigated for sawdust within the above ranges for comparison.

5.2.1.5 TG-MS analysis

In case of sawdust, at temperatures below 500ºC or 650ºC the thermal degradation of the non-aromatic compounds and the breakdown of the aliphatic side groups and functional groups occurred, and the maximum release of the non-condensable gases took place, as evident from the release peaks shown in Fig. 5.2.1.4 (b). At higher temperatures, the aromatic compounds present in the biomass, and also formed during pyrolysis, combine into bigger units, releasing their oxygen heteroatoms in the form of H_2O, CO and CO_2, while a decrease in the noticeable of the peaks can be observed. Methane also formed in both territory, but its potency decreased with temperature. Conflicting with sawdust, for KAG, along with other gases, SO_2 and H_2S were released throughout the thermal degradation process (Fig. 5.2.1.4 (a)). This was mostly because of the sulphated polysaccharide moiety in the KAG structure, whose decomposition began from 125°C and persisted throughout the entire degradation zone. The maximum SO_2 peak was achieved at ~ 300°C and 950° C.

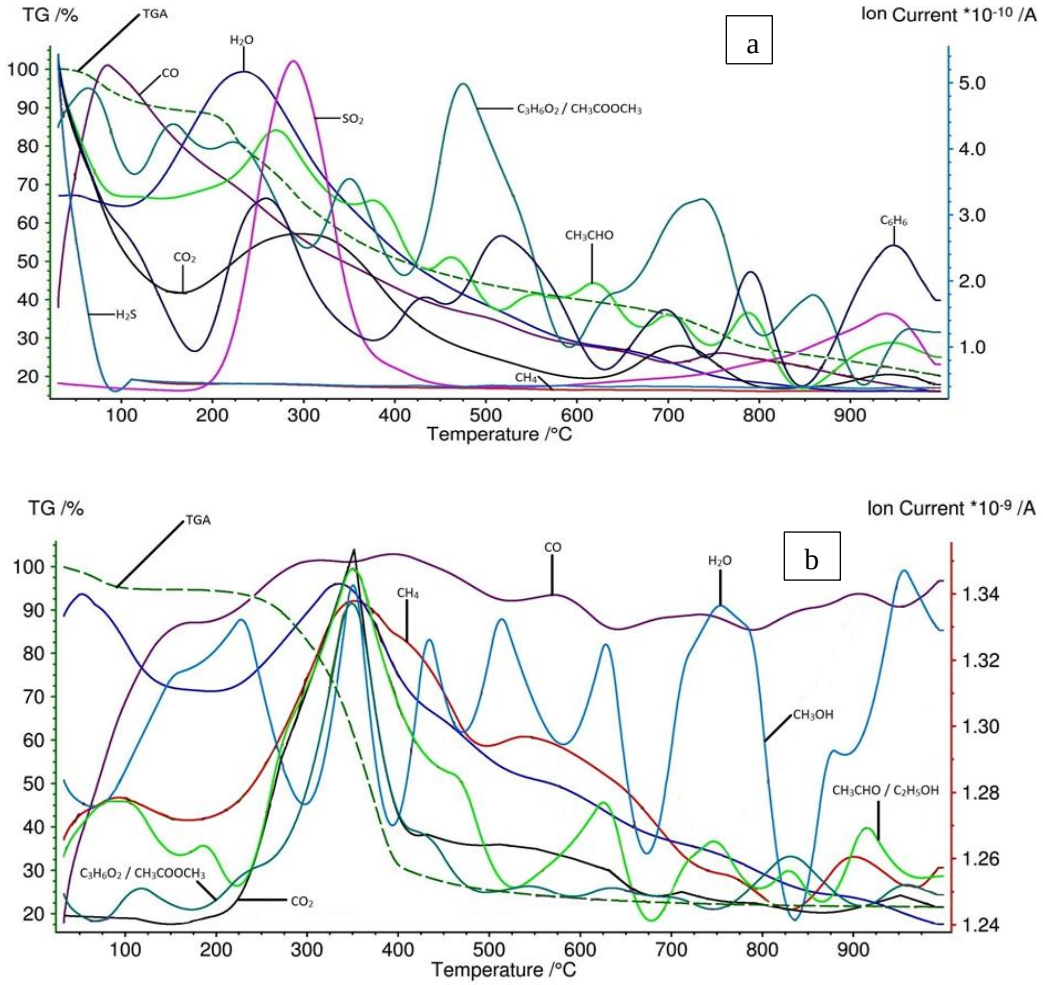

FIGURE 5.2.1.4: The TG-MS (Thermogravimetric-mass spectrometry) curve of (a) KAG (b) Sawdust, showing probable gaseous compounds liberated during pyrolysis from temperature.

5.2.1.6 Possible routes of utilisation of KAG for energy application through thermo-chemical means – experimental investigations

From the TG-MS studies, it could be proposed that the most suitable operating temperature for thermochemical conversion of KAG lies in the range of 450- 620^{o}C, whereby sulphur compound emission in lowest. Nonetheless, to make sure of experimental suitability of the TG-MS results, both downdraft gasification and slow pyrolysis studies were investigated.

5.2.1.7 Case study of downdraft gasification of KAG

For experimental trial, water washed and sun-dried KAG was fed into a traditional 15 kg h^{-1} downdraft gasifier which was previously utilized for the gasification of jatropha shells [81]. The gasifier and 10 kWe engine were operated for 2 h for continuing at full load. Despite, throughout the entire operation, sufficient SOx emissions were noticed. Gasification for energy needs high temperatures ~ 700 - 900^{o}C, which is suitable to yield large quantity of sulphur oxide emissions according to TG-MS data, and if the syn-gas is the main aim for power production directly, it is recommended to deter the gasification of KAG, because of the corrosive nature of the SOx mixed with syn-gas. The SOx in the syn-gas has the negative tendency to cause engine damage. After 2 h of run, the gasifier performance degraded gradually and enough power could not be produced even when fresh charge of seaweed was supplied. Scrutiny of the gasifier unit the following day exhibited the formation of soft solid lumps which most probably had restricted further downward flow of KAG. The high ash content of the KAG along with their woolly nature was undoubtedly the contributing factors behind its inappropriate fuel response. The substantial base-to-acid ratio in the ash might also be accountable. As mentioned early, κ-carrageenan is a sulfated polysaccharide, whereas a fraction of the sulfate moiety finishes in the ash, and a fraction is lost as gaseous emissions. To fight with the SO_x formation, when the granules were assorted with hydrated lime at a ratio of 3.33:1 and charged in the gasifier, the product gas produced SOx emissions were reduced to minimum, however, assorting with lime generated more ash and more solid handling was required. The problem of inappropriate heat transfer throughout the granules prevented the use of KAG in gasifier in improper form.

5.2.1.8 Case study of slow pyrolysis of KAG

The experimental set up for the pyrolysis experiment was performed in a stainless steel fixed bed horizontal reactor whose one end was adjoined to nitrogen flow system and other end attached to silicon tube connected to a condenser. Nitrogen flow rate was kept 200 cm^3 min^{-1} and maintained throughout the experimental condition. The reactor has a heating coil surrounded on its outer surface and inserted in a thermally insulating structure. A K-type thermocouple was placed in the middle of the reactor to measure the temperature of the bulk sample bed. Profile of temperature was in the axial direction of the reactor and the extreme ends revealed about 5 % lesser temperature than the middle. The heating rate of the reactor was set to 20 K min^{-1} (similar to TG-MS studies). For the experiments, 500 g of

washed KAG, well dried in oven at 110°C for 1 h was inserted into the reactor. A packed bed lime scrubber at the outlet was placed during temperature rise upto 500°C in order to minimize the gaseous sulphur compounds release during experiment. Bio-oil yield was optimum at 500°C, after carrying out experiments at temperatures 300°C, 400°C, 500°C, and 600°C. The design of the condenser was made in such way that maximum oil yield could be achieved for each experiment and no carry-over of oil with the gas was possible. The condenser unit was placed in ice bath for proper condensation. The gas from the condenser was subjected to pass through activated carbon bed and dilute sodium hydroxide solution to remove it completely from the non-condensed tarry matter present in the gas. Pyrolysis was investigated till about 4 hr until oil yield and yield of non-condensable gases became almost zero. The product yields were expressed as the average of at least three with experimental measurement error < ± 1%. Powder XRD was studied on the bio-char/ash mixture. Fig. 5.2.1.6 (a) provides proof of the aphthitalite phase [$K_3Na(SO_4)_2$] in the bio-char/ash mixture.

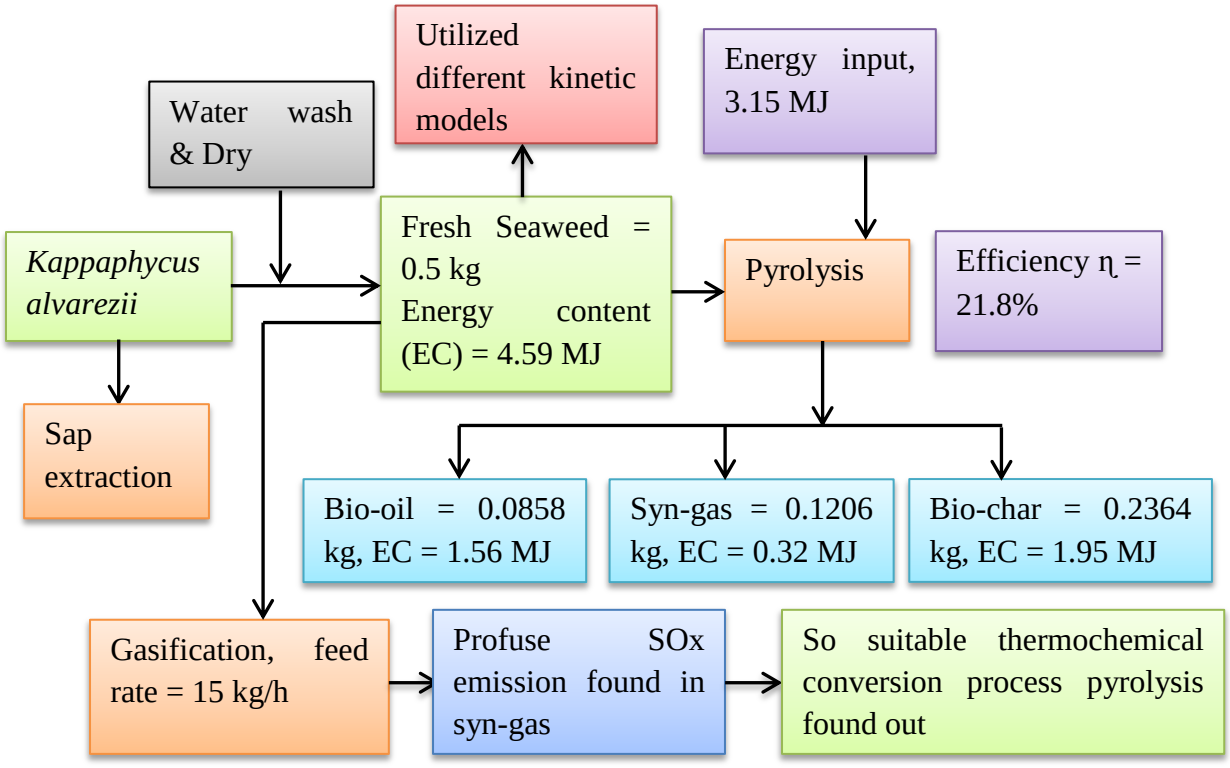

FIGURE 5.2.1.5: The overall mass and energy balance of KAG slow pyrolysis and depiction of end products range 100 – 1000 °C at 20 K min^{-1}.

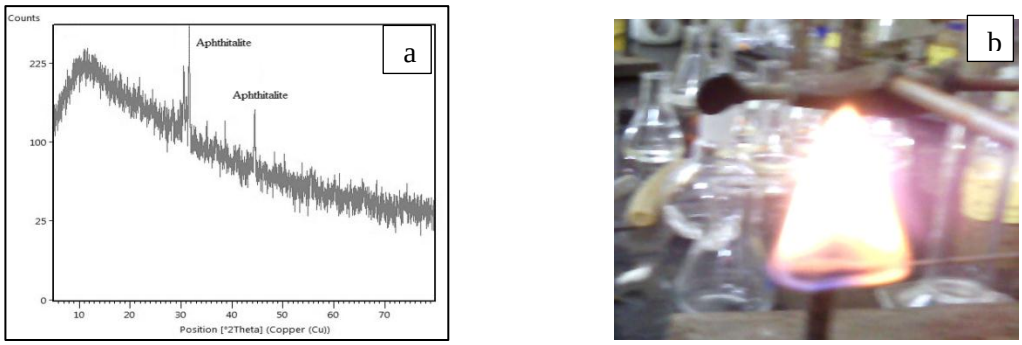

FIGURE 5.2.1.6: Powder XRD (a) studies obtained from the gasifier and burning flame of moisture free crude oil (b).

This was used as K-S fertilizer. The average product yield of bio-oil, bio-char/ash and syn-gas obtained during pyrolysis were 28.6, 47.28 and 24.12 wt.% respectively. The moisture free bio-oil had gross calorific value 18.23 MJ kg^{-1} measured by the bomb calorimeter, which burnt with a flame as shown in Fig. 5.2.1.6 (b). The calorific value of the moisture free bio-oil was upgraded to 41.10 MJ kg^{-1} by a simple organic reduction. It is a cheap and sustainable alternative for furnace oil utilized in boilers. The energy balance on the slow pyrolysis process was calculated as 21.8 % efficiency (Fig. 5.2.1.5). In this process diagram, the actual mass of the components and their energy content values in MJ have been accounted. The efficiency of the process can be enhanced by improving the syn-gas for heating purpose during the thermochemical conversion process.

5.2.2 Case study of gasification of KAG in 5 kW downdraft gasifier

Initially, the water washed and sun-dried seaweed was fed into a conventional 15 kg h^{-1} downdraft gasifier which was used previously for gasification of Jatropha shells as mentioned previous section. So, to avoid this problem, an improved another gasifier (5 kg h^{-1}) was thus designed to combat these problems and Fig. 5.2.1.7 shows the schematic diagram of the unit. The gasifier has two hollow metallic cylinders with annular space within. The top part of the two cylinders was sealed and the base of the cylinders was supported on a metallic rectangular box comprising a screw-driven conveyer which assisted to remove ash. The conveyer was controlled by a programmable timer (800XC – 22.5 Din Rail Analog Timer) to ensure that the residence time was controlled in a way that lumps or clinkers did not form. The ash was deposited at the bottom of this rectangular box. Biomass was fed in the smaller cylinder fitted with an air-tight lid. There were six

holes (each 1cm dia.) about 10 cm from the top of the gasifier. These holes were connected by stainless steel tubes to the ignition point. All these tubes passed through the annular space between the cylinders. These tubes assisted in providing air supply for partial oxidation. The air was pre-heated by the syngas, improving the overall energy efficiency of the unit. Charcoal required in the reduction zone was placed at the bottom of the small cylinder just below the ignition point and the top of the charcoal bed was filled with biomass. Generally 2 to 3 kg charcoal was used and 10 to 15 kg biomass could be fed at a time into the gasifier.

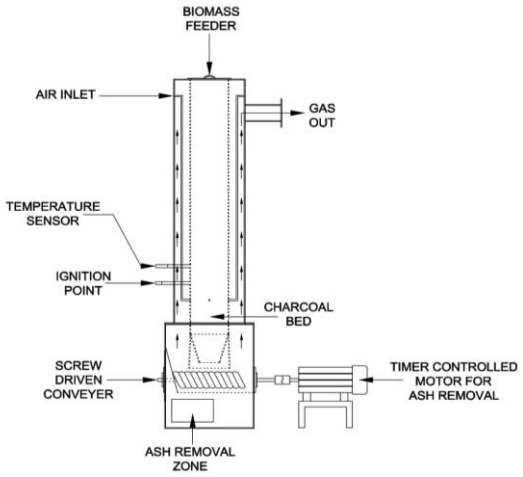

Figure 5.2.1.7: Schematic diagram of the downdraft gasifier used for gasification of the seaweeds granules.

Carbon dioxide formed in the combustion zone passed through the charcoal bed that is reduction zone to form the syn-gas. The syn-gas was sucked out through the annular space as a blower has connected to the system. In our previous study with *Jatropha* shells, the syn-gas was subjected to wet scrubbing which, though efficient, was tedious and messy. In the present unit, dry scrubbing of the hot gas was introduced. A cyclone separator was positioned next to the top of the gasifier to separate tar and particulate matter from the syn-gas. The cleaned gas from the cyclone was thereafter cooled to near ambient temperature in a gas cooling system consisting of a small blower (55 W; 1400 rpm). As a special precaution, the cooled gas was passed through a double filter system consisting of two chambers containing sawdust and cotton filter. The gas was sucked out by a 2844 rpm air blower, the outlet of which was adjoined to a dual fuel engine of 5 kW rating. The engine was operated initially with diesel and as the gas generation built up the diesel consumption

was reduced to idling level. On an average the engine could run on 15-20% diesel and rest on syn-gas. Schematic diagram of the overall unit is shown in Fig. 5.2.1.8.

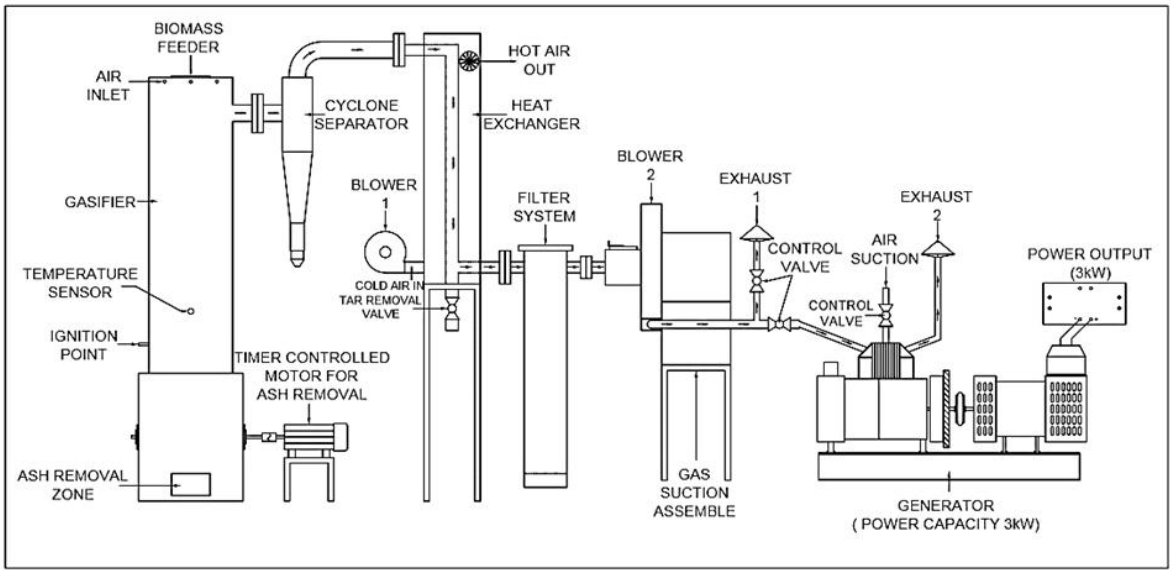

Figure 5.2.1.8: Outline of the 3 kWe gasifier with gas cleaning, cooling systems and coupled to a dual fuel engine.

Photograph of the gasifier along with lighting load in running condition is shown in Fig. 5.2.1.9.

Figure 5.2.1.9: Generation of 3 kWe power (lighting load) by the engine-gasifier running on the pelletized granules.

In a typical operation, the granular mass was pelletized in a pelletizer (rated capacity 0.5 HP) with 0.5 % oil cake as binder to circumvent the problem of direct use of the fluffy and low bulk density granules. The gasifier was run initially for 2 h without any load and thereafter for 4 h with 3 kWe lighting load as shown in table 5.2.1.5.

Table 5.2.1.5: The output power and the variation of combustible gas composition on lighting load basis.

Time (h)	Current (A)	Voltage (V)	PF	Power (kW)	CO (%)	CH_4 (%)	H_2 (%)
3rd	11.3	222.7	1	2.51	10.19	1.02	6.2
4th	11.2	221.3	1	2.49	10.21	1.4	6.25
5th	11.2	219.2	1	2.46	10.22	1.68	6.27
6th	11.1	217.9	1	2.44	10.23	1.71	6.29

5.3 Harnessing energy from selected seaweeds: *Ulva fasciata, Gracilaria corticata,* and *Sargassum tenerrimum* via slow pyrolysis

5.3.1 Introduction

If we look at the availability of seaweed species in India, more than 800 seaweed species of 29 orders belonging to the different classes have already been reported [82]. The global production of seaweed was found to be around 7.5 to 8 million tons of wet seaweeds being produced along the coastal region of worldwide in every year [83]. There are huge variation of production of seaweed in India which is due to the climate suitability on the seaweed species. It was reported by earlier that the estimated productivity of seaweed is more than 100000 ton wet weight consisting of 6000 ton agar yielding seaweeds, 16000 ton of algin yielding seaweed, 8000 ton of carrageenan yielding seaweeds and the remaining 70000 ton of edible and green seaweed [84, 85].

The main objective of this section is to describe briefly about the characterization of some marine biomass and to investigate the energy derivation of selective seaweeds like *Ulva fasciata, Gracilaria corticata*, and *Sargassum tenerrimum*. But it is essential to grasp the source, cultivation location, and the potential source of different feed-stocks.

The green seawseed species *Ulva* which proliferates rapidly; the availability of this species is very high as it is found all over the world. Some species *Ulva fasciata, Ulva lactuca, Ulva rigida*, belongs to the class of chlorophyta which are most commonly available in India. Under the aegis of global energy crisis marine macroalgae species have achieved considerable global attention as a source of third generation biofuels [86 - 89]. N. Trivedi et al. [90] investigated about the enzymatic hydrolysis and the production bioethanol from green alga *Ulva fasciata*. Typical composition of *Ulva fasciata* is given below: carbohydrate: 43 ± 4.5; protein: 14.4 ± 2.2; Lipid: 1.83 + 0.0 and cellulose: 15 ± 2.3 on relative % dry weight basis and the proximate analysis was provided later this section.

Gracilaria corticata has chemical composition as follows: carbohydrate: 46.79 ± 1.5; protein: 15.0 ± 1.4; lipid: 1.53 ± 0.7 on relative dry weight basis. M. Kumar at el. investigated about the *Sargassum tenerrimum* seaweeds species and its chemical composition was found out as follows: carbohydrate: 30.30 ± 1.55; protein: 10.75 ± 0.75; lipid: 2.03 ± 0.35 and the rest is determined by proximate analysis as described later [91]. A.K. Siddhanta et al. studied the profiling of cellulose content in Indian seaweed species. The cellulose contents were estimated as 12 seaweed species belonging to different families e.g. red, green, and brown in Indian seawaters [92].

The present study is mainly focussed about the characterization of the selected marine algae, pyrolysis mechanism with kinetic study and the characterization of the bio-oil derived from slow pyrolysis process and the characterization of the obtained bio-char as a solid fuel or potential source as a soil nutrient.

5.3.2 Material and method

The green seaweed *Ulva fasciata* (UF) Delile and *Gracilaria corticata* (GC) (Chlorophyceae) was collected from Veraval (N 20°54.870, E 70°20.830) coast of Gujarat, *Sargassum tenerrimum* (ST) J. Agardh (20.54°N and 70.20°E) belong to Phaeophyceae, India. The Seaweed samples were washed thoroughly with tap water to remove salts, epiphytes and debris and dried to a constant weight at temperature of 30°C. After drying,

the seaweed samples were powdered using grinder for chemical composition analysis and further analysis.

5.3.3 The effect of physical properties on pyrolysis and kinetic study

The inherent property of any biomass cannot be changed in order to get the better results, but the pre-treatment might have been a good option to change some of the properties, especially for marine macroalgae. Since the algae contains impurities such as different salts, epiphytes, debris, etc. they can be removed by cleansing with water effectively. Fig. 5.3.1.1(a, b, c) shows the proximate, ultimate and CV analysis of the biomass.

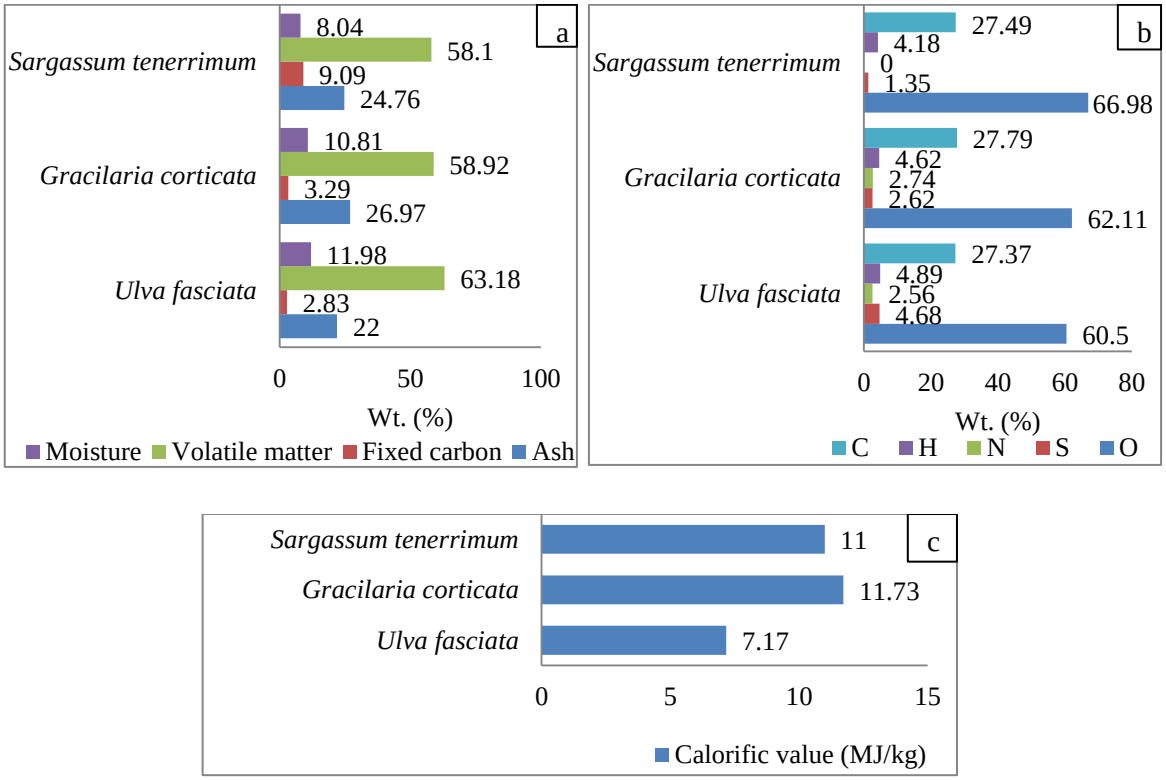

FIGURE 5.3.1.1: Proximate (a), ultimate (b) and calorific value (c) analysis for the three seaweed species.

The result shows the marine macroalgae contains quite high moisture content, oxygen content is found high in ultimate analysis for all species which was found to be highest for ST, followed by GC and UF. The volatile matter is found to be reasonable for all marine algae but this value was comparatively lower than terrestrial or agricultural biomass due to

high ash content in marine algae. Fixed carbon is found high in ST, followed by GC and UF. The CV of marine algae is very low due to the presence of high inert ash in the biomass. The ultimate analysis also shows the carbon content of each alga is reasonable, and sulphur content is found to be highest in UF. The high sulphur content is generally responsible for reducing the CV of the algae as the result shows in Fig. 5.3.1.1 (c).

5.3.4 Thermal decomposition of three seaweed species

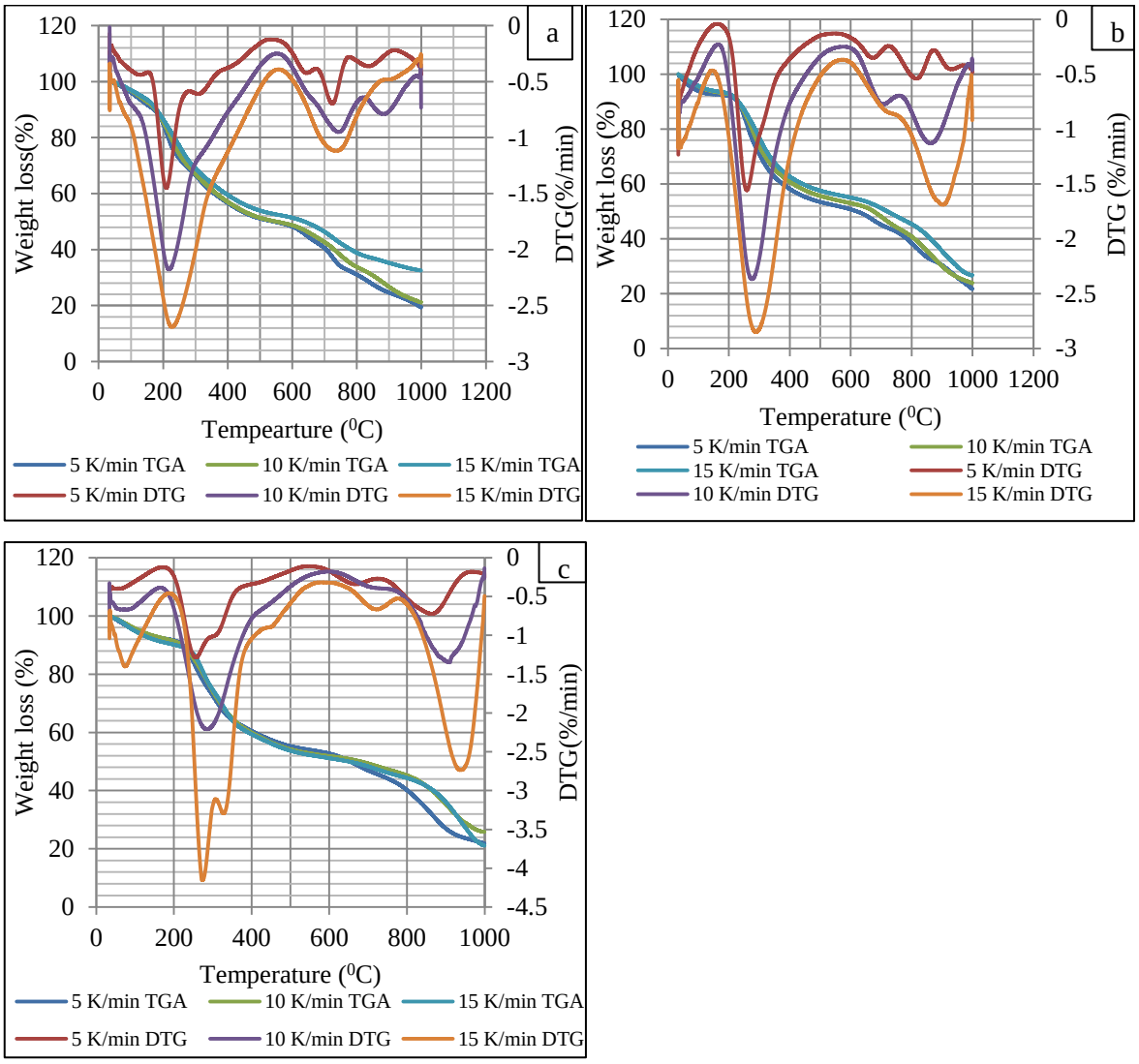

FIGURE 5.3.1.2: TGA and DTG plots of *Ulva fasciata* (a), *Gracilaria corticata* (b), *Sargassum tenerrimum* (c), are marine macroalgae.

It is already discussed how the proximate, ultimate and fuel value of the seaweeds affect pyrolysis, and gasification. Fig. 5.3.1.2 (a, b, c) shows the TGA and DTG curves for 5, 10

and 15 K min^{-1} of respective seaweeds. First for UF, the TGA curves at all the heating rates there is a loss of moisture. The moisture removal starts from around 50 – 60°C which continues upto 130°C. The moisture removable zone increases with increasing heating rate due to decrease in the residence time in any given temperature range.

The weight loss because of evolution of the volatiles from the seaweed species was investigated considering three selective temperature zones (a) 150 – 260°C, 530 – 800°C and 800 – 900°C for UF, (b) 125 – 270°C, 270 – 350°C and 580 - 760°C for GC, (c) 180 – 330°C, 580 – 730°C and 750 – 950°C for ST. The total degradation zones of seaweeds and the average rate of degradation (ROD) are presented in tables 5.3.1.1, 5.3.1.2 and 5.3.1.3 for respective seaweeds. The common feature among the seaweeds was that the degradation started at temperatures of 200°C and continued upto 400 – 500°C and then decreased. For UF, the degradation increased again from 600°C to 800°C and it slightly increased again from 800°C to 950°C. Whereas for GC and ST the degradation zone was almost same as UF with small variation of peaks due to the lack of uniformity of its chemical composition within its structure.

TABLE 5.3.1.1: Weight loss pattern and rate of degradation (ROD) of UF.

Samples	**Rate of heating (K/min)**	**Weight loss (%) at different temperature zones**					
		150 – 260°C		530 – 800°C		800 – 900°C	
Ulva fasciata		Wt. loss (%)	ROD (%/min)	Wt. loss (%)	ROD (%/min)	Wt. loss (%)	ROD (%/min)
	5	22.52	1.01	39.28	0.65	20.58	1.02
	10	22.25	2.02	33.33	1.22	21.31	2.11
	15	20.05	2.70	27.06	1.49	4.63	1.36

Table 5.3.1.1 shows the weight loss pattern in samples of 5, 10, 15 K min^{-1} at selected major degradation temperature zones. The weight loss was found maximum at 530 – 800°C which decreased with increasing the rate of heating as indicated for all temperature ranges, except for 10 K min^{-1} at 800 – 900°C.

Similarly, for GC the selected degradation temperature zones were a bit lower than UL as shown in table 5.3.1.2. The reason could be the presence of high ash content and the low carbohydrate content. High ash content in any biomass reduces the melting temperature and acts as a catalyst, but only selective mineral contents such as K, Na or alkaline earth metals are responsible. The weight loss found highest at 270 – 350°C was followed by 580 – 760°C and 125 – 270°C. With increasing the rate of heating, the weight loss in samples decreased at 125 – 270°C, while for 270 – 350°C and 580 – 760°C the weight loss increased with increasing the rate of heating.

TABLE 5.3.1.2: Weight loss pattern and rate of degradation (ROD) of GC.

Samples	**Rate of heating (K/min)**	**Weight loss (%) at different temperature zones**					
Gracilaria corticata		125 – 270°C		270 – 350°C		580 – 760°C	
		Wt. loss (%)	ROD (%/min)	Wt. loss (%)	ROD (%/min)	Wt. loss (%)	ROD (%/min)
	5	16.21	0.55	20.08	1.24	18.40	0.51
	10	13.18	0.86	21.03	2.44	18.85	1.04
	15	3.81	0.53	28.65	2.84	21.10	1.31

Finally, table 5.3.1.3 shows the weight loss pattern and rate of degradation of ST.

TABLE 5.3.1.3: Weight loss pattern and rate of degradation (ROD) of ST.

Samples	**Rate of heating (K/min)**	**Weight loss (%) at different temperature zones**					
Sargassum tenerrimum		180 – 330°C		580 – 730°C		700 – 950°C	
		Wt. loss (%)	ROD (%/min)	Wt. loss (%)	ROD (%/min)	Wt. loss (%)	ROD (%/min)
	5	27.68	0.91	15.12	0.50	50.0	0.99
	10	26.31	1.74	7.96	0.52	39.02	1.94
	15	25.52	2.53	9.87	0.98	42.46	3.16

The rate of degradation is best described by the heat transfer limitation. At lower heating rates the curves are quite flat than at higher rates. As it is now well established that the marine biomass is a poor conductor of heat, so there exists a temperature gradient throughout the cross-section of the biomass. Hence at lower heating rates, the temperature profile along the cross-section can be predicted linear as both the outer surface and the inner core of the biomass gets same temperature at a particular time as sufficient time is given for heating. On the other hand, at higher rate of heating, a substantial difference in temperature profile exists along the cross-section of the marine biomass. The difference in total degradation at a higher heating rate to that of a lower heating rate may also point to the fact that completion of reaction at the higher rate of heating is not achieved. The less residence time implies incomplete evolution of the volatile matters at lower temperature ranges. Hence, at the higher heating rate a higher percentage of weight loss should be observed, but in case the seaweeds species the weight loss is very versatile, and dis-uniformity is observed.

5.3.5 Kinetics parameters of three seaweed species

Many researchers have been worked on the kinetic of pyrolysis on different substrates. Due to the compositional complexity of different organic wastes, it is impossible to accept the same model of degradation. Therefore, the rate of decomposition is calculated by the Arrhenius rate equation as described in earlier section 5.1.2.2. The kinetics of the pyrolysis for the three seaweeds species at different heating rates is given in table 5.3.1.4. It shows the heating rates affect the reaction kinetics. The order of reaction is higher at a slower rate of heating, but in some cases, the order increases at higher rate of heating, which may be due to more degradation. The activation energy for each marine alga varies due to the variation of decomposition temperature for different composition. For UF, the overall activation energy decreases with increasing rate of heating, as at lower heating rate the residence time is more and more prominent weight loss pattern is observed. Unlike UF, the GC exhibits lowest activation energy at 10 K min^{-1} and similar pattern is noticed for ST. Fig. 5.3.1.3 shows the product yield distribution of three seaweed species.

TABLE 5.3.1.4: Kinetics parameters of three seaweed species.

Rate of	**Temperature Zone**

heating	Kinetics parameters	*Ulva fasciata*			*Gracilaria corticata*			*Sargassum tenerrimum*		
		150-260 °C	530-800 °C	800-900 °C	125-270 °C	270-350 °C	580-760 °C	180-330 °C	580-730 °C	750-950 °C
5^0C min^{-1}	R^2	0.69	0.77	0.77	0.59	0.71	0.93	0.93	0.95	0.97
	A (min^{-1})	6.69×10^3	2.57×10^2	0.11	1.37×10^4	0.75	4.20×10^3	1.98×10^7	4.64×10^5	2.35×10^5
	E (kJ/mol)	45.46	71.75	6.78	48.18	11.62	91.04	84.80	123.05	141.59
	n	0.53	0.45	0.12	0.70	0.097	0.38	1.97	0.99	0.87
10^0C min^{-1}		150-260 °C	530-800 °C	800-900 °C	115-265 °C	265-350 °C	570-815 °C	180 - 330 °C	580-730 °C	750-950 °C
	R^2	0.88	0.95	0.96	0.57	0.83	0.89	0.92	0.93	0.94
	A (min^{-1})	3.53×10^2	1.52×10^2	2.67×10^2	1.59×10^3	0.55	7.13×10^3	5.05×10^3	9.91×10^1	1.18×10^5
	E (kJ/mol)	31.79	63.76	73.32	36.88	7.27	92.41	48.32	56.69	114.49
	n	0.32	0.27	0.063	0.59	0.037	0.58	0.42	0.013	0.23
15^0C min^{-1}		150-260 °C	530-800 °C	850-900 °C	115-220 °C	220-370 °C	580-820 °C	180-330 °C	600-750 °C	750-950 °C
	R^2	0.85	0.93	0.89	0.55	0.52	0.84	0.89	0.95	0.96
	A (min^{-1})	1.17×10^1	1.07×10^2	7.23	2.70×10^6	0.15	8.68×10^3	3.23×10^4	1.81×10^2	1.37×10^4
	E (kJ/mol)	17.35	58.05	30.38	60.0	3.68	97.61	55.43	58.66	114.45
	n	0.11	0.23	0.0203	0.81	0.057	0.40	0.39	0.109	0.038

5.3.6 The Bio-oils characterization

The physio-chemical properties of bio-oils are listed in table 5.3.1.5. The fundamental properties of each crude bio-oil that is without treatment are taken as viscosity, density, pH and moisture content. The viscosity of each bio-oil is almost same range; no difference is there, similarly for density. But pH of each bio-oil shows a contrasting result as for UF it is highly acidic, for GC it is moderately acidic and for ST it is almost neutral. The presence of aldehydes and sulphonated groups makes the bio-oil acidic for UF. The moisture free bio-oils were also characterized by its CV, density, viscosity, and elemental analysis. The highest CV is found for ST followed by GC and UF and its values are listed in table 5.3.1.5. The density for each bio-oil was found to be indeed high after moisture elimination and simultaneously, the viscosity of bio-oils increased due to the removal of moisture. Macroalgae yields less bio-oil due to high amount of ash in it, lack of cellulose, hemicellulose, and lignin contents and high oxygen content (Figure 5.3.1.3).

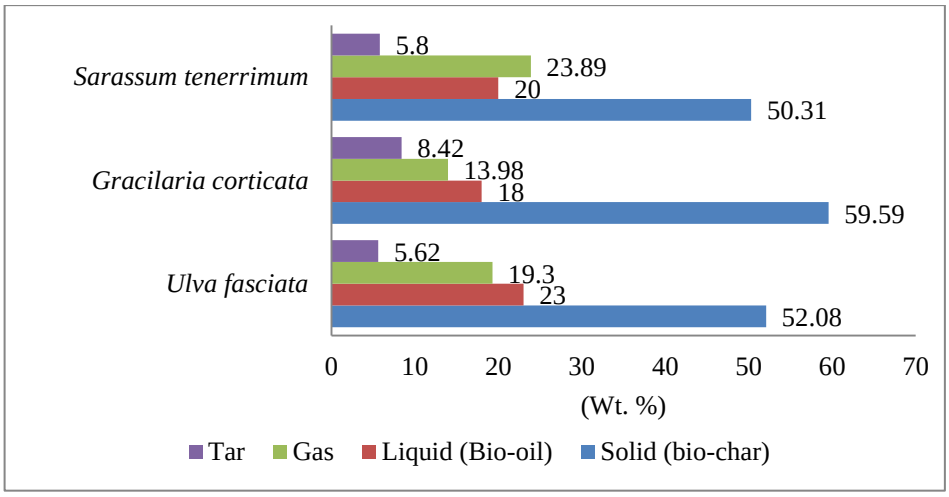

FIGURE 5.3.1.3: Products yield of UF, GC and ST.

TABLE 5.3.1.5: Physio-chemical Properties of Bio-oil obtained from slow pyrolysis from UF, GC and ST.

Physio-chemical Properties of Bio-oil obtained at 500°C			
	Ulva fasciata	*Gracilaria corticata*	*Sargassum tenerrimum*
Viscosity (cP) @ 30°C	1.21	1.32	1.25
Density (gm/ml) @ 30°C	0.92	0.87	0.89
pH	2.15	4.66	6.5
Moisture content (%)	45.12	42.32	46.32
Ultimate analysis (moisture free)			
GCV (MJ/kg)	27.86	29.42	33.35
Density (gm/ml) @ 30°C	1.127	1.08	1.03
Viscosity (cP) @ 30°C	217.13	211.6	202.3
Elemental (wt. %)			
C	53.66	63.53	69.15
H	5.66	7.12	8.39
S	0.43	0.92	0.35
N	4.42	9.46	4.03
O	25.83	18.97	18.08
H/C molar ratio	1.06	1.34	1.45
O/C molar ratio	0.30	0.22	0.19

The elemental analysis exhibited high content of carbon in ST followed by GC and UF. The bio-oils are further characterized by GC-MS (Fig. 5.3.1.5, 5.3.1.6, and 5.3.1.7) and

FT-IR (Fig. 5.3.1.4) from which the product yield distribution is evaluated as shown in table 5.3.1.6. The result shows contrasting functional groups among the seaweed species.

Firstly, for UF, compositions are hydrocarbons including alkane and alkene (4.72%), nitrogen containing compounds (8.52%), alcohol (10.04%), phenol (6.89%) and aldehyde (58.75%).

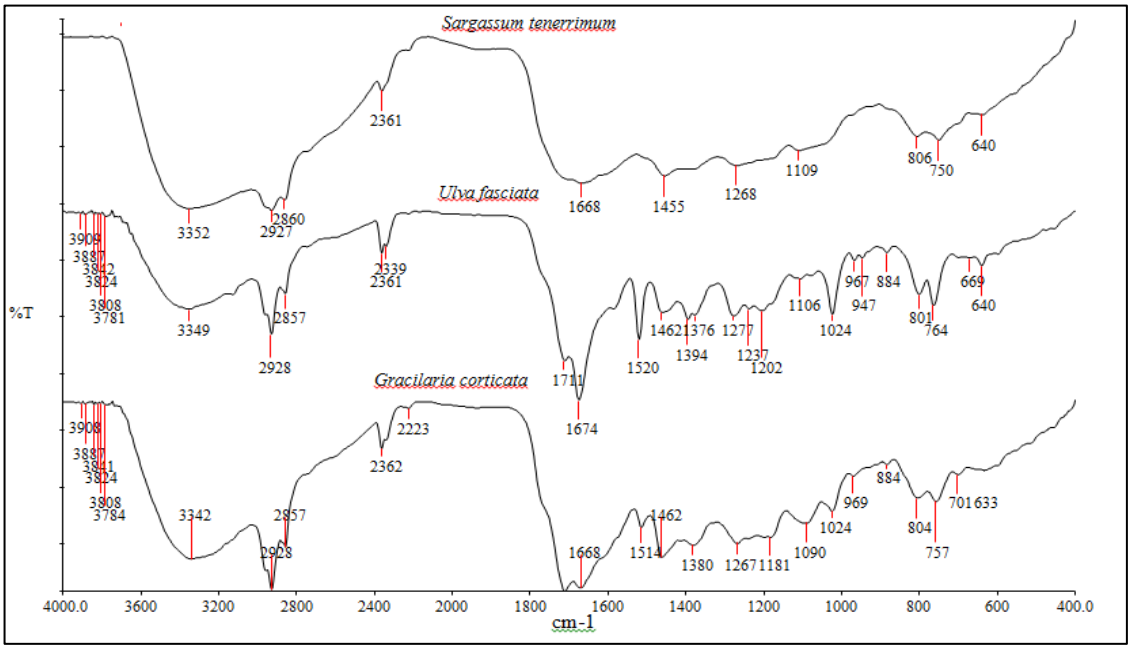

FIGURE 5.3.1.4: FT-IR analysis of obtained bio-oil from UL, GC and ST.

The oxygenated compounds containing the functional group C = O, O – H, C – O, and aromatic compounds reduces the calorific value. Whereas, for GC and ST, the oxygenated compounds containing groups are less compared to UF. The most visible thing in ST is the improved quality as shown in table 5.3.6 and its value is 33.35 MJ/kg. FT-IR was also used to identify the chemical bonds and functional groups present in the bio-oil samples. The functional group identified through the FT-IR analysis for the bio-oils is shown in table 5.3.1.7.

TABLE 5.3.1.6: Distribution and yield (area %) of bio-oil composition obtained from three seaweed species at 500°C.

Temperatures	**Area (%)**	**Area (%)**	**Area (%)**
	Ulva fasciata	*Gracilaria corticata*	*Sargassum tenerrimum*

Aromatic hydrocarbons	1.2	4.21	1.48
Hydrocarbons (alkane + alkene)	4.72	14.3	11.19
Heterocyclic compounds	-	-	-
Total			
Nitrogen-containing organic compounds	8.52	26.99	17.88
Total			
other organic compounds			
Alcohols	10.04	17.0	17.25
Phenols	6.89	5.62	14.72
Ester	0.69	2.31	2.18
Ethers	0.17	-	1.04
Aldehydes	58.75	1.86	-
Ketones	3.9	9.61	15.34
Sulphonate groups	0.32	5.34	-
Carboxylic acids and derivatives, etc.	3.77	11.76	17.86
Total	98.97	99.0	98.94

TABLE 5.3.1.7: Functional groups identification of the bio-oil for *Ulva fasciata*, *Gracilaria corticata* and *Sargassum tenerrimum*.

Frequency range (cm^{-1})	**Groups**	**Class of compounds**
3650-3200	O-H (Stretching)	H-bonded, water impurities
3100-3000	C-H (Stretching)	Aromatic groups
3000-2800	C-H (Stretching)	Alkanes
1775-1650	C = O (Stretching)	Ketones, aldehyde, carboxylic acid and its derivatives.
1680-1575	C = C (Stretching)	Alkenes
1550-1475	$-NO_2$ (Stretching)	Nitrogenous compounds
1490-1325	C-H (bending)	Alkanes
1350-1140	S = O	Sulphur's related compounds
1300-1000	C-O **(**stretching)	Alcohols, ethers, esters, carboxylic acids, phenol.
900-690	O-H (bending)	Aromatic compounds, alkenes.

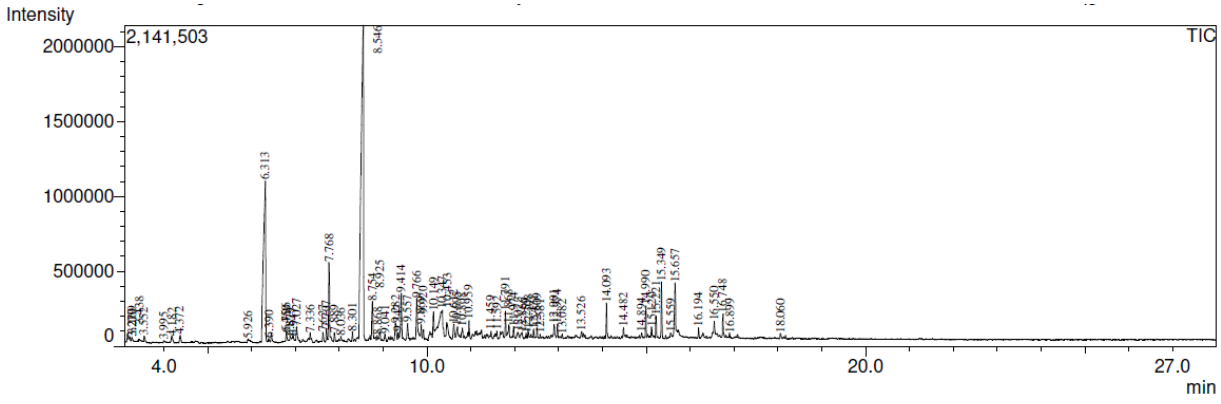

FIGURE 5.3.1.5: Chromatogram diagram of extracted bio-oil from *Ulva fasciata*.

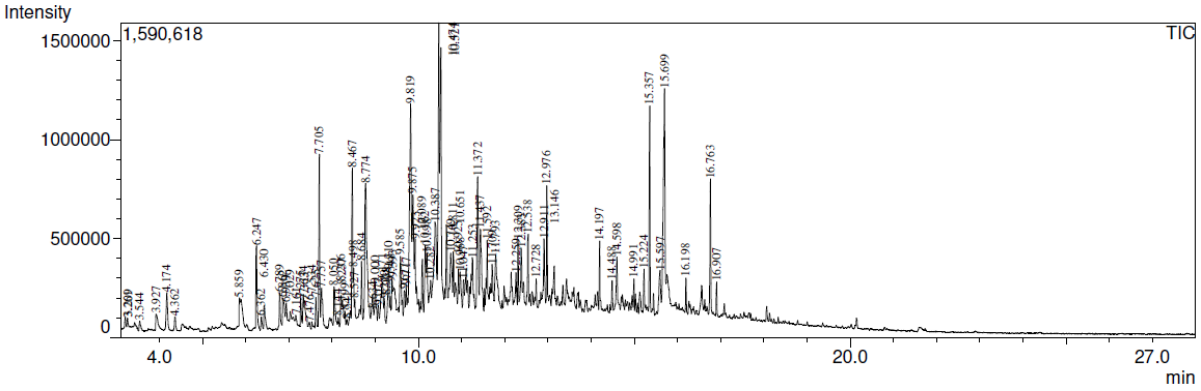

FIGURE 5.3.1.6: Chromatogram diagram of extracted bio-oil from *Gracilaria corticata*.

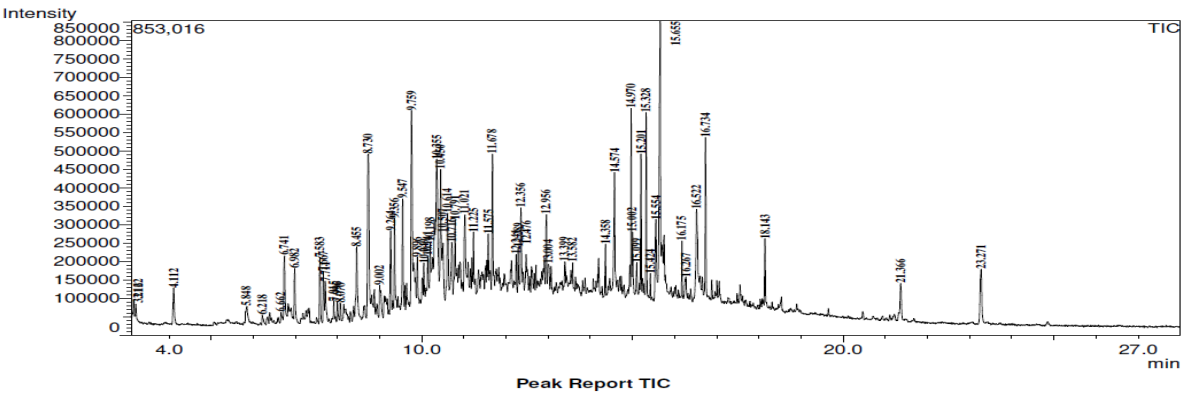

FIGURE 5.3.1.7: Chromatogram diagram of extracted bio-oil from *Sargassum tenerrimum*.

5.3.7 The Bio-chars from macro-algal pyrolysis

The bio-char obtained after the slow pyrolysis in the reactor is a potential solid fuel in thermochemical conversions for producing syn-gas either thermal or electrical applications and can be used as a solid soil nutrient for enrichment. The complete fuel characterization of three seaweed species bio-chars obtained at 500°C pyrolysis temperature are shown in Fig. 5.3.1.8 (a, b, c).

The result confirms that there is a drastic change in proximate analysis in all four parameters. First, the moisture content was reduced to a large extent from its raw biomass. But there is a contrasting result in volatile matter. For ST the volatile matter reduces to 24.06 % from 58.10%.

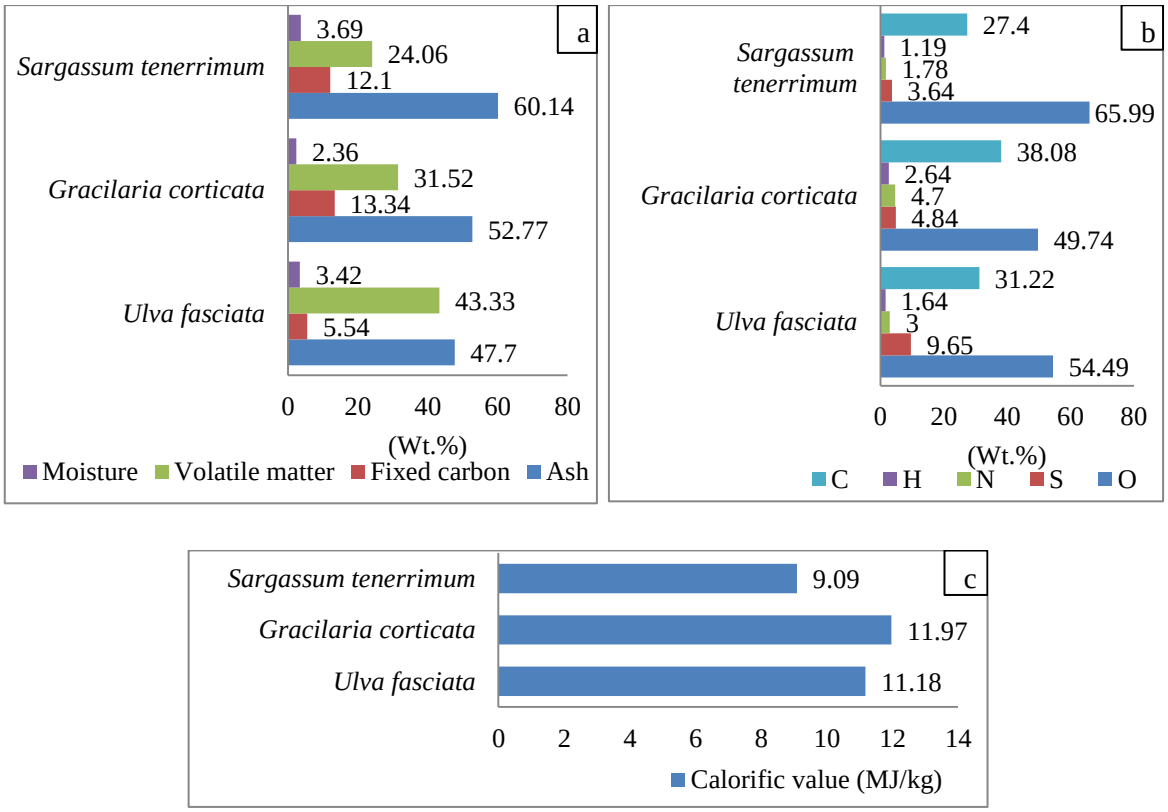

FIGURE 5.3.1.8: Proximate (a), ultimate (b) and CV (c) analysis of Bio-chars obtained from slow pyrolysis.

The condensable phase condenses as bio-oil and the noncondensable phase evolves as syn-gas during pyrolysis. While for GC the volatile matter reduces to 31.52% from 58.92% and similarly for UF devolatized matter is 31.41% on dry weight basis. The fixed carbon and other parameters are a relative parameter in proximate analysis and its higher value just improved the fuel quality. The main problem is that the seaweed species contains high ash which creates hindrance in thermochemical conversions. It was found the highest ash is in ST followed by GC and UF. The ultimate analysis exhibits the elemental analysis of the obtained bio-chars. The elements such as carbon and hydrogen are responsible for improving the fuel quality while other elements such as oxygen, sulphur and high ash content are trustworthy for bringing down the calorific value of the bio-chars as shown in Fig. 5.3.1.8 (c). Table 5.3.1.8 shows the result of ash composition for each seaweed species.

TABLE 5.3.1.8: The ash composition of three seaweeds species selectively measured.

Elements	*Ulva fasciata* (%wt.)	*Gracilaria Corticata* (%wt.)	*Sargassum tenerrimum*
Si	0.97	0.97	0.96
Al	0.37	2.41	0.25
Ca	17.50	8.10	19.60
K	4.28	21.14	26.12
Mg	12.22	0.009	3.91
Na	5.33	5.48	17.32
Fe	0.21	0.81	0.25
P	3.23	0.68	0.89
Ti	0.005	0.01	0.005

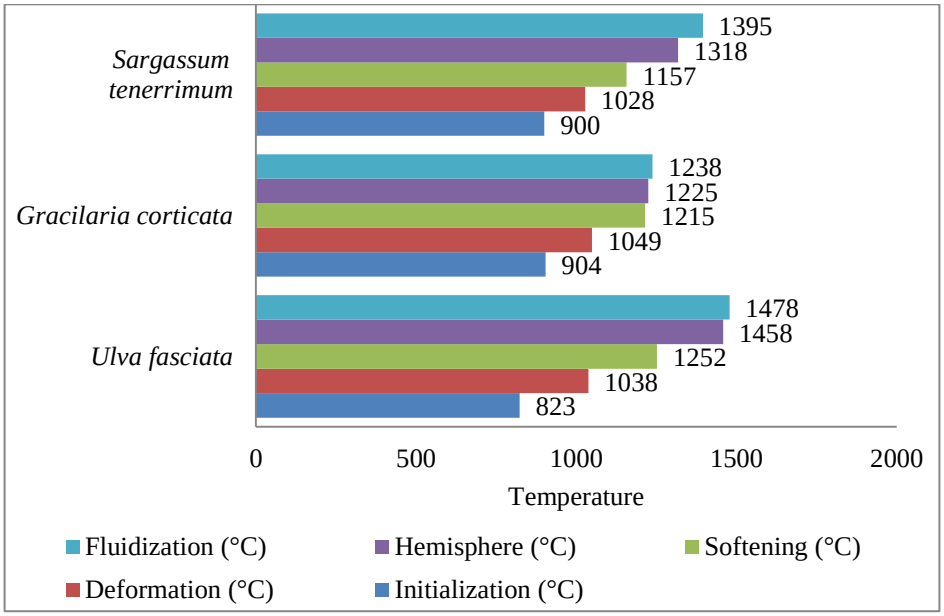

FIGURE 5.3.1.9: The ash fusion test of the three seaweeds species, (a) *Ulva fasciata*, (b) *Gracilaria corticata*, (c) *Sargassum tenerrimum*.

The Fig. 5.3.1.9 shows the ash fusion temperatures of each seaweed species. The deformation temperature for each seaweed ash is from around 1000°C. The softening temperatures are 1252, 1215, 1157°C, hemisphere temperature 1458, 1225, 1318 and fluidization temperature 1478, 1238, 1395°C for UF, GC and ST. So the obtained bio-chars can be used in thermochemical conversions such as gasifier, but the only constraint is the operating temperature should be less than 1000°C temperature.

5.3.8 LCA analysis

In the present LCA study, we used GaBi software (thinkstep) with (ECOINVENT 3.0) database for analysing the current process with the aim of energy consumption and environment evaluation. Life cycle impact assessment (LCIA) has selectively been done for the process of pyrolysis of *Ulva fasciata* seaweed biomass (0.5 kg) to yield three products, viz., syn-gas (0.289 MJ), moisture free bio-oil (1.76 MJ) and bio-char (2.89 MJ equivalent to 0.2604 kg) and 0.0281 kg tar. Unallocated impacts for the overall algal pyrolytic process revealed that the electricity accounted for almost 98.41% of the ReCiPe 1.08 Midpoint (H) climate change impact (excluding or including biogenic carbon di-oxide). The impacts for climate change has next highest (1.54%) due to ethyl acetate used during separation of water from bio-oil, while climate change impacts due to other processes (material of machinery used, were almost negligible). The total climate change impact was 2.05 kg CO_2-equivalent for the unallocated process (Fig. 5.3.1.10). Hence, it is prudent to make efforts towards reducing the requirement of electricity and solvent for further decreasing the climate change impacts.

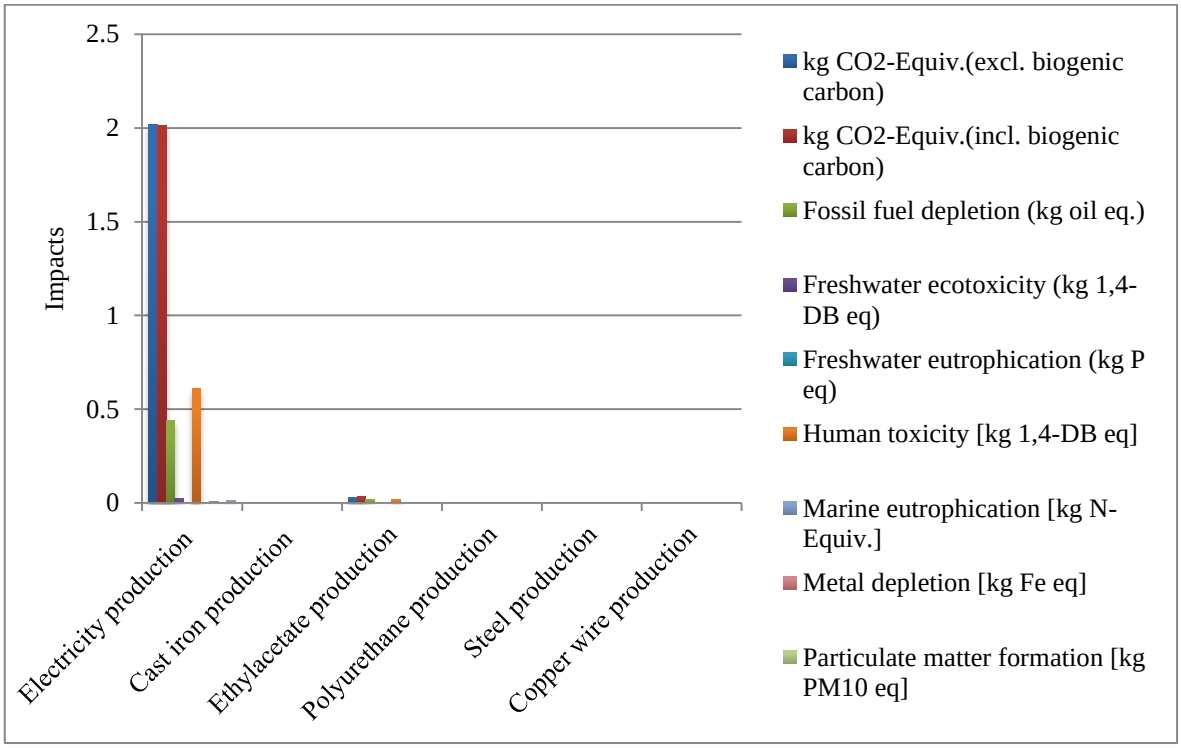

Figure 5.3.1.10: Impacts (unallocated) across various environmental impact categories for 0.5 kg *Ulva fasciata* seaweed pyrolysis due to the constituent production processes.

Similarly, impacts across various other environmental categories has been also assessed, viz., - Agricultural land occupation [m^2a], Fossil depletion [kg oil eq], Freshwater ecotoxicity [kg 1,4-DB eq] , Freshwater eutrophication [kg P eq] , Human toxicity [kg 1,4-DB eq] , Ionising radiation [kg U235 eq] , Marine ecotoxicity [kg 1,4-DB eq] , Marine eutrophication [kg N-Equiv.] , Metal depletion [kg Fe eq] , Natural land transformation [m2], Ozone depletion [kg CFC-11 eq], Particulate matter formation [kg PM10 eq], Photochemical oxidant formation [kg NMVOC], Terrestrial acidification [kg SO_2 eq], Urban land occupation [m^2a], Water depletion [m^3] (Fig. 5.3.1.10). It was found that contribution to these impacts has also attributed mostly due to electricity, which ranged from almost 71% in case of Ozone depletion to 98.4% in case of fresh water eutrophication. Similar to that of climate change impact, the use of ethyl acetate contributed higher to the other impact categories as well. The Life cycle assessment method has been further used to determine the allocated impacts of each of the products based on the price. The electricity consumption can be reduced by utilizing renewable energy such as solar electricity to make the process sustainable.

References:

1. RN Singh, DK Vyas, NSL Srivastava, M Narra, (2008), SPRERI experience on holistic approach to utilize all parts of Jatropha curcas fruit for energy, Renewable Energy, 33, 1868–73.

2. PK Ghosh et al., (2010), Process for the preparation of fatty acid methyl ester from triglyceride oil by transesterification, US Patent 7666234.

3. PK Ghosh et al., WO2011027353 (Filing date 22-09-2011, Publication date 29-03-2012) – Integrated process for the production of jatropha methyl ester and by products.

4. A Ghosh, DR Chaudhary, MP Reddy, SN Rao, J Chikara, JB Pandya, et al., (2007), Prospects for jatropha methyl ester (biodiesel) in India, International Journal of Environmental Studies, 64, 659–74.

5. D Fairless, (2007), Biofuel: the little shrub that could – maybe, Nature, 449 (7163), 652–5.

6. AK Tiwari, A Kumar, H Raheman, (2007), Biodiesel production from jatropha oil (Jatropha curcas) with high free fatty acids: an optimized process, Biomass Bioenergy, 31(8), 569–75.

7. R Sarin, M Sharma, S Sinharay, RK Malhotra, (2007), Jatropha–Palm biodiesel blends: an optimum mix for Asia, Fuel, 86, 1365–71.

8. PK Sahoo, LM Das, (2009), Combustion analysis of Jatropha, Karanja and Polanga based biodiesel as fuel in a diesel engine, Fuel, 88(6), 994–9.

9. SR Kalbande, GR More, RG Nadre, (2008), Biodiesel production from non-edible oils of Jatropha and Karanj for utilization in electrical generator, Bioenergy Research, 1(2), 170–8.

10. HJ Berchmans, S Hirata, (2008), Biodiesel production from crude Jatropha curcas L. seed oil with a high content of free fatty acids, Bioresource Technology, 99(6), 1716–21.

11. PT Vasudevan, M Briggs, (2008), Biodiesel production—current state of the art and challenges, Journal of Industrial Microbiology and Biotechnology, 35(5), 421–30.

12. H Zhou, H Lu, B Liang, (2006), Solubility of multicomponent systems in the biodiesel production by transesterification of Jatropha curcas L. oil with methanol, Journal of Chemical & Engineering Data, 51(3), 1130–5.

13. N Foidl, G Foidl, M Sanchez, M Mittelbach, Hackel, (1996), Jatropha curcas L. a source for the production of biofuel in Nicaragua, Bioresource Technology, 58(1), 77–82.

14. P Chitra, P Venkatachalam, A Sampathrajan, (2005), Optimisation of experimental conditions for biodiesel production from alkali-catalysed transesterification of Jatropha curcus oil, Energy for Sustainable Development, 9(3), 13–8.

15. MY Koh, TIM Ghazi, (2011), A review of biodiesel production from Jatropha curcas L. oil, Renewable & Sustainable Energy Reviews, 15(5), 2240–51.

16. SH Shuit, KT Lee, AH Kamaruddin, S Yusup, (2010), Reactive extraction and in situ esterification of Jatropha curcas L. seeds for the production of biodiesel, Fuel, 89(2), 527–30.

17. D-AZ Wever, HJ Heeres, AA Broekhuis, (2012), Characterization of Physic nut (Jatropha curcas L.) shells, Biomass Bioenergy, 37, 177–87.

18. DK Vyas, RN Singh, (2007), Feasibility study of Jatropha seed husk as an open core gasifier feedstock, Renewable Energy, 32, 512–7.

19. NA Pambudi, S Torii, H Saptoadi, W Sumbodo, M Syamsiro, UB Surono, (2010), Experimental study on combustion of biobriquettes jatropha curcas solid waste, Environmental Engineering and Management, 20(2), 133–6.

20. SV Loo, J Koppejan, (2008), The handbook of biomass combustion and cofiring, London: Earthscan.

21. D Gunarathne, (2012), Optimization of the performance of down-draft biomass gasifier installed at National Engineering Research & Development (NERD) Centre of Sri Lanka, Master of Science Thesis EGI.

22. P Basu, (2010), Biomass gasification and pyrolysis practical design and theory. UK: Elsevier Inc.

23. Anjireddy Bhavanam, RC Sastry, (2011), Biomass gasification processes in downdraft fixed bed reactors: a review, International Journal of Chemical Engineering and Applications, 2(6), 425–33.

24. ZA Zainal, A Rifau, GA Quadir, KN Seetharamu, (2002), Experimental investigation of a downdraft biomass gasifier, Biomass Bioenergy, 23, 283–9.

25. DL Pyle, C A Zaror, (1984), Heat transfer and kinetics in the low temperature pyrolysis of solids, Chemical Engineering Science, 39, 147−158.

26. T Sonobe, N Worasuwannarak, (2008), Kinetic analyses of biomass pyrolysis using the distributed activation energy model, Fuel 87, 414−421.

27. L Gasparovic, Z Korenova, L Jelemensky, (2009), Kinetic study of wood chips decomposition by TGA, Presented at the 36th International Conference of SSCHE, Tatranśke Matliare, Slovakia, May 25−29.

28. AGW Bradbury, Y Sakai, F Shafizadeh, (1979), A Kinetic Model for Pyrolysis of Cellulose, Journal of Applied Polymer Science, 23, 3271−3280.

29. H Haykiri-Acma, S Yaman, S Kucukbayrak, (2006), Effect of heating rate on the pyrolysis yields of rapeseed, Renewable Energy, 31, 803−810.

30. JJM Orfão, FJA Antunes, JL Figueiredo, (1999), Pyrolysis kinetics of lignocellulosic materials-three independent reactions model, Fuel, 78, 349−358.

31. P Das, M Dinda, N Gosai, S Maiti, (2015), High energy density bio-oil via slow pyrolysis of Jatropha curcas shells, Energy Fuels, 29, 4311–4320.

32. H Yang, R Yan, H Chen, C Zheng, DH Lee, DT Liang, (2006), In-Depth Investigation of Biomass Pyrolysis Based on Three Major Components: Hemicellulose, Cellulose and Lignin, Energy Fuels, 20, 388−393.

33. S Maiti, S Purakayastha, B Ghosh, (2007), Thermal characterization of mustard straw and stalk in nitrogen at different heating rates, Fuel, 86, 1513−1518.

34. R Bilbao, JF Mastral, ME Aldea, J Ceamanos, (1997), Kinetic study for the thermal decomposition of cellulose and pine sawdust in an air atmosphere, Journal of Analytical and Applied Pyrolysis, 39, 53−64.

35. R Ball, AC McIntosh, J Brindley, (2004), Feedback processes in cellulose thermal decomposition: implications for fire-retarding strategies and treatments, Combustion Theory and Modelling, 8, 281−291.

36. AE Pűtűn, E Apaydun, E Pűtűn, (2002), Bio-oil production from pyrolysis and steam pyrolysis of soybean-cake: product yields and composition, Energy, 27, 703−713.

37. AE Pűtűn, E Apaydun, E Pűtűn, (2004), Rice straw as a bio-oil source via pyrolysis and steam pyrolysis, Energy, 29, 2171−2180.

38. N Özbay, AE Pűtűn, BB Uzun, E Pűtűn, (2001), Bio-crude from biomass pyrolysis of cottonseed cake, Renewable Energy, 24, 615−625.

39. HPS Makkar, K Becker, F Sporer and M Wink, (1997), Studies on nutritive potential and toxic constituents of different provenances of jatropha carcass, Journal of agricultural food chemistry, 45, 3152 – 3157.

40. D Wever, HJ Heeres, AA Broekhuis, (2012), Characterization of Physic nut (Jatropha curcas L.) shells, Biomass Bioenergy, 37, 177−187.

41. S Sadasivam, A Manickam, (1992), Biochemical Methods for Agricultural Sciences; Wiley Eastern Ltd.: New Delhi, 14−15.

42. HD Goering, PJ Vansoest, (1975), Forage Fibre Analyses; U.S. Department of Agriculture, Agricultural Research Service, Agriculture Handbook No. 379; U.S. Government Printing Office: Washington, DC.

43. DM Updegroff, (1969), Semimicro determination of cellulose in biological materials, Analytical Biochemistry, 32, 420−424.

44. E Salehi, J Abedi, T Harding, (2007), Bio-oil from sawdust: pyrolysis of sawdust in a fixed-bed system, Energy Fuels, 23, 3767−3772.

45 P Basu, (2010), Biomass Gasification and Pyrolysis Practical Design and Theory; Elsevier Inc.: London.

46. D Undurraga, P Poirrier, R Chamy, (2016), Microalgae growth kinetic model based on the PSII quantum yield and its utilization in the operational curves construction, Algal Research, 17, 330–40.

47. C Azar, K Lindgren, BA Andersson, (2003), Global energy scenarios meeting stringent CO2 constraints—cost-effective fuel choices in the transportation sector, Energy Policy 31, 961–976.

48. AV Bridgwater, D Meier, D Radlein, (1999), An overview of fast pyrolysis of biomass, Organic Geochemistry, 30, 1479–1493.

49. A Demirbas, (2007), Progress and recent trends in biofuels, Progress in Energy Combustion science, 33, 1–18.

50. A Cadenas, S Cabezudo, (1998). Biofuels as sustainable technologies: perspectives for less developed countries, Technological Forecasting and Social Change, 58, 83–103.

51. T Minowa, S Yokoyama, M Kishimoto, T Okakura, (1995), Oil Production from Algal Cells of Dunaliella tertiolecta by Direct Thermochemical Liquefaction, Fuel, 74, 1735−1738.

52. T Brown, P Duan, P Savage, (2010), Hydrothermal Liquefaction and Gasification of Nannochloropsis sp., Energy Fuels, 24, 3639−3646.

53. P Duan, P Savage, (2011), Hydrothermal Liquefaction of Microalga with Heterogeneous Catalysts, Industrial & Engineering Chemistry Research, 50, 52−61.

54. P Biller, A Ross, (2011), Potential Yields and Properties of Oil from the Hydrothermal Liquefaction of Microalgae with Different Biochemical Content, Bioresource Technology, 102, 215−225.

55. D Zhou, L Zhang, S Zhang, H Fu, J Chen, (2010), Hydrothermal liquefaction of macroalgae enteromorpha prolifera to bio-oil, Energy Fuels, 24, 4054–4061.

56. D Vardon, B Sharma, J Scott, G Yu, Z Wang, L Schideman, (2011), Chemical properties of biocrude oil form the hydrothermal liquefaction of spirulina algae, swine manure and digested anaerobic sludge, Bioresource Technology, 102, 8295–8303.

57. P Valdez, J Dickinson, P Savage, (2011), Characterization of product fractions from hydrothermal liquefaction of Nannochloropsis sp. and the influence of solvents, Energy Fuels, 25, 3235–3243.

58. U Jena, K Daa, J Kastner, (2011), Effect of Operating Conditions of Thermochemical Liquefaction on Biocrude Production from Spirulina platensis, Bioresource Technology 102, 6221−6229.

59. S Ceylan, Y Topcu, Z Ceylan, (2014), Thermal behaviour and kinetics of alga Polysiphonia elongata biomass during pyrolysis, Bioresource Technology, 171, 193–198.

60. G Yu, Y Zhang, L Schideman, T Funk, Z Wang, (2011), Distributions of Carbon and Nitrogen in the Products from Hydrothermal Liquefaction of Low-Lipid Microalgae, Energy and Environmental Science 4, 4587−4595.

61. Z Shuping, W Yulong, Y Mingde, L Chun, T Junmao, (2010), Pyrolysis characteristics and kinetics of the marine microalgae Dunaliella tertiolecta using thermogravimetric analyzer, Bioresource Technology 101, 359–365.

62. L Alba, C Torri, C Samor, J van der Spek, D Fabbri, S Kerstn, D Brilman, (2012), Hydrothermal Treatment (HTT) of Microalgae: Evaluation of the Process as Conversion Method in an Algae Biorefinery Concept, Energy Fuels, 26, 642−657.

63. S Thangalazhy-Gopakumar, S Adhikari, SA Chattanathan, RB Gupta, (2012), Catalytic pyrolysis of green algae for hydrocarbon production using H+ ZSM-5 catalyst. Bioresource Technology, 118, 150–157.

64. H Yang, R Yan, T Chin, DT Liang, H Chen, C Zheng, (2004), Thermogravimetric analysis-Fourier transform infrared analysis of palm oil waste pyrolysis, Energy Fuel, 18, 1814–21.

65. MJ Antal, G Varhegyi, E Jakab, (1998), Cellulose pyrolysis kinetics: revisited, Industrial & Engineering Chemistry Research, 37, 1267–75.

66. H Teng, YC Wei, (1998), Thermogravimetric studies on the kinetics of rice hull pyrolysis and the influence of water treatment, Industrial & Engineering Chemistry Research, 37, 3806 − 11.

67. S Kim, H Vu Ly, G Choi, J Kim, HC Woo, (2012), Pyrolysis characteristics and kinetics of the alga Saccharina japonica, Bioresource Technology, 123, 445–451.

68. S Kim, H Vu Ly, J Kim, G Choi, HC Woo,(2013), Thermogravimetric characteristics and pyrolysis kinetics of Alga Sagarssum sp. biomass, Bioresource Technology, 139, 242–248.

69. M Heydari, M Rahman, R Gupta, (2015), Kinetic Study and Thermal Decomposition Behavior of Lignite Coal, International Journal of Chemical Engineering Article ID 481739, 9 pages.

70. K Eswaran, PK Ghosh, AK Siddhanta, PPeriyasamy, AS Mehta, (2005) U.S. Patent 6893479, May 17.

71. D Mondal, M Sharma, P Maiti, K Prasad, R Meena, AK Siddhanta, P Bhatt, S Ijardar, VP Mohandas, A Ghosh, K Eswaran, BG Shah, PK Ghosh, (2013), Process for improved seaweed biomass conversion for fuel intermediates, agricultural nutrients and fresh water. RSC Advances 3, 17989–17997.

72. Y Khambhaty, K Mody, MR Gandhi, S Thampy, P Maiti, H Brahmbhatt, K Eswaran, PK Ghosh, (2012), Kappaphycus alvarezii as a source of bioethanol, Bioresource Technology, 2012, 180–185.

73. C Roger, (1984), The Chemical Composition of Wood. U.S. Department of Agriculture, Forest Service, Forest Products Laboratory, Madison, WI 53705.

74. HL Friedman, (1964), Journal of Polymer Science Part C 6, 183.

75. J Flynn, L Wall, (1966), A quick, direct method for the determination of activation energy from thermogravimetric data, Journal of Polymer Science, Polymer Letters 4, 323–8.

76. T Ozawa, (1965), A new method of analyzing thermogravimetric data, Bulletin of the Chemical Society of Japan, 38, 1881–6.

77. T Akahira, T Sunose, (1971), Joint convention of four electrical institutes. Sci. Technol. 16, 22–31.

78. H Kissinger, (1956), Variation of peak temperature with heating rate in differential thermal analysis, Journal of Research of the National Bureau of Standards, 57, 217–21.

79. K Slopiecka, P Bartocci, F Fantozzi, (2012), Thermogravimetric analysis and kinetic study of poplar wood pyrolysis, Applied Energy, 97, 491–7.

80. Young-H Park, J Kim, Seung-S Kim, Young-K Park, (2009), Pyrolysis characteristics and kinetics of oak trees using thermogravimetric analyzer and micro-tubing reactor, Bioresource Technology, 100, 400–405.

81. S Maiti, P Bapat, P Das, PK Ghosh, (2014), Feasibility study of jatropha shell gasification for captive power generation in biodiesel production process from whole dry fruits, Fuel, 121, 126–132.

82. RM Oza, SH Zaidi, (2001), A revised checklist of Indian marine algae, CSMCRI, Bhavnagar, pp 24–29

83. DJ McHugh, (2003), A guide to the seaweed industry, FAO Fisheries Technical Paper,441, p. 105.

84. P Kaladharan and N Kaliaperumal, (1999), Seaweed Industry in India, Central Marine Fisheries Research Institute, Kochi-682014, India.Quarterly (Vol. 22, No.1).

85. PV Subba Rao and Vaibhav A Mantri. Indian seaweed resources and sustainable utilization: Scenario at the dawn of a new century. Review article. Marine Algae and

Marine Environment Division, Central Salt and Marine Chemicals Research Institute (CSIR), Gijubhai Badheka Marg, Bhavnagar 364 002, India.

86. SJ Horn, IM Aasen, K Østgaard, (2000), Ethanol production from seaweed extract, Journal of Industrial Microbiology and Biotechnology, 25, 249–254.

87. CS Goh, KT Lee, (2010), A visionary and conceptual macroalgae-based thirdgeneration bioethanol (TGB) biorefinery in Sabah, Malaysia as an underlay for renewable and sustainable development, Renewable and Sustainable Energy Reviews, 14, 842–848.

88. Prasanta Das, Dibyendu Mondal, Subarna Maiti, (2017), Thermochemical conversion pathways of Kappaphycus alvarezii granules through study of kinetic models, Bioresource Technology, 234, 233–242.

89. X Wang, XH Liu, and GY Wang, (2011), Two-stage hydrolysis of invasive algal feedstock for ethanol fermentation, Journal of Integrative Plant Biology, 53, 246–252.

90. Nitin Trivedi, Vishal Gupta, CRK Reddy, Bhavanath Jha, (2013), Enzymatic hydrolysis and production of bioethanol from common macrophytic green alga Ulva fasciata Delile, Bioresource Technology, 150, 106–112.

91. Manoj Kumar, Puja Kumari, Nitin Trivedi, Mahendra K Shukla, Vishal Gupta, CRK Reddy, Bhavanath Jha, (2011), Minerals, PUFAs and antioxidant properties of some tropical seaweeds from Saurashtra coast of India, Journal Applied Phycology 23, 797–810.

92. AK Siddhanta, Kamalesh Prasad, Ramavatar Meena, Gayatri Prasad, Gaurav K Mehta, Mahesh U. Chhatbar, Mihir D Oza, Sanjay Kumar, Naresh D Sanandiya, (2009), Profiling of cellulose content in Indian seaweed species, Bioresource Technology, 100, 6669–6673.

CHAPTER – 6

Concluding Remarks and Future Studies

6.1 Introduction

The sequences of this PhD thesis are presented to give an insight of the energy scenario both in the world and India. Current trend is mainly focussed on the renewable energy sectors such as solar energy, bio-energy, wind energy, etc. Energy is a daily need in every household. The over reliance on conventional energy sources for our daily requirements is indeed huge. Also burning these energy sources causes several problems associated with health, environment, and soil. The underpinning of this PhD thesis is to explore different renewable bio-energy sources. The selection of wasteland derived biomass and marine macroalgae as solid fuel is the main theme of the thesis. The entire PhD work is analysed and this can be categorized in six salient features.

(1) The selection of problem which exists

(2) Suitable justification for a proper solution

(3) Find the originality and novelty of the solution

(4) Suitable methodology adoption for solving the problems and

(5) The ultimate outcome of the research work

The PhD thesis based on the above parameters have been discussed and presented.

6.2 Summary and discussion

The objective for selecting these biomasses is to avoid controversy over the food vs. energy. These crops have very good potential to compete with the conventional energy sources and may be substituted for energy application in near future. For this, each biomass from different category has been investigated for the fuel characterization prior to thermochemical conversion processes, mainly in gasification, pyrolysis, and steam gasification.

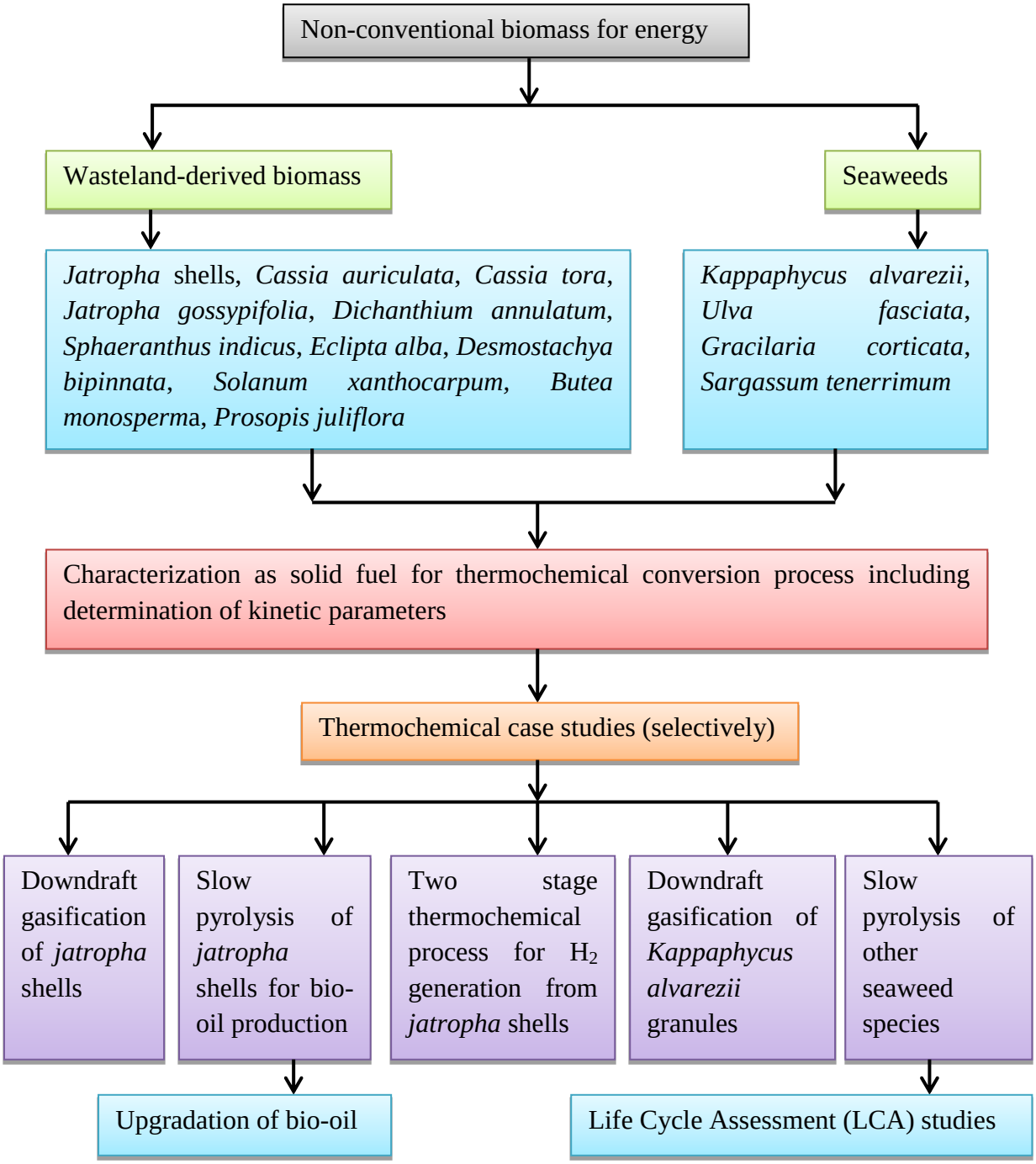

FIGURE 6.1: Schematic diagram of all the work.

The kinetic study was undertaken to explore the devolatilization process i.e. pyrolysis. Figure 6.1 shows the overall work carried out in the present thesis. The non-conventional biomasss including wasteland-derived as well as seaweeds characterized as solid fuel by standard methods. Chapter 1 reviews energy scenario in the world and India covering the past, present, and future energy scenario of conventional energy sources for both the cases. Then, the different thermochemical conversion process gasification, pyrolysis, combustion, and steam gasification are described. The end product from each process is described in this chapter. The review of the chapter 2 provides literature survey of thermochemical conversion routes. The first literature survey describes about biomass for thermochemical conversion process. The second literature survey includes overview of gasification technology. It covers several areas starting from the discovery of the technology to several types of gasifier. The third literature survey reviews the pyrolysis process, effect of physical and chemical characteristics on bio-oil yield, description of different methodologies, and the bio-oil from different feedstocks. The fourth literature survey provides information about the different kinetic models which assists in understanding the pyrolysis process. The last and final literature survey brings about steam gasification process which includes the reaction mechanism and an overview of the steam gasification technology.

The chapter 3 gives the necessary information about the aim and scope of the work. This chapter describes about the overview of the renewable technologies and the objective of the research work. The chapter 4 describes about the different methodologies that were adopted for the determination of solid fuel characterization of wasteland derived biomass. Based on fuel characterization of the different biomass some of them were investigated for the experimental case studies and some were predicted for possible thermochemical routes. The chapter 5 reviews all the experimental case studies commencing from the jatropha curcas shells to macroalgae. Chapter 5 is divided into different sections for each experimental case study. The first section contains the gasification of jatropha shells which is followed by bio-oil production and steam gasification of bio-chars obtained after the slow pyrolysis of the same biomass. The next section provides valuable information about the gasification and bio-oil production from *Kappaphycus alvarezii* granules and other seaweed species.

6.3 Avenues of the prospective work

The entire thesis deals with the characterization of different kind of biomass, experimental investigation of selective biomass such as gasification of jatropha curcas shells, pyrolysis of the same biomass, and the obtained bio-char in steam gasification. The marine macroalgae *Kappaphycus alvarezii* granules are investigated in gasification and for bio-oil production. Other seaweed species *Ulva fasciata, Gracilaria corticata, and Sargassum tenerrimum* are also investigated for the bio-oil production via slow pyrolysis process. The wasteland biomass species are predicted for their suitability in thermochemical conversion processes based on solid fuel characterization. The gasification of jatropha curcas shells was investigated at a pilot scale level, but it can be positively upgraded for industrial scale level. The bio-oil production from jatropha shells via slow pyrolysis process was carried out in a lab scale pyrolyzer for the preliminary study, while there is a potential to investigate the same at the industrial scale which might assist for its commercial application. However, to do so, more parametric studies and optimization are required. Similarly, the gasification of *Kappaphycus alvarezii* – a macroalgae was investigated a typical downdraft gasifier can be implemented at the industrial scale level. Other seaweed species, such as *Ulva fasciata, Gracilaria corticata,* and *Sargassum tenerrimum*, were also investigated for the bio-oil production at a lab scale level. There are some biomasses which are enriched with high K^+ content or other valuable mineral contents. Detailed process development is required to extract these products. Another interesting activity could be to improve the calorific value of bio-oil through use of suitable catalysts to make the process economic. There are catalysts like acid based such as silica sulphuric acid [1]; Mo-based sulphide catalysts and noble metal catalysts such as palladium, Ru/TiO_2, etc [2]. These are useful to upgrade calorific value of bio-oil. Hydrogen content in the syn-gas from steam gasification of bio-char can be improved through use of different organic or inorganic catalyst. The bio-char obtained from slow pyrolysis of jatropha shells can be utilized for the preparation of activated carbon which is a highly porous material which has industrial applications. It would be very difficult to cover all the research areas in this thesis. So in future, some additional research work could be carried out and make a significant contribution to alleviate the problems faced.

References:

[1] Zhijun Zhang, Shujuan Sui, Fengqiang Wang, Qingwen Wang and Charles U. Pittman, Jr., (2013), Catalytic Conversion of Bio-Oil to Oxygen-Containing Fuels by Acid-Catalyzed Reaction with Olefins and Alcohols over Silica Sulfuric Acid, Energies, 6, 4531–4550.

[2] Huamin Wang, Suh-Jane Lee, Mariefel Valenzuela Olarte, and Alan H. Zacher, (2016), Bio-oil stabilization by hydrogenation over reduced metal catalysts at low temperatures, ACS Sustainable Chemistry & Engineering, 4 (10), 5533–5545.

Appendix – I

Pictures of Ash Fusion Temperatures of Ash Cone for Wasteland derived Biomass and for three other Seaweed species, *Ulva fasciata, Sargassum tenerrimum, Gracilaria corticata, and Kappaphycus alvarezii.*

Samples	Initialization	Deformation	Softening	Hemisphere	Fluidization
JG		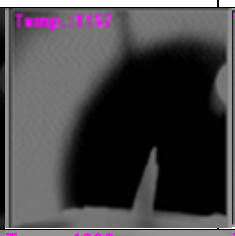	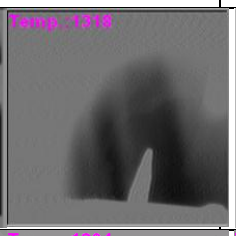	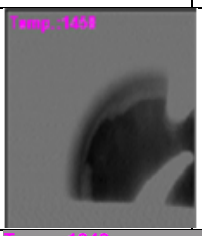	Fluidization temperature more than 1500°C
CT			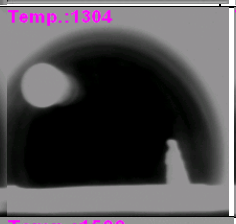	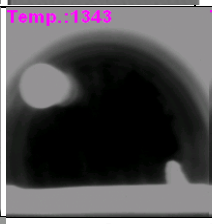	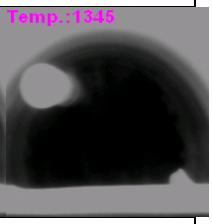
CA				Hemisphere and Fluidization temperatures more than 1500°C	
DB	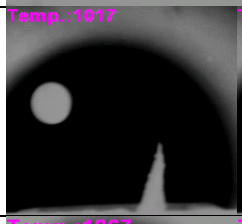	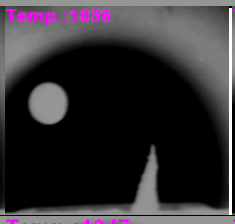		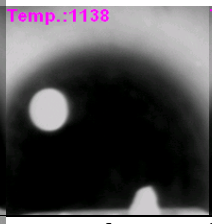	
SI	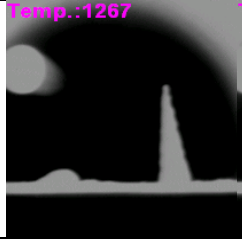	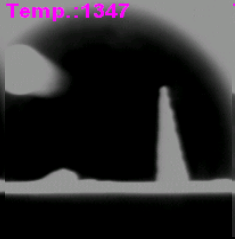		Hemisphere and Fluidization temperatures more than 1500°C	

DA	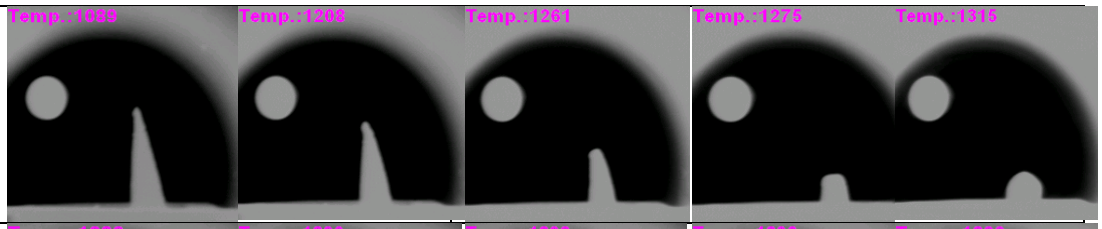				
SX	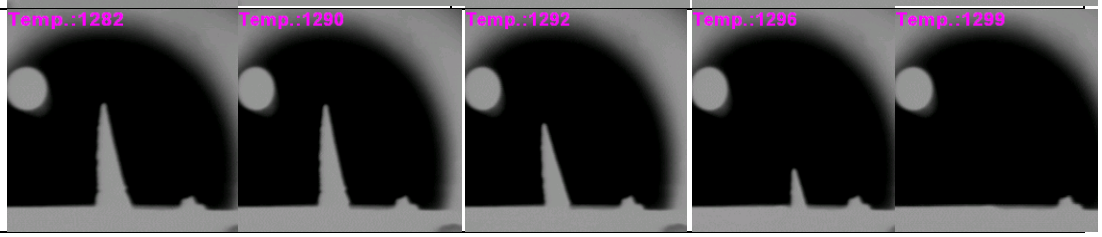				

	Initialization	Deformation	Softening	Hemisphere	Fluidization
EA	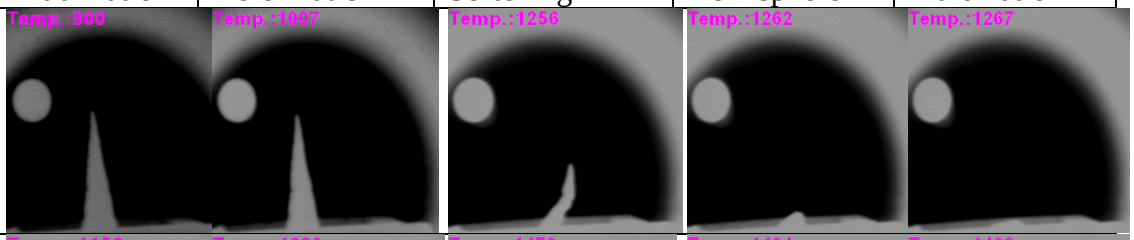				
PJ	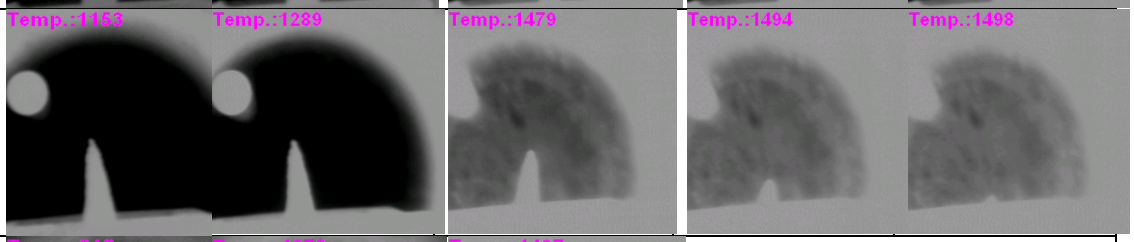				
BM	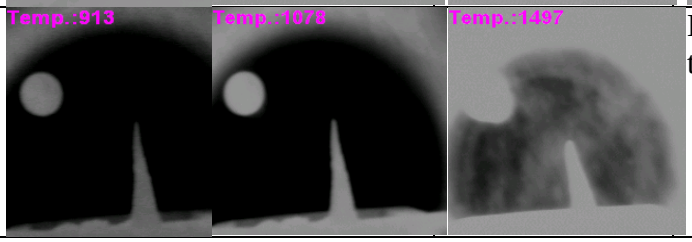			Hemisphere and Fluidization temperatures more than 1500°C	

AFT of *Ulva faciata*

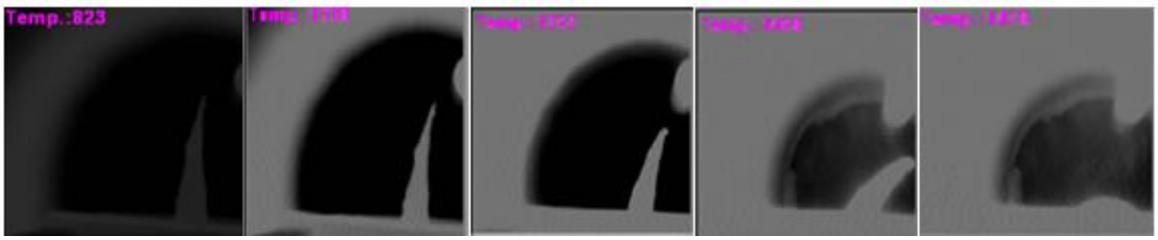

AFT of *Sargassum tenerrimum*

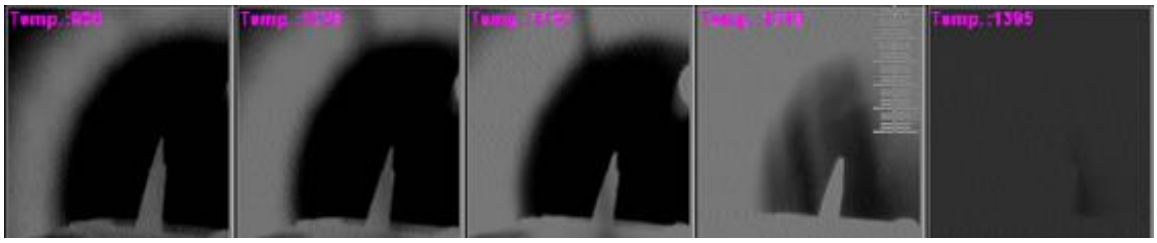

AFT of *Gracilaria corticata*

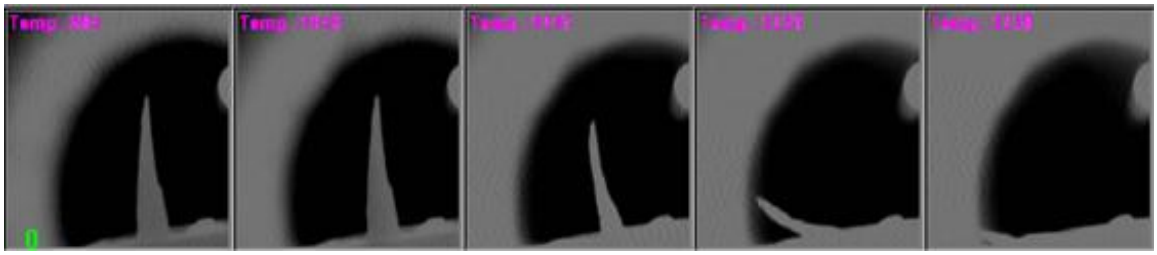

AFT of *Kappaphycus alvarezii* (Water washed granules)

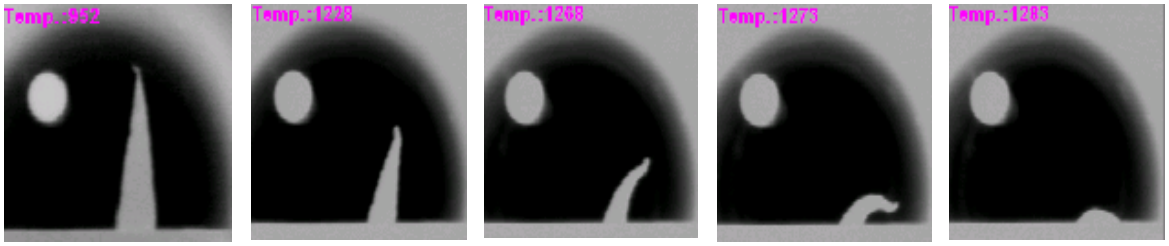

Annexure - XIX

List of Publications

1. Subarna Maiti, Pratap Bapat, **Prasanta Das**, Pushpito K. Ghosh. Feasibility study of jatropha shell gasification for captive power generation in biodiesel production process from whole dry fruits. **Fuel** 121 (2014) 126–132. IF = 4.6.

2. **Prasanta Das**, Milan Dinda, Nehal Gosai, and Subarna Maiti. High Energy Density Bio-oil via Slow Pyrolysis of Jatropha curcas Shells. **Energy Fuels** 2015, 29, 4311−4320. IF = 3.09.

3. **Prasanta Das**, Dibyendu Mondal, Subarna Maiti. Thermochemical conversion pathways of Kappaphycus alvarezii granules through study of kinetic models. **Bioresource Technology** 234 (2017) 233–242. IF = 5.65.

4. **Prasanta Das**, Samir Charola, Milan Dinda, Himanshu Patel, Subarna Maiti. Hydrogen from empty cotton boll agro-waste via thermochemical route and feasibility study of operating an IC engine in continuous mode. **International journal of hydrogen energy** 42 (2017) 14471 – 14484. IF = 3.58.

[5] Sumit Sahitya, Hasan Baig, Ruchita Jani, Nirav Gadhiya, **Prasanta Das**, Tapas K. Mallick, and Subarna Maiti." Hydrogen rich syn-gas from Jatropha curcas shell biomass char in Fresnel lens solar concentrator assembly". **Energy and Fuel**, DOI**:** 10.1021/acs.energyfuels.7b01406. IF = 3.09.

[6] Fabian Müller, Himanshu Patel, Dario Blumenthal, Peter Pozivil, **Prasanta Das**, Christian Wieckert, Pratyush Maiti, Subarna Maiti and Aldo Steinfeld. "Co-production of syngas and potassium-based fertilizer by solar-driven thermochemical conversion of crop residues". **Fuel processing technology**, Amsterdam: Elsevier, 2017. (Just accepted manuscript). IF = 3.75.

List of Patent

1. Process for potash recovery from biomethanated spent wash with concomitant environmental remediation of effluent. Inventors: Pratyush Maiti, Subarna Maiti, Soumya Halder, Krishna Kanta Ghara, **Prasanta Das**, S. K. Charola and Neha P. Patel. Patent filed in CSIR, New Delhi, India. Pub. No. WO/2017/042832, International Application No. PCT/IN2016/050298.